ARCHIVES OF MECHANICS **Appears since 1949**

Aims and Scope

ARCHIVES OF MECHANICS provides a forum for original research on mechanics of solids, fluids and discrete systems, including the development of mathematical methods for solving mechanical problems. The journal encompasses all aspects of the field, with the emphasis placed on:

- mechanics of materials: elasticity, plasticity, time-dependent phenomena, phase transformation, damage, fracture; physical and experimental foundations, micromechanics, thermodynamics, instabilities
- methods and problems in continuum mechanics: general theory and novel applications, thermomechanics, structural analysis, porous media, contact problems
- dynamics of material systems
- fluid flows and interactions with solids

Address of the Editorial Office:
Institute of Fundamental Technological Research
Świętokrzyska 21
PL 00-049 Warsaw, Poland

Tel.: (48-22) 826 60 22, Fax: (48-22) 826 98 15, E-mail: publikac@ippt.gov.pl

Abstracted/indexed in:

Applied Mechanics Reviews, Current Mathematical Publications, Mathematical Reviews, MathSci, Zentralblatt für Mathematik, UnCover.

Polish Academy of Sciences

Institute of Fundamental Technological Research

Archives of Mechanics

Archiwum Mechaniki Stosowanej

volume 52 issue 1

Agencja Reklamowo-Wydawnicza A. Grzegorczyk
Warszawa 2000

SUBSCRIPTIONS

Address of the Editorial Office: Archives of Mechanics
Institute of Fundamental Technological Research, Świętokrzyska 21
PL 00-049 Warsaw, Poland
Tel.: (48-22) 826 60 22, Fax: (48-22) 826 98 15, E-mail: publikac@ippt.gov.pl

Subscription orders for all journals edited by IFTR may be sent directly to the Editorial Office of the Institute of Fundamental Technological Research

Subscription rates

Annual subscription rate (2000) including postage is US $ 192.
Please transfer the subscription fee to our bank account: Payee: IPPT PAN,
Bank: PKO SA. IV O/Warszawa,
Account no. 12401053-40054492-3000-401112-001.

All journals edited by IFTR are available also through:

- Foreign Trade Enterprise ARS POLONA Krakowskie Przedmieście 7, 00-068 Warszawa, Poland fax: (48-22) 826 86 73
- RUCH S.A. ul. Towarowa 28, 00-958 Warszawa, Poland fax:(48-22) 620 17 62
- Agencja Reklamowo-Wydawnicza A. Grzegorczyk, Bitwy Warszawskiej 1920r. 3, 00-973 Warszawa, Poland tel./fax: (48-22) 822 49 36

Warunki prenumeraty

Redakcja przyjmuje prenumeratę na wszystkie czasopisma wydawane przez IPPT PAN. Bieżące numery można nabyć a także zaprenumerować roczne wydanie Archiwum Mechaniki Stosowanej bezpośrednio w Dziale Wydawnictw IPPT PAN, Świętokrzyska 21, 00-049 Warszawa, Tel.: (48-22) 826 60 22; Fax: (48-22) 826 98 15.
Cena rocznej prenumeraty z bonifikatą (na rok 2000) dla krajowego odbiorcy wynosi 150 zł

Również można je nabyć, a także zamówić (przesyłka za zaliczeniem pocztowym) we Wzorcowni Ośrodka Rozpowszechniania Wydawnictw Naukowych PAN,
00-818 Warszawa, ul. Twarda 51/55, tel. (48-22) 697 88 35.
Wpłaty na prenumeratę przyjmują także jednostki kolportażowe RUCH S.A. Oddział Krajowej Dystrybucji Prasy, 00-958 Warszawa, ul. Towarowa 28. Konto: PBK.S.A. XIII Oddział Warszawa nr 11101053-16551-2700-1-67. Dostawa odbywa się pocztą zwykłą w ramach opłaconej prenumeraty z wyjątkiem zlecenia dostawy pocztą lotniczą, której koszt w pełni pokrywa zleceniodawca. Tel.: (48-22) 620 10 39, fax: (48-22) 620 17 62

Arkuszy wydawniczych 14.6. Arkuszy drukarskich 16,60/A5.
Papier offset. kl III 70 g. B1.
Oddano do składania w styczniu 2000 r. Druk ukończono w lutym 2000 r.
Skład i łamanie: G. Wasilewska. Druk i oprawa: Drukarnia OMIKRON, Stare Babice ul. Kutrzeby 15.

Arch. Mech., **52**, 1, pp. 3–23, Warszawa 2000

Propagation and reflectivity of transient heat waves

M. ROMEO

D.I.B.E., Università di Genova,
via Opera Pia, 11/a, 16145 Genova, Italy
e-mail: romeo@dibe.unige.it

We consider a rigid heat conductor characterized by two relaxation times and derive a linear hyperbolic equation for the temperature which can properly describe heat waves. The wave splitting technique is applied to the propagation problem whose solution is expressed in the form of the Laplace transform of the wave propagator. The reflectivity of a heat pulse is then obtained at an interface between two different conductors. Explicit results for both the propagation and the reflection probelms are worked out under suitable conditions which allow for a second sound propagation in low temperature rigid conductors. The characteristic relaxation times of a reflecting conductor are also determined as the solution of an inverse reflection problem.

1. Introduction

A large part of the recent theories of heat conduction is modelled in such a way as to comply with the fundamental requirement of a finite propagation speed. Beside the strong physical motivation which supports these theories, a growing experimental evidence of heat waves seems to point out that the usual diffusion equation for the temperature fails in describing transient phenomena in special circumstances [1, 2]. Heat waves (second sound) have been detected in liquid helium II and in dielectric crystals in narrow ranges of very low temperatures [3, 4]. Hyperbolic heat conduction has been also observed in processed meat at room temperatures [5]. In this last case the use of a Cattaneo's type constitutive equation for the heat flux has been proved to give excellent agreement with experimental results. The heat flux in Cattaneo's constitutive model is characterized by an exponential kernel with a single relaxation time and represents the most simple generalization to the Fourier's law allowing for a hyperbolic heat equation. On the other hand, experimental results on solid heat conductors at low temperatures suggest that different relaxation times exist in connection with different mechanisms of heat conduction. This is due to the fact that any conductor possesses substructures which relax at different rates. Really, heat can be carried by free electrons or by ballistic phonons, transmitted by electron-electron,

electron-phonon or phonon-phonon collisions and by interactions of phonons and electrons with the lattice impurities. In many cases, a realistic model can be obtained accounting for only two or three different mechanisms which compete in heat transport.

In the present paper we introduce a phenomenological model for a rigid conductor adopting a constitutive equation for the heat flux characterized by an exponential kernel with two different relaxation times. We show that, along with a linearized form of the balance of energy, this assumption yields a hyperbolic heat equation which generalizes the Cattaneo model. The coefficients of the heat equation are shown to depend essentially on the relaxation times which ultimately characterize the conductor's behaviour. The remainder of the paper is devoted to the analysis of the linearized hyperbolic system for the temperature θ and the heat flux q within the phenomenological model previously outlined. In some sense, this analysis extends the results obtained in [6] for a rigid conductor governed by the Cattaneo model. Transient wave solutions are studied and expressed in terms of the Laplace transform of a wave propagator. As shown in the last section, explicit inversion of the solution can be carried out under suitable conditions on the relaxation times which allow for second sound propagation in low temperature conductors. As it occurs in all propagation phenomena, the interaction of transient heat waves with an interface between different heat conductors, plays a fundamental role in many direct and inverse problems. For this reason we have applied the usual wave splitting technique to analyze the reflectivity of heat pulses on a discontinuity surface within the conductor. The procedure parallels the known approaches on wave propagation in dissipative media and leads to a reflectivity function characterized by the relaxation times of both sides of the interface. In the last section it is also shown that reflected pulses can be exploited to determine the relaxation times of the reflecting conductor. This inverse problem is solved in the case in which the incoming wave is a second sound pulse.

2. Heat flux with two relaxation times

Let us consider a rigid isotropic heat conductor which occupies an unbounded region $\mathcal{B}$ of the physical space. The absolute temperature $\theta = \theta(\mathbf{x}, t)$ is taken as a bounded function of the position and time, defined on the vector space $V \times \mathbb{R}$ where $V \subset \mathbb{R}^3$. A constitutive model accounting for a finite speed of heat propagation in a rigid conductor was introduced by GURTIN and PIPKIN [7] within the thermodynamic theory of materials with memory. In the linear approximation they obtained the following expression for the heat flux in an isotropic conductor:

$$\mathbf{q}(\mathbf{x},t) = -\int_0^\infty a(s)\ \mathbf{g}(\mathbf{x},t-s)\,\mathrm{d}s, \tag{2.1}$$

where $\mathbf{g}(\mathbf{x},t) = \nabla\theta(\mathbf{x},t)$ is the temperature gradient. If $a(s) = \frac{\kappa}{\tau}\exp(-s/\tau)$, from Eq. (2.1) follows the Cattaneo's equation,

$$\tau\ \partial_t\mathbf{q} + \mathbf{q} = -\kappa\ \mathbf{g}, \tag{2.2}$$

where κ and τ are respectively the heat conductivity and the characteristic relaxation time. In [7] it is assumed that the free energy density ψ, the entropy density η and the heat flux $\mathbf{q}$ depend on the summed histories of θ and $\mathbf{g}$, i.e., $\bar{\theta}^t(s) = \int_0^s \theta(t-\lambda)\,d\lambda$ and $\bar{\mathbf{g}}^t(s) = \int_0^s \mathbf{g}(t-\lambda)\,d\lambda$. However, as shown by MORRO [8], an effective model, compatible with a finite speed of heat propagation can be obtained by replacing the dependence on $\bar{\theta}^t$ and $\bar{\mathbf{g}}^t$ with the dependence on the histories $\theta^t(s) = \theta(t-s)$ and $\mathbf{g}^t(s) = \mathbf{g}(t-s)$. The qualitative features of the model, with respect to heat waves, do not change if we restrict the constitutive functionals to the form

$$\psi = \Psi(\theta,\mathbf{g}^t), \quad \eta = N(\theta,\mathbf{g}^t), \quad \mathbf{q} = \mathbf{Q}(\theta,\mathbf{g}^t). \tag{2.3}$$

As an example, a Maxwell-Cattaneo kernel for Eq. (2.1) has been considered in [8] assuming a quadratic dependence of ψ on the heat flux. As shown in [9], this assumption is required by the compatibility of Eq. (2.2) with thermodynamics. Consistently with the analysis in [8], we generalize here the previous example assuming that the relaxation kernel $a(s)$ be characterized by two different times τ_1 and τ_2. More precisely, we assume that Eqs. $(2.3)_3$ and $(2.3)_1$ take the following form

$$\mathbf{q}(\mathbf{x},t) = -\sum_{i=1}^{2}\kappa_i[\theta(\mathbf{x},t)]\int_0^\infty \frac{\exp(-s/\tau_i)}{\tau_i}\ \mathbf{g}(\mathbf{x},t-s)\,ds, \tag{2.4}$$

$$\psi(\mathbf{x},t) = \varphi[\theta(\mathbf{x},t)] + \sum_{i,j=1}^{2}\beta_{ij}[\theta(\mathbf{x},t)]\left[\int_0^\infty \frac{\exp(-s/\tau_i)}{\tau_i}\mathbf{g}(\mathbf{x},t-s)\,ds\right]\left[\int_0^\infty \frac{\exp(-s/\tau_j)}{\tau_j}\mathbf{g}(\mathbf{x},t-s)\,ds\right]. \tag{2.5}$$

The quantities $\kappa_i(\theta)$ $(i=1,2)$ in (2.4) are supposed to be C^2 functions of θ and the relaxation times $\tau_i > 0$ $(i=1,2)$ are taken to be constant. In Eq. (2.5) $\varphi(\theta)$ is a convex function and the entries of the symmetric matrix β_{ij} are supposed to

be C^2 functions of θ. The model (2.4) – (2.5) applies, in general, to composite materials in which different substructures relax at different rates. Specifically, as illustrated in the next section, it can be applied to rigid dielectrics at low temperatures where phonon normal processes and umklapp processes occur with different frequencies.

In order to obtain thermodynamic restrictions on $\kappa_i(\theta)$ and $\beta_{ij}(\theta)$, we exploit the balance equation for the energy density $e(\mathbf{x}, t)$,

$$\rho \partial_t e = -\nabla \cdot \mathbf{q} + r, \tag{2.6}$$

together with the second law in the form of the following inequality for the entropy density η,

$$\rho \partial_t \eta \geq -\nabla \cdot \frac{\mathbf{q}}{\theta} + \frac{r}{\theta}, \tag{2.7}$$

where ρ is the (constant) mass density and r is the heat supply of external sources. Accounting for the thermodynamic relation $\psi = e - \theta\eta$, Eqs. (2.6) and (2.7) yield the Clausius-Duhem inequality in the following form:

$$-\rho \partial_t \psi - \frac{\rho}{\theta}(e - \psi)\partial_t \theta \geq \frac{1}{\theta}\mathbf{q} \cdot \mathbf{g}, \tag{2.8}$$

Posing

$$\Phi_i(\mathbf{x}, t) = \int_0^\infty \frac{1}{\tau_i} \exp(-s/\tau_i)\ \mathbf{g}(\mathbf{x}, t - s)\, ds, \qquad i = 1, 2,$$

we have

$$\partial_t \Phi_i = \frac{1}{\tau_i}(\mathbf{g} - \Phi_i), \qquad i = 1, 2. \tag{2.9}$$

Exploiting this result and substituting (2.5) and (2.4) into (2.8) we obtain

$$-\frac{\rho}{\theta}\partial_t \theta \left[e - \varphi + \theta\varphi' - \sum_{i,j=1}^{2} (\beta_{ij} - \theta\beta'_{ij}) \Phi_i \cdot \Phi_j \right]$$

$$-\rho \sum_{i,j=1}^{2} \beta_{ij} \left[\left(\frac{1}{\tau_i}\Phi_j + \frac{1}{\tau_j}\Phi_i \right) \cdot \mathbf{g} - \left(\frac{1}{\tau_i} + \frac{1}{\tau_j} \right) \Phi_i \cdot \Phi_j \right]$$

$$\geq -\frac{1}{\theta} \sum_{i=1}^{2} \kappa_i \Phi_i \cdot \mathbf{g}.$$

where prime denotes differentiation with respect to θ. Since β_{ij} and κ_i do not depend on $\partial_t \theta$, we obtain

$$e = \varphi - \theta\varphi' + \sum_{i,j=1}^{2} (\beta_{ij} - \theta\beta'_{ij}) \Phi_i \cdot \Phi_j, \tag{2.10}$$

$$\rho\theta \sum_{i,j=1}^{2} \beta_{ij} \left[\left(\frac{1}{\tau_i} \Phi_j + \frac{1}{\tau_j} \Phi_i \right) \cdot \mathbf{g} - \left(\frac{1}{\tau_i} + \frac{1}{\tau_j} \right) \Phi_i \cdot \Phi_j \right] \leq \sum_{i=1}^{2} \kappa_i \Phi_i \cdot \mathbf{g}. \tag{2.11}$$

Adapting to our purposes a lemma shown in [8] and accounting for the independence of β_{ij} and κ_i on $\mathbf{g}^t$, inequality (2.11) ultimately gives

$$\kappa_i = 2\rho\theta \sum_{j=1}^{2} \beta_{ij} \frac{1}{\tau_j}, \tag{2.12}$$

$$\sum_{i,j=1}^{2} \beta_{ij} \left(\frac{1}{\tau_i} + \frac{1}{\tau_j} \right) \Phi_i \cdot \Phi_j \geq 0.$$

In view of the symmetry of β_{ij}, we conclude that the matrix $B_{ij} = \beta_{ij}/\tau_i$ is positive semidefinite and the same holds for the matrix β_{ij}. These facts imply

$$\kappa := \kappa_1 + \kappa_2 \geq 0, \tag{2.13}$$

$$\gamma := \frac{\kappa_1}{\tau_1} + \frac{\kappa_2}{\tau_2} \geq 0. \tag{2.14}$$

From (2.10) and (2.5) we also have

$$\eta = -\theta^2 \left[\varphi' + \frac{1}{\theta} \sum_{i,j=1}^{2} \beta_{ij} \Phi_i \cdot \Phi_j \right].$$

We remark that models which are characterized by only one relaxation time yield a Cattaneo's constitutive equation for the heat flux. This fact is apparent from Eqs. (2.4) and (2.9). The usual Fourier law $\mathbf{q} = -\kappa\mathbf{g}$ follows from (2.4) in the stationary case where κ, given by (2.13), is the heat conductivity of the medium.

3. Hyperbolic heat equation

Owing to Eqs. (2.10), (2.12) and (2.4), the balance of energy density (2.6) takes the form

$$-\theta\partial_t\theta\varphi'' - \sum_{i,j=1}^{2} \left[(\beta_{ij} - \theta\beta'_{ij}) \left(\frac{1}{\tau_i} + \frac{1}{\tau_j} \right) + \theta\partial_t\theta\beta''_{ij} \right] \Phi_i \cdot \Phi_j \tag{3.1}$$

$$+4\theta \sum_{i,j=1}^{2} \beta'_{ij} \frac{\Phi_i}{\tau_j} \cdot \mathbf{g} - 2\theta \sum_{i,j=1}^{2} \beta_{ij} \frac{1}{\tau_j} \nabla \cdot \Phi_i - \frac{r}{\rho} = 0.$$

Looking at a result which bear evidence of the essential features of the model with two relaxation times, we search for a linearized form of Eq. (3.1). Since thermal equilibrium is characterized by $\theta(\mathbf{x},t)=\theta_0$ and $\Phi_i(\mathbf{x},t)=0$ $(i=1,2)$, we retain only linear terms in the derivatives of θ and Φ_i. In absence of external heat supplies we obtain

$$\chi\partial_t\theta(\mathbf{x},t)=2\sum_{i,j=1}^{2}\beta_{ij}^0\frac{1}{\tau_j}\nabla\cdot\Phi_i, \tag{3.2}$$

where $\chi=-\varphi''(\theta_0)$ and $\beta_{ij}^0=\beta_{ij}(\theta_0)$. We note that, in view of the previous hypotheses we have $\chi>0$. Eq. (3.2) allows us to arrive at a linearized heat equation in a differential form. To this aim we observe that in view of Eq. (2.9), successive differentiation of Eq. (3.2) with respect to t gives

$$\begin{aligned}
&2\sum_{i,j}^{2}\beta_{ij}^0\frac{1}{\tau_i}\frac{1}{\tau_j}\nabla\cdot\Phi_i=2\sum_{i,j}^{2}\beta_{ij}^0\frac{1}{\tau_i}\frac{1}{\tau_j}\nabla\cdot\mathbf{g}-\chi\partial_t^2\theta,\\
&2\sum_{i,j}^{2}\beta_{ij}^0\frac{1}{\tau_i^2}\frac{1}{\tau_j}\nabla\cdot\Phi_i=2\sum_{i,j}^{2}\beta_{ij}^0\frac{1}{\tau_i}\frac{1}{\tau_j}\left[\frac{1}{\tau_i}\nabla\cdot\mathbf{g}-\partial_t\nabla\cdot\mathbf{g}\right]+\chi\partial_t^3\theta.
\end{aligned} \tag{3.3}$$

Since $\tau_1\neq\tau_2$ and assuming $\kappa_i\neq 0$ $(i=1,2)$, system (3.3) can be solved for $\nabla\cdot\Phi_i$, $(i=1,2)$. Substituting these results into (3.2) we arrive at the following heat equation

$$\begin{aligned}
-\partial_t\theta=(\tau_1+\tau_2)\partial_t^2\theta+\tau_1\tau_2\partial_t^3\theta-\frac{2}{\chi}\Bigg[&\left(\frac{\beta_{11}^0}{\tau_1}+\frac{\beta_{22}^0}{\tau_2}+\beta_{12}^0\left(\frac{1}{\tau_1}+\frac{1}{\tau_2}\right)\right)\Delta\theta\\
&+\left(\beta_{11}^0\frac{\tau_2}{\tau_1}+\beta_{22}^0\frac{\tau_1}{\tau_2}+2\beta_{12}^0\right)\partial_t\Delta\theta\Bigg].
\end{aligned} \tag{3.4}$$

This is an hyperbolic differential equation which, according to (2.14) admits wave propagation with the speed

$$v=\left[\frac{\gamma}{\rho\theta_0\chi}\right]^{1/2}=\left[\frac{2}{\chi}\sum_{i,j=1}^{2}\beta_{ij}^0\frac{1}{\tau_i}\frac{1}{\tau_j}\right]^{1/2}. \tag{3.5}$$

The quantities β_{ij}^0 are phenomenological coefficients whose values can be assigned by experimental data. In particular, if the heat conductivity κ and the wave speed v are given, Eqs. (2.13),(2.14) and (3.5) allow us to obtain β_{11}^0 and β_{22}^0 to within the choice of β_{12}^0. Since β_{ij}^0 is required to be positive semidefinite, we can fix β_{12}^0

under the only restriction $|\beta_{12}^0| \leq \sqrt{\beta_{11}^0 \beta_{22}^0}$. The most simple choice is $\beta_{12}^0 = 0$. In this case we obtain

$$\beta_{11}^0 = \frac{\tau_1^2}{\tau_2 - \tau_1}\left[v^2\tau_2 - \frac{\kappa}{2\rho\theta_0}\right], \qquad \beta_{22}^0 = \frac{\tau_2^2}{\tau_1 - \tau_2}\left[v^2\tau_1 - \frac{\kappa}{2\rho\theta_0}\right]. \tag{3.6}$$

The present phenomenological model is then reduced to the knowledge of the relaxation times τ_1 and τ_2.

A relevant application of the result (3.4) can be found in the problem of heat conduction in a rigid dielectric at low temperatures (see[1, 10]). In this context, a theory of the phonon gas has been developed which considers relaxation phenomena as the result of phonon's interactions. In particular, in a dielectric heat conductor two characteristic times can be introduced in connection with phonon's resistive processes which do not conserve momentum, and normal processes which conserve momentum (see [11]).We remark that in our model τ_1 and τ_2 are phenomenological quantities which are not necessarily ascribed respectivly to resistive and normal processes. However, a comparison with the 9-fields theory shows that the heat equation (3.4) has the same form of that obtained from system (3.56) in [10] where two relaxation times τ_R and τ_N account for resistive processes and normal processes, respectively. In fact Eqs. (3.56) in [10], can be rewritten as

$$\begin{aligned} \partial_t e + c^2 \nabla \cdot \mathbf{p} &= 0, \\ \partial_t \mathbf{p} + \frac{1}{3}\nabla e + \nabla \cdot \mathbf{N} &= -\frac{1}{\tau_R}\mathbf{p}, \\ \partial_t \mathbf{N} + \frac{2}{5}c^2\left(\nabla \mathbf{p} - \frac{1}{3}(\nabla \cdot \mathbf{p})\,\mathbf{1}\right) &= -\frac{1}{\tau}\mathbf{N}, \end{aligned} \tag{3.7}$$

where e is the energy density of phonons, $\mathbf{p}$ is the phonon momentum, $\mathbf{N}$ is the deviatoric part of the momentum flux of phonons, c is the Debye speed and $1/\tau = 1/\tau_R + 1/\tau_N$. Eliminating $\mathbf{p}$ and $\mathbf{N}$ from (3.7), we obtain the following equation for e,

$$-\frac{1}{\tau_R \tau}\partial_t e = \left(\frac{1}{\tau_R} + \frac{1}{\tau}\right)\partial_t^2 e + \partial_t^3 e - \frac{c^2}{3}\left(\frac{1}{\tau}\Delta e + \frac{9}{5}\partial_t \Delta e\right). \tag{3.8}$$

In [10] the energy density is supposed to obey the Debye law for phonons even in non-equilibrium. This fact means that $e = e(\theta)$ where θ is the absolute temperature of the conductor. In particular, the linearized form used in [10]

$$e = e_0 + \alpha(\theta - \theta_0), \tag{3.9}$$

with e_0 and α constant, turns out to be equivalent to the linearized version of (2.10). Substitution of (3.9) into (3.8) gives

$$-\partial_t\theta = (\tau_R + \tau)\partial_t^2\theta + \tau_R\tau\partial_t s\theta - \frac{c^2}{3}\left(\tau_R\Delta\theta + \frac{9}{5}\tau_R\tau\partial_t\Delta\theta\right). \tag{3.10}$$

Equation (3.10) has the same form of (3.4) provided that $1/\tau_1$ and $1/\tau_2$ are identified respectively with the relaxation frequencies $1/\tau_R$ and $1/\tau$. We finally observe that, actually and independently on their physical interpretation, the phenomenological times τ_1 and τ_2 have to be evalued by a measure of some relaxation properties of the conductor. In the last section we turn the evaluation of $1/\tau_1$ and $1/\tau_2$ into an inverse problem for the reflection of transient heat waves.

4. Wave splitting for transient heat waves

Having introduced Cartesian coordinates (x, y, z), we suppose that the region occupied by the rigid heat conductor corresponds to the half-space $V = \{(x, y, z) \in \mathbb{R}^3 |\ x \geq 0\}$ and denote by $\mathcal{S}$ the boundary plane surface $x = 0$. We assume that a uniform heat pulse is generated at $x = 0$, for $t > 0$ and that temperature perturbations are absent throughout V for $t \leq 0$. We restrict the analysis to the one-dimensional problem considering only the component $q_x =: q$ of $\mathbf{q}$. Looking for definite results, in the following we shall discard external heat supplies. From (2.4) and (2.6) we obtain a linear integro-differential system for θ and q in the form

$$q(x,t) = -\int_0^\infty \left(\frac{\kappa_1}{\tau_1}\exp(-s/\tau_1) + \frac{\kappa_2}{\tau_2}\exp(-s/\tau_2)\right)\partial_x\theta(x, t-s)\,ds, \tag{4.1}$$

$$\rho\theta_0\chi\partial_t\theta(x,t) = -\partial_x q(x,t), \tag{4.2}$$

together with the conditions

$$\theta(0,t) = \hat{\theta}(t), \qquad \text{or} \qquad q(0,t) = \hat{q}(t), \qquad \forall t > 0, \tag{4.3}$$

$$\theta(x,t) = \theta_0, \qquad \forall x \geq 0, \quad \forall t \leq 0. \tag{4.4}$$

In Eq. (4.1) it is understood that the quantities κ_1 and κ_2 are evaluated at $\theta = \theta_0$. After differentiating (4.1) with respect to time and taking into account (4.4), we get

$$\partial_t q(x,t) = \gamma K[\partial_x\theta(x,\cdot)](t), \tag{4.5}$$

where the linear integral operator K is defined as

$$(4.6)\qquad (Kf)(t) = -f(t) + \frac{1}{\gamma}\int_0^t \left(\frac{\kappa_1}{\tau_1}\exp(-s/\tau_1) + \frac{\kappa_2}{\tau_2}\exp(-s/\tau_2)\right) f(t-s)\,ds,$$

for any bounded $f(t)$, $(t \in \mathbb{R}^+)$. By the use of the Laplace transforms it is easy to show that K admits the following inverse

$$(4.7)\qquad (K^{-1}f)(t) = -f(t) - \frac{\gamma}{\kappa}\int_0^t \left[1 + \frac{\kappa_1\kappa_2}{\gamma^2}\left(\frac{1}{\tau_2} - \frac{1}{\tau_1}\right)^2 \exp\left(-\frac{\kappa}{\tau_1\tau_2\gamma}s\right)\right] f(t-s)\,ds.$$

Then, Eqs. (4.5) and (4.2) can be rewritten as

$$(4.8)\qquad \partial_x \begin{pmatrix} \theta \\ q \end{pmatrix} = \begin{pmatrix} 0 & \gamma^{-1}K^{-1} \\ -\rho\theta_0\chi & 0 \end{pmatrix} \partial_t \begin{pmatrix} \theta \\ q \end{pmatrix}.$$

Equation (4.8) is analogous to the system (2.2) of WALL and OLSSON [6], where a Maxwell-Cattaneo equation is analyzed. Adopting a wave splitting technique, we parallel the analysis of [6] in the homogeneous case. Accordingly, we introduce the quantity $(\theta^+, \theta^-)^T$ in the following way:

$$(4.9)\qquad \begin{pmatrix} \theta^+ \\ \theta^- \end{pmatrix} = \mathbf{D}^{-1} \begin{pmatrix} \theta - \theta_0 \\ q \end{pmatrix},$$

where

$$(4.10)\qquad \mathbf{D} = \begin{pmatrix} 1 & 1 \\ -\gamma P & \gamma P \end{pmatrix},$$

and we look for the linear operator P which diagonalizes the matrix in the right-hand side of (4.8). Substituting (4.9) and (4.10) into (4.8) we obtain

$$(4.11)\qquad \partial_x \begin{pmatrix} \theta^+ \\ \theta^- \end{pmatrix} = \frac{1}{2} \begin{pmatrix} \frac{1}{v^2}P^{-1} - K^{-1}P & \frac{1}{v^2}P^{-1} + K^{-1}P \\ -\frac{1}{v^2}P^{-1} - K^{-1}P & -\frac{1}{v^2}P^{-1} + K^{-1}P \end{pmatrix} \partial_t \begin{pmatrix} \theta^+ \\ \theta^- \end{pmatrix},$$

where the definition (3.5) has been used. Imposing the diagonalization condition we have

$$(4.12)\qquad \frac{1}{v^2}(P^{-1}f)(t) = -[(K^{-1}P)f](t),$$

for any bounded $f(t)$, $t \in \mathbb{R}^+$. In view of Eq. (4.7) and making use of the Laplace transforms, Eq. (4.12) yields

$$(4.13) \qquad (P^{-1}f)(t) = \pm v f(t) \pm v \int_0^t \left[F_1(\tau) + F_2(\tau) \int_0^\tau F_1(\xi) F_2(\tau - \xi)\, d\xi \right] f(t-\tau)\, d\tau,$$

where

$$F_1(t) = \frac{1}{2\tau_1} \exp\left(-\frac{t}{2\tau_1}\right) \left[I_0\left(\frac{t}{2\tau_1}\right) + I_1\left(\frac{t}{2\tau_1}\right) \right],$$

$$(4.14) \qquad F_2(t) = \frac{1}{2\tau_2}\left(1 - \frac{\kappa}{\tau_1\gamma}\right) \exp\left[-\frac{t}{2\tau_2}\left(1 + \frac{\kappa}{\tau_1\gamma}\right)\right] \times \left\{ I_0\left[\frac{t}{2\tau_2}\left(1 - \frac{\kappa}{\tau_1\gamma}\right)\right] + I_1\left[\frac{t}{2\tau_2}\left(1 - \frac{\kappa}{\tau_1\gamma}\right)\right] \right\},$$

and where I_0 and I_1 are modified Bessel functions. The sign in (4.13) can be chosen according to the meaning of θ^+ and θ^- as forward and backward propagating modes. Then, Eq. (4.11) reduces to

$$(4.15) \qquad \partial_x \begin{pmatrix} \theta^+ \\ \theta^- \end{pmatrix} = \frac{1}{v} \begin{pmatrix} -1 - F_1 * - F_2 * - F_1 * F_2 * & 0 \\ 0 & 1 + F_1 * + F_2 * + F_1 * F_2 * \end{pmatrix} \partial_t \begin{pmatrix} \theta^+ \\ \theta^- \end{pmatrix},$$

where the asterisk denotes time convolution, i.e.,

$$[a(\cdot) * b(\cdot)](t) = \int_0^t a(\tau) b(t-\tau)\, d\tau.$$

Since forward and backward modes propagate independently in opposite directions, for definiteness let us consider only one mode, say θ^+. We can write

$$(4.16) \qquad \partial_x \theta^+(x,t) = -\frac{1}{v} \{ [\delta(\cdot) + F_1(\cdot) + F_2(\cdot) + F_1 * F_2(\cdot)] * \partial_{(\cdot)} \theta^+(x,\cdot) \}(t).$$

Equation (4.16) can be transformed into an integro-differential equation for a wave propagator $\mathcal{P}^+(x,t)$, defined as

$$\theta^+(x,t) = [\mathcal{P}^+(x,\cdot) * \theta^+(0,\cdot)](t).$$

Substituting into (4.16) we obtain

$$\partial_x[\mathcal{P}^+(x,\cdot) * \theta^+(0,\cdot)(t)] = -\frac{1}{v}\partial_t[(1 + F_1 + F_2 + F_1 * F_2) * \mathcal{P}^+(x,\cdot) * \theta^+(0,\cdot)(t)]. \tag{4.17}$$

In deriving Eq. (4.17) we have exploited the result $\theta^+(x,0) = 0, \forall x \geq 0$, which follows from (4.4), (4.9) and (4.13). The application of Laplace transforms to Eq. (4.17) allows us to obtain

$$\mathcal{L}\mathcal{P}^+(x,s) = \exp\left[-\frac{x}{v}s(1 + \mathcal{L}F_1(s) + \mathcal{L}F_2(s) + \mathcal{L}F_1(s)\mathcal{L}F_2(s))\right], \tag{4.18}$$

where we have taken into account the condition $\mathcal{P}^+(0,t) = \delta(t)$. Making use of (4.14) we get

$$\mathcal{L}\mathcal{P}^+(x,s) = \exp\left[-\frac{x}{v}\sqrt{\frac{s(s+1/\tau_1)(s+1/\tau_2)}{s + \dfrac{\kappa}{\tau_1\tau_2\gamma}}}\right]. \tag{4.19}$$

We note that in a phenomenological model with a single relaxation time, the Laplace transform in Eq. (4.19) can be easily inverted to give the wave propagator for a Cattaneo type heat equation (see [6]). This can be performed by letting $\tau_2 \to \infty$ in (4.19). We obtain

$$\mathcal{P}_1^+(x,t) = \exp(-t/(2\tau_1)) \left\{\delta\left(t - \frac{x}{v}\right) + \mathcal{H}\left(t - \frac{x}{v}\right)\frac{x}{2\tau_1 v}\frac{I_1\left[\dfrac{1}{2\tau_1}\sqrt{t^2 - (x/v)^2}\right]}{\sqrt{t^2 - (x/v)^2}}\right\}, \tag{4.20}$$

where $\mathcal{H}(t)$ is the Heaviside unit step function. An analytical inversion of the Laplace transform in (4.19) will be accomplished under suitable approximations in the last section. To this end we give here an alternative form of the previous result. Without loss of generality we can choose $\tau_1 > \tau_2$, such that, owing to (2.12) and (2.13), the quantity

$$\sqrt{\frac{s+1/\tau_2}{s + \dfrac{\kappa}{\tau_1\tau_2\gamma}}} = \left[1 - \frac{1}{\tau_2}\frac{1 - \dfrac{\kappa}{\tau_1\gamma}}{s + 1/\tau_2}\right]^{-1/2}$$

can be expanded into a binomial series. We obtain

$$\mathcal{LP}^+(x,s) = \exp\left\{-\frac{x}{v}\sqrt{s(s+1/\tau_1)}\sum_{k=0}^{\infty}\frac{(2k-1)!!}{(2k)!!}\left[\frac{1}{\tau_2}\frac{1-\dfrac{\kappa}{\tau_1\gamma}}{s+1/\tau_2}\right]^k\right\}. \tag{4.21}$$

5. Reflectivity of heat waves

Let us consider two half-spaces $V_a = \{\mathbf{x}\in\mathbb{R}^3|\ x\le 0\}$ and $V_b = \{\mathbf{x}\in\mathbb{R}^3|\ x > 0\}$ occupied respectively by two different homogeneous rigid heat conductors, modelled as in Sec. 2. They are taken to be in a thermodynamic equilibrium state at the temperature θ_0. The constitutive parameters $\rho, \kappa_1, \kappa_2, \tau_1, \tau_2$ are supposed to be constant in V_a and V_b and discontinuous at the common plane boundary $\mathcal{S}, (x=0)$ of the two conductors. In the following we shall use the suffixes a and b to denote quantities pertaining respectively to V_a and V_b. The continuity of θ and q at the surface $\mathcal{S}$ implies

$$\begin{pmatrix}\theta\\ q\end{pmatrix}(0^+,t) = \begin{pmatrix}\theta\\ q\end{pmatrix}(0^-,t), \qquad \forall\, t\in\mathbb{R}^+, \tag{5.1}$$

where 0^+ and 0^- refer respectively to the limiting values from the right and from the left of $x=0$. Since θ_0 is the common temperature of both conductors, from (4.9) we have

$$\left[\mathbf{D}_b\begin{pmatrix}\theta^+\\ \theta_-\end{pmatrix}\right](0^+,t) = \left[\mathbf{D}_a\begin{pmatrix}\theta^+\\ \theta^-\end{pmatrix}\right](0^-,t), \qquad \forall\, t\in\mathbb{R}^+, \tag{5.2}$$

where

$$\mathbf{D}_b = \begin{pmatrix}1 & 1\\ -\gamma_b P_b & \gamma_b P_b\end{pmatrix}, \qquad \mathbf{D}_a = \begin{pmatrix}1 & 1\\ -\gamma_a P_a & \gamma_a P_a\end{pmatrix}.$$

Multiplicating Eq. (5.2) from the left by $\mathbf{D}_b^{-1}$ we arrive at

$$\begin{pmatrix}\theta^+\\ \\ \theta^-\end{pmatrix}(0^+,t) \tag{5.3}$$

$$= \frac{1}{2}\begin{pmatrix}1+\dfrac{\gamma_a}{\gamma_b}P_b^{-1}*P_a & 1-\dfrac{\gamma_a}{\gamma_b}P_b^{-1}*P_a\\ 1-\dfrac{\gamma_a}{\gamma_b}P_b^{-1}*P_a & 1+\dfrac{\gamma_a}{\gamma_b}P_b^{-1}*P_a\end{pmatrix}\begin{pmatrix}\theta^+\\ \\ \theta^-\end{pmatrix}(0^-,t).$$

Now we introduce a reflectivity function $R(t)$ by the following definition,

$$\theta^-(0^-,t) = [R(\cdot) * \theta^+(0^-,\cdot)](t),$$

and substitute into (5.3) to obtain

$$\theta^+(0^+,t) = \frac{1}{2}[\delta(\cdot) + \frac{\gamma_a}{\gamma_b}P_b^{-1} * P_a(\cdot) + R(\cdot) - \frac{\gamma_a}{\gamma_b}P_b^{-1} * P_a * R(\cdot)] * \theta^+(0^-,t),$$

(5.4)

$$\theta^-(0^+,t) = \frac{1}{2}[\delta(\cdot) - \frac{\gamma_a}{\gamma_b}P_b^{-1} * P_a(\cdot) + R(\cdot) + \frac{\gamma_a}{\gamma_b}P_b^{-1} * P_a * R(\cdot)] * \theta^+(0^-,t).$$

Owing to the causality principle we pose $\theta^-(0^+,t) = 0, \forall\, t \in \mathbb{R}^+$. Then, in view of the arbitrariness of $\theta^+(0^-,t)$, Eq. (5.4) yields

$$\delta(t) + R(t) - \frac{\gamma_a}{\gamma_b}P_b^{-1} * P_a(t) + \frac{\gamma_a}{\gamma_b}P_b^{-1} * P_a * R(t) = 0. \tag{5.5}$$

Applying the Laplace transforms to Eq. (5.5) and accounting for the expression of P derived in the previous section, we arrive at

$$\mathcal{L}R(s) = \frac{\sqrt{H(s)} - \sigma}{\sqrt{H(s)} + \sigma}, \tag{5.6}$$

where

$$H(s) = \frac{\left(s + \frac{1}{\tau_1^b}\right)\left(s + \frac{1}{\tau_2^b}\right)\left(s + \frac{\kappa^a}{\tau_1^a\tau_2^a\gamma_a}\right)}{\left(s + \frac{1}{\tau_1^a}\right)\left(s + \frac{1}{\tau_2^a}\right)\left(s + \frac{\kappa^b}{\tau_1^b\tau_2^b\gamma_b}\right)}, \tag{5.7}$$

and $\sigma = \sqrt{\rho_b\chi_b\gamma_b}/\sqrt{\rho_a\chi_a\gamma_a}$. An inversion of the Laplace transform in Eq. (5.6) can be performed by writing

$$H(s) = 1 + \frac{A_1}{s + s_1} + \frac{A_2}{s + s_2} + \frac{A_3}{s + s_3},$$

where $s_1 = 1/\tau_1^a$, $s_2 = 1/\tau_2^a$, $s_3 = \kappa_b/(\tau_1^b\tau_2^b\gamma_b)$, and

$$A_i = \left\{ -s_i^3 + \left(\frac{1}{\tau_1^b} + \frac{1}{\tau_2^b} + \frac{\kappa^a}{\tau_1^a \tau_2^a \gamma_a} \right) s_i^2 \right.$$
$$- \left(\frac{1}{\tau_1^b \tau_2^b} + \frac{\kappa^a}{\tau_1^a \tau_2^a \tau_1^b \gamma_a} + \frac{\kappa^a}{\tau_1^a \tau_2^a \tau_2^b \gamma_a} \right) s_i$$
$$\left. + \frac{\kappa^a}{\tau_1^a \tau_2^a \tau_1^b \tau_2^b \gamma_a} \right\} [(s_{i+1} - s_i)(s_{i+2} - s_i)]^{-1}$$

for $i = 1, 2, 3$. The final result is

$$R(t) = \int_0^\infty N(\xi)[G_1(\xi, \cdot) * G_2(\xi, \cdot) * G_3(\xi, \cdot)](t)\, d\xi, \tag{5.8}$$

where

$$N(\xi) = \exp(-\xi) \left[2\sigma^2 \exp(\sigma^2 \xi) \operatorname{erfc}(\sigma \sqrt{\xi}) - \frac{2\sigma}{\sqrt{\pi \xi}} + 1 \right], \tag{5.9}$$

and

$$G_i(\xi, t) = \exp(-t s_i) \left[\delta(t) - \sqrt{\frac{A_i \xi}{t}} J_1(2\sqrt{A_i \xi t}) \right], \quad i = 1, 2, 3. \tag{5.10}$$

with J_1 Bessel function of order 1. In view of Eqs. (5.8) – (5.10) we can write

$$R(t) = \nu \sum_{i=1}^{3} \mathrm{e}^{-t s_i} \delta(t) + \widetilde{R}(t),$$

where

$$\nu = \int_0^\infty N(\xi)\, d\xi = \frac{1 - \sigma}{1 + \sigma}$$

is the (instantaneous) attenuation factor and where $\widetilde{R}(t)$ yields the part of the reflected field due to convolution. Both ν and $\widetilde{R}(t)$ are characterized by the relaxation times τ_1 and τ_2 and by the partial heat conductivities κ_1 and κ_2 in a and b. As shown in the next section, if the quantities pertaining to the conductor a are known, the reflection data can be used to gain informations about the characteristic parameters in b.

6. Application to the second sound and the inverse problem

The analysis of experimental results on heat pulses in dielectric crystals has shown that second sound propagates only if θ_0 falls into a narrow range of

absolute temperatures [12]. This property, called window condition, has been interpreted on the basis of phonons' model by saying that, in sufficiently pure crystals, second sound appears when the temperature is low enough to prevent resistive processes and high enough to allow for normal processes. Applying our phenomenological model to this problem we assume $1/\tau_1$ and $1/\tau_2$ to represent two characteristic frequencies accounting for resistive processes and normal processes. This hypothesis is justified by the identifications due to the comparison of the heat Eq. (3.4) with Eq. (3.10), obtained in phonon's model [10] (see the end of Sec. 3). Then the window condition holds when we have $1/\tau_1 \ll 1/\tau_2$. We exploit this condition to derive an explicit solution to the propagation and the reflection problems.

We firstly consider the wave propagator $\mathcal{P}^+(x,t)$ in the form (4.21). According to Eqs. (3.5) we can write

$$\mathcal{L}\mathcal{P}^+(x,s) = \exp\left[-\frac{x}{v}\sqrt{s(s+1/\tau_1)}\sum_{k=0}^{\infty}\frac{(2k-1)!!}{(2k)!!}\left(\frac{1-\dfrac{\kappa}{2\rho\theta_0\tau_1 v^2}}{1+s\tau_2}\right)^k\right]. \tag{6.1}$$

A first approximation of Eq. (6.1) can be worked out under the window conditon assuming $\tau_2 \ll \tau_1$. Retaining only the terms for $k=0$ and $k=1$ in the binomial series, we get

$$\mathcal{L}\mathcal{P}^+(x,s) = \exp\left[-\frac{x}{v}\sqrt{s(s+1/\tau_1)}\right]\exp\left[-\frac{x}{2v\tau_2}\frac{s}{s+1/\tau_2}\right]. \tag{6.2}$$

The Laplace transform in (6.2) can be easily inverted to give

$$\mathcal{P}^+(x,t) = \exp\left(-\frac{x}{2v\tau_2}\right)\left[\mathcal{P}_1^+(x,\cdot) * \mathcal{Q}(x,\cdot)(t)\right], \tag{6.3}$$

where $\mathcal{P}_1^+(x,t)$ is given by (4.20) and where

$$\mathcal{Q}(x,t) = \exp(-t/\tau_2)\delta(t) + \exp(-t/\tau_2)\frac{1}{\tau_2}\sqrt{\frac{x}{2vt}}I_1\left(\frac{1}{\tau_2}\sqrt{\frac{2x}{v}t}\right).$$

To point out the role of normal processes in determining the wave propagator we rewrite Eq. (6.3) in terms of the nondimensional quantities $a = x/v\tau_2$, $q = \tau_2/2\tau_1$, $\lambda = t/\tau_2$. We obtain

$$\mathcal{P}^+(a,\lambda) = \mathrm{e}^{a(1/2-q)-\lambda}\delta(\lambda-a) + \mathrm{e}^{a(1/2-q)-\lambda}\frac{1}{\tau_2}\sqrt{\frac{a}{2(\lambda-a)}}\, I_1\left(\sqrt{2a(\lambda-a)}\right) + aq\frac{1}{\tau_2}\mathrm{e}^{-\frac{a}{2}-\lambda q}\frac{I_1(q\sqrt{\lambda^2-a^2})}{\sqrt{\lambda^2-a^2}} + \mathrm{e}^{-\frac{a}{2}-\lambda}\int_a^\lambda \mathrm{e}^{\xi(q-1)}\frac{1}{\tau_2^2}\frac{\sqrt{\frac{a}{2(\lambda-\xi)}}}{\sqrt{\xi^2-a^2}} I_1\left[q\sqrt{\xi^2-a^2}\right]\, I_1\left[\sqrt{2a(\lambda-\xi)}\right]\, d\xi. \tag{6.4}$$

The first term at the right-hand side of (6.4) is the hyperbolic part of the propagator which leaves the boundary pulse undistorted but attenuated in amplitude, owing to the few resistive processes. The second term takes into account the effect of normal processes. It is the leading term and it rapidly decreases with λ. The third term is a slow decreasing function of λ, essentially due to the resistive processes. The fourth term is a mixed, quantitatively minor contribution. The effect of such propagator on a half-gaussian pulse at $x = 0$, $\theta^+(0,t) = \mathrm{e}^{-bt^2}$, $(t > 0)$, is shown in Fig. 1 for different values of τ_2. It is evident how a second sound pulse arises if τ_2 is notably smaller than τ_1. Figure 1 is in agreement with the experimental evidence of second sound in low-temperature very pure crystals (see [3]), and with the numerical results according to the 9-fields theory by [10] where a second sound pulse develops for small values of the relaxation time associated with normal processes.

Now we consider the problem of the reflectivity at the interface $\mathcal{S}$ between the half-spaces V_a and V_b occupied by two different rigid conductors. On the basis of the results obtained in Sec. 5 we suppose that the medium in V_a is a highly pure crystal which complies with the window condition at the temperature θ_0. This assumption implies that the function $H(s)$, given in (5.7), can be approximated to

$$H(s) = h\left[1 + \frac{1}{\tau s} - \frac{1}{\tau}\frac{\left(1-\frac{\tau}{\tau_1}\right)\left(1-\frac{\tau}{\tau_2}\right)}{s+\frac{\tau}{\tau_1\tau_2}}\right], \tag{6.5}$$

where τ_1 and τ_2 are the relaxation times pertinent to the conductor placed in V_b, and

$$h = \frac{\kappa^a}{\tau_1^a\gamma_a}, \qquad \tau = \frac{\kappa^b}{\gamma_b}.$$

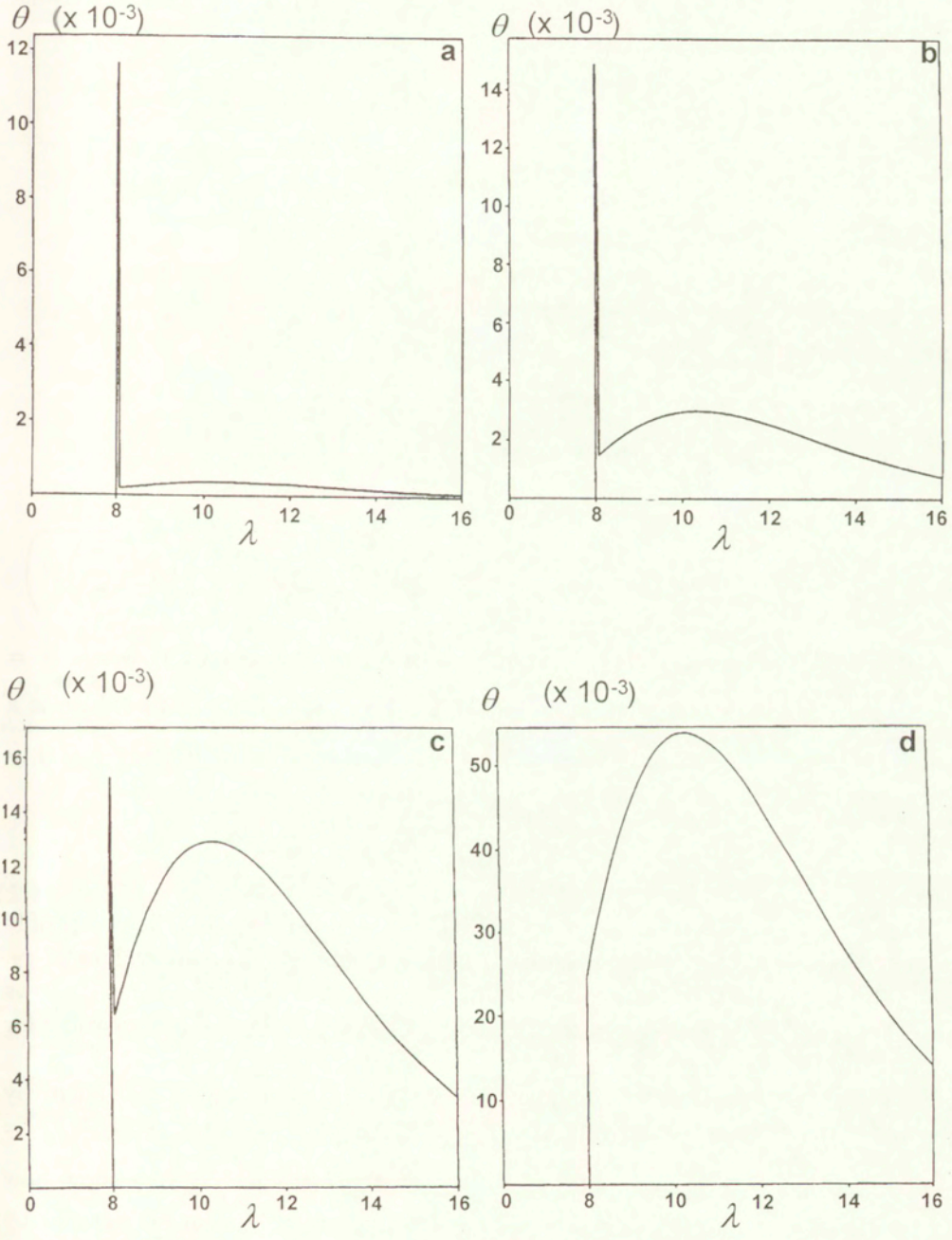

FIG. 1. Temperature at $x = av\tau_2$ as function of $\lambda = t/\tau_2$ for an half-Gaussian pulse $\theta^+(0,t) = \mathrm{e}^{-bt^2}$, $t > 0$, for $a = 8, b = 10^6 s^{-2}$, $\tau_1 = 5$ s, and (a)$\tau_2 = 0.5$s, (b)$\tau_2 = 0.2$s, (c)$\tau_2 = 0.1$s, (d)$\tau_2 = 0.05$ s.

Substitution of Eq. (6.5) into (5.6) and application of the inverse Laplace transform yields

$$R(t) = \nu \exp\left(-\frac{\tau}{\tau_1\tau_2}t\right)\delta(t) + \widetilde{R}(t) \tag{6.6}$$

where

$$\widetilde{R}(t) = \int_0^\infty [-L_1(\xi,t) - L_2(\xi,t) + L_1(\xi,\cdot) * L_2(\xi,\cdot)(t)]\, N(\xi)\, d\xi, \tag{6.7}$$

with

$$\begin{aligned} L_1(\xi,t) &= \sqrt{\frac{\xi}{\tau t}} J_1\left(2\sqrt{\frac{\xi t}{\tau}}\right), \\ L_2(\xi,t) &= \exp(-\frac{\tau}{\tau_1\tau_2}t)\sqrt{\frac{1}{\tau}\left(1-\frac{\tau}{\tau_1}\right)\left(1-\frac{\tau}{\tau_2}\right)\frac{\xi}{t}} \\ &\qquad J_1\left(2\sqrt{\frac{1}{\tau}\left(1-\frac{\tau}{\tau_1}\right)\left(1-\frac{\tau}{\tau_2}\right)\xi t}\right). \end{aligned} \tag{6.8}$$

In (6.6) and (6.7) ν and $N(\xi)$ are given by Eqs. (5.11) and (5.9) where $\sigma = \sqrt{h\frac{\rho_b\chi_b\gamma_b}{\rho_a\chi_a\gamma_a}}$ (hereafter we shall assume $\sigma \leq 1$). From the result (6.6), which is a special case of that obtained in Sec. 5, we obtain the reflected field at $x = 0$ in the form

$$\theta^-(0^-,t) = \nu\theta^+(0^-,t) + \int_0^t \widetilde{R}(s)\theta^+(0^-,t-s)\, ds. \tag{6.9}$$

In Fig. 2 we have shown an incoming half-Gaussian pulse and its reflected profile at $x = 0$, given by Eq. (6.9) when $\sigma = 0, (\nu = 1)$ for two different values of τ_2. The reflected pulse turns out to be notably sharpened by reflection and it shows a negative tail ($\theta < \theta_0$) at $x = 0$. The effect of sharpening is more relevant for smaller values of τ_2.

Now we assume that a boundary pulse $\theta^+(0^-,t)$ be given at $\mathcal{S}$. Then, by the reflection data, we can estimate the quantities $\theta_0^- := \theta^-(0^-,0)$, $(\theta^-)_0' := \frac{d}{dt}\theta^-(0^-,0)|_{t=0}$, $(\theta^-)_0'' := \frac{d^2}{dt^2}\theta^-(0^-,0)|_{t=0}$ at the interface $\mathcal{S}$. We show how the parameter σ and the relaxation times τ_1 and τ_2 in V_b can be derived by $\theta_0^-, (\theta^-)_0', (\theta^-)_0''$. To this end we observe that by successive differentiation of (6.9) with respect to t and evaluating the results at $t = 0$, we obtain

$$\nu = \frac{\theta_0^-}{\theta_0^+}, \tag{6.10}$$

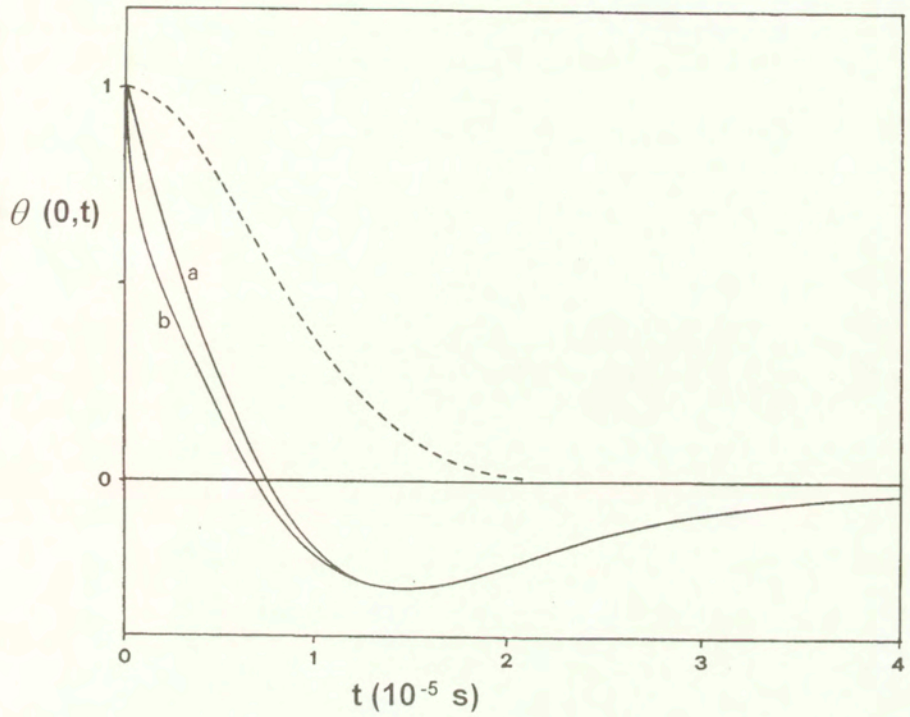

FIG. 2. Incident (dashed) and reflected (solid) temperature pulses for $\sigma = 0$ ($\nu = 1$). A half-Gaussian profile $\theta^+(0,t) = \mathrm{e}^{-bt^2}$ is assumed with $b = 10^{10}\mathrm{s}^{-2}, \tau = 10^{-5}\mathrm{s}, \tau_1 = 5 \cdot 10^{-6}\mathrm{s}$ and (a)$\tau_2 = 5 \cdot 10^{-6}\mathrm{s}$, (b)$\tau_2 = 10^{-6}$ s.

$$\widetilde{R}(0) = \frac{1}{(\theta_0^+)^2}[\theta_0^+(\theta^-)_0' - \theta_0^-(\theta^+)_0'],$$

(6.11)

$$\widetilde{R}'(0) = \frac{1}{(\theta_0^+)^3}\{\theta_0^+[\theta_0^+(\theta^-)_0'' - \theta_0^-(\theta^+)_0''] + (\theta^+)_0'[\theta_0^-(\theta^+)_0' - \theta_0^+(\theta^-)_0']\}.$$

From Eqs. (6.10) and (5.11) we obtain the value of the parameter σ. Concerning the quantities $\widetilde{R}(0), \widetilde{R}'(0)$, they can be written in terms of the relaxation times τ_1 and τ_2. In fact, evaluating L_1, L_2 and their derivatives for $t = 0$, by Eqs. (6.8) we have

$$L_1(\xi,0) = \frac{\xi}{\tau}, \qquad L_2(\xi,0) = \frac{1}{\tau}\left(1 - \frac{\tau}{\tau_1}\right)\left(1 - \frac{\tau}{\tau_2}\right)\xi,$$

(6.12)

$$L_1'(\xi,0) = -\frac{\xi^2}{2\tau^2}, \qquad L_2'(\xi,0) = -\left(1 - \frac{\tau}{\tau_1}\right)\left(1 - \frac{\tau}{\tau_2}\right)\left[\frac{\xi}{\tau_1\tau_2} + \frac{\xi^2}{2\tau^2}\left(1 - \frac{\tau}{\tau_1}\right)\left(1 - \frac{\tau}{\tau_2}\right)\right].$$

Substitution of (6.12) into (6.7) yields

$$\widetilde{R}(0) = -\frac{2\nu_1}{\tau} + \nu_1\left(\frac{1}{\tau_1} + \frac{1}{\tau_2} - \frac{\tau}{\tau_1\tau_2}\right),$$

$$\widetilde{R}'(0) = -\frac{\nu_1}{\tau_1\tau_2}\left[1 - \tau\left(\frac{1}{\tau_1} + \frac{1}{\tau_2} - \frac{\tau}{\tau_1\tau_2}\right)\right] - \frac{\nu_2}{2}\left(\frac{1}{\tau_1} + \frac{1}{\tau_2} - \frac{\tau}{\tau_1\tau_2}\right)^2, \tag{6.13}$$

where

$$\nu_1 = \int_0^\infty N(\xi)\xi\,\mathrm{d}\xi = \frac{\sigma^2 + \sigma + 1}{(\sigma+1)^2},$$

$$\nu_2 = \int_0^\infty N(\xi)\xi^2\,\mathrm{d}\xi = \frac{4\sigma^3 + 11\sigma^2 + 9\sigma + 4}{2(\sigma+1)^3}.$$

Solving the system (6.13) for τ_1 and τ_2 we explicitly obtain

$$\frac{1}{\tau_1} = a - \sqrt{a^2 - 4b}, \qquad \frac{1}{\tau_2} = a + \sqrt{a^2 - 4b}, \tag{6.14}$$

with

$$a = \frac{\tau}{\nu_1 + \widetilde{R}(0)\tau}\left[\widetilde{R}'(0) + \frac{\nu_2}{2}\left(\frac{\widetilde{R}(0)}{\nu_1} + \frac{2}{\tau}\right)^2\right] + \frac{2}{\tau} + \frac{\widetilde{R}(0)}{\nu_1},$$

$$b = \frac{1}{\nu_1 + \widetilde{R}(0)\tau}\left[\widetilde{R}'(0) + \frac{\nu_2}{2}\left(\frac{\widetilde{R}(0)}{\nu_1} + \frac{2}{\tau}\right)^2\right]. \tag{6.15}$$

Owing to (6.14), (6.15) and (6.11), the relaxation times turn out to be uniquely determined by the reflection data.

7. Conclusion

In the first part of this paper we have shown that, within the linear theory of heat conduction, a phenomenological model accounting for two relaxation times yields a hyperbolic heat equation which can be effective in describing the observed phenomena on the propagation of heat pulses. In the second part of the paper we have applied the wave splitting analysis to our phenomenological model. The solution of the propagation problem has been written in terms of the

Laplace transform of a propagator kernel. An inverse transform is explicitly obtained in the case of a low temperature conductor under the "window condition" which allows for second sound propagation. The hyperbolicity of the governing system leads to the natural question on the reflectivity of heat pulses. Beside its intrinsic intersest, we have considered the solution to this problem as a means to determine the characteristic relaxation times of a given rigid conductor when the reflection data on its boundary are available. In particular we have assumed that the incoming wave propagates in a highly pure crystal and impinges on the boundary of a unknown conducting specimen. However, the same procedure can be performed for any case in which the relaxation times of one of the two conductors are known.

Acknowledgments

The research leading to this work was performed under the auspicies of G.N.F.M.

References

1. D.D. JOSEPH and L. PREZIOSI, *Heat waves*, Rev. Modern Physics, **61**, 41–73, 1989.
2. D.D. JOSEPH and L. PREZIOSI, *Addendum to the paper "Heat waves"*, Rev. Modern Physics, **62**, 375–391, 1990.
3. H.E. JACKSON, C.T. WALKER and T.F. MCNELLY, *Second sound in NaF*, Phys. Rev. Lett., **25**, 26, 1970.
4. H.E. JACKSON and C.T. WALKER, *Thermal conductivity, second sound and phonon-phonon interactions in NaF*, Phys. Rev., **B 3**, 1428, 1971.
5. K. MITRA, S. KUMAR, A. VEDAVARZ and M.K. MOALLEMI, *Experimental evidence of hyperbolic heat conduction in processed meat*, J. Heat Transfer, **117**, 568–573, 1995.
6. D.J.N. WALL and P.Olsson, *Invariant imbedding and hyperbolic heat waves*, J. Math. Phys., **38**, 1723–1749, 1997.
7. M.E. GURTIN and A.C. PIPKIN, *A general theory of the heat conduction with finite wave speeds*, Arch. Ration. Mech. Anal., **31**, 113–126, 1968.
8. A. MORRO, *Temperature waves in rigid materials with memory*, Meccanica, **12**, 73–77, 1977.
9. B.D. COLEMAN, M. FABRIZIO and D.R. OWEN, *On the thermodynamics of second sound in dielectric crystals*, Arch. Ration. Mech. Anal., **80**, 135–158, 1982.
10. W. DREYER and H. STRUCHTRUP, *Heat pulse experiments revisited*, Cont. Mech. and Thermodyn., **5**, 3–50, 1993.
11. J. CALLAWAY, *Model for lattice thermal conductivity at low temperatures*, Phys. Rev., **113**, 1046, 1959.
12. C.C. ACKERMANN and R.A. GUYER, *Temperature pulses in dielectric solids*, Ann. Phys., **50**, 128, 1968.

Received April 20, 1998; new version January 4, 1999.

Arch. Mech., **52**, 1, pp. 25–53, Warszawa 2000

Laminar dispersed two-phase flows at low concentration – I. Generalised system of equations

J. L. ACHARD and A. CARTELLIER

Laboratoire des Écoulements Géophysiques et Industriels
CNRS-UJF-INPG, B.P. 53X, 38041 Grenoble Cedex, France
e-mail: Jean-Luc.Achard@hmg.inpg.fr

TO REPRESENT MULTIDIMENSIONAL FLOWS of particle-fluid mixtures, Eulerian two-fluid models are currently used nowadays. Even if there are no pure turbulence effects in the carrier phase flow, many closure laws are required in order to supplement the conservation equations. To furnish a systematic method for deriving such closure laws that are valid at least for spherical solid inclusions, a generalised system of equations is proposed in this first paper (hereafter referred to as part I) of a sequence. It is based on the coupling of two sets of equations, one for each phase: the continuous phase is represented by an extension of a hierarchy of equations proposed by Lundgren for treating flows in porous media, and the dispersed phase by an adaptation of the well- known B.B.G.K.Y. hierarchy. The first-order equations of both hierarchies correspond to the conservation equations of standard two-fluid models; they contain the usual unknown terms. In our approach these terms appear to be provided by the second-order equations. Unfortunately, as is usual in other similar statistical theories, the second-order equations contain extra uknown terms which figure in the third-order equations and so on. Formulating closure equations is replaced by the broader problem of truncating the generalised system of equations via a perturbation method based on diluteness.

1. Introduction

IN ORDER TO OBTAIN multidimensional equations which relate the macroscopic phase properties of two-phase flows, several averaging processes have been proposed by (among others) DELHAYE and ACHARD [6]. They consist in applying time or space-averaging operators to a given system composed of local instant field equations that are valid each phase, supplemented by jump conditions at the interface. As it has been pointed out (HINCH [9]), ensemble-averaging operators applied over a set of "macroscopically equivalent" realisations have to be introduced in preference to other averaging processes. However, all these processes lead to formally identical mass, momentum and energy conservation equations. These provide a rational basis for many models used in engineering and especially for the most sophisticated ones, i.e., two-fluid and multidimensional models, which are starting to be used widely for numerical simulation purposes.

A consistent model for any two-phase flow phenomenon must therefore be based upon the above equations; furthermore it must include appropriate closure laws (improperly referred to as constitutive equations, or rheological relationships). In fact, these laws constitute the essential part of a given model since they express, inter alia, how the fluids are coupled. There is still a lack of knowledge about these closure laws, the derivation of which generally appears in a separate second step, as intuitive grafts upon well-established conservation equations. Progress may be made by settling for something less than complete generality. Indeed, even if we restrict our interest, as in this paper, to dispersed two-phase flows (i) carrying spherical inclusions (ii) which are small compared to the length scale of the averaged fields, (iii) are composed of incompressible and Newtonian fluids, (iv) where no heat transfer and no phase change occur, (v) under negligible interparticle collision conditions (vi) which remain "laminar" at all times, with possibly significant inertia effects, averaged equations nevertheless require many laws, the rational derivation and indeed the validity of which are not guaranteed.

The most promising way to improve our ability to model dispersed two-phase flows lies in an approach which mixes kinetic theory concepts and classical continuum mechanics. VAN and WIJNGAARDEN [16] was one of the first authors to introduce an equation for the bubble number density in order to handle variations in their radius. Many of these studies proceed intuitively rather than rigorously (ACHARD [1]), even if the modelling of pure turbulence effects is left aside. Fortunately, exceptions exist (BIESHEUVEL VAN and WIJNGAARDEN [2]) and among these, two series of careful studies attempt to be as systematic as possible as we shall. They where proposed by ZHANG and PROSPERETTI [17, 19] and by KOCH and his collaborators (KUMARAN and KOCH [13]; KOCH [12]). In order to represent the dispersed phases, both authors start from a sort of Liouville equation (named N-particle Smoluchowski equation by the latter and equation for the number of realisations by the former). The continuous phase is governed by creeping flow equations for the latter and by potential flow equations for the former. Due to their general formalism, several new results were obtained in their specific applications.

In the forthcoming sequence of papers, a new method pertaining to this school of thought is presented in detail; emphasis will be put on methodology. In the first place, our work will concentrate on extending and then connecting in a consistent way two hierarchies of equations existing in the literature: the well-known B.B.G.K.Y. hierarchy for the dispersed phase (GRAD [8]) and the Lundgren hierarchy for the continuous phase (LUNDGREN [15]), which was introduced initially to treat flows in porous media. Its essential feature is to produce, as a rule, all the standard conservation equations and most of the required constitutive equations at the same time, and in an unified manner.

The rest of the paper is organised as follows. The class of two-phase flows to which our theory applies will be defined in Sec. 2. In Sec. 3, we present the basic statistical tools and the main averaged variables which will be used. Most of them are conditional upon the presence of several inclusions and require specific equations which are given precisely by the revisited B.B.G.K.Y. and Lundgren hierarchies. Complete derivation of these hierarchies is a long and difficult process which will be discussed in the following two Secs. 4 and 5. The main limitations of our theory are recalled in Sec. 6 while further developments are briefly outlined.

2. Deterministic equations

2.1. Inclusion equations

The first step here is to see how far the usual starting particle equations in Statistical Mechanics (S.M.) differ from the starting inclusion equations in our method. To begin with, there is a striking difference: both phases will be modelled by equations provided by Continuum Mechanics and any molecular effects will be neglected. With regard to the continuous phase, the usual field equations are inevitably used. These consist of conservation equations (mass, linear and angular momentum and energy) supplemented by constitutive and state laws appropriate to the continuous phase material. All these equations obviously have no counterpart in S.M. With regard to the dispersed phase, we have to adopt a lumped formulation for the thermomechanical fields inside a typical inclusion. Such a lumped model is essential in order to deal with a finite number of overall particle characteristics whose values at time t correspond to n generalised coordinates (g.c.), written for short, $\mathbf{z} = [z^1, z^2, ..., z^n]$. Among these, we may distinguish an external part giving the location of an inclusion centre $\mathbf{x}$ and its unit orientation vectors, from an internal part ξ giving its intrinsic condition and specifying for instance its linear and angular velocities, its size, its temperature or even certain spherical modes in the case of deformable inclusions. To obtain such a formulation, if it exists, it is necessary to make certain approximations that exploit the physical peculiarities of the micro problem under consideration, and among others the smallness of the inclusion.

Turning now to the simplified case treated in this paper, where the inclusions are identical, spherical, rigid, with a radius a: they may represent solid particles, highly viscous droplets or small bubbles with surfactants; the equations of rigid body motion will be applied. Collisions will also be excluded. For both phases gravity may act and affect the motion of the mixture. The physical 3-D domain occupied by the mixture is denoted by $\mathcal{V}_x^c$. The boundaries $\partial\mathcal{V}^c$ of $\mathcal{V}_x^c$ may consist of rigid walls $\partial\mathcal{V}_w^c$ as well as fluid surfaces $\partial\mathcal{V}_f^c$ through which inclusions

(and carrying fluid) are injected or removed at a prescribed rate. Note that the physical 3-D domain allowed for inclusions is not $\mathcal{V}_x^c$ but more precisely, $\mathcal{V}_x^d$, the reduced domain which is obtained by excluding all positions $\mathbf{x}$ such that $|\mathbf{x} - \mathbf{x}_{\partial\mathcal{V}_w^c}| < a$ from $\mathcal{V}_x^c$ (*impermeability* of solid walls). Its boundaries are denoted $\partial\mathcal{V}^d$.

Supposing provisionally distinguishable inclusions, let $\mathbf{z}_j = (\mathbf{x}_j, \mathbf{u}_j, \boldsymbol{\omega}_j)(j = 1, 2, ..., N)$ the motion of the jth inclusion in its generalized own space $\mu_{z_j}(n = 9)$ where $\mathbf{x}_j$ or $x_j^i(i = 1, 2, 3)$ denotes its position, $\mathbf{u}_j$ or u_j^i its translational velocity and $\boldsymbol{\omega}_j$ or ω_j^i its angular velocity. The density ρ^d within each inclusion is homogeneous so that the mass of the jth inclusion is $m = 4\pi\rho^d a^3/3$ and its moment of inertia is $I = 2ma^2/5$. Such a motion $\mathbf{z}_j(t)$ obeys the following equations:

$$\frac{d\mathbf{x}_j(t)}{dt} = \mathbf{u}_j(t), \tag{2.1}$$

$$m\frac{d\mathbf{u}_j(t)}{dt} = \mathbf{F}_j(t) + \mathbf{F}_j^e(t), \tag{2.2}$$

$$I\frac{d\boldsymbol{\omega}_j(t)}{dt} = \mathbf{K}_j(t), \tag{2.3}$$

where $\mathbf{F}_j$, $\mathbf{K}_j$ and $\mathbf{F}_j^e$ are, respectively, the force and torque exerted by the fluid on inclusion j, and the external force acting on this inclusion. No external couple acts on it. Here the boundary terms are:

$$\mathbf{F}_j = \int_{S(\mathbf{x}_j)} \mathbf{n}_j^d \cdot \mathbb{T}^c dS \quad \text{and} \quad \mathbf{K}_j = \int_{S(\mathbf{x}_j)} (\mathbf{x} - \mathbf{x}_j(t)) \wedge \mathbf{n}_j^d \cdot \mathbb{T}^c dS,$$

where $S(\mathbf{x}_j)$ is the surface of the inclusion centered at $\mathbf{x}_j(t)$ and $\mathbf{n}_j^d$ a unit normal to it, exterior to phase d. For the sake of simplicity the superscript d will usually be omitted and this unit vector will be defined as $\mathbf{n}_j = (\mathbf{x} - \mathbf{x}_j(t))/a$.

Now, consider the whole population of inclusions. Its state, at any time t, is specified by the location of one point, called a phase point, or a *configuration* of the system $Z_N(t) = [\mathbf{z}_1(t), \mathbf{z}_2(t), ..., \mathbf{z}_N(t)]$. The corresponding Euclidean space of $n\mathbf{N}$ dimensions is the phase space, denoted by Γ; it is equal to the Cartesian product of all μ_{z_i}. Of course the particle coordinates are arbitrary within each domain, except for the restrictions $|\mathbf{x}_i - \mathbf{x}_j| > 2a$ for any couple of (i, j) having distinct values (*non-overlapping* of nondeformable particles).

The continuous fluid is Newtonian and therefore the stress tensor $\mathbb{T}^c$ is defined by $\mathbb{T}^c = -p^c\mathbb{I} + 2\mu^c\mathbb{D}(\mathbf{v}^c)$, where $\mathbb{D}(\mathbf{v}^c)$, the rate of deformation tensor, is the

symmetric part of the velocity gradient $\mathbb{D}() = \left[\frac{\partial}{\partial \mathbf{x}}()\right]^s$. Of course $\mathbf{F}_j^e = m\mathbf{g}$ as the body force is just gravity. The fluid velocity field satisfies the classical equation

$$\mathbf{v}^c(\mathbf{x}, t) = \mathbf{v}_j^d(\mathbf{x}, t) \qquad \text{for} \quad |\mathbf{x} - \mathbf{x}_j(t)| = a \tag{2.4}$$

at the surface of the inclusions and $\mathbf{v}_j^d$ is the velocity field inside the jth inclusion. Each inclusion is subject to a rigid motion, thus:

$$\mathbf{v}_j^d(\mathbf{x}, t) = \mathbf{u}_j(t) + \boldsymbol{\omega}_j(t) \wedge [\mathbf{x} - \mathbf{x}_j(t)] \qquad \text{for} \quad |\mathbf{x} - \mathbf{x}_j(t)| \leq a. \tag{2.5}$$

It will be assumed that collisions between inclusions are unlikely to occur or are soft enough not to give rise to significant pressure impulses. Taking into account collisions would mean supplementing motion Eqs. (2.1), (2.2) and (2.3) with jump conditions relating translational and angular velocities before and after each interaction.

Several fine-grained functions can be defined describing the complete structure of the dispersed phase in $\mathcal{V}_x^d$. These are the dispersed phase indicator (or structural, or characteristic) function X^d equalling unity inside the inclusion and zero otherwise, and the velocity field of the dispersed phase. In the case under consideration, they are:

$$X^d(Z_N; \mathbf{x}) = \sum_{j=1}^{N} H(a - |\mathbf{x} - \mathbf{x}_j|) = 1 - X^c, \tag{2.6}$$

$$\begin{aligned} X^d(Z_N; \mathbf{x})\mathbf{v}^d(Z_N; \mathbf{x}) &= \sum_{j=1}^{N} H(a - |\mathbf{x} - \mathbf{x}_j|)\mathbf{v}_j^d(\mathbf{x}, t) \\ &= \sum_{j=1}^{N} H(a - |\mathbf{x} - \mathbf{x}_j|)(\mathbf{u}_j + \omega_j \wedge (\mathbf{x} - \mathbf{x}_j)), \end{aligned} \tag{2.7}$$

where H is the Heaviside step function defined as zero when its argument is negative and one otherwise.

2.2. Ambient fluid equations

Formulating local instant field equations in the sense of generalised functions (g.f.) before averaging them, offers several advantages which are well-known today in two-phase flows as well as in intermittent turbulent flows after the original LEWI thesis [14] and DOPAZO paper [7], respectively. First, time and space differential operators in the sense of g.f. commute with averaging operators;

second, applying averaging operators to equations in their ordinary sense requires a different set of calculations concerning the interfacial source terms, whereas equations in the sense of g.f. require a single step operation; finally, these source terms have a mathematical form which will help in finding the closure models. The first step in obtaining continuous phase equations in sense of g.f. is to make these equations valid throughout space-time $\mathbb{R}^3 \times \mathbb{R}$, i.e. even outside the mixture domain $\mathcal{V}_x^c$ and inside each inclusion where $|\mathbf{x} - \mathbf{x}_j| < a$. The velocity $\mathbf{v}^c(\mathbf{x}, t)$ and the pressure $p^c(\mathbf{x}, t)$ which enter the Navier-Stokes and continuity equations are thus extended outside phase c; the precise value of these extended fields is irrelevant with respect to the fields $X^c\mathbf{v}^c(\mathbf{x}, t)$ and $X^c p^c(\mathbf{x}, t)$, which vanish inside the inclusions. Thus, $X^c\mathbf{v}^c(\mathbf{x}, t)$ and $X^c p^c(\mathbf{x}, t)$ will be treated as regular g.f. We shall also introduce a singular g.f., the surface Dirac g.f. δ_Σ, which restricts a volume integration to one over the surface $\Sigma(\Sigma = \cup S(\mathbf{x}_j), j = 1, ..., N.)$, representing the interface. Collecting all inclusion effects, we indeed find $\delta_\Sigma = \sum_{j=1}^{N} \delta(P_j)|\text{grad}\, P_j|$. An obvious choice for P_j is the radial coordinate of a spherical co-ordinate system having its origin at the centre of the jth sphere i.e. $P_j(\mathbf{x}, t) = a - |\mathbf{x} - \mathbf{x}_j(t)| = a - r_j$ for which we observe $|\text{grad}\, P_j| = 1$.

The following extended equations are then valid for each member of the ensemble or realisations:

$$\left\{X^c \frac{\partial}{\partial \mathbf{x}} \cdot \mathbf{v}^c\right\} = 0 \quad \text{and} \quad \left\{X^c \frac{\partial}{\partial t}\mathbf{v}^c\right\} + \left\{X^c \frac{\partial}{\partial \mathbf{x}} \cdot \mathbf{v}^c\mathbf{v}^c\right\} - \left\{X^c \frac{\partial}{\partial \mathbf{x}} \cdot \mathbb{T}^c\right\} \Big/ \rho^c - \{X^c \mathbf{g}\} = 0, \tag{2.8}$$

where $\mathbb{T}^c$ denotes the stress tensor defined above and $\mathbf{g}$ the body force density; $\{f\}$ is the regular g.f. associated with the usual function f which here is piecewise continuous. The above equations are coupled by the non-slip condition (2.4) at the interface $S(\mathbf{x}_j)$ of each particle.

Several formulas are available (BOUIX [3]) for transforming each g.f. associated with derivatives in the usual sense of functions (i.e. $\{X^c \partial \mathbf{v}^c/\partial t\}$ or equivalently $\{\partial(X^c\mathbf{v}^c)/\partial t\}$) into derivatives in the sense of g.f. of the same functions (i.e. $\partial X^c\mathbf{v}^c/\partial t$). They are basically similar to integration by parts formulas. The continuity equation in the g.f. sense becomes:

$$\frac{\partial}{\partial t}X^c + \frac{\partial}{\partial \mathbf{x}} \cdot (X^c\mathbf{v}^c) = 0. \tag{2.9}$$

Note that a similar continuity equation for the dispersed phase can be obtained by replacing the superscript c by d. On the other hand, the momentum equation

calls for the following relation to be satisfied:

$$\left\{X^c \frac{\partial}{\partial \mathbf{x}} \cdot \mathbb{T}^c\right\} = \frac{\partial}{\partial \mathbf{x}} \cdot \{X^c \mathbb{T}^c\} + \mathbf{n}^c \cdot \mathbb{T}^c \delta_\Sigma \tag{2.10}$$

in which the divergence argument can be written in turn:

$$\{X^c \mathbb{T}^c\} = -X^c p^c \mathbb{I} + 2\mu^c \mathbb{D}(X^c \mathbf{v}^c) + 2\mu^c \mathbb{F}^c \delta_\Sigma. \tag{2.11}$$

Taking the divergence of (2.11):

$$\frac{\partial}{\partial \mathbf{x}} \cdot \{X^c \mathbb{T}^c\} = -\frac{\partial}{\partial \mathbf{x}}(X^c p^c) + \mu^c \Delta(X^c \mathbf{v}^c) + \mu^c \frac{\partial}{\partial \mathbf{x}} \left[\frac{\partial}{\partial \mathbf{x}} \cdot (X^c \mathbf{v}^c)\right] + 2\mu^c \frac{\partial}{\partial \mathbf{x}} \cdot (\mathbb{F}^c \delta_\Sigma), \tag{2.12}$$

where Δ represents the Laplace operator; the singular g.f. $\mathbb{F}^c \delta_\Sigma = [\mathbf{v}^c \mathbf{n}^c]^s \delta_\Sigma$ is the fine-grained extra deformation tensor, and the singular g.f. $\mathbf{n}^c \cdot \mathbb{T}^c \delta_\Sigma = (-\mathbf{n}^c p^c + 2\mu^c \mathbf{n}^c \cdot \mathbb{D}(\mathbf{v}^c))\delta_\Sigma$ is the fine grained interfacial stress exerted by the continuous phase upon the inclusions; $\mathbf{n}^c (= -\mathbf{n}^d = -\mathbf{n})$ is the unit normal exterior to phase c. Another expression of $\{X^c \mathbb{T}^c\}$ is proposed by JOSEPH and LUNDGREN [10], extending $\mathbf{v}^c$ and p^c inside the inclusions: the pressure is made to vanish and the velocity is assumed to be given by (2.5); they obtain:

$$\{X^c \mathbb{T}^c\} = -X^c p^c \mathbb{I} + 2\mu^c \mathbb{D}(X^c \mathbf{v}^c + X^d \mathbf{v}^d). \tag{2.13}$$

Comparing (2.11) and (2.13) gives $\mathbf{n}^c \cdot \mathbb{T}^c \delta_\Sigma = \mathbb{D}(X^d \mathbf{v}^d)$. The momentum equations in the g.f. sense, where $\nu^c = \mu^c / \rho^c$, can be easily obtained once (2.11) and (2.13) are known. The former expression yields:

$$\frac{\partial X^c \mathbf{v}^c}{\partial t} + \frac{\partial}{\partial \mathbf{x}} \cdot (X^c \mathbf{v}^c \mathbf{v}^c) = -\frac{1}{\rho^c} \frac{\partial}{\partial \mathbf{x}}(X^c p^c) + \nu^c \Delta(X^c \mathbf{v}^c) + \nu^c \frac{\partial}{\partial \mathbf{x}} \left[\frac{\partial}{\partial \mathbf{x}} \cdot (X^c \mathbf{v}^c)\right] + 2\nu^c \frac{\partial}{\partial \mathbf{x}} \cdot (\mathbb{F}^c \delta_\Sigma) + \frac{1}{\rho^c} \mathbf{n}^c \cdot \mathbb{T}^c \delta_\Sigma + X^c \mathbf{g}. \tag{2.14}$$

Strictly speaking all the above fine-grained equations are incomplete since they do not involve a singular g.f. relative to the walls, as for instance $\mathbb{F}^c \delta_{\partial \mathcal{V}^c} = -[\mathbf{v}^c \mathbf{n}^b]^s \delta_{\partial \mathcal{V}^c}$, where $\mathbf{n}^b$ is the unit normal interior to $\mathcal{V}_x^c$. Presenting all these g.f.'s would be of no interest, since in contrast to the interfacial g.f.'s, which evolve randomly, they still remain g.f.'s after averaging. Once this process is completed, it is more convenient to rule out the g.f. approach to the equations.

At the boundary of the $\mathcal{V}_x^c$ domain, it should simply be recalled that an equation similar to (2.4) holds, namely:

$$\mathbf{v}^c(\mathbf{x},t) = \mathbf{v}^b(\mathbf{x},t) \qquad \text{for} \quad \mathbf{x} \quad \text{on} \quad \partial\mathcal{V}^c, \tag{2.15}$$

where $\mathbf{v}^b$ is a prescribed velocity on the boundaries.

3. Probability concepts

3.1. Reduced densities and observation or μ_z-space

Thus far our considerations have only been dynamic, and probability considerations have not been introduced. Once initial conditions for the above equations have been specified, the inclusions and the carrying phase behave in a deterministic fashion. However, from a practical point of view, these initial conditions are random. In our case, where the continuous phase flow is assumed to remain laminar each time (it might be laminar at the beginning and then turn turbulent, i.e. unstable, by the very presence of the inclusions), one is tempted to consider the hydrodynamic fields as continuous functionals of the dispersed phase initial data alone; under this assumption, any field (say $\mathbf{v}^c(s;\mathbf{x},0)$, s representing a sample point) would not be an independent random variable but rather it might be introduced as an implicit and regular functional of an initial configuration $Z_N(s;0)$, which would be compatible with the laws of hydrodynamics and would continue to be so at any point $(\mathbf{x},t)$; this view is incorrect in general since the fluid has its own degrees of freedom which are independent of those of the inclusions, but it is correct in the limit of potential flows or of creeping flows; it is also correct for steady initial conditions of general types of flows. For arbitrary initial conditions, the above functional may exist only if the admissible initial fields $\mathbf{v}^c(s;\mathbf{x},0)$ are restricted by requiring each of them to be the result of a given configuration; thus, the probability density function (p.d.f.) f_N describing the entire system, will be allowed to include only Z_N in its arguments. Other special randomizing effects arise when Brownian motion is significant or when collisions have to be treated. They are also excluded from this study.

Thus, as in S.M., only the initial p.d.f. $\mathrm{f}_N(Z_N;0)$, given over Γ, will serve as the initial condition of the so-called Liouville equation whose solution is $\mathrm{f}_N(Z_N;t)$; this p.d.f. is symmetric with respect to the N inclusions (which are in fact assumed to be indistinguishable) and normalized to one. As a rule, such a p.d.f., which may provide any kind of averaged value, is too detailed a state variable. The reduced p.d.f. f_r of order $r (r = 1,2,...)$, which gives the probability of observing the r first inclusions at the points $\mathbf{z}_1,...,\mathbf{z}_r$ (an *r-configuration* in a reduced part of the Γ-space) and which are defined by integrating over the coordinates of the $N-r$ remaining inclusions, are more suitable; they are solutions

of the B.B.G.K.Y. hierarchy defined over the various r-time Cartesian products of μ_{z_i}.

Since no two inclusions of the same coordinates are distinguishable, it is more physically meaningful to see whether r prescribed values $(\mathbf{z}, \mathbf{z}^\circ, ...)$ are occupied by any set of r inclusions irrespective of their labels, instead of following an *r-configuration*. The 9, 18,...- D spaces ("observation spaces"), where such *mechanical states* are observed, are denoted by μ_z, $\mu_z \otimes \mu_{z^\circ}$, ... and various dispersed phase state variables and their equations will be defined over them in Sec. 4. Due to the non-overlapping condition, some regions must in fact be cut out and the resulting spaces are then denoted μ_{zz°, $\mu_{zz^\circ z^{\circ\circ}}$... Such a notation change will be extended to "restricted" Cartesian products of ordinary physical spaces. Over $\mu_{zz^\circ z^{\circ\circ}}$... we introduce $\mathrm{f}^{(r)}(\mathbf{z}, \mathbf{z}^\circ, \mathbf{z}^{\circ\circ}, ...)$, the mean number of mechanical states per unit volume, which is equal to $A_N^r \mathrm{f}_r(\mathbf{z}\mathbf{z}^\circ, \mathbf{z}^{\circ\circ}, ...)$, where $A_N^r = N!/(N - \mathbf{r})!$ is the number of configurations leaving a mechanical state unchanged.

The basic tool of this approach is the "fine-grained density" defined by:

$$f_i(s; \mathbf{z}, t) = \delta\{\mathbf{z} - \mathbf{z}_i(s,t)\} = \delta\{\mathbf{x} - \mathbf{x}_i(s,t)\}\ \delta\{\mathbf{u} - \mathbf{u}_i(s,t)\}$$

$$\delta\{\boldsymbol{\omega} - \boldsymbol{\omega}_i(s,t)\}.$$

Such an irregular field of events allows a fine-grained number density $n(s; \mathbf{z}, t) = \Sigma f_i(s; \mathbf{z}, t)$ to be defined, including the contributions of all inclusions. Defining $\mathrm{f}^{(1)}$ as an average number density in the μ_z-space, we can write $\mathrm{f}^{(1)} = E[n] = NE[f_1] = N\mathrm{f}_1$. The mean values of the products $n(\mathbf{z})[n(\mathbf{z}^\circ) - \delta(\mathbf{z} - \mathbf{z}^\circ)]$, $n(\mathbf{z})[n(\mathbf{z}^{\circ\circ}) - \delta(\mathbf{z} - \mathbf{z}^{\circ\circ}) - \delta(\mathbf{z}^\circ - \mathbf{z}^{\circ\circ})]$..., can be connected with higher-order distribution functions, $\mathrm{f}^{(2)}$, $\mathrm{f}^{(3)}$...

3.2. General averaging formulas

Introducing the above fine-gradient density indeed offers one way of defining f_r or $\mathrm{f}^{(r)}$ without using f_N. As it is possible to derive equations for various fine-grained densities, f_1, $f_1 f_2^\circ$, $f_1 f_2^\circ f_3^{\circ\circ}$... (for brevity $f_j^\circ = f_j(\mathbf{z}^\circ)$...) then, by averaging the latter, the first members of the B.B.G.K.Y. hierarchy can be obtained as far as desired in the observation spaces (KLIMONTOVICH [11]): the Liouville equation is by-passed. For the theory developed in this paper, the B.B.G.K.Y. hierarchy will be stopped at the second order equation. In the averaging process, dispersed phase fields $\psi(\mathbf{z})$ appear as $\left(\sum_i f_i\right)\psi(\mathbf{z}) = \sum_i f_i \psi(\mathbf{z}_i)$; $\left(\sum_i \sum_{i \neq j} f_i f_j^\circ\right)\psi\zeta^\circ(\mathbf{z}, \mathbf{z}^\circ) = \sum_i \sum_{i \neq j} f_i f_j^\circ \psi(\mathbf{z}_i)\zeta(\mathbf{z}_j)$. So, besides

$\mathrm{f}_1(\mathbf{z})$, $\mathrm{f}_2(\mathbf{z}, \mathbf{z}^\circ)$, ... the first dispersed phase-averaged variables in the μ_z and μ_{zz° – spaces are:

$$\overline{\psi}^1(\mathbf{z}) = \sum_i E\left[f_i \psi(\mathbf{z}_i)\right] / \sum_i E[f_i] = E[f_1 \psi(\mathbf{z}_1)]/\mathrm{f}_1, \tag{3.1}$$

$$\overline{\psi\zeta^\circ}^2(\mathbf{z}, \mathbf{z}^\circ) = \sum_i \sum_{i \neq j} E\left[f_i f_j^\circ \psi(\mathbf{z}_i)\zeta(\mathbf{z}_j)\right] / \sum_i \sum_{i \neq j} E[f_i f_j^\circ] \tag{3.2}$$

$$= E[f_1 f_2^\circ \psi(\mathbf{z}_1)\zeta(\mathbf{z}_2)]/\mathrm{f}_2.$$

In most cases, averaged variables come out as straightforward explicit functions of $\mathbf{z}$ and $\mathbf{z}^{\circ\circ}$... and do not depend on time, i.e. $\mathbf{u}_1\boldsymbol{\omega}_1$ and $\mathbf{u}_1\mathbf{u}_2$ become simply $\mathbf{u}\boldsymbol{\omega}$ and $\mathbf{u}\mathbf{u}^\circ$.

The next step in our approach will be to switch from observation spaces to ordinary 3-space domains or Cartesian products of them. Transforming each member of the B.B.G.K.Y. hierarchy into moment equations simplifies the dispersed phase dynamics formulation since the number of independent variables is considerably reduced. First moments equations are obtained by averaging the f_1 equation over internal coordinates in μ_z-space, higher order moments are introduced by averaging the f_2 equation and so on. The most common moments are $\phi^{(1)}$, the (average) number density defined in $\mathcal{V}_x^d$ and $\phi^{(2)}$, the pair number density defined in the pair physical space $\mathcal{V}_{xx^\circ}^d$ (see above the definition of μ_{zz° which is similar)

$$\phi^{(1)}(\mathbf{x}, t) = E\left[\sum_i \varphi_i\right] = NE[\varphi_1] = N\phi_1(\mathbf{x}, t),$$

$$\phi^{(2)}(\mathbf{x}, \mathbf{x}^\circ, t) = E\left[\sum_j \sum_{i \neq j} \varphi_i \varphi_j\right] = N(N-1)E[\varphi_1 \varphi_2] \tag{3.3}$$

$$= N(N-1)\phi_2(\mathbf{x}, \mathbf{x}^\circ, t),$$

where the fine-grained density $\varphi_i(\mathbf{x}, t) = \delta\{\mathbf{x} - \mathbf{x}_i(s, t)\}$ has been introduced. Here and below, conditional averaged values of ψ, are denoted by an overscale; italic superscripts indicate the number of points occupied by inclusions in observation spaces while standard superscripts indicate the number of observation points in the physical spaces. Other moments of any order can be considered as inner products over various observation spaces. Let $\langle \mathrm{f}_i \rangle$ be such an ith order moment ($i = 1, 2...$) obtained by multiplying by f_i the quantity appearing to the left of

the semicolon. For instance, the first-order and second-order moments can be written:

$$\overline{\psi}^1(\mathbf{x},t) = \sum_i E[\varphi_i \psi(\mathbf{x}_i)] \Big/ \sum_i E[\varphi_i] = \int \overline{\psi}^1 \mathrm{f}_1 d\mathbf{u} d\omega / \phi_1 = \langle \overline{\psi}^1; \mathrm{f}_1 \rangle / \phi_1, \tag{3.4}$$

$$\overline{\psi\zeta^\circ}^2(\mathbf{x},\mathbf{x}^\circ,t) = \sum_i \sum_{i\neq j} E[\varphi_i \varphi_j^\circ \psi(\mathbf{x}_i)\zeta(\mathbf{x}_j)] \Big/ \sum_i \sum_{i\neq j} E[\varphi_i \varphi_j^\circ] = \int \overline{\psi\zeta^\circ}^2 \mathrm{f}_2 d\mathbf{u} d\omega d\mathbf{u}^\circ d\omega^\circ / \phi_2 = \langle \overline{\psi\zeta^\circ}^2; \mathrm{f}_2 \rangle / \phi_2, \tag{3.5}$$

after having specified $d\xi = d\mathbf{u}d\omega$. The most common averages are cross-correlations between inclusion velocities observed at two positions such as $\overline{\mathbf{u}\mathbf{u}^\circ}^2(\mathbf{x},\mathbf{x}^\circ)$, $\overline{\boldsymbol{\omega}\mathbf{u}^\circ}^2(\mathbf{x},\mathbf{x}^\circ)$ or $\overline{\mathbf{u}\boldsymbol{\omega}^\circ}^2(\mathbf{x},\mathbf{x}^\circ)$. Given two observation locations $\mathbf{x}$ and $\mathbf{x}^\circ$, each being occupied by an inclusion, $\overline{\mathbf{u}}^2(\mathbf{x},\mathbf{x}^\circ)$ (respectively $\overline{\mathbf{u}^\circ}^2(\mathbf{x},\mathbf{x}^\circ)$) is the averaged velocity computed at $\mathbf{x}$ (respectively at $\mathbf{x}^\circ$). For the first case, where $\zeta^\circ = 1$, $\overline{\mathbf{u}}^2(\mathbf{x},\mathbf{x}^\circ)$ can be interpreted as the averaged velocity at $\mathbf{x}$, conditional upon the presence of an another inclusion at $\mathbf{x}^\circ$, this leads to the possible notation $\overline{\mathbf{u}}^2(\mathbf{x},\mathbf{x}^\circ) = \overline{\mathbf{u}}^2(\mathbf{x}|\mathbf{x}^\circ)$. Similarly we can write $\overline{\mathbf{u}^\circ}^2(\mathbf{x},\mathbf{x}^\circ) = \overline{\mathbf{u}}^2(\mathbf{x}^\circ|\mathbf{x})$. The correlations $\overline{\mathbf{u}\mathbf{u}}^2(\mathbf{x}|\mathbf{x}^\circ)$ and $\overline{\boldsymbol{\omega}\mathbf{u}}^2(\mathbf{x},\mathbf{x}^\circ)$ are also averages of the same type. In contrast to the tensor $\overline{\mathbf{u}\mathbf{u}^\circ}^2(\mathbf{x},\mathbf{x}^\circ)$, the tensor $\overline{\mathbf{u}\mathbf{u}}^2(\mathbf{x}|\mathbf{x}^\circ)$ is not symmetrical with respect to $\mathbf{x}$ and $\mathbf{x}^\circ$. In the following, when the arguments are not explicity stated for the sake of simplicity, the supercript "$\circ$" (respectively no superscript) over a function, such as $\overline{\mathbf{u}^\circ}^2$ (respectively $\overline{\mathbf{u}}^2$) will indicate that its first spatial argument is $\mathbf{x}^\circ$ (respectively $\mathbf{x}$), the condition being specified at $\mathbf{x}$ (respectively $\mathbf{x}^\circ$).

On the other hand, continuous phase fine-grained variables, which appear as X^c ψ^c are only defined in the physical domain $\mathcal{V}_x^c$ occupied by the mixture; they can also be averaged subject to various constraints. The event "there is the continuous phase at $\mathbf{x}$", i.e. $X^c = 1$, has a finite probability equal to the average of X^c, the local continuous phase volume fraction or concentration $\alpha^{c1}(\mathbf{x}) = E[X^c]$. The simplest conditional average corresponding to this constraint is the standard conditional phase average of ψ^c, which has the notation $\overline{\psi}^{c1}(\mathbf{x}) = E[X^c\psi^c]/\alpha^{c1}(\mathbf{x})$ so that conditional averaged values of ψ^c are also designated by an overscore. We will also need the conditioned concentration:

$$\alpha^{c2}(\mathbf{x}^\circ,t|\mathbf{x}) = \sum_i E[X_i^c(\mathbf{x}^\circ,t)]/\phi^{(1)}(\mathbf{x},t) = E[X_1^c(\mathbf{x}^\circ,t)\varphi_1(\mathbf{x},t)]/\phi_1(\mathbf{x},t) \tag{3.6}$$

where X_i^c is a partial indicator function in which the ith inclusion is excluded

from X^c (see (2.6)); the second-order average is

$$\overline{\psi^c}^2(\mathbf{x}^\circ|\mathbf{x}) = E[X_1^c \psi^c(\mathbf{x}^\circ)\varphi_1(\mathbf{x})]/\alpha^{c2}(\mathbf{x}^\circ|\mathbf{x})\phi_1(\mathbf{x}). \tag{3.7}$$

The overscore bears an index indicating the number of contraints, e.g. $X^c = 1$, plus the number of neighbouring points occupied by inclusions. All the above conditioned variables (3.6) and (3.7) are defined over a region denoted by $\mathcal{V}^c_{x,x^\circ}$ which is $\mathcal{V}^c_{x^\circ} \otimes \mathcal{V}^d_x$, from which some inaccessible region due to the finite inclusions size (i.e. $|\mathbf{x}^\circ - \mathbf{x}| < 2a$) in the carrying flow has been removed. Likewise, averages such as $\overline{\psi}^{c3}(\mathbf{x}^{\circ\circ}|\mathbf{x}, \mathbf{x}^\circ)$ will be introduced at the third order, i.e. for two fixed inclusions. Defining them means introducing an additional partial indicator function $X^c_{i,j}$ in which the ith and jth inclusions are excluded from X^c. The relevant space (denoted $\mathcal{V}^c_{x,x^\circ,x^{\circ\circ}}$) is $\mathcal{V}^c_{x^{\circ\circ}} \otimes \mathcal{V}^d_{x^\circ x}$ from which some region is removed, and so on. Finally, composite averages such as $\alpha^{c2}(\mathbf{x}^\circ|\mathbf{z})$ and $\overline{\psi}^{c2}(\mathbf{x}^\circ|\mathbf{z})$ will be encountered.

It is worth recalling that a dispersed phase description can also be produced parallelling the description we have just given for continuous phase modelling. It would be suitable for standard two-phase flow models. In these models, dispersed phase variables as well as continuous phase ones are defined directly as moments in ordinary physical 3D-space from equations like those presented in Sec. 2.2 for the continuous phase. The averages associated with X^d (the dispersed phase volume fraction) and $\mathbf{v}^d$ obtained from a standard averaging process for local instantaneous dispersed equations are simply:

$$E[X^d(\mathbf{x})] = \alpha^{d1}(\mathbf{x}) = 1 - \alpha^{c1}(\mathbf{x}) \quad \text{and} \quad E[X^d \mathbf{v}^d(\mathbf{x})|X^d = 1] = E[\mathbf{v}^d X^d]/\alpha^{d1} = \overline{\mathbf{v}}^{d1}(\mathbf{x}). \tag{3.8}$$

$$E[X^d(\mathbf{x}^\circ)|\mathbf{x}_1 = \mathbf{x}] = \alpha^{d2}(\mathbf{x}^\circ|\mathbf{x}) = 1 - \alpha^{c2}(\mathbf{x}^\circ|\mathbf{x}) \quad \text{and} \quad E[X^d \mathbf{v}^d(\mathbf{x}^\circ)|\mathbf{x}_1 = \mathbf{x}, X^d = 1] = \overline{\mathbf{v}}^{d2}(\mathbf{x}^\circ|\mathbf{x}). \tag{3.9}$$

In our approach, these standard dispersed phase variables will appear incidentally in interaction terms; they will be considered as provisional quantities which will be transformed into variables such as (3.4) and (3.5); thus the way of describing both phases will ultimately be unsymmetrical.

4. Averaging process for the dispersed phase

The Klimontovich approach begins by a preparatory step which amounts to formulating local instant field equations in the sense of generalised functions (g.f.); it parallels the approach for the continuous phase in Sec. 2.2.

4.1. The Klimontovich equations

To obtain the equation for f_1 (CERCIGNANI [5]) in $\mu_{\mathbf{z}}$, we first determine the derivative with respect to time of this fine-grained function; inserting (2.1), (2.2) and (2.3), we obtain:

$$\frac{\partial f_1}{\partial t} + \mathbf{u}_1 \cdot \frac{\partial f_1}{\partial \mathbf{x}} + [m^{-1}\mathbf{F}_1 + \mathbf{g}] \cdot \frac{\partial f_1}{\partial \mathbf{u}} + I^{-1}\mathbf{K}_1 \cdot \frac{\partial f_1}{\partial \boldsymbol{\omega}} = 0. \tag{4.1}$$

It must be stressed that taking into account collisions would have introduced extra terms which would have meant generalising our analysis. $\mathbf{F}_1$ and $\mathbf{K}_1$ are composite quantities since they involve properties associated with both phases. On the one hand, $\mathbf{F}_1$ and $\mathbf{K}_1$ represent the resulting stress and torque exerted by the continuous phase upon the first inclusion with coordinates $\mathbf{z}_1$. On the other hand, their effects are described by two linear functionals of $p^c[Z_N; \tilde{\mathbf{x}}, t]$ and $\mathbf{v}^c[Z_N; \tilde{\mathbf{x}}, t]$, where $\tilde{\mathbf{x}}$ is such that $(\tilde{\mathbf{x}} - \mathbf{x}_1)/a = \mathbf{n}$. Let $d\Omega$ be an element of solid angle on the sphere of unit radius, i.e. $a^2 d\Omega = dS$. The only points which contribute to the integral are thus $\tilde{\mathbf{x}} = \mathbf{x}_1 + a\mathbf{n}$ for all $\mathbf{n}$ on this sphere:

$$\mathbf{F}_1(Z_N; t) = a^2 \int_{S(\mathbf{x}_1)} \{\mathbf{n} \cdot X^c \mathbb{T}^c\}(Z_N; \tilde{\mathbf{x}}, t) d\Omega, \tag{4.2}$$

$$\mathbf{K}_1(Z_N; t) = a^3 \int_{S(\mathbf{x}_1)} \mathbf{n} \wedge \{\mathbf{n} \cdot X^c \mathbb{T}^c\}(Z_N; \tilde{\mathbf{x}}, t) d\Omega, \tag{4.3}$$

$$= a^3 \mathcal{E} : \int_{S(\mathbf{x}_1)} \{\mathbf{nn} \cdot X^c \mathbb{T}^c\}(Z_N; \tilde{\mathbf{x}}, t) d\Omega,$$

where $\mathcal{E}$ is the antisymmetric alternating tensor. Equation (4.1) can be rearranged as:

$$\frac{\partial f_1}{\partial t} + \frac{\partial}{\partial \mathbf{x}} \cdot (f_1 \mathbf{u}_1) + m^{-1} \frac{\partial}{\partial \mathbf{u}} \cdot (f_1 \mathbf{F}_1) + \frac{\partial}{\partial \mathbf{u}} \cdot (f_1 \mathbf{g}) + I^{-1} \frac{\partial}{\partial \boldsymbol{\omega}} \cdot (f_1 \mathbf{K}_1) = 0. \tag{4.4}$$

This is the first equation of the Klimontovich hierarchy written in μ_z-space. Following the same line of calculations, we can obtain the equation for $f_1 f_2$ in μ_{zz°-space:

$$d\frac{\partial f_1 f_2}{\partial t} + \frac{\partial}{\partial \mathbf{x}} \cdot (f_1 f_2 \mathbf{u}_1) + \frac{\partial}{\partial \mathbf{x}^\circ} \cdot (f_1 f_2 \mathbf{u}_2) + m^1 \frac{\partial}{\partial \mathbf{u}} \cdot (f_1 f_2 \mathbf{F}_1) + m^{-1} \frac{\partial}{\partial \mathbf{u}^\circ} \cdot (f_1 f_2 \mathbf{F}_2) + \frac{\partial}{\partial \mathbf{u}} \cdot (f_1 f_2 \mathbf{g}) + \frac{\partial}{\partial \mathbf{u}^\circ} \cdot (f_1 f_2 \mathbf{g}) + I^{-1} \frac{\partial}{\partial \omega} \cdot (f_1 f_2 \mathbf{K}_1) + I^{-1} \frac{\partial}{\partial \omega^\circ} \cdot (f_1 f_2 \mathbf{K}_2) = 0. \tag{4.5}$$

$\mathbf{F}_2$ and $\mathbf{K}_2$ have the same structure as $\mathbf{F}_1$ and $\mathbf{K}_1$, $S(\mathbf{x}_1)$ being changed into $S(\mathbf{x}_2)$. The procedure could have been continued to give the next product $f_1 f_2 f_3$ and so on. Finally, the equations for the fine-grained number densities $n(\mathbf{z})$ and $n(\mathbf{z})[n(\mathbf{z}^\circ) - \delta(\mathbf{z} - \mathbf{z}^\circ)]$ can be obtained by combining equations for f_i and $f_i f_j$ which are similar to (4.4) and (4.5).

4.2. The revisited B.B.G.K.Y. hierarchy

The B.B.G.K.Y. hierarchy is obtained by averaging the entire sequence of Klimontovich equations. As far as g.f. are concerned, it is well known that $E[O(g)] = O(E[g])$, O being any differential operator whatever. The equation for f_1 is derived first.

$$\frac{\partial}{\partial t}\mathrm{f}_1 + \frac{\partial}{\partial \mathbf{x}} \cdot \mathrm{f}_1 \mathbf{u} + m^{-1} \frac{\partial}{\partial \mathbf{u}} \cdot \mathrm{f}_1 \overline{\mathbf{F}}^1 + \frac{\partial}{\partial \mathbf{u}} \cdot \mathrm{f}_1 \mathbf{g} + I^{-1} \frac{\partial}{\partial \omega} \cdot \mathrm{f}_1 \overline{\mathbf{K}}^1 = 0, \tag{4.6}$$

where the averaged force and the averaged torque exerted upon an inclusion which is known to be centred at $\mathbf{x}$ and to have internal coordinates equal to ξ are defined by:

$$\overline{\mathbf{F}}^1(\mathbf{z}) = E[f_1 \mathbf{F}_1]/\mathrm{f}_1 = a^2 \int_{S(\mathbf{x})} \mathbf{n} \cdot \overline{X^c \mathbb{T}^{c2}}(\mathbf{x} + a\mathbf{n}|\mathbf{z}) d\Omega,$$

$$\overline{\mathbf{K}}^1(\mathbf{z}) = E[f_1 \mathbf{K}_1]/\mathrm{f}_1 = a^3 \mathcal{E} : \int_{S(\mathbf{x})} \mathbf{n}\mathbf{n} \cdot \overline{X^c \mathbb{T}^{c2}}(\mathbf{x} + a\mathbf{n}|\mathbf{z}) d\Omega. \tag{4.7}$$

The local averaged force around the test inclusion is obtained by selecting formula (2.13) to express the fine-grained stress field:

$$\mathbf{n} \cdot \overline{X^c \mathbb{T}^{c2}}(\tilde{\mathbf{x}}|\mathbf{z}) = E[\{f_1 \mathbf{n} \cdot X_1^c \mathbb{T}^c\}]/\mathrm{f}_1(\mathbf{z}) = -\alpha^{c2} \overline{p}^{c2} \mathbf{n} + 2\mu^c \mathbf{n} \cdot \mathbb{D}[\overline{\mathbf{v}}^{c2} + \alpha^{d2}(\overline{\mathbf{v}}^{d2} - \overline{\mathbf{v}}^{c2})]. \tag{4.8}$$

The same formula will be used throughout the article in any kind of averaging stress field around test inclusions. The positions of the inclusion centres which contribute to this integral are such that $\tilde{\mathbf{x}} = \mathbf{x} + a\mathbf{n}$.

The above averaging procedure can be extended to derive the equation for f_2:

$$\frac{\partial}{\partial t}\mathrm{f}_2 + \frac{\partial}{\partial \mathbf{x}} \cdot \mathrm{f}_2 \mathbf{u} + \frac{\partial}{\partial \mathbf{x}^\circ} \cdot \mathrm{f}_2 \mathbf{u}^\circ + m^{-1} \frac{\partial}{\partial \mathbf{u}} \cdot \mathrm{f}_2 \overline{\mathbf{F}}^2 + m^{-1} \frac{\partial}{\partial \mathbf{u}^\circ} \cdot \mathrm{f}_2 \overline{\mathbf{F}^\circ}^2 + \frac{\partial}{\partial \mathbf{u}} \cdot \mathrm{f}_2 \mathbf{g} + \frac{\partial}{\partial \mathbf{u}^\circ} \cdot \mathrm{f}_2 \mathbf{g} + I^{-1} \frac{\partial}{\partial \boldsymbol{\omega}} \cdot \mathrm{f}_2 \overline{\mathbf{K}}^2 + I^{-1} \frac{\partial}{\partial \boldsymbol{\omega}^\circ} \cdot \mathrm{f}_2 \overline{\mathbf{K}^\circ}^2 = 0, \tag{4.9}$$

where the averaged force exerted at time t upon an inclusion which is known to be located at $\mathbf{z}$ and to have a companion inclusion at $\mathbf{z}^\circ$ is:

$$\overline{\mathbf{F}}^2(\mathbf{z}|\mathbf{z}^\circ) = E[f_1 f_2 \mathbf{F}_1]/\mathrm{f}_2 = a^2 \int_{S(\mathbf{x})} \mathbf{n} \cdot \overline{X^c \mathbb{T}^{c3}}(\mathbf{x} + a\mathbf{n}|\mathbf{z}, \mathbf{z}^\circ) d\Omega \tag{4.10}$$

where the local averaged stress at the surface of the test inclusion is:

$$\mathbf{n} \cdot \overline{X^c \mathbb{T}^{c3}}(\tilde{\mathbf{x}}|\mathbf{z}, \mathbf{z}^\circ) = E[f_1 f_2 \mathbf{n} \cdot X^c_{1,2} \mathbb{T}^c]/f_2(\mathbf{z}, \mathbf{z}^\circ) = -\alpha^{c3} \overline{p}^{c3} \mathbf{n} + 2\mu^c \mathbf{n} \cdot \mathbb{D}[\overline{\mathbf{v}}^{c3} + \alpha^{d3}(\overline{\mathbf{v}}^{d3} - \overline{\mathbf{v}}^{c3})]. \tag{4.11}$$

The position of the inclusion centres which contribute to this integral are such that $\tilde{\mathbf{x}} = \mathbf{x} + a\mathbf{n}$.

The point here is to distinguish between averaging $f_1 f_2 \mathbf{F}_1$ which leads to (5.15) and averaging $f_1 f_2 \mathbf{F}_2$ which leads to $\overline{\mathbf{F}^\circ}^2 = E[f_1 f_2 \mathbf{F}_2]/\mathrm{f}_2 = \overline{\mathbf{F}}^2(\mathbf{z}^\circ|\mathbf{z})$. Both quantities differ because $\overline{\mathbf{F}}^2(\cdot|\cdot)$ is not symmetrical with respect to its two spatial arguments.

All the results which have just been obtained for the averaged force can be extented directly to the averaged torque. Furthermore the equations for $\mathrm{f}^{(1)}$ and $\mathrm{f}^{(2)}$ can be obtained readily by averaging the equations for the afore-mentioned fine-grained number densities.

4.3. Moment equations

The first two members of the B.B.G.K.Y. hierarchy above are written in μ_z and μ_{zz}-spaces either in terms of f_1 and f_2 or in terms of $\mathrm{f}^{(1)}$ and $\mathrm{f}^{(2)}$. The latter form will be adopted. Transforming them into moment equations over the physical spaces $\mathcal{V}_x^d$ and $\mathcal{V}_{xx^\circ}^d$ instead of the μ_z and μ_{zz°-spaces is a standard process. The first-order moment equations of interest here are the averaged simple number density $\phi^{(1)}$, the averaged linear velocity $\overline{\mathbf{u}}^1$ and the averaged angular velocity $\overline{\boldsymbol{\omega}}^1$:

$$\frac{\partial}{\partial t}\phi^{(1)} + \frac{\partial}{\partial \mathbf{x}} \cdot \left(\phi^{(1)} \overline{\mathbf{u}}^1\right) = 0, \tag{4.12}$$

$$\frac{\partial}{\partial t}\left(\phi^{(1)}\overline{\mathbf{u}}^{1}\right)+\frac{\partial}{\partial \mathbf{x}}\cdot\sum_{i=1}^{N}E[\varphi_i\mathbf{u}_i\mathbf{u}_i]=\phi^{(1)}\mathbf{g}+m^{-1}\phi^{(1)}\overline{\mathbf{F}}^{1}, \tag{4.13}$$

$$\frac{\partial}{\partial t}\left(\phi^{(1)}\overline{\boldsymbol{\omega}}^{1}\right)+\frac{\partial}{\partial \mathbf{x}}\cdot\sum_{i=1}^{N}E[\varphi_i\boldsymbol{\omega}_i\mathbf{u}_i]=I^{-1}\phi^{(1)}\overline{\mathbf{K}}^{1}, \tag{4.14}$$

where the resultant force $\overline{\mathbf{F}}^{1}$ and torque $\overline{\mathbf{K}}^{1}$ experienced by the first inclusion located at $\mathbf{x}$, whatever its translational or rotational velocities, were defined using (3.7) as:

$$\overline{\mathbf{F}}^{1}(\mathbf{x})=\langle\overline{\mathbf{F}}^{I};f_1\rangle/\phi_1=a^2\int\limits_{S(\mathbf{x})}\mathbf{n}\cdot\overline{X^c\mathbb{T}^{c2}}(\mathbf{x}+a\mathbf{n}|\mathbf{x})d\Omega, \tag{4.15}$$

$$\overline{\mathbf{K}}^{1}(\mathbf{x})=\langle\overline{\mathbf{K}}^{I};f_1\rangle/\phi_1=a^3\mathcal{E}:\int\limits_{S(\mathbf{x})}\mathbf{nn}\cdot\overline{X^c\mathbb{T}^{c2}}-(\mathbf{x}+a\mathbf{n}|\mathbf{x})d\Omega, \tag{4.16}$$

where the local averaged stress at the test inclusion surface is defined by:

$$\begin{aligned}\mathbf{n}\cdot\overline{X^c\mathbb{T}^{c2}}(\tilde{\mathbf{x}},t|\mathbf{x})=\mathbf{n}\cdot E[\varphi_1X_1^c\mathbb{T}^c]/\phi_1(\mathbf{x})=-\alpha^{c2}\overline{p}^{c2}\mathbf{n}\\ +2\mu^c\mathbf{n}\cdot\{\mathbb{D}[\overline{\mathbf{v}}^{c2}+\alpha^{d2}(\overline{\mathbf{v}}^{d2}-\overline{\mathbf{v}}^{c2})]\}.\end{aligned} \tag{4.17}$$

The expression of this stress will be simplified in Sec. 5.3.

We also need the equation governing the second-order moments. Starting from (4.9), we determine the second-order moment equations for the three variables, the averaged pair number density $\phi^{(2)}(\mathbf{x},\mathbf{x}^\circ,t)$, the linear velocity $\overline{\mathbf{u}^\circ}^2$ and angular velocity $\overline{\boldsymbol{\omega}^\circ}^2$, which are conditionally averaged upon the presence of an inclusion at $\mathbf{x}$

$$\frac{\partial}{\partial t}\phi^{(2)}+\frac{\partial}{\partial \mathbf{x}}\cdot\left(\phi^{(2)}\overline{\mathbf{u}}^{2}\right)+\frac{\partial}{\partial \mathbf{x}^\circ}\cdot\left(\phi^{(2)}\overline{\mathbf{u}^{\circ 2}}\right)=0, \tag{4.18}$$

$$\begin{aligned}\frac{\partial}{\partial t}\left(\phi^{(2)}\overline{\mathbf{u}^{\circ 2}}\right)+\frac{\partial}{\partial \mathbf{x}^\circ}\cdot\sum_{i=1}\sum_{j\neq i}E[\varphi_i\varphi_j\mathbf{u}_j\mathbf{u}_j]\\ +\frac{\partial}{\partial \mathbf{x}}\cdot\sum_{i=1}\sum_{j\neq i}E[\varphi_i\varphi_j\mathbf{u}_i\mathbf{u}_j]=\phi^{(2)}\mathbf{g}+m^{-1}\phi^{(2)}\overline{\mathbf{F}^{\circ 2}},\end{aligned} \tag{4.19}$$

$$\begin{aligned}\frac{\partial}{\partial t}\left(\phi^{(2)}\overline{\boldsymbol{\omega}^{\circ 2}}\right)+\frac{\partial}{\partial \mathbf{x}^\circ}\cdot\sum_{i=1}\sum_{j\neq i}E[\varphi_i\varphi_j\mathbf{u}_j\boldsymbol{\omega}_j]\\ +\frac{\partial}{\partial \mathbf{x}}\cdot\sum_{i=1}\sum_{j\neq i}E[\varphi_i\varphi_j\mathbf{u}_i\boldsymbol{\omega}_j]=I^{-1}\phi^{(2)}\overline{\mathbf{K}^{\circ 2}},\end{aligned} \tag{4.20}$$

where the resultant force $\overline{\mathbf{F}^{\circ 2}}$ and torque $\overline{\mathbf{K}^{\circ 2}}$ experienced by the test inclusion located at $\mathbf{x}^\circ$ and conditionally averaged upon the presence of another inclusion at $\mathbf{x}$, are:

$$\overline{\mathbf{F}^{\circ 2}} = \overline{\mathbf{F}}^2(\mathbf{x}^\circ|\mathbf{x}) = \langle \overline{\mathbf{F}^{\circ 2}}; f_2\rangle/\phi_2 = a^2 \int_{S(\mathbf{x})} \mathbf{n}\cdot\overline{X^c\mathbb{T}^{c3}}(\mathbf{x}^\circ + a\mathbf{n}|\mathbf{x},\mathbf{x}^\circ)d\Omega, \tag{4.21}$$

$$\begin{aligned}\overline{\mathbf{K}^{\circ 2}} = \overline{\mathbf{K}}^2(\mathbf{x}^\circ|\mathbf{x}) &= \langle \overline{\mathbf{K}^{\circ 2}}; f_2\rangle/\phi_2 \\ &= a^3\mathcal{E} : \int_{S(\mathbf{x})} \mathbf{nn}\cdot\overline{X^c\mathbb{T}^{c3}}(\mathbf{x}^\circ + a\mathbf{n}|\mathbf{x},\mathbf{x}^\circ)d\Omega,\end{aligned} \tag{4.22}$$

where the local averaged stress at the test inclusion surface is defined by

$$\begin{aligned}\mathbf{n}\cdot\overline{X^c\mathbb{T}^{c3}}(\tilde{\mathbf{x}}|\mathbf{x},\mathbf{x}^\circ) &= \mathbf{n}\cdot E[\varphi_1\varphi_2 X^c_{1,2}\mathbb{T}^c]/\phi_2(\mathbf{x},\mathbf{x}^\circ) \\ &= -\alpha^{c3}\overline{p}^{c3}\mathbf{n} + 2\mu^c\mathbf{n}\cdot\mathbb{D}[\overline{\mathbf{v}^{c3}} + \alpha^{d3}(\overline{\mathbf{v}}^{d3} - \overline{\mathbf{v}}^{c3})].\end{aligned} \tag{4.23}$$

4.4. The dispersed phase pseudo-turbulent tensors

When considering first order Eqs. (4.13) and (4.14), two types of correlation functions appear, namely $E[\varphi_i\mathbf{u}_i\mathbf{u}_i]$ and $E[\varphi_i\mathbf{u}_i\boldsymbol{\omega}_i]$. As usual, these averages should be transformed into products of their averages plus a component due to pulsation effects around these averages. To this end, a fluctuation field is defined via $\varphi_1(\mathbf{x})\mathbf{u}_1 = \varphi_1(\mathbf{x})\overline{\mathbf{u}}^1 + \varphi_1(\mathbf{x})\mathbf{u}'_1$ for the first correlation and, using (3.4), it may be noted that

$$\begin{aligned}\sum_{i=1}^N E[\varphi_i\mathbf{u}'_i\mathbf{u}'_i] = NE[\varphi_1\mathbf{u}'_1\mathbf{u}'_1] = NE[\varphi_1(\mathbf{u}_1 - \overline{\mathbf{u}}^1)(\mathbf{u}_1 - \overline{\mathbf{u}}^1] = \phi^{(1)}\overline{\mathbf{u}}^1\overline{\mathbf{u}}^1 \\ -2\overline{\mathbf{u}}^1 NE(\varphi_1\mathbf{u}_1) + NE[\varphi_1\mathbf{u}_1\mathbf{u}_1] = \sum_{i=1}^N E[\varphi_i\mathbf{u}_i\mathbf{u}_i] - \phi^{(1)}\overline{\mathbf{u}}^1\overline{\mathbf{u}}^1.\end{aligned} \tag{4.24}$$

So the overall correlation function which is the first term in the r.h.s. may be considered as the sum of two terms: the mean flow convection term $\phi^{(1)}\overline{\mathbf{u}}^1\overline{\mathbf{u}}^1$ of the dispersed phase and a second one which measures the linear velocity pulsations experienced by any inclusion passing through $\mathbf{x}$. It is the first-order agitation (or pseudo-turbulent) tensor of the dispersed phase:

$$\mathbb{A}^1_{uu}(\mathbf{x}) = \sum_{i=1}^N E[\varphi_i\mathbf{u}'_i\mathbf{u}'_i] \tag{4.25}$$

where the superscript indicates the order of the fluctuating field and where the subscript $_{uu}$ indicates which phase velocities are considered to be correlated: here the dispersed phase velocity is correlated with itself. Later (Sec. 5.3) similar functions will be introduced for the continuous phase velocity ($_{vv}$). Finaly, a second fluctuation field $\boldsymbol{\omega}'_1$ can be introduced and a second first-order pseudo-turbulent tensor $\mathbb{A}^1_{u\omega} = \sum_{i=1}^{N} E[\varphi_i \boldsymbol{\omega}'_i \mathbf{u}'_i]$ can be defined.

Other velocity variance tensors are expected to occur. When consdering second-order Eqs. (4.19) and (4.20), four types of correlation function appear, namely $E[\varphi_i\varphi_j\mathbf{u}_i\mathbf{u}_j]$, $E[\varphi_i\varphi_j\mathbf{u}_i\boldsymbol{\omega}_j]$ on one side, and $E[\varphi_i\varphi_j\mathbf{u}_i\mathbf{u}_j]$, $E[\varphi_i\varphi_j\mathbf{u}_j\boldsymbol{\omega}_j]$ on the other side. Extra fluctuation fields have to be defined in order to obtain breakdowns such as (4.24). To begin with, they are $\varphi_i(\mathbf{x})\varphi_j(\mathbf{x}^\circ)\mathbf{u}_i = \varphi_i(\mathbf{x})\varphi_j(\mathbf{x}^\circ)\overline{\mathbf{u}}^2 + \varphi_i(\mathbf{x})\varphi_j(\mathbf{x}^\circ)\mathbf{u}''_i$ and $\varphi_i(\mathbf{x})\varphi_j(\mathbf{x}^\circ)\mathbf{u}_j = \varphi_i(\mathbf{x})\varphi_j(\mathbf{x}^\circ)\overline{\mathbf{u}^{\circ 2}} + \varphi_i(\mathbf{x})\varphi_j(\mathbf{x}^\circ)\mathbf{u}^{\circ''}_2$. Inserting the latter field into the second order correlation function $E[\varphi_i\varphi_j\mathbf{u}_j\mathbf{u}_j]$ gives:

$$\sum_{i=1}\sum_{j\neq i} E[\varphi_i\varphi_j\mathbf{u}_j\mathbf{u}_j] = N(N-1)E[\varphi_1\varphi_2\overline{\mathbf{u}}^{\circ 2}\overline{\mathbf{u}}^{\circ 2}] \tag{4.26}$$

$$+N(N-1)E[\varphi_1\varphi_2\mathbf{u}^{\circ''}_2\mathbf{u}^{\circ''}_2] = \phi^{(2)}\overline{\mathbf{u}}^{\circ 2}\overline{\mathbf{u}}^{\circ 2} + \mathbb{A}^2_{uu^\circ}(\mathbf{x}^\circ,\mathbf{x}),$$

where a second-order unsymmetrical tensor $\mathbb{A}^2_{uu^\circ}(\mathbf{x}^\circ,\mathbf{x})$ which measures the rotationless agitation experienced by any inclusion fixed at $\mathbf{x}^\circ$ provided that there is a second inclusion at $\mathbf{x}$.

Inserting both fluctuation fields into $E[\varphi_i\varphi_j\mathbf{u}_i\mathbf{u}_j]$ leads to a similar breakdown:

$$\sum_{i=1}\sum_{j\neq i} E[\varphi_i\varphi_j\mathbf{u}_i\mathbf{u}_j] = N(N-1)E[\varphi_1\varphi_2\overline{\mathbf{u}}^2\overline{\mathbf{u}^{\circ 2}}] \tag{4.27}$$

$$+N(N-1)E[\varphi_1\varphi_2\mathbf{u}''_1\mathbf{u}^{\circ''}_2] = \phi^{(2)}\overline{\mathbf{u}}^2\overline{\mathbf{u}^{\circ 2}} + \mathbb{A}^2_{uu^\circ}(\mathbf{x}^\circ,\mathbf{x}),$$

where a second-order symmetrical tensor $\mathbb{A}^2_{uu^\circ}(\mathbf{x}^\circ,\mathbf{x})$ which measures the linear velocity correlation between any pair of inclusions located at $\mathbf{x}$ and $\mathbf{x}^\circ$.

Finally, extra fluctuation fields $\boldsymbol{\omega}''_i$ and $\boldsymbol{\omega}^{\circ''}_j$, can be introduced to describe the rotational contribution to inclusion agitation and to display (unsymmetrical) second order pseudo-turbulent tensors $\mathbb{A}^2_{\omega^\circ u}$ and $\mathbb{A}^2_{\omega^\circ u^\circ}$.

It is obvious that the physical origin of these tensors is the same. It has nothing to do with usual turbulence in a single-phase flow. Interactions between inclusions via a medium evolving with its own dynamics set up a highly nonlinear process which reveals itself in an apparently random pulsating motion of both phases super-imposed on their mean motion (unconditioned and conditioned by different test inclusions). Moreover, as far as the continuous phase is concerned,

fluctuations result from local distortions in fluid flow streamlines, including possibly the wakes caused by the submerged inclusions. Note that the latter origin has already been pointed out by BUYEVICH and SHCHELCHKOVA [4].

4.5. The simplified form of the momentum equations

Breaking down the pseudo-turbulent correlation functions allows the momentum equations of any order to be simplified by means of some straightforward transformations. Indeed, the simplified forms follow from both dispersed phase continuity equations of the same order. For the first order:

$$\frac{\partial}{\partial t}\overline{\mathbf{u}}^1 + \overline{\mathbf{u}}^1 \cdot \frac{\partial}{\partial \mathbf{x}}\overline{\mathbf{u}}^1 = -(\phi^{(1)})^{-1}\frac{\partial}{\partial \mathbf{x}} \cdot \mathbb{A}^1_{uu} + m^{-1}\overline{\mathbf{F}}^1 + \mathbf{g}, \tag{4.28}$$

$$\frac{\partial}{\partial t}\overline{\omega}^1 + \overline{\mathbf{u}}^1 \cdot \frac{\partial}{\partial \mathbf{x}}\overline{\omega}^1 = -(\phi^{(1)})^{-1}\frac{\partial}{\partial \mathbf{x}} \cdot \mathbb{A}^1_{\omega u} + I^{-1}\overline{\mathbf{K}}^1, \tag{4.29}$$

and for the second order:

$$\frac{\partial}{\partial t}\overline{\mathbf{u}^{\circ 2}} + \overline{\mathbf{u}^{\circ 2}} \cdot \frac{\partial}{\partial \mathbf{x}^\circ}\overline{\mathbf{u}^{\circ 2}} + \overline{\mathbf{u}^2} \cdot \frac{\partial}{\partial \mathbf{x}}\overline{\mathbf{u}^{\circ 2}} = -(\phi^{(2)})^{-1}\frac{\partial}{\partial \mathbf{x}^\circ} \cdot \mathbb{A}^2_{u^\circ u^\circ} - (\phi^{(2)})^{-1}\frac{\partial}{\partial \mathbf{x}} \cdot \mathbb{A}^2_{uu^\circ} + m^{-1}\overline{\mathbf{F}}^{\circ 2} + \mathbf{g}, \tag{4.30}$$

$$\frac{\partial}{\partial t}\overline{\omega^{\circ 2}} + \overline{\mathbf{u}^{\circ 2}} \cdot \frac{\partial}{\partial \mathbf{x}^\circ}\overline{\boldsymbol{\omega}^{\circ 2}} + \overline{\mathbf{u}}^2 \cdot \frac{\partial}{\partial \mathbf{x}}\overline{\boldsymbol{\omega}^{\circ 2}} = -(\phi^{(2)})^{-1}\frac{\partial}{\partial \mathbf{x}^\circ} \cdot \mathbb{A}^2_{\omega^\circ u^\circ} - (\phi^{(2)})^{-1}\frac{\partial}{\partial \mathbf{x}} \cdot \mathbb{A}^2_{\omega^\circ u} + I^{-1}\overline{\mathbf{K}^{\circ 2}}. \tag{4.31}$$

Many differences can be pointed out with analogous kinetic equations (in their original or moment form) which appear in classical S.M. The most striking one lies in the expression (i.e. 4.15, 4.16, 4.21 and 4.22) of the resultant forces and torques experienced by the test inclusion located at $\mathbf{x}$ or else at $\mathbf{x}^\circ$, and conditionally averaged depending on whether or not another inclusion is present at $\mathbf{x}$. They do not rely on inclusion interactions but on the adjacent carrying phase effects (conditionally averaged).

These momentum equations must be supplemented by the continuity Eqs. (4.12) and (4.18) which have just been used. The latter is an equation for the averaged pair density and it should be replaced by:

$$\frac{\partial \chi_2^\circ}{\partial t} + \frac{\partial}{\partial \mathbf{x}^\circ} \cdot \left[\chi_2^\circ \overline{\mathbf{u}^{\circ 2}}\right] = -\overline{\mathbf{u}}^2 \cdot \frac{\partial \chi_2^\circ}{\partial \mathbf{x}} - (\chi_2^\circ/\phi_1)\frac{\partial}{\partial \mathbf{x}} \cdot \left[(\overline{\mathbf{u}}^2 - \overline{\mathbf{u}}^1)\phi_1\right] \tag{4.32}$$

where the conditional density is defined as

$$\chi_2^\circ = \chi_2(\mathbf{x}^\circ|\mathbf{x}) = \phi_2(\mathbf{x}, \mathbf{x}^\circ)/\phi_1(\mathbf{x}) \tag{4.33}$$

4.6. Boundary conditions

Two types of condition on the boundaries of $\mathcal{V}_x^d$ and on the external boundaries of $\mathcal{V}_{x,x^\circ}^d$ have to be distinguished depending on whether these boundaries are close to an impermeable wall (i.e. $\partial\mathcal{V}_w^c$) or are permeable fluid limits (i.e. $\partial\mathcal{V}_f^c$). Near a wall, the soft collision assumption introduced in Sec. 2 entails velocity continuity conditions:

$$\overline{\mathbf{u}}^1(\mathbf{x}+a\mathbf{n}^b) - a\overline{\boldsymbol{\omega}}^1(\mathbf{x}+a\mathbf{n}^b)\wedge\mathbf{n}^b = \mathbf{v}^b(\mathbf{x}),\ \mathbf{x}\ \text{ on }\ \partial\mathcal{V}_w^c,$$

(4.34)

$$\overline{\mathbf{u}}^2(\mathbf{x}^\circ+a\mathbf{n}^b|\mathbf{x}) - a\overline{\boldsymbol{\omega}}^2(\mathbf{x}^\circ+a\mathbf{n}^b|\mathbf{x})\wedge\mathbf{n}^b = \mathbf{v}^b(\mathbf{x}^\circ),\ \ \mathbf{x}^\circ \text{ on }\ \partial\mathcal{V}_w^c.$$

On the internal boundaries of $\mathcal{V}_{\mathbf{x},\mathbf{x}^\circ}^d$ a similar velocity continuity condition holds:

$$\overline{\mathbf{u}}^2(\mathbf{x}+2a\mathbf{n}|\mathbf{x}) - a\overline{\boldsymbol{\omega}}^2(\mathbf{x}+2a\mathbf{n}|\mathbf{x})\wedge\mathbf{n} = \overline{\mathbf{u}}^2(\mathbf{x}|\mathbf{x}+2a\mathbf{n}) + a\overline{\boldsymbol{\omega}}^2(\mathbf{x}|\mathbf{x}+2a\mathbf{n})\wedge\mathbf{n},\tag{4.35}$$

where $\mathbf{n} = \mathbf{x}^\circ - \mathbf{x}/|\mathbf{x}^\circ - \mathbf{x}|$ is the unit normal along the centre line. No condtion can be prescribed for the density fields such as $\phi_1(\mathbf{x})$ and $\chi_2(\mathbf{x}^\circ|\mathbf{x})$ on all these types of boundaries.

When they pass the fluid boundary of $\partial\mathcal{V}^d$, which coincides with $\partial\mathcal{V}_f^c$ the linear $\mathbf{u}^f$ and angular $\boldsymbol{\omega}^f$ velocities of the inclusions must be given:

$$\overline{\mathbf{u}}^1(\mathbf{x}) = \mathbf{u}^f(\mathbf{x}),\ \ \mathbf{x}\ \text{ on }\partial\mathcal{V}_f^c\ \text{ and }\ \overline{\mathbf{u}}^2(\mathbf{x}^\circ|\mathbf{x}) = \mathbf{u}^f(\mathbf{x}^\circ),\ \ \mathbf{x}^\circ\ \text{ on }\partial\mathcal{V}_f^c \tag{4.36}$$

$$\overline{\boldsymbol{\omega}}^1(\mathbf{x}) = \boldsymbol{\omega}^f(\mathbf{x}),\ \ \mathbf{x}\text{ on }\partial\mathcal{V}_f^c\ \text{ and }\ \overline{\boldsymbol{\omega}}^2(\mathbf{x}^\circ|\mathbf{x}) = \boldsymbol{\omega}^f(\mathbf{x}^\circ),\ \ \mathbf{x}^\circ\text{ on }\partial\mathcal{V}_f^c \tag{4.37}$$

Densities have also to be specified on this fluid part:

$$\phi_1(\mathbf{x}) = \varphi^f(\mathbf{x}),\ \ \mathbf{x}\ \text{ on }\partial\mathcal{V}_f^c\ \text{ and }\ \chi_{\circ 2}(\mathbf{x}^\circ|\mathbf{x}) = \varphi^f(\mathbf{x}^\circ),\ \ \mathbf{x}^\circ\text{ on }\partial\mathcal{V}_f^c \tag{4.38}$$

so that the rate at which they are injected into the system under study or picked off can be known by using (4.36). The overall flux imposed on $\partial\mathcal{V}_f^c$ is assumed to satisfy $\int_{\partial\mathcal{V}_f} \phi_1\overline{\mathbf{u}}^1\cdot\mathbf{n}^f dS = 0$ at any time (where $\mathbf{n}^f$ denotes the unit normal interior to $\partial\mathcal{V}_f^c$). Hence the total number of inclusions is conserved as expressed by the normalization conditions for $\phi_1(\mathbf{x}^\circ)$ and $\chi_2(\mathbf{x}^\circ|\mathbf{x})$ over $\mathcal{V}_{x^\circ}^d$ and $\mathcal{V}_{x,x^\circ}^d$ respectively:

$$\int_{\mathcal{V}_x^d}\phi_1(\mathbf{x})d\mathbf{x} = 1,\qquad \int_{\mathcal{V}_{x,x^\circ}^d}\chi_2(\mathbf{x}^\circ|\mathbf{x})d\mathbf{x}^\circ = 1. \tag{4.39}$$

5. Averaging process for the continuous phase

5.1. The extra fine-grained densities equations

The parallel between the fine-grained equations for both phases is achieved by deriving, for positions in the continuous phase, new equations in the g.f. sense relative to one neighbouring fixed inclusion centre, two fixed inclusion centres, and so on...; these govern mixed fine-grained variables such as $\varphi_i(\mathbf{x},t)X_i^c(\mathbf{x}^\circ,t)$, $\varphi_i(\mathbf{x},t)X_i^c\psi^c(\mathbf{x}^\circ,t)$ and $\varphi_i(\mathbf{x}^\circ,t)\varphi_j(\mathbf{x},t)X_{i,j}^c(\mathbf{x}^{\circ\circ},t)$, $\varphi_i(\mathbf{x}^\circ,t)\varphi_j(\mathbf{x},t)X_{i,j}^c\psi^c(\mathbf{x}^{\circ\circ},t)$ respectively, and they complete the fine-grained equations of Sec. 2.2. By averaging them, a whole sequence of conditionally averaged equations can be produced. In our theory this sequence will be presented up to the third order. LUNDGREN [15] proposed a similar hierarchy of averaged equations directly, without obtaining fine-grained equations beforehand. Furthermore, as the dispersed phase in his case was the immobile matrix of a porous medium, he did not observe some extra terms induced by the motion of test inclusions.

To obtain first the equations to the second order, i.e. with one fixed inclusion, say the first one, consider the following extended equations:

$$\left\{\varphi_1 X_1^c \frac{\partial}{\partial \mathbf{x}^\circ}\cdot(\mathbf{v}^c)\right\} = 0, \tag{5.1}$$

$$\left\{\varphi_1 X_1^c \frac{\partial \mathbf{v}^c}{\partial t}\right\} + \left\{\varphi_1 X_1^c \frac{\partial}{\partial \mathbf{x}^\circ}\cdot(\mathbf{v}^c\mathbf{v}^c)\right\} - \left\{\varphi_1 X_1^c \frac{\partial}{\partial \mathbf{x}^\circ}\cdot\mathbb{T}^c\right\}\Big/\rho^c - \{\varphi_1 X_1^c \mathbf{g}\} = 0. \tag{5.2}$$

As in Sec. 2.2, each g.f. associated with derivatives in the usual sense of functions (i.e. $\{\varphi_1 X_1^c \partial \mathbf{v}^c/\partial t\}$) can be transformed into derivatives in the sense of g.f. of the same functions (i.e. $\partial\varphi_1 X_1^c \mathbf{v}^c/\partial t$). First, the continuity equation conditioned by the presence of an inclusion centre at point $\mathbf{x}$ presents an unexpected extra volume source term in its r.h.s., due to the motion of the test inclusion:

$$\frac{\partial \varphi_1 X_1^c}{\partial t} + \frac{\partial}{\partial \mathbf{x}^\circ}\cdot(\varphi_1 X_1^c \mathbf{v}^c) = -\frac{\partial}{\partial \mathbf{x}}\cdot(\varphi_1 X_1^c \mathbf{u}_1). \tag{5.3}$$

The momentum equation conditioned by the presence of an inclusion centre at point $\mathbf{x}$ is obtained by treating (5.2) in the same way and by introducing the partial surface Dirac g.f. δ_Σ^1 from which the first inclusion surface is excluded:

$$\frac{\partial \varphi_1 X_1^c \mathbf{v}^c}{\partial t} + \frac{\partial}{\partial \mathbf{x}^\circ} \cdot (\varphi_1 X_1^c \mathbf{v}^c \mathbf{v}^c) = -\frac{1}{\rho^c} \frac{\partial}{\partial \mathbf{x}^\circ} (\varphi_1 X_1^c p^c) + \nu^c \Delta^\circ (\varphi_1 X_1^c \mathbf{v}^c) + \nu^c \frac{\partial}{\partial \mathbf{x}^\circ} \left[\frac{\partial}{\partial \mathbf{x}^\circ} \cdot (\varphi_1 X_1^c \mathbf{v}^c) \right] + 2\nu^c \frac{\partial}{\partial \mathbf{x}^\circ} \cdot \left(\mathbb{F}^c \varphi_1 \delta_\Sigma^1 \right) + \frac{1}{\rho^c} \mathbf{n}^c \cdot \mathbb{T}^c \varphi_1 \delta_\Sigma^1 - \frac{\partial}{\partial \mathbf{x}} \cdot [\varphi_1 X_1^c \mathbf{u}_1 \mathbf{v}^c] + \varphi_1 X_1^c \mathbf{g}, \tag{5.4}$$

where $\mathbb{F}^c \varphi_1 \delta_\Sigma^1$ is the fine-grained extra deformation tensor and $\mathbf{n}^c \cdot \mathbb{T}^c \varphi_1 \delta_\Sigma^1$ is the fine-grained interfacial stress exerted upon the inclusions, when the first inclusion centre is at point $\mathbf{x}$. Again, our method allows an extra momentum source term to appear due to the motion of the test inclusion.

To obtain the third-order continuous phase equations, i.e. with two fixed inclusions, the following extended equations are considered:

$$\left\{ \varphi_1 \varphi_2 X_{1,2}^c \frac{\partial}{\partial \mathbf{x}^{\circ\circ}} \cdot (\mathbf{v}^c) \right\} = 0, \tag{5.5}$$

$$\left\{ \varphi_1 \varphi_2 X_{1,2}^c \frac{\partial \mathbf{v}^c}{\partial t} \right\} + \left\{ \varphi_1 \varphi_2 X_{1,2}^c \frac{\partial}{\partial \mathbf{x}^{\circ\circ}} \cdot (\mathbf{v}^c \mathbf{v}^c) \right\} - \left\{ \varphi_1 \varphi_2 X_{1,2}^c \frac{\partial}{\partial \mathbf{x}^{\circ\circ}} \cdot \mathbb{T}^c \right\} / \rho^c - \{ \varphi_1 \varphi_2 X_{1,2}^c \mathbf{g} \} = 0. \tag{5.6}$$

Using transformations like those used above for the second-order equations, one obtains fine-grained continuity and momentum equations similar to (5.3) and (5.4) respectively.

5.2. The revisited Lundgren hierarchy

The Lundgren hierarchy is obtained by averaging the entire sequence of fine-grained equations written for the continuous phase. The property $E[O(f)] = O(E[f])$ will be used again repeatedly. Averaging Eqs. (2.9) and (2.14), and using the various definitions of hydrodynamic variables given in Sec. 3, the first-order equations, valid over $\mathcal{V}_x^c$, are:

$$\frac{\partial \alpha^{c1}}{\partial t} + \frac{\partial}{\partial \mathbf{x}} \cdot (\alpha^{c1} \overline{\mathbf{v}}^{c1}) = 0 \tag{5.7}$$

$$\frac{\partial \alpha^{c1} \overline{\mathbf{v}}^{c1}}{\partial t} + \frac{\partial}{\partial \mathbf{x}} \cdot E[X^c \mathbf{v}^c \mathbf{v}^c] = -\frac{1}{\rho^c} \frac{\partial}{\partial \mathbf{x}} (\alpha^{c1} \overline{p}^{c1}) + \nu^c \Delta (\alpha^{c1} \overline{\mathbf{v}^{c1}}) + \nu^c \frac{\partial}{\partial \mathbf{x}} \left[\frac{\partial}{\partial \mathbf{x}} \cdot (\alpha^{c1} \overline{\mathbf{v}}^{c1}) \right] + 2\nu^c \frac{\partial}{\partial \mathbf{x}} \cdot E[\mathbb{F}^c \delta_\Sigma] + \frac{1}{\rho^c} E[\mathbf{n}^c \cdot \mathbb{T}^c \delta_\Sigma] + \alpha^{c1} \mathbf{g}. \tag{5.8}$$

Next, we can derive the second-order equations, valid over $\mathcal{V}^c_{x,x^\circ}$, by summing the continuity Eq. (5.3) and the momentum Eq. (5.4) over all fixed inclusions and averaging them. Repeating the process, the third-order equations, valid over $\mathcal{V}^c_{x,x^\circ,x^{\circ\circ}}$, are obtained by summing and averaging the corresponding continuity momentum equations.

Now we turn our attention to the important problem of the non-closedness of the Lundgren hierarchy. This characteristic is apparent when examining the interfacial terms in the momentum equations at each order. Considering for example Eq. (5.8), these terms, i.e. $2\nu^c \partial\overline{\partial} x \cdot (E[\mathbb{F}^c \delta_\Sigma]$ and $E[\mathbf{n}^c \cdot \mathbb{T}^c \delta_\Sigma]/\rho^c$, are respectively the averaged extra-deformation tensor and the averaged interfacial force density. The presence of the Dirac function inside the average operator indicates some conditional averaging; as we shall see more precisely in the next paper, this means that one inclusion has to be fixed. At the second order, clearly, these corresponding interaction terms involve one more fixed inclusion and so on.

5.3. Boundary conditions

Continuity equations and non-slip conditions hold on boundaries $\partial\mathcal{V}^c$ of $\mathcal{V}^c_x$, and on the external boundaries of $\mathcal{V}^c_{x,x^\circ}$, $\mathcal{V}^c_{x,x^\circ,x^{\circ\circ}}$. Consequently various conditional averagings of (2.15) give:

$$\overline{\mathbf{v}}^{c1}(\mathbf{x}) = \mathbf{v}^b(\mathbf{x}), \quad \mathbf{x} \text{ on } \partial\mathbf{V}^c; \quad \overline{\mathbf{v}}^{c2}(\mathbf{x}^\circ|\mathbf{x}) = \mathbf{v}^b(\mathbf{x}^\circ), \quad \mathbf{x}^\circ \text{ on } \partial\mathcal{V}^c \tag{5.9}$$

$$\text{and } \overline{\mathbf{v}}^{c3}(\mathbf{x}^{\circ\circ}|\mathbf{x}^\circ, \mathbf{x}) = \mathbf{v}^b(\mathbf{x}^{\circ\circ}), \quad \mathbf{x}^{\circ\circ} \text{ on } \partial\mathcal{V}^c.$$

Conditions of this type have also to be specified on the internal boundaries of $\mathcal{V}^c_{x,x^\circ}$, $\mathcal{V}^c_{x,x^\circ,x^{\circ\circ}}$. They are based on fine grained mass balance equations and non-slip conditions valid on the test inclusions. The corresponding averaged forms at $\mathbf{x}^\circ = \mathbf{x} + a\mathbf{n}$ and at $\mathbf{x}^{\circ\circ} = \mathbf{x}^\circ + a\mathbf{n}$, are (see 2.4):

$$\overline{\mathbf{v}}^{c2}(\mathbf{x} + a\mathbf{n}|\mathbf{x} = \overline{\mathbf{u}}^1(\mathbf{x}) + a\overline{\boldsymbol{\omega}}^1(\mathbf{x}) \wedge \mathbf{n},$$

(5.10)

$$\overline{\mathbf{v}}^{c3}(\mathbf{x}^\circ + a\mathbf{n}|\mathbf{x}^\circ, \mathbf{x}) = \overline{\mathbf{u}}^2(\mathbf{x}^\circ|\mathbf{x}) + a\overline{\boldsymbol{\omega}}^2(\mathbf{x}^\circ|\mathbf{x}) \wedge \mathbf{n}.$$

An extra average boundary condition is obtained by interchanging $\mathbf{x}^\circ$ and $\mathbf{x}$ in the last equation. In this way all the equations of the Lundgren hierarchy are connected to the moment equations of the dispersed phase.

Strictly speaking, there are no particular boundary conditions for α^{c1}, α^{c2}, and α^{c3} which might be associated with field equations such as (5.7) and (5.8), while there are conditions for the densities such as (4.38). Nevertheless, to simplify interfacial momentum conditions $\alpha^{cj} = 1, (j = 1, 2, 3, ...)$ on the walls $\partial\mathcal{V}^c_w$ will be used. This condition is valid if the inclusions keep their spherical shape

when they collide instantaneously. Similar conditions are valid on the surface of the test inclusion. All these conditions are dynamic in nature and correspond to an idealised mechanical response of the inclusion material. For instance, they allow the local averaged stress tensor at the surface $\mathbf{x}^\circ = \mathbf{x} + a\mathbf{n}$ of the test inclusion centred at $\mathbf{x}$ to be simplified, see (4.17), to give:

$$\overline{X^c\mathbb{T}^{c2}}(\mathbf{x}+a\mathbf{n}|\mathbf{x}) = E[\varphi_1 X^c\mathbb{T}^c]/\phi_1(\mathbf{x}) = -\overline{p}^{c2}\mathbb{I} + 2\mu^c\left\{\mathbb{D}(\overline{\mathbf{v}}^{c2}) + \left[(\overline{\mathbf{v}}^{d2} - \overline{\mathbf{v}}^{c2})\frac{\partial}{\partial\mathbf{x}}\alpha^{d2}\right]^s\right\}. \tag{5.11}$$

Here we have distinguished an extra viscous term with a non-zero gradient of α^{d2}. It is represented by a symmetrical tensor involving the relative velocity. The velocity difference depends on momentum exchanges during collisions. In our case, it should be recalled that collisions are assumed to be soft enough not to give rise to significant pressure impulses and the conditional averaged continuous phase velocity merges with the inclusion velocity (5.10) at the point of impact; as a consequence, this extra term will be neglected. Of course, all the results which have just been obtained for the resultant averaged stress can be extended directly to the resultant averaged torque.

Likewise, the local averaged stress tensor (4.23) at the surface $\mathbf{x}^{\circ\circ} = \mathbf{x}^\circ + a\mathbf{n}$ of the test inclusion centred at $\mathbf{x}^\circ$, when another inclusion is centred at $\mathbf{x}$, becomes:

$$\begin{aligned}\overline{X^c\mathbb{T}^{c3}}(\mathbf{x}^\circ + a\mathbf{n}|\mathbf{x},\mathbf{x}^\circ) &= E[\varphi_1\varphi_2 X^c\mathbb{T}^c]/\phi_2(\mathbf{x},\mathbf{x}^\circ) \\ &= -\overline{p}^{c3}\mathbb{I} + 2\mu^c\left\{\mathbb{D}(\overline{\mathbf{v}}^{c3}) + \left[(\overline{\mathbf{v}}^{d3} - \overline{\mathbf{v}}^{c3})\frac{\partial}{\partial\mathbf{x}}\alpha^{d3}\right]^s\right\},\end{aligned} \tag{5.12}$$

where the last viscous term is neglected as above. An extra averaged boundary condition is obtained by interchanging $\mathbf{x}^\circ$ and $\mathbf{x}$.

5.4. The pseudo-turbulent tensors in the continuous phase

In the three first-order momentum equations, we are faced with correlations between continuous phase velocities such as $E[X^c\mathbf{v}^c\mathbf{v}^c(\mathbf{x})]$, $E[\varphi_i X_i^c\mathbf{v}^c\mathbf{v}^c(\mathbf{x}^\circ)]$ and $E[\varphi_i\varphi_j X_{i,j}^c\mathbf{v}^c\mathbf{v}^c(\mathbf{x}^{\circ\circ})]$. These functions can be broken down like the corresponding dispersed phase correlations. The first-order fluctuation field is given via $X^c\mathbf{v}^c(\mathbf{x}) = X^c\overline{\mathbf{v}}^{c1}(\mathbf{x}) + X^c\mathbf{v}^{c'}(\mathbf{x})$ and yields

$$E[X^c\mathbf{v}^c\mathbf{v}^c] = E[X^c\overline{\mathbf{v}}^{c1}\overline{\mathbf{v}}^{c1}] + E[X^c\mathbf{v}^{c'}\mathbf{v}^{c'}] = \alpha^{c1}\overline{\mathbf{v}}^{c1}\overline{\mathbf{v}}^{c1}(\mathbf{x}) + E[X^c\mathbf{v}^{c'}\mathbf{v}^{c'}], \tag{5.13}$$

since the conditional average $\mathbf{v}'^{c1}$ is zero and $(X^c)^2 = X^c$. The first term in the r.h.s. of (5.13) gives rise to the mean flow convection term of the continuous phase in the first order momentum equation. The second one, which measures the agitation in the continuous phase, is the first-order agitation or pseudo-turbulent tensor relative to this phase:

$$\mathbb{A}^1_{vv}(\mathbf{x}) = E[X^c \mathbf{v}^{c'} \mathbf{v}^{c'}]. \tag{5.14}$$

Now, let us consider the second-order fluctuation field defined by

$$\varphi_i(\mathbf{x}) X_i^c \mathbf{v}^c(\mathbf{x}^\circ) = \varphi_i(\mathbf{x}) X_i^c \overline{\mathbf{v}}^{c2}(\mathbf{x}^\circ|\mathbf{x}) + \varphi_i(\mathbf{x}) X_i^c \mathbf{v}^{c''}(\mathbf{x}^\circ). \tag{5.15}$$

Inserting this equation into the overall second-order correlation function gives

$$\sum_{i=1}^{N} E[\varphi_i X_i^c \mathbf{v}^c \mathbf{v}^c] = N E[\varphi_1 X_1^c \overline{\mathbf{v}}^{c2} \overline{\mathbf{v}}^{c2}] + \sum_{i=1}^{N} E[\varphi_i X_i^c \mathbf{v}^{c''} \mathbf{v}^{c''}] \tag{5.16}$$

$$= \phi^{(1)}(\mathbf{x}) \alpha^{c2}(\mathbf{x}^\circ|\mathbf{x}) \overline{\mathbf{v}}^{c2} \overline{\mathbf{v}}^{c2}(\mathbf{x}^\circ|\mathbf{x}) + \mathbb{A}^2_{v^\circ v^\circ}(\mathbf{x}^\circ|\mathbf{x}),$$

where the second-order agitation tensor for the continuous phase $\mathbb{A}^2_{v^\circ v^\circ}(\mathbf{x}^\circ|\mathbf{x})$ has been introduced.

Likewise at the third-order, we arrive at

$$\sum_{i}^{N} \sum_{i \neq j}^{N-1} E[\varphi_i \varphi_j X_{i,j}^c \mathbf{v}^c \mathbf{v}^c] = N(N-1) E[\varphi_1 X_{1,2}^c \overline{\mathbf{v}}^{c2} \overline{\mathbf{v}}^{c2}] \tag{5.17}$$

$$+ \sum_{i=1}^{N} \sum_{i \neq j}^{N-1} E[\varphi_i \varphi_j X_{i,j}^c \mathbf{v}^{c''} \mathbf{v}^{c''}] = \phi^{(2)}(\mathbf{x}^\circ, \mathbf{x}) \alpha^{c3}(\mathbf{x}^{\circ\circ}|\mathbf{x}^\circ, \mathbf{x}) \overline{\mathbf{v}}^{c3} \overline{\mathbf{v}}^{c3}(\mathbf{x}^{\circ\circ}|\mathbf{x}^\circ, \mathbf{x})$$

$$+ \mathbb{A}^3_{v^{\circ\circ} v^{\circ\circ}}(\mathbf{x}^{\circ\circ}|\mathbf{x}^\circ, \mathbf{x}).$$

Furthermore, test inclusion motions generate at any order new correlation terms which are revealed by our approach. In mass equations, there are $E[X_i^c \varphi_i \mathbf{u}_i]$, $E[X_{i,j}^c \varphi_i \varphi_j \mathbf{u}_i]$ and $E[X_{i,j}^c \varphi_i \varphi_j \mathbf{u}_j]$. Some simple transformations are helpful to interpret these terms and these will be proposed in a future paper (part III). These same work will be carried out for $E[X_i^c \varphi_i \mathbf{u}_i \mathbf{v}^c]$, $E[X_{i,j}^c \varphi_i \varphi_j \mathbf{u}_i \mathbf{v}^c]$ and $E[X_{i,j}^c \varphi_i \varphi_j \mathbf{u}_j \mathbf{v}^c]$, which appear in the momentum equations. Cross-correlation agitation tensors between both phases (vu) have to be defined in this way.

5.5. The simplified form of the continuity and momentum equations

With all these definitions at hand, the momentum equations for the three first orders can now be simplified by means of certain transformations that are similar

to those used in Sec. 4.5 for the dispersed phase equations and which are standard in two-phase flow modelling. They are based on using continuity equations. Moreover, all the pressure and viscous terms in the momentum equations will be broken down in such a way that all the terms which look like single-phase flow terms will be placed in the l.h.s. and extra terms which are specific to a two-phase flow case will be placed in the r.h.s.

Consider the first order. By substituting (5.7), (5.13) and (5.14) in (5.8) it is easily found that the first-order momentum equation at $\mathbf{x}$ becomes:

$$\alpha^{c1}\left(\frac{\partial \overline{\mathbf{v}}^{c1}}{\partial t}+\overline{\mathbf{v}}^{c1}\cdot\frac{\partial}{\partial \mathbf{x}}\overline{\mathbf{v}}^{c1}+\left(\frac{\partial}{\partial \mathbf{x}}\overline{p}^{c1}\right)/\rho^c-\nu^c\Delta(\overline{\mathbf{v}}^{c1})\right. \tag{5.18}$$

$$\left.-\nu^c\frac{\partial}{\partial \mathbf{x}}\left[\frac{\partial}{\partial \mathbf{x}}\cdot\overline{\mathbf{v}}^{c1}\right]-\mathbf{g}\right)=\left(\overline{p}^{c1}\mathbb{I}/\rho^c-2\nu^c\mathbb{D}(\overline{\mathbf{v}}^{c1})\right)\cdot\frac{\partial}{\partial \mathbf{x}}\alpha^{d1}-2\nu^c\frac{\partial}{\partial \mathbf{x}}$$

$$\cdot\left[\overline{\mathbf{v}}^{c1}\frac{\partial}{\partial \mathbf{x}}\alpha^{d1}\right]^s+2\nu^c\frac{\partial}{\partial \mathbf{x}}\cdot E[\mathbb{F}^c\delta_\Sigma]+E[\mathbf{n}^c\cdot\mathbb{T}^c\delta_\Sigma]/\rho^c-\frac{\partial}{\partial \mathbf{x}}\cdot\mathbb{A}^1_{vv}.$$

The second and third-order momentum equations

$$\alpha^{c2}\left\{\frac{\partial \overline{\mathbf{v}}^{c2}}{\partial t}+\overline{\mathbf{v}}^{c2}\cdot\frac{\partial}{\partial \mathbf{x}^\circ}\overline{\mathbf{v}}^{c2}+\left(\frac{\partial}{\partial \mathbf{x}^\circ}\overline{p}^{c2}\right)/\rho^c-\nu^c\Delta^\circ(\overline{\mathbf{v}}^{c2})\right. \tag{5.19}$$

$$\left.-\nu^c\frac{\partial}{\partial \mathbf{x}^\circ}\left[\frac{\partial}{\partial \mathbf{x}^\circ}\cdot\overline{\mathbf{v}}^{c2}\right]-\mathbf{g}\right\}=\left(\overline{p}^{c2}\mathbb{I}/\rho^c-2\nu^c\mathbb{D}^\circ(\overline{\mathbf{v}}^{c2})\right)\cdot\frac{\partial}{\partial \mathbf{x}^\circ}\alpha^{d2}$$

$$-2\nu^c\frac{\partial}{\partial \mathbf{x}^\circ}\cdot\left[\overline{\mathbf{v}}^{c2}\frac{\partial}{\partial \mathbf{x}^\circ}\alpha^{d2}\right]^s+2\nu^c(\phi_1)^{-1}\frac{\partial}{\partial \mathbf{x}^\circ}\cdot E[\mathbb{F}^c\varphi_1\delta^1_\Sigma]$$

$$+(\rho^c\phi_1)^{-1}E[\mathbf{n}^c\cdot\mathbb{T}^c\varphi_1\delta^1_\Sigma]-(\phi^{(1)})^{-1}\frac{\partial}{\partial \mathbf{x}^\circ}\cdot\mathbb{A}^2_{v^\circ v^\circ}$$

$$-(\phi_1)^{-1}\frac{\partial}{\partial \mathbf{x}}\cdot E[\varphi_1 X_1^c\mathbf{u}_1\mathbf{v}^c]+(\phi_1)^{-1}\overline{\mathbf{v}}^{c2}\cdot\frac{\partial}{\partial \mathbf{x}}E[\varphi_1 X_1^c\mathbf{u}_1]$$

$$\alpha^{c3}\left\{\frac{\partial \overline{\mathbf{v}}^{c3}}{\partial t}+\overline{\mathbf{v}}^{c3}\cdot\frac{\partial}{\partial \mathbf{x}^{\circ\circ}}\overline{\mathbf{v}}^{c3}+\left(\frac{\partial}{\partial \mathbf{x}^{\circ\circ}}\overline{p}^{c3}\right)/\rho^c-\nu^c\Delta^{\circ\circ}(\overline{\mathbf{v}}^{c3})\right. \tag{5.20}$$

$$\left.-\nu^c\frac{\partial}{\partial \mathbf{x}^{\circ\circ}}\left[\frac{\partial}{\partial \mathbf{x}^{\circ\circ}}\cdot\overline{\mathbf{v}}^{c3}\right]-\mathbf{g}\right\}=\left(\overline{p}^{c3}\mathbb{I}/\rho^c-2\nu^c\mathbb{D}^{\circ\circ}(\overline{\mathbf{v}}^{c3})\right)\cdot\frac{\partial}{\partial \mathbf{x}^{\circ\circ}}\alpha^{d3}$$

(5.20) [cont.]
$$-2\nu^c \frac{\partial}{\partial \mathbf{x}^{\circ\circ}} \cdot \left[\overline{\mathbf{v}}^{c3} \frac{\partial}{\partial \mathbf{x}^{\circ\circ}} \alpha^{d3} \right]^s + 2\nu^c (\phi_2)^{-1} \frac{\partial}{\partial \mathbf{x}^{\circ\circ}} \cdot E[\mathbb{F}^c \varphi_1 \varphi_2 \delta_\Sigma^{1,2}]$$

$$+(\rho^c \phi_2)^{-1} E[\mathbf{n}^c \cdot \mathbb{T}^c \varphi_1 \varphi_2 \delta_\Sigma^{1,2}] - (\phi^{(2)})^{-1} \frac{\partial}{\partial \mathbf{x}^{\circ\circ}} \cdot \mathbb{A}^3_{v^{\circ\circ} v^{\circ\circ}}$$

$$-(\phi_2)^{-1} \frac{\partial}{\partial \mathbf{x}} \cdot E[X^c_{1,2} \varphi_1 \varphi_2 \mathbf{u}_1 \mathbf{v}^c] - (\phi_2)^{-1} \frac{\partial}{\partial \mathbf{x}^\circ} \cdot E[X^c_{1,2} \varphi_1 \varphi_2 \mathbf{u}_2 \mathbf{v}^c]$$

$$+(\phi_2)^{-1} \overline{\mathbf{v}}^{c3} \cdot \frac{\partial}{\partial \mathbf{x}} E[X^c_{1,2} \varphi_1 \varphi_2 \mathbf{u}_1] + (\phi_2)^{-1} \overline{\mathbf{v}}^{c3} \cdot \frac{\partial}{\partial \mathbf{x}^\circ} E[X^c_{1,2} \varphi_1 \varphi_2 \mathbf{u}_2]$$

may also be simplified in a similar way thanks to the averaged continuous phase continuity equations at the corresponding order, derived from Sec. 5.1, i.e.

(5.21)
$$\frac{\partial \alpha^{c2} \phi_1}{\partial t} + \frac{\partial}{\partial \mathbf{x}^\circ} \cdot (\alpha^{c2} \phi_1 \overline{\mathbf{v}}^{c2}) = -\frac{\partial}{\partial \mathbf{x}} \cdot E[\varphi_1 X^c_1 \mathbf{u}_1],$$

(5.22)
$$\frac{\partial \alpha^{c3} \phi_2}{\partial t} + \frac{\partial}{\partial \mathbf{x}^{\circ\circ}} \cdot (\alpha^{c3} \phi_2 \overline{\mathbf{v}}^{c3}) = -\frac{\partial}{\partial \mathbf{x}} \cdot E[\varphi_1 \varphi_2 X^c_{1,2} \mathbf{u}_1]$$

$$-\frac{\partial}{\partial \mathbf{x}^\circ} \cdot E[\varphi_1 \varphi_2 X^c_{1,2} \mathbf{u}_2].$$

Moreover, the continuous phase continuity equations themselves can also be simplified from the dispersed phase continuity Eqs. (4.12) and (4.18).

6. Conclusions

This part I presents a general statistical method for deriving averaged equations for non-turbulent dispersed flows. It belongs to a developing class of methods which mixes the kinetic theory of gases and classical continuum mechanics approaches. Probability in our case refers merely to repeated trials which are themselves a practical consequence of apprehending systems with a large number of degrees of freedom. The only randomising effect comes from the initial conditions of the dispersed phase. Brownian motion and collisions between inclusions are not taken into account.

In standard two-fluid models, the dispersed phase is poorly defined by two single moments, the averaged local volume fraction and the averaged velocity. Here, it is possible to use a natural way of introducing hidden characteristics of the dispersed phase. For instance, the averaged angular velocity field has been introduced. Provided inclusions can be defined by a finite number of parameters with their own equation of evolution, other types of inclusion may be envisaged,

e.g. oscillating bubbles in an acoustic field, non-spherical particles orientating themselves in a shear flow, particles having a dipole interacting with an external electromagnetic field, etc. As a rule, an infinite number of coordinates are strictly required in more complex cases, such as spherical fluid inclusions with some viscosity, immersed in another fluid and inclusions with some deformability (thus requiring conditions to be prescribed for the component of stress normal to the inclusion surface); in fact, only a finite number of them prove to be necessary. It must be admitted that in many real cases, particles often have irregular shapes which may be either permanent (solid particles) or continuously developing (distorted bubbles). Thus, it may be too complicated to enlarge the set of geometrical characteristics of a particle to many extra parameters. Because of these mathematical and physical difficulties, our method is obviously not able to treat all practical flow problems even if they are dilute and laminar. However, in many cases, it continues to serve one important purpose. It can be used as a reliable guide for proposing new closure laws and to assess their validity, either by indicating their structure or by providing the order of magnitude of certain coefficients.

The obtained hierarchies now have to be truncated simultaneously using the same perturbation method involving a small parameter. In many statistical theories devoted to two-phase flows, the assumption of diluteness has been introduced. Our approach presented in a future paper is also based on the same parameter, i.e. the spatially averaged dispersed phase volume fraction. Note that the precision of our approach is somewhat restricted from the outset since only the first order equations of these hierarchies (second- and third-order equations for the dispersed and continuous phases respectively) can be derived in practice, at least if nonlinear terms are kept. On the other hand, there will be no *a priori* assumption about homogeneity of the dispersed phase volume fraction since all evolution equations controlling this phase are available. However, the equations defined at the end of this paper are not yet ready to be treated by any asymptotic method. In subsequent papers they will be simplified beforehand and all the terms appearing in them will receive a straightforward interpretation.

References

1. J. L. ACHARD, *Contribution à l'étude dynamique des écoulements diphasiques gaz-liquide*, I.N.P. Grenoble, Doctorat d'État 1978.

2. A. BIESHEUVEL and L. VAN WIJNGAARDEN, *Two-phase flow equation for a dilute dispersion of gas bubbles in liquid*, J. Fluid Mech., **148**, 301–318, 1984.

3. M. BOUIX, *Les fonctions généralisées ou distributions*, Masson 1964.

4. Y. A. BUYEVICH and I. N. SHCHELCHKOVA, *Flow of dense suspensions*, Prog. Aerospace Sci., **18**, 121–150, 1978.

5. C. CERCIGNANI, *Kinetic theory and gas dynamics*, Springer, 1988.

6. J. M. DELHAYE and J. L. ACHARD, *On the use of averaging operators in two phase flow modeling* [in:] Symp. Thermal Hydraulic Aspects of Nuclear Reactor Safety [Ed.] O.C. Jones and S.G. Bankoff, ASME, New York, 5–78, 1977.

7. C. DOPAZO, *On conditioned averages for intermittent turbulent flows*, J. Fluid Mech., **81**, 433–438, 1977.

8. H. GRAD, *Principles of the kinetic theory of gases*, Handbuch der Physik, **12**, Springer, 1958.

9. E. J. HINCH, *An averaged-equation approach to particle interactions in a fluid suspension*, J. Fluid Mech., **83**, 695–720, 1977.

10. D. D. JOSEPH and T. S. LUNDGREN, *Ensemble averaged and mixture theory equations for incompressible fluid-particle suspensions*, Int. J. Multiphase Flow, **16**, 35–42, 1990.

11. YU L. KLIMONTOVICH, *The statistical theory of non-equilibrium processes in a plasma*, Pergamon, 1967.

12. D. L. KOCH, *Hydrodynamic diffusion in dilute sedimenting suspensions at moderate Reynolds numbers*, Phys. Fluids, **5**, 1141–1155, 1993.

13. V. KUMARAN and D. L. KOCH, *The effects of hydrodynamic interactions on the average properties of a bidisperse suspension of high Reynolds number, low Weber number bubbles*, Phys. Fluids, **A 5**, 1123–1134, 1993.

14. J. LEWI, *Contribution à l'étude dynamique des écoulements diphasiques gaz liquide*, Paris VI, Doctorat d'État, 1975.

15. T. S. LUNDGREN, *Slow flow through stationary random beds and suspensions of spheres*, J. Fluid Mech., **51**, 273–299, 1972.

16. VAN L. WIJNGAARDEN, *On the equations of motion for mixtures of liquid and gas bubbles*, J. Fluid Mech., **33**, 465–474, 1968.

17. D. Z. ZHANG and A. PROSPERETTI, *Effective equations for disperse two-phase flows and their closure in the dilute limit*, J. Fluid Mech., **26**, 245–268, 1995.

18. D. Z. ZHANG and A. PROSPERETTI, *Momentum and energy equations for disperse two-phase flows and their closure for dilute suspensions*, Int. J. Multiphase Flow, **23**, 425–453, 1997.

Received September 21, 1998; revised version October 11, 1999.

Arch. Mech., **52**, 1, pp. 55–88, Warszawa 2000

Irreducible representations for constitutive equations of anisotropic solids II: crystal and quasicrystal classes D_{2m+1d}, D_{2m+1} and C_{2m+1v}

H. XIAO, O.T. BRUHNS and A. MEYERS

Institute of Mechanics I, Ruhr-University Bochum
D-44780 Bochum, Germany

A SIMPLE, UNIFIED PROCEDURE is applied to derive irreducible nonpolynomial representations for scalar-, vector-, skewsymmetric and symmetric second order tensor-valued anisotropic constitutive equations involving any finite number of vector variables and second order tensor variables. In this part, our concern is for all crystal classes and quasicrystal classes D_{2m+1d}, D_{2m+1} and C_{2m+1v} for all integers $m \geq 1$.

1. Introduction

IN CONTINUUM PHYSICS, complicated and varied macroscopic physical behaviours of anisotropic solids are modelled by scalar-, vector- and second order tensor-valued functions of vector variables and second order tensor variables, commonly known as material constitutive equations. Material objectivity and material symmetry place a combined invariance restriction under the material symmetry group on the tensor function forms of material constitutive equations. General reduced forms, or representations, of material constitutive equations under the just-mentioned universal invariance restriction, constitute a rational basis for consistent mathematical modelling of complex material behaviours. In the past decades, this aspect was extensively studied. Now many results for polynomial representations and some results for nonpolynomial representations are available. For detail, see, e.g., the monographs by TRUESDELL and NOLL [11], SPENCER [10], BOEHLER [4], RYCHLEWSKI [7], ERINGEN and MAUGIN [5], KIRAL and ERINGEN [6], BETTEN [2], SMITH [9], and the recent reviews by BETTEN [1], RYCHLEWSKI and ZHANG [8] and ZHENG [21], *et al.* Some references are listed in Part I of this series of paper.

Although now many results in many cases are available, general aspects of tensor function representations, especially nonpolynomial representations, are still under investigation, which are concerned with any finite number of vector variables and tensor variables and all kinds of material symmetry groups including

the 32 crystal classes and all denumerably infinitely many quasicrystal classes. As compared with polynomial representations, nonpolynomial representations are not only more general both in notion and in scope, but may furnish more compact representations for constitutive equations, as noted by WANG [12] for isotropic cases and by BOEHLER [3 – 4] for anisotropic cases. There are relatively few results for irreducible nonpolynomial representations for the foregoing general cases, except for those concerning some simple material symmetry groups (see the related references in Part I of this series, i.e. XIAO, BRUHNS and MEYERS [20]. Henceforth, the just-mentioned reference will be simply referred to as Part I). In a series of work consisting of three parts, we aim to provide irreducible nonpolynomial representations for scalar-, vector-, skewsymmetric and symmetric second order tensor-valued anisotropic constitutive equations of any finite number of vector variables and second order tensor variables relative to all crystal and quasicrystal classes as subgroups of the cylindrical group $D_{\infty h}$. In the second part, we consider the crystal and quasicrystal classes D_{2m+1d}, D_{2m+1} and C_{2m+1v} for all integers $m \geq 1$.

As it has been done in Part I, we shall apply a unified procedure based on [13 – 15] and [18] to derive the desired functional bases and generating sets. For a detailed account of such a unified procedure and for notations and preliminaries, refer to Secs. 2 – 3 in Part I and the related reference therein.

2. Crystal and quasicrystal classes D_{2m+1d}

The classes at issue are of the form

$$D_{2m+1d}(\mathbf{n},\mathbf{e}) = \{\pm\mathbf{R}_{\mathbf{n}}^{2k\pi/2m+1}, \pm\mathbf{R}_{\mathbf{a}_k}^{\pi} | \mathbf{a}_k = \mathbf{R}_{\mathbf{n}}^{2k\pi/2m+1}\mathbf{e}, \quad k = 1, \cdots, 2m+1\}\,. \tag{2.1}$$

They include the trigonal crystal class D_{3d} as the particular case when $m = 1$. Henceforth, $\mathbf{a}$ will be used to represent one of the *two-fold axis* vectors $\mathbf{a}_1, \cdots, \mathbf{a}_{2m+1}$.

2.1. Single variables

(i) A single vector $\mathbf{u}$

Each anisotropic function of a vector variable $\mathbf{u}$ under the group D_{2m+1d} may be extended as an isotropic function of the three variables $(\mathbf{u}, \mathbf{E}\boldsymbol{\eta}_{2m}(\overset{\circ}{\mathbf{u}}), \mathbf{n}\otimes\mathbf{n})$ (see Theorem 1 in XIAO [15]). Applying the related result for isotropic functions and following the unified procedure outlined in Sec. 3 in Part I, we construct the following table.

V $\{\mathbf{u}, \mathbf{u} \times \boldsymbol{\eta}_{2m}(\overset{\circ}{\mathbf{u}}), \alpha_{2m+1}(\overset{\circ}{\mathbf{u}})\boldsymbol{\eta}_{2m}(\overset{\circ}{\mathbf{u}})\}$ $(\equiv V_{2m+1}(\mathbf{u}))$

Skw $\{\mathbf{E}\boldsymbol{\eta}_{2m}(\overset{\circ}{\mathbf{u}}), \mathbf{u} \wedge (\mathbf{u} \times \boldsymbol{\eta}_{2m}(\overset{\circ}{\mathbf{u}})), \alpha_{2m+1}(\overset{\circ}{\mathbf{u}})\mathbf{u} \wedge \boldsymbol{\eta}_{2m}(\overset{\circ}{\mathbf{u}})\}$
$(\equiv \mathrm{Skw}_{2m+1}(\mathbf{u}))$

Sym $\{\mathbf{I}, \mathbf{n} \otimes \mathbf{n}, \overset{\circ}{\mathbf{u}} \otimes \overset{\circ}{\mathbf{u}}, \mathbf{n} \vee (\mathbf{n} \times \boldsymbol{\eta}_{2m}(\overset{\circ}{\mathbf{u}})), \overset{\circ}{\mathbf{u}} \vee (\mathbf{u} \times \boldsymbol{\eta}_{2m}(\overset{\circ}{\mathbf{u}})),$
$\alpha_{2m+1}(\overset{\circ}{\mathbf{u}})(\overset{\circ}{\mathbf{u}} \vee \boldsymbol{\eta}_{2m}(\overset{\circ}{\mathbf{u}}) - (\mathbf{u} \cdot \mathbf{n})\mathbf{n} \vee \boldsymbol{\eta}_{2m}(\overset{\circ}{\mathbf{u}}))\}$ $(\equiv \mathrm{Sym}_{2m+1}(\mathbf{u}))$

R $\mathbf{r} \cdot \mathbf{u}, [\mathbf{r}, \mathbf{u}, \boldsymbol{\eta}_{2m}(\overset{\circ}{\mathbf{u}})], \alpha_{2m+1}(\overset{\circ}{\mathbf{u}})\, \overset{\circ}{\mathbf{r}} \cdot \boldsymbol{\eta}_{2m}(\overset{\circ}{\mathbf{u}})$;
$\mathrm{tr}\mathbf{H}(\mathbf{E}\boldsymbol{\eta}_{2m}(\overset{\circ}{\mathbf{u}})), [\mathbf{u}, \mathbf{H}\mathbf{u}, \boldsymbol{\eta}_{2m}(\overset{\circ}{\mathbf{u}})], \alpha_{2m+1}(\overset{\circ}{\mathbf{u}})\boldsymbol{\eta}_{2m}(\overset{\circ}{\mathbf{u}}) \cdot \mathbf{H}\mathbf{u}$;
$\mathrm{tr}\mathbf{C}, \mathbf{n} \cdot \mathbf{C}\mathbf{n}, \overset{\circ}{\mathbf{u}} \cdot \overset{\circ}{\mathbf{C}}\overset{\circ}{\mathbf{u}}, [\mathbf{n}, \boldsymbol{\eta}_{2m}(\overset{\circ}{\mathbf{u}}), \overset{\circ}{\mathbf{C}}\,\mathbf{n}], [\mathbf{u}, \boldsymbol{\eta}_{2m}(\overset{\circ}{\mathbf{u}}), \overset{\circ}{\mathbf{C}}\overset{\circ}{\mathbf{u}}]$,
$\alpha_{2m}(\overset{\circ}{\mathbf{u}})(\boldsymbol{\eta}_{2m}(\overset{\circ}{\mathbf{u}}) \cdot \overset{\circ}{\mathbf{C}}\overset{\circ}{\mathbf{u}} - (\mathbf{u} \cdot \mathbf{n})\boldsymbol{\eta}_{2m}(\overset{\circ}{\mathbf{u}}) \cdot \overset{\circ}{\mathbf{C}}\,\mathbf{n})$;
$\{(\mathbf{u} \cdot \mathbf{n})^2, |\overset{\circ}{\mathbf{u}}|^2, \alpha_{4m+2}(\overset{\circ}{\mathbf{u}}), (\mathbf{u} \cdot \mathbf{n})\beta_{2m+1}(\overset{\circ}{\mathbf{u}})\}$ $(\equiv I_{2m+1}(\mathbf{u}))$.

First, we show that the presented set $I_{2m+1}(\mathbf{u})$ of invariants is a desired functional basis. In fact, an isotropic functional basis of $(\mathbf{u}, \mathbf{E}\boldsymbol{\eta}_{2m}(\overset{\circ}{\mathbf{u}}), \mathbf{n} \otimes \mathbf{n})$ is given by

$$|\mathbf{u}|^2, (\mathbf{u} \cdot \mathbf{n})^2, \mathbf{u} \cdot (\mathbf{E}\boldsymbol{\eta}_{2m}(\overset{\circ}{\mathbf{u}}))^2\mathbf{u}, \mathbf{u} \cdot (\mathbf{n} \otimes \mathbf{n})(\mathbf{E}\boldsymbol{\eta}_{2m}(\overset{\circ}{\mathbf{u}}))\mathbf{u},$$
$$\mathbf{u} \cdot (\mathbf{E}\boldsymbol{\eta}_{2m}(\overset{\circ}{\mathbf{u}}))\,(\mathbf{n} \otimes \mathbf{n})(\mathbf{E}\boldsymbol{\eta}_{2m}(\overset{\circ}{\mathbf{u}}))^2\mathbf{u}.$$

In deriving the above basis, many redundant invariants have been removed by using the equalities

$$(\mathbf{n} \otimes \mathbf{n})^2 = \mathbf{n} \otimes \mathbf{n}, \quad (\mathbf{E}\boldsymbol{\eta}_{2m}(\overset{\circ}{\mathbf{u}}))^2\mathbf{n} = -|\overset{\circ}{\mathbf{u}}|^{4m}\mathbf{n}. \tag{2.2}$$

Then, using the second equality above and the identity

$$(\mathbf{E}\mathbf{u})\mathbf{v} = \mathbf{v} \times \mathbf{u}, \tag{2.3}$$

as well as the decomposition formula (2.15) in Part I, we know that the first four invariants in the foregoing basis yield the set $I_{2m+1}(\mathbf{u})$ of invariants and, moreover, the last invariant given before is redundant. Thus, the presented set $I_{2m+1}(\mathbf{u})$ is a desired functional basis. It may readily be proved that this basis is irreducible.

Next, we prove that the two presented sets $V_{2m+1}(\mathbf{u})$ and $\mathrm{Skw}_{2m+1}(\mathbf{u})$ supply a desired vector generating set and a desired skewsymmetric tensor generating set, respectively. In fact, let $\mathbf{u} \times \boldsymbol{\eta}_{2m}(\overset{\circ}{\mathbf{u}}) = \mathbf{0}$. Then $\mathbf{u} = x\mathbf{a}_k$ or $\mathbf{u} = x\mathbf{n}$. It can easily be shown that the foregoing two sets obey the criterion (2.3) given in

Part I. Now let $\mathbf{u} \times \boldsymbol{\eta}_{2m+1}(\overset{\circ}{\mathbf{u}}) \neq \mathbf{0}$. Then we have (see (2.5), (2.6) and (2.8) in Part I)

$$\mathit{\Gamma}(\mathbf{u}, \mathbf{E}\boldsymbol{\eta}_{2m}(\overset{\circ}{\mathbf{u}})) \subset C_{2h}(\boldsymbol{\eta}_{2m}(\overset{\circ}{\mathbf{u}})) \subset D_{\infty h}(\mathbf{n}),$$

and therefore we have $\mathit{\Gamma}(\mathbf{u}, \mathbf{E}\boldsymbol{\eta}_{2m}(\overset{\circ}{\mathbf{u}}), \mathbf{n} \otimes \mathbf{n}) = \mathit{\Gamma}(\mathbf{u}, \mathbf{E}\boldsymbol{\eta}_{2m}(\overset{\circ}{\mathbf{u}}))$. From the latter and the criterion (2.3) given in Part I, we infer that for the case for $\mathbf{u}$ at issue, isotropic generating sets for the three variables $(\mathbf{u}, \mathbf{E}\boldsymbol{\eta}_{2m}(\overset{\circ}{\mathbf{u}}), \mathbf{n}\otimes\mathbf{n})$ are obtainable from those for the two variables $(\mathbf{u}, \mathbf{E}\boldsymbol{\eta}_{2m}(\overset{\circ}{\mathbf{u}}))$. By applying the related result for isotropic functions we know that, for the vector-valued and skewsymmetric tensor-valued cases, the latter are just given by the two presented sets $V_{2m+1}(\mathbf{u})$ and $\mathrm{Skw}_{2m+1}(\mathbf{u})$.

Finally, we show that the presented set $\mathrm{Sym}_{2m+1}(\mathbf{u})$ supplies a desired symmetric tensor generating set. To this end we prove that this set obeys the criterion (2.3) given in Part I. When $\overset{\circ}{\mathbf{u}} = \mathbf{0}$, the just-mentioned fact is evidently true. Now let $\overset{\circ}{\mathbf{u}} \neq \mathbf{0}$. Then the triplet $(\mathbf{n}, \overset{\circ}{\mathbf{u}}, \mathbf{n}\times \overset{\circ}{\mathbf{u}})$, denoted by $(\mathbf{e}_3, \mathbf{e}_1, \mathbf{e}_2)$, is an orthogonalized basis of the vector space V, and hence the six tensors $\mathbf{e}_i \vee \mathbf{e}_j$, $i,\ j = 1, 2, 3$, form an orthogonalized basis of the symmetric tensor space Sym. It is easily understood that the first three generators in the set $\mathrm{Sym}_{2m+1}(\mathbf{u})$ yield the three tensors $\mathbf{e}_i \otimes \mathbf{e}_i$, i=1, 2, 3. Thus, we have

$$\text{rank}\ \ \mathrm{Sym}_{2m+1}(\mathbf{u}) = 3 + \text{rank}\{\mathbf{G}_1, \mathbf{G}_2, \mathbf{G}_3\},$$

where the $\mathbf{G}_i$ are used to denote the last three generators in the set $\mathrm{Sym}_{2m+1}(\mathbf{u})$, i.e.

$$\mathbf{G}_1 = \mathbf{n} \vee (\mathbf{n} \times \boldsymbol{\eta}),\ \mathbf{G}_2 = \overset{\circ}{\mathbf{u}} \vee (\mathbf{u} \times \boldsymbol{\eta}),\ \ \mathbf{G}_3 = \alpha_{2m+1}(\overset{\circ}{\mathbf{u}})(\overset{\circ}{\mathbf{u}} \vee \boldsymbol{\eta} - (\mathbf{u} \cdot \mathbf{n})\mathbf{n} \vee \boldsymbol{\eta}),$$

with $\boldsymbol{\eta} = \boldsymbol{\eta}_{2m}(\overset{\circ}{\mathbf{u}})$. We have

$$\begin{aligned}
\Delta &= \begin{vmatrix} \mathbf{G}_1 : (\mathbf{e}_1 \vee \mathbf{e}_2) & \mathbf{G}_1 : (\mathbf{e}_2 \vee \mathbf{e}_3) & \mathbf{G}_1 : (\mathbf{e}_3 \vee \mathbf{e}_1) \\ \mathbf{G}_2 : (\mathbf{e}_1 \vee \mathbf{e}_2) & \mathbf{G}_2 : (\mathbf{e}_2 \vee \mathbf{e}_3) & \mathbf{G}_2 : (\mathbf{e}_3 \vee \mathbf{e}_1) \\ \mathbf{G}_3 : (\mathbf{e}_1 \vee \mathbf{e}_2) & \mathbf{G}_3 : (\mathbf{e}_2 \vee \mathbf{e}_3) & \mathbf{G}_3 : (\mathbf{e}_3 \vee \mathbf{e}_1) \end{vmatrix} \\
&= 8\alpha_{2m+1}(\overset{\circ}{\mathbf{u}}) \begin{vmatrix} 0 & \alpha_{2m+1}(\overset{\circ}{\mathbf{u}}) & \beta_{2m+1}(\overset{\circ}{\mathbf{u}}) \\ xy^2\alpha_{2m+1}(\overset{\circ}{\mathbf{u}}) & 0 & -y^2\beta_{2m+1}(\overset{\circ}{\mathbf{u}}) \\ -y^2\beta_{2m+1}(\overset{\circ}{\mathbf{u}}) & x\beta_{2m+1}(\overset{\circ}{\mathbf{u}}) & -x\alpha_{2m+1}(\overset{\circ}{\mathbf{u}}) \end{vmatrix} \\
&= 8y^4(\alpha_{2m+1}(\overset{\circ}{\mathbf{u}}))^2(x^2y^{4m} + (\beta_{2m+1}(\mathbf{u}))^2),
\end{aligned}$$

where $x = \mathbf{u} \cdot \mathbf{n}$ and $y = |\ \overset{\circ}{\mathbf{u}}\ |$. Hence, for $\overset{\circ}{\mathbf{u}} \neq \mathbf{0}$ we deduce

$$\text{rank Sym}_{2m+1}(\mathbf{u}) = \begin{cases} 6 \text{ if } \Delta \neq 0\,, \\ 4 \text{ if } \alpha_{2m+1}(\overset{\circ}{\mathbf{u}}) = 0\,, \\ 4 \text{ if } x = \beta_{2m+1}(\overset{\circ}{\mathbf{u}}) = 0\,. \end{cases}$$

From these results and

$$\Gamma(\mathbf{u}) \cap D_{2m+1d} = \begin{cases} C_{1h}(\mathbf{a}_k) \text{ if } \alpha_{2m+1}(\overset{\circ}{\mathbf{u}}) = 0\,, \\ C_2(\mathbf{a}_k) \text{ if } x = \beta_{2m+1}(\overset{\circ}{\mathbf{u}}) = 0\,, \end{cases}$$

for $\overset{\circ}{\mathbf{u}} \neq \mathbf{0}$, as well as Table 3 given in Sec. 2 in Part I, we infer that the set $\text{Sym}_{2m+1}(\mathbf{u})$ obeys the criterion (2.3) in Part I.

Each generating set presented is minimal and, of course, irreducible.

(ii) A skewsymmetric tensor $\mathbf{W}$

Skw $\{\mathbf{W}, \mathbf{E}\boldsymbol{\eta}_{2m}(\mathbf{Wn}), \mathbf{W}(\mathbf{E}\boldsymbol{\eta}_{2m}(\mathbf{Wn})) - (\mathbf{E}\boldsymbol{\eta}_{2m}(\mathbf{Wn}))\mathbf{W}\}$
$(\equiv \text{Skw}_{2m+1}(\mathbf{W}))$

Sym $\{\mathbf{I}, \mathbf{n} \otimes \mathbf{n}, \mathbf{Wn} \otimes \mathbf{Wn}, \mathbf{n} \vee \mathbf{Wn}, \mathbf{W}(\mathbf{E}\boldsymbol{\eta}_{2m}(\mathbf{Wn})) + (\mathbf{E}\boldsymbol{\eta}_{2m}(\mathbf{Wn}))\mathbf{W},$
$\mathbf{W}^2\mathbf{n} \vee (\mathbf{n} \times \boldsymbol{\eta}_{2m}(\mathbf{Wn}))\}$ $(\equiv \text{Sym}_{2m+1}(\mathbf{W}))$

R $\text{tr}\mathbf{H}\ \mathbf{W}, \text{tr}\mathbf{H}(\mathbf{E}\boldsymbol{\eta}_{2m}(\mathbf{Wn})), \text{tr}\mathbf{H}\ \mathbf{W}(\mathbf{E}\boldsymbol{\eta}_{2m}(\mathbf{Wn}))$; $\text{tr}\mathbf{C}, \mathbf{n} \cdot \mathbf{Cn},$
$(\mathbf{Wn}) \cdot \overset{\circ}{\mathbf{C}}\ \mathbf{Wn}, (\overset{\circ}{\mathbf{C}}\ \mathbf{n}) \cdot \mathbf{Wn}, \text{tr}\overset{\circ}{\mathbf{C}}\ \mathbf{W}(\mathbf{E}\boldsymbol{\eta}_{2m}(\mathbf{Wn})), [\mathbf{n}, \boldsymbol{\eta}_{2m}(\mathbf{Wn}), \overset{\circ}{\mathbf{C}}\ \mathbf{W}^2\mathbf{n}];$
$\{(\text{tr}\mathbf{W}\ \mathbf{N})^2, |\mathbf{Wn}|^2, \beta_{2m+1}(\mathbf{Wn}), (\text{tr}\mathbf{W}\ \mathbf{N})\alpha_{2m+1}(\mathbf{Wn})\}$ $(\equiv I_{2m+1}(\mathbf{W}))$.

The proof for the above results is as follows. Anisotropic functions of the skewsymmetric tensor $\mathbf{W}$ under the group D_{2m+1d} may be extended as isotropic functions of the extended set $(\mathbf{W}, \mathbf{E}\boldsymbol{\eta}_{2m}(\mathbf{Wn}), \mathbf{n} \otimes \mathbf{n})$ (see Theorem 1 in XIAO [15]). Applying the related result for scalar-valued isotropic functions, we derive an isotropic functional basis of the extended variables $(\mathbf{W}, \mathbf{E}\boldsymbol{\eta}_{2m}(\mathbf{Wn}), \mathbf{n} \otimes \mathbf{n})$ as follows:

$$\text{tr}\mathbf{W}^2, |\mathbf{Wn}|^2, \text{tr}\mathbf{W}(\mathbf{E}\boldsymbol{\eta}_{2m}(\mathbf{Wn})), \text{tr}\mathbf{W}(\mathbf{E}\boldsymbol{\eta}_{2m}(\mathbf{Wn}))(\mathbf{n} \otimes \mathbf{n}),$$
$$\text{tr}\mathbf{W}^2(\mathbf{E}\boldsymbol{\eta}_{2m}(\mathbf{Wn}))(\mathbf{n} \otimes \mathbf{n}).$$

In deriving the above result, many obviously redundant invariants have been removed by using the equalities

$$(\mathbf{n} \otimes \mathbf{n})^2 = \mathbf{n} \otimes \mathbf{n},\ (\mathbf{E}\boldsymbol{\eta}_{2m}(\mathbf{Wn}))^2 = \boldsymbol{\eta}_{2m}(\mathbf{Wn}) \otimes \boldsymbol{\eta}_{2m}(\mathbf{Wn})$$
$$-|\mathbf{Wn}|^{4m}\mathbf{I},\ \ \boldsymbol{\eta}_{2m}(\mathbf{Wn}) \cdot \mathbf{n} = 0.$$

Moreover, with the aid of the decomposition formula (2.16) given in Part I, we infer that, of the foregoing basis, the third invariant is equal to the fourth invariant and hence redundant. The other four invariants form the presented set $I_{2m+1}(\mathbf{W})$ of invariants.

Next, we show that the presented set $\mathrm{Skw}_{2m+1}(\mathbf{W})$ is a desired skewsymmetric tensor generating set. Two cases are considered. First, let $\mathbf{W}$ and $\mathbf{E}\boldsymbol{\eta}_{2m}(\mathbf{Wn})$ be linearly independent, i.e., either of them is nonvanishing and their axis vectors are noncollinear. Then we have (see (2.6) in Part I)

$$\Gamma(\mathbf{W}, \mathbf{E}\boldsymbol{\eta}_{2m}(\mathbf{Wn})) = S_2 = \Gamma(\mathbf{W}, \mathbf{E}\boldsymbol{\eta}_{2m}(\mathbf{Wn}), \mathbf{n} \otimes \mathbf{n}).$$

From this fact and the criterion (2.3) in Part I it follows that for the case at issue, an isotropic skewsymmetric tensor generating set for $(\mathbf{W}, \mathbf{E}\boldsymbol{\eta}_{2m}(\mathbf{Wn}))$ supplies an isotropic skewsymmetric tensor generating set for $(\mathbf{W}, \mathbf{E}\boldsymbol{\eta}_{2m}(\mathbf{Wn}), \mathbf{n} \otimes \mathbf{n})$. By applying the related result for isotropic functions we know that the former is just given by the set $\mathrm{Skw}_{2m+1}(\mathbf{W})$. Second, let $\mathbf{W}$ and $\mathbf{E}\boldsymbol{\eta}_{2m}(\mathbf{Wn})$ be linearly dependent. Then we have $(\mathrm{tr}\mathbf{W}^2)(\mathrm{tr}\mathbf{H}^2) - (\mathrm{tr}\mathbf{WH})^2 = 0$ with $\mathbf{H} = \mathbf{E}\boldsymbol{\eta}_{2m}(\mathbf{Wn})$. Hence we derive $\mathbf{W} = c\mathbf{Ez}$ with $\mathbf{z} \in \{\mathbf{n}, \mathbf{a}_1, \cdots, \mathbf{a}_{2m+1}\}$. Evidently, for the case at issue, a single generator $\mathbf{W}$ is enough to form a desired generating set.

Finally, we show that the presented set $\mathrm{Sym}_{2m+1}(\mathbf{W})$ is a desired symmetric tensor generating set. Towards this goal, we show that this set obeys the criterion (2.3) given in Part I. In fact, let $\mathbf{Wn} \neq \mathbf{0}$. Then the triplet $(\mathbf{n}, \mathbf{Wn}, \mathbf{n} \times \mathbf{Wn})$, denoted by $(\mathbf{e}_1, \mathbf{e}_2, \mathbf{e}_3)$, is an orthogonalized basis of the vector space $\mathbf{V}$, and hence the six symmetric tensors $\mathbf{e}_i \vee \mathbf{e}_j$, $i, j = 1, 2, 3$ form an orthogonalized basis of the symmetric tensor space Sym. In the presented set $\mathrm{Sym}_{2m+1}(\mathbf{W})$, the first four generators yield $\mathbf{e}_3 \otimes \mathbf{e}_3$ and $\mathbf{e}_i \vee \mathbf{e}_j$, $i, j = 1, 2$. For the last two generators in the set $\mathrm{Sym}_{2m+1}(\mathbf{W})$, denoted by $\mathbf{G}_1$ and $\mathbf{G}_2$, by using the formulas (2.6) and $(2.28)_{2,3}$ in Part I we have

$$\begin{aligned}
\Delta &= \begin{vmatrix} \mathbf{G}_1 : (\mathbf{e}_1 \vee \mathbf{e}_3) & \mathbf{G}_1 : (\mathbf{e}_2 \vee \mathbf{e}_3) \\ \mathbf{G}_2 : (\mathbf{e}_1 \vee \mathbf{e}_3) & \mathbf{G}_2 : (\mathbf{e}_2 \vee \mathbf{e}_3) \end{vmatrix} \\
&= 4 \begin{vmatrix} x\beta_{2m+1}(\mathbf{Wn}) & y^2\alpha_{2m+1}(\mathbf{Wn}) \\ -y^2\alpha_{2m+1}(\mathbf{Wn}) & xy^2\beta_{2m+1}(\mathbf{Wn}) \end{vmatrix} \\
&= 4y^2(x^2(\beta_{2m+1}(\mathbf{Wn}))^2 + y^2(\alpha_{2m+1}(\mathbf{Wn}))^2),
\end{aligned}$$

where $x = \mathrm{tr}\mathbf{WN}$ and $y = |\mathbf{Wn}|$. Hence, for $\mathbf{Wn} \neq \mathbf{0}$ we deduce

$$\mathrm{rank}\ \mathrm{Sym}_{2m+1}(\mathbf{W}) \geq \begin{cases} \mathrm{rank}\{\mathbf{I}, \mathbf{n} \otimes \mathbf{n}, \mathbf{Wn} \otimes \mathbf{Wn}, \mathbf{n} \vee \mathbf{Wn}\} \\ = 4 \quad \text{if} \quad \Delta = 0, \quad \text{i.e.} \ \mathbf{W} = c\mathbf{Ea}_k, \\ 6 \quad \text{if} \quad \Delta \neq 0. \end{cases}$$

From the latter and $\Gamma(\mathbf{W}) \cap D_{2m+1d} = C_{2h}(\mathbf{a}_k)$ for $\mathbf{W} = c\mathbf{E}\mathbf{a}_k \neq \mathbf{O}$, as well as Table 3 given in Sec. 2 in Part I, we infer that for $\mathbf{W}\mathbf{n} \neq \mathbf{0}$, the set $\mathrm{Sym}_{2m+1}(\mathbf{W})$ obeys the criterion (2.3) given in Part I. Moreover, it can readily be shown that the same is true for $\mathbf{W}\mathbf{n} = \mathbf{0}$, i.e. $\mathbf{W} = c\mathbf{E}\mathbf{n}$.

Either of the two presented generating sets is minimal and, of course, irreducible.

(iii) A single symmetric tensor $\mathbf{A}$

Anisotropic functions of the symmetric tensor variable $\mathbf{A}$ under the group D_{2m+1d} may be extended as isotropic functions of the four variables $(\mathbf{A}, \mathbf{E}\boldsymbol{\eta}_{2m}(\overset{\circ}{\mathbf{A}}\,\mathbf{n}), \mathbf{E}\boldsymbol{\eta}_m(\mathbf{q}(\mathbf{A})), \mathbf{n} \otimes \mathbf{n})$ (see Theorem 1 in XIAO [15]). Applying this fact and the related result for isotropic functions, one can immediately derive complete representations for the anisotropic functions at issue. However, the results thus obtained need not be irreducible. Removing the redundant elements and then following the unified procedure in Sec. 3 in Part I, we arrive at the desired irreducible representations.

$$
\begin{aligned}
\mathrm{Skw}\quad & \{\beta_{2m+1}(\mathbf{q}(\mathbf{A}))\mathbf{N}, \mathbf{E}\boldsymbol{\pi}_m(\mathbf{q}(\mathbf{A})), \mathbf{E}\boldsymbol{\eta}_{2m}(\overset{\circ}{\mathbf{A}}\,\mathbf{n}), \overset{\circ}{\mathbf{A}}\,\mathbf{n} \wedge \overset{\circ}{\mathbf{A}}{}^2\mathbf{n}, \\
& \alpha_{2m+1}(\overset{\circ}{\mathbf{A}}\,\mathbf{n})\mathbf{N} + \mathbf{E}\boldsymbol{\rho}_m(\mathbf{q}(\mathbf{A}))\} \ (\equiv \mathrm{Skw}_{2m+1}(\mathbf{A})) \\
\mathrm{Sym}\quad & \{\mathbf{I}, \mathbf{n} \otimes \mathbf{n}, \overset{\circ}{\mathbf{A}}, \overset{\circ}{\mathbf{A}}\,\mathbf{n} \otimes \overset{\circ}{\mathbf{A}}\,\mathbf{n}, \mathbf{n} \vee (\mathbf{n} \times \boldsymbol{\eta}_{2m}(\overset{\circ}{\mathbf{A}}\,\mathbf{n})), \\
& \overset{\circ}{\mathbf{A}}\,\mathbf{n} \vee (\mathbf{n} \times \boldsymbol{\eta}_{2m}(\overset{\circ}{\mathbf{A}}\,\mathbf{n})), \boldsymbol{\Phi}_{2m}(\mathbf{q}(\mathbf{A})), \\
& \mathbf{n} \vee (\mathbf{n} \times \boldsymbol{\eta}_m(\mathbf{q}(\mathbf{A}))), \mathbf{A}_\mathbf{e}(\mathbf{E}\boldsymbol{\eta}_m(\mathbf{q}(\mathbf{A}))) - (\mathbf{E}\boldsymbol{\eta}_m(\mathbf{q}(\mathbf{A})))\mathbf{A}_\mathbf{e}\} \\
& (\equiv \mathrm{Sym}_{2m+1}(\mathbf{A})) \\
R\quad & (\mathrm{tr}\mathbf{H}\mathbf{N})\beta_{2m+1}(\mathbf{q}(\mathbf{A})), \mathrm{tr}\mathbf{H}(\mathbf{E}\boldsymbol{\pi}_m(\mathbf{q}(\mathbf{A}))), \mathrm{tr}\mathbf{H}(\mathbf{E}\boldsymbol{\eta}_{2m}(\overset{\circ}{\mathbf{A}}\,\mathbf{n})), \\
& (\mathrm{tr}\mathbf{H}\mathbf{N})J(\mathbf{A}), (\mathrm{tr}\mathbf{H}\mathbf{N})\alpha_{2m+1}(\overset{\circ}{\mathbf{A}}\,\mathbf{n}) + \mathrm{tr}\mathbf{H}(\mathbf{E}\boldsymbol{\rho}_m(\mathbf{q}(\mathbf{A}))); \\
& \{\mathbf{n} \cdot \mathbf{A}\mathbf{n}, \mathrm{tr}\mathbf{A}, |\overset{\circ}{\mathbf{A}}\,\mathbf{n}|^2, |\mathbf{q}(\mathbf{A})|^2, \mathbf{n} \cdot \overset{\circ}{\mathbf{A}}{}^3\mathbf{n}, \beta_{2m+1}(\overset{\circ}{\mathbf{A}}\,\mathbf{n}), \\
& \alpha_{2m+1}(\mathbf{q}(\mathbf{A})), \\
& [\mathbf{n}, \overset{\circ}{\mathbf{A}}{}^2\mathbf{n}, \boldsymbol{\eta}_{2m}(\overset{\circ}{\mathbf{A}}\,\mathbf{n})]\} \ (\equiv I_{2m+1}(\mathbf{A})).
\end{aligned}
$$

Here and henceforth, $\boldsymbol{\pi}_m((\mathbf{q}(\mathbf{A}))$ and $\boldsymbol{\rho}_m(\mathbf{q}(\mathbf{A}))$ is used to denote two vector-valued polymonial functions of the symmetric tensor $\mathbf{A}$ defined by

$$
\boldsymbol{\rho}_m(\mathbf{q}(\mathbf{A})) = \begin{cases} |\mathbf{q}(\mathbf{A})|^{m+1}\boldsymbol{\eta}_m(\mathbf{q}(\mathbf{A})) & \text{if } m \text{ is an odd number}, \\ |\mathbf{q}(\mathbf{A})|^m \mathbf{A}_\mathbf{e}\boldsymbol{\eta}_m(\mathbf{q}(\mathbf{A})) & \text{if } m \text{ is an even number}, \end{cases} \tag{2.4}
$$

$$\pi_m(\mathbf{q}(\mathbf{A})) = \begin{cases} |\mathbf{q}(\mathbf{A})|^{m-1}\mathbf{A}_e\eta_m(\mathbf{q}(\mathbf{A})) \text{ if } m \text{ is an odd number}, \\ |\mathbf{q}(\mathbf{A})|^{m}\eta_m(\mathbf{q}(\mathbf{A})) \text{ if } m \text{ is an even number}, \end{cases} \tag{2.5}$$

In the table given, the two sets $\mathrm{Sym}_{2m+1}(\mathbf{A})$ and $I_{2m+1}(\mathbf{A})$, cited from XIAO [16] and XIAO [17] separately, supply a desired irreducible symmetric tensor generating set and a desired irreducible functional basis, respectively. In the tables given here and in **(vi)** we omit the invariants provided by the scalar products of the symmetric tensor variable $\mathbf{C} \in \mathrm{Sym}$ and the presented symmetric tensor generators. In the final general result that will be given by Theorem 4, we intend to cite directly the related results recently established by the authors (Xiao, Bruhns & Meyers [19]), which are simpler and more compact than the foregoing invariants from the scalar product. Moreover, using the equality (2.7) below and noticing that the invariant $|\overset{\circ}{\mathbf{A}}\,\mathbf{n}|(\mathbf{Hn})\cdot\overset{\circ}{\mathbf{A}}\,\mathbf{n}$ is redundant, we know the scalar product $\mathrm{tr}\mathbf{H}(\overset{\circ}{\mathbf{A}}\,\mathbf{n}\wedge\overset{\circ}{\mathbf{A}}{}^2\mathbf{n})$ may be replaced by the invariant $(\mathrm{tr}\mathbf{HN})J(\mathbf{A})$, as has been done.

In what follows we prove that the presented set $\mathrm{Skw}_{2m+1}(\mathbf{A})$ is a desired irreducible skewsymmetric tensor generating set. First, we show that this set obeys the criterion (2.3) in Part I. The case when $\overset{\circ}{\mathbf{A}} = \mathbf{O}$ is trivial. Let $\overset{\circ}{\mathbf{A}} \neq \mathbf{O}$. By using the equalities

$$\mathbf{A}_e\eta_m(\mathbf{q}(\mathbf{A})) = \alpha_{m+1}(\mathbf{q}(\mathbf{A}))\mathbf{e} + \beta_{m+1}(\mathbf{q}(\mathbf{A}))\mathbf{e}', \tag{2.6}$$

$$\overset{\circ}{\mathbf{A}}\,\mathbf{n}\wedge\overset{\circ}{\mathbf{A}}{}^2\mathbf{n} = |\overset{\circ}{\mathbf{A}}\,\mathbf{n}|^2\mathbf{n}\wedge\overset{\circ}{\mathbf{A}}\,\mathbf{n} + J(\mathbf{A})\mathbf{N}, \tag{2.7}$$

and setting $\mathbf{q} = \mathbf{q}(\mathbf{A})$ and $D = \mathrm{rank}\,\mathrm{Skw}_{2m+1}(\mathbf{A})$, we deduce

$$D \geq \begin{cases} \mathrm{rank}\{\mathbf{N}, \mathbf{E}\pi_m(\mathbf{q}), \mathbf{E}\rho_m(\mathbf{q})\} = 3 \quad \text{if} \quad \beta_{2m+1}(\mathbf{q}) \neq 0, \\ \mathrm{rank}\{\mathbf{N}, \mathbf{E}\eta_{2m}(\overset{\circ}{\mathbf{A}}\,\mathbf{n}), \mathbf{n}\wedge\overset{\circ}{\mathbf{A}}\,\mathbf{n}\} = 3 \quad \text{if} \quad \beta_{2m+1}(\mathbf{q}) = 0, \\ \alpha_{2m+1}(\overset{\circ}{\mathbf{A}}\,\mathbf{n}) \neq 0, \\ \mathrm{rank}\{\mathbf{E}\eta_{2m}(\overset{\circ}{\mathbf{A}}\,\mathbf{n}), \mathbf{N}, \mathbf{E}\pi_m(\mathbf{q})\} = 3 \quad \text{if} \quad \alpha_{2m+1}(\overset{\circ}{\mathbf{A}}\,\mathbf{n}) = 0, \\ J(\mathbf{A}) \neq 0, \\ \mathrm{rank}\{\mathbf{n}\wedge\overset{\circ}{\mathbf{A}}\,\mathbf{n}, \mathbf{E}\pi_m(\mathbf{q})\} \geq 1 \quad \text{if} \quad \alpha_{2m+1}(\overset{\circ}{\mathbf{A}}\,\mathbf{n}) = \beta_{2m+1}(\mathbf{q}) \\ = J(\mathbf{A}) = 0. \end{cases}$$

It is clear that the above four cases for $\overset{\circ}{\mathbf{A}} \neq \mathbf{O}$ exhaust all possible cases. The last case yields

$$\overset{\circ}{\mathbf{A}} = x\mathbf{n}\vee\mathbf{a}_k + y(\mathbf{a}_k\otimes\mathbf{a}_k - \mathbf{a}'_k\otimes\mathbf{a}'_k),\ \mathbf{a}'_k = \mathbf{n}\times\mathbf{a}_k,\ x^2 + y^2 \neq 0.$$

This indicates that one of the two-fold axis vectors of the group D_{2m+1d} is an eigenvector of $\mathbf{A}$. Hence we have

$$\alpha_{2m+1}(\overset{\circ}{\mathbf{A}}\,\mathbf{n}) = \beta_{2m+1}(\mathbf{q}(\mathbf{A})) = J(\mathbf{A}) = 0 \Longrightarrow C_{2h}(\mathbf{a}_k) \subset \Gamma(\mathbf{A}) \cap D_{2m+1d}.$$

From the above facts and Table 2 given in Sec. 2 in Part I, we infer that the presented set $\mathrm{Skw}_{2m+1}(\mathbf{A})$ obeys the criterion (2.3) in Part I and hence is the desired skewsymmetric tensor generating set. Furthermore, let $\mathbf{A}_1 = \mathbf{e} \vee \mathbf{e}'$ and $\mathbf{A}_2 = \mathbf{n} \vee \mathbf{e}$. Then we have $\dim \mathrm{Skw}(\Gamma(\mathbf{A}_i) \cap D_{2m+1d}) = \dim \mathrm{Skw}(S_2) = 3$ and $\overset{\circ}{\mathbf{A}}_1\,\mathbf{n} = \mathbf{0}$ and $\mathbf{q}(\mathbf{A}_2) = \mathbf{0}$. From these facts we deduce that the five generators in the set $\mathrm{Skw}_{2m+1}(\mathbf{A})$ are irreducible.

2.2. D_{2m+1d}-irreducible sets of two variables

(iv) The D_{2m+1d}-irreducible set $(\mathbf{u}, \mathbf{v})$ of two vectors

$$\begin{aligned}
V\quad & V_{2m+1}(\mathbf{u}) \cup V_{2m+1}(\mathbf{v}) \cup \{\mathbf{u} \times \boldsymbol{\eta}_{2m}(\overset{\circ}{\mathbf{v}}), \mathbf{v} \times \boldsymbol{\eta}_{2m}(\overset{\circ}{\mathbf{u}})\} \\
& (\equiv V_{2m+1}(\mathbf{u}, \mathbf{v})) \\
\mathrm{Skw}\quad & \mathrm{Skw}_{2m+1}(\mathbf{u}) \cup \mathrm{Skw}_{2m+1}(\mathbf{v}) \cup \{\mathbf{u} \wedge \mathbf{v}, \\
& (\mathbf{u} \cdot \mathbf{n})^{2m+1}\, \overset{\circ}{\mathbf{v}} \wedge (\mathbf{n} \times \boldsymbol{\eta}_{2m}(\overset{\circ}{\mathbf{v}})) + (\mathbf{v} \cdot \mathbf{n})^{2m+1}\, \overset{\circ}{\mathbf{u}} \wedge (\mathbf{n} \times \boldsymbol{\eta}_{2m}(\overset{\circ}{\mathbf{u}}))\} \\
& (\equiv \mathrm{Skw}_{2m+1}(\mathbf{u}, \mathbf{v})) \\
\mathrm{Sym}\quad & \mathrm{Sym}_{2m+1}(\mathbf{u}) \cup \mathrm{Sym}_{2m+1}(\mathbf{v}) \cup \{\mathbf{u} \vee \mathbf{v}, \\
& (\mathbf{u} \cdot \mathbf{n})^{2m+1}\, \overset{\circ}{\mathbf{v}} \vee (\mathbf{n} \times \boldsymbol{\eta}_{2m}(\overset{\circ}{\mathbf{v}})) + (\mathbf{v} \cdot \mathbf{n})^{2m+1}\, \overset{\circ}{\mathbf{u}} \vee (\mathbf{n} \times \boldsymbol{\eta}_{2m}(\overset{\circ}{\mathbf{u}}))\} \\
& (\equiv \mathrm{Sym}_{2m+1}(\mathbf{u}, \mathbf{v})) \\
R\quad & \mathbf{r} \cdot V_{2m+1}(\mathbf{z}), \mathbf{H} : \mathrm{Skw}_{2m+1}(\mathbf{z}), \mathbf{C} : \mathrm{Sym}_{2m+1}(\mathbf{z}),\ \mathbf{z} = \mathbf{u},\ \mathbf{v}; \\
& [\mathbf{r}, \mathbf{u}, \boldsymbol{\eta}_{2m}(\overset{\circ}{\mathbf{v}})], [\mathbf{r}, \mathbf{v}, \boldsymbol{\eta}_{2m}(\overset{\circ}{\mathbf{u}})]; \mathbf{u} \cdot \mathbf{H}\mathbf{v}; \mathbf{u} \cdot \overset{\circ}{\mathbf{C}}\,\mathbf{v}; \\
& (\mathbf{u} \cdot \mathbf{n})^{2m+1}[\mathbf{n}, \boldsymbol{\eta}_{2m}(\overset{\circ}{\mathbf{v}}), \mathbf{H}\mathbf{v}] + (\mathbf{v} \cdot \mathbf{n})^{2m+1}[\mathbf{n}, \boldsymbol{\eta}_{2m}(\overset{\circ}{\mathbf{u}}), \mathbf{H}\mathbf{u}]; \\
& (\mathbf{u} \cdot \mathbf{n})^{2m+1}[\mathbf{n}, \boldsymbol{\eta}_{2m}(\overset{\circ}{\mathbf{v}}), \overset{\circ}{\mathbf{C}}\,\mathbf{v}] + (\mathbf{v} \cdot \mathbf{n})^{2m+1}[\mathbf{n}, \boldsymbol{\eta}_{2m}(\overset{\circ}{\mathbf{u}}), \overset{\circ}{\mathbf{C}}\,\mathbf{u}]; \\
& I_{2m+1}(\mathbf{u}) \cup I_{2m+1}(\mathbf{v}) \cup \{(\mathbf{u} \cdot \mathbf{n})(\mathbf{v} \cdot \mathbf{n}), \mathbf{u} \cdot \mathbf{v}\}\ (\equiv I_{2m+1}(\mathbf{u}, \mathbf{v})).
\end{aligned}$$

To prove the above results, we first work out the D_{2m+1d}-irreducible set $(\mathbf{u}, \mathbf{v})$, specified by (see (3.1) in Part I)

$$\Gamma(\mathbf{u}, \mathbf{v}) \cap D_{2m+1d} \neq \Gamma(\mathbf{z}) \cap D_{2m+1d},\ \mathbf{z} = \mathbf{u},\ \mathbf{v}.$$

It is evident that $\mathbf{u}$ and $\mathbf{v}$ are linearly independent, i.e. $\mathbf{u} \times \mathbf{v} \neq \mathbf{0}$. Moreover, we

have

$$\Gamma(\mathbf{z}) \cap D_{2m+1d} \neq C_1, \text{ i.e., } \operatorname{rank} V_{2m+1}(\mathbf{z}) \neq 3,\ \mathbf{z} = \mathbf{u},\ \mathbf{v}.$$

The latter yields

$$\alpha_{2m+1}(\overset{\circ}{\mathbf{z}})((\beta_{2m+1}(\overset{\circ}{\mathbf{z}}))^2 + (\mathbf{z}\cdot\mathbf{n})^2|\overset{\circ}{\mathbf{z}}|^{4m}) = 0,\ \mathbf{z} = \mathbf{u},\ \mathbf{v}.$$

Hence, each vector $\mathbf{z} \in \{\mathbf{u}, \mathbf{v}\}$ takes one of the forms

$$c\mathbf{a},\ c \neq 0; \quad a\mathbf{n} + b\mathbf{n} \times \mathbf{a},\ a^2 + b^2 \neq 0\,. \tag{2.8}$$

Considering the combinations of the above forms and excluding the cases

$$\mathbf{u} = x\mathbf{a},\ \mathbf{v} = y\mathbf{a};\ \mathbf{u} = a\mathbf{n} + b\mathbf{n} \times \mathbf{a},\ \mathbf{v} = x\mathbf{n} + y\mathbf{n} \times \mathbf{a},$$

which violate the D_{2m+1d}-irreducibility condition for $(\mathbf{u}, \mathbf{v})$, we derive the following three disjoint cases for the D_{2m+1d}-irreducible set $(\mathbf{u}, \mathbf{v})$:

(c1) $\mathbf{u} = x\mathbf{e},\ \mathbf{v} = y\mathbf{a},\ \mathbf{a} \neq \mathbf{e},\ xy \neq 0$;

(c2) $\mathbf{u} = x\mathbf{e},\ \mathbf{v} = y\mathbf{n} \times \mathbf{a} + z\mathbf{n},\ x(y^2 + z^2) \neq 0$;

(c3) $\mathbf{u} = x\mathbf{n} \times \mathbf{e} + w\mathbf{n},\ \mathbf{v} = y\mathbf{n} \times \mathbf{a} + z\mathbf{n},\ \mathbf{a} \neq \mathbf{e},\ xy \neq 0$.

Then, for case (c1) we have

$$\begin{aligned}
\operatorname{rank} V_{2m+1}(\mathbf{u}, \mathbf{v}) &\geq \operatorname{rank}\{\mathbf{u}, \mathbf{v}, \mathbf{v} \times \boldsymbol{\eta}_{2m}(\overset{\circ}{\mathbf{u}})\} = 3,\\
\operatorname{rank}\ \operatorname{Skw}_{2m+1}(\mathbf{u}, \mathbf{v}) &\geq \operatorname{rank}\{\mathbf{E}\boldsymbol{\eta}_{2m}(\overset{\circ}{\mathbf{u}}), \mathbf{E}\boldsymbol{\eta}_{2m}(\overset{\circ}{\mathbf{v}}), \mathbf{u} \wedge \mathbf{v}\} = 3,\\
\operatorname{rank}\ \operatorname{Sym}_{2m+1}(\mathbf{u}, \mathbf{v}) &\geq \operatorname{rank}(\operatorname{Sym}_{2m+1}(\mathbf{u}) \cup \operatorname{Sym}_{2m+1}(\mathbf{v}))\\
&= \operatorname{rank}(\operatorname{Sym}(C_2(\mathbf{e})) \cup \operatorname{Sym}(C_2(\mathbf{a}))) = 6.
\end{aligned}$$

In deriving the last expression above, the formula (2.4) in Part I is used. For case (c2) we have the first expression above and

$$\begin{aligned}
\operatorname{rank}\ \operatorname{Skw}_{2m+1}(\mathbf{u}, \mathbf{v}) \geq \operatorname{rank}\{&\mathbf{E}\boldsymbol{\eta}_{2m}(\mathbf{u}), \mathbf{u} \wedge \mathbf{v}, \mathbf{E}\boldsymbol{\eta}_{2m}(\overset{\circ}{\mathbf{v}}),\\
&\overset{\circ}{\mathbf{u}} \wedge(\mathbf{n} \times \boldsymbol{\eta}_{2m}(\overset{\circ}{\mathbf{u}}))\} = 3,
\end{aligned}$$

$$\begin{aligned}
\operatorname{rank}\ \operatorname{Sym}_{2m+1}(\mathbf{u}, \mathbf{v}) \geq \operatorname{rank}\{&\mathbf{I}, \mathbf{n} \otimes \mathbf{n}, \overset{\circ}{\mathbf{u}} \otimes \overset{\circ}{\mathbf{u}}, \mathbf{n} \vee (\mathbf{n} \vee \boldsymbol{\eta}_{2m}(\overset{\circ}{\mathbf{u}}),\\
&\mathbf{u} \vee \mathbf{v}, \overset{\circ}{\mathbf{u}} \vee(\mathbf{n} \times \boldsymbol{\eta}_{2m}(\overset{\circ}{\mathbf{u}}))\} = 6.
\end{aligned}$$

For case (c3) we have the second expression for case (1) and

$$\begin{aligned}
\operatorname{rank} V_{2m+1}(\mathbf{u}, \mathbf{v}) &\geq \operatorname{rank}(V_{2m+1}(\mathbf{u}) \cup V_{2m+1}(\mathbf{v}))\\
&= \operatorname{rank}(V(C_{1h}(\mathbf{e})) \cup V(C_{1h}(\mathbf{a}))) = 3,
\end{aligned}$$

$$\operatorname{rank}\ \mathrm{Sym}_{2m+1}(\mathbf{u},\mathbf{v}) \geq \operatorname{rank}(\mathrm{Sym}_{2m+1}(\mathbf{u}) \cup \mathrm{Sym}_{2m+1}(\mathbf{v}))$$
$$= \operatorname{rank}(\mathrm{Sym}(C_{1h}(\mathbf{e})) \cup \mathrm{Sym}(C_{1h}(\mathbf{a}))) = 6\,.$$

In the above, Eq. (2.4) in Part I is used again. From the above results we infer that the three sets of generators at issue obeys the criterion (2.3) in Part I, and hence they supply desired vector, skewsymmetric tensor and symmetric tensor generating sets. Further, by considering the two pairs: $\mathbf{u}_1 = \mathbf{n}$ and $\mathbf{v}_1 = \mathbf{e}$, $\mathbf{u}_2 = \mathbf{e}$ and $\mathbf{v}_2 = \mathbf{n}$, we deduce that the respective last two generators in the three presented generating sets are irreducible.

Finally, it is evident that the presented set $I_{2m+1}(\mathbf{u},\mathbf{v})$ of invariants determines a functional basis of the two variables $(\mathbf{u},\mathbf{v})$ under the cylindrical group $D_{\infty h}(\mathbf{n})$.

(v) The D_{2m+1d}-irreducible set $(\mathbf{W},\boldsymbol{\Omega})$ of two skewsymmetric tensors

$$\begin{aligned}
\mathrm{Skw}\quad & \{\mathbf{W},\boldsymbol{\Omega},\mathbf{W}\boldsymbol{\Omega}-\boldsymbol{\Omega}\mathbf{W}\}\\
\mathrm{Sym}\quad & \mathrm{Sym}_{2m+1}(\mathbf{W})\cup\mathrm{Sym}_{2m+1}(\boldsymbol{\Omega})\cup\{\mathbf{W}\boldsymbol{\Omega}+\boldsymbol{\Omega}\mathbf{W},\\
& |\mathrm{tr}\boldsymbol{\Omega}\mathbf{N}|(\mathrm{tr}\boldsymbol{\Omega}\mathbf{N})\mathbf{W}\mathbf{n}\vee\mathbf{N}\mathbf{W}\mathbf{n}+|\mathrm{tr}\mathbf{W}\mathbf{N}|(\mathrm{tr}\mathbf{W}\mathbf{N})\boldsymbol{\Omega}\mathbf{n}\vee\mathbf{N}\boldsymbol{\Omega}\mathbf{n}\}\\
R\quad & \mathrm{tr}\mathbf{H}\mathbf{W},\mathrm{tr}\mathbf{H}\boldsymbol{\Omega};\mathbf{C}:\mathrm{Sym}_{2m+1}(\mathbf{W}),\mathbf{C}:\mathrm{Sym}_{2m+1}(\boldsymbol{\Omega})\\
& \mathrm{tr}\mathbf{H}\mathbf{W}\boldsymbol{\Omega};\ \mathrm{tr}\overset{\circ}{\mathbf{C}}\,\mathbf{W}\boldsymbol{\Omega},\\
& |\mathrm{tr}\boldsymbol{\Omega}\mathbf{N}|(\mathrm{tr}\boldsymbol{\Omega}\mathbf{N})[\mathbf{n},\mathbf{W}\mathbf{n},\overset{\circ}{\mathbf{C}}\,\mathbf{W}\mathbf{n}]+|\mathrm{tr}\mathbf{W}\mathbf{N}|(\mathrm{tr}\mathbf{W}\mathbf{N})[\mathbf{n},\boldsymbol{\Omega}\mathbf{n},\overset{\circ}{\mathbf{C}}\,\boldsymbol{\Omega}\mathbf{n}];\\
& I_{2m+1}(\mathbf{W})\cup I_{2m+1}(\boldsymbol{\Omega})\cup\{\mathrm{tr}\mathbf{W}\boldsymbol{\Omega}\}.
\end{aligned}$$

The proof for the above results is the same as that given for the corresponding case (v) in Sec. 4 in Part I.

(vi) The D_{2m+1}-irreducible set $(\mathbf{W},\mathbf{A})$ of a skewsymmetric tensor and a symmetric tensor

$$\begin{aligned}
\mathrm{Skw}\quad & \mathrm{Skw}_{2m+1}(\mathbf{A})\cup\{\mathbf{W},\overset{\circ}{\mathbf{A}}\,\mathbf{W}+\mathbf{W}\,\overset{\circ}{\mathbf{A}},(\mathbf{E}:\mathbf{W})\wedge\boldsymbol{\eta}_m(\mathbf{q}(\mathbf{A}))\}\\
& (\equiv\mathrm{Skw}_{2m+1}(\mathbf{W},\mathbf{A}))\\
\mathrm{Sym}\quad & \mathrm{Sym}_{2m+1}(\mathbf{W})\cup\mathrm{Sym}_{2m+1}(\mathbf{A})\cup\{(\mathrm{tr}\mathbf{W}\mathbf{N})(\overset{\circ}{\mathbf{A}}\,\mathbf{N}-\mathbf{N}\,\overset{\circ}{\mathbf{A}}),\\
& (\mathrm{tr}\mathbf{W}\mathbf{N})((-1)^m\,\overset{\circ}{\mathbf{A}}\,\mathbf{n}\vee\boldsymbol{\eta}_{2m}(\overset{\circ}{\mathbf{A}}\,\mathbf{n})+\mathbf{n}\vee\boldsymbol{\rho}_m(\mathbf{q}(\mathbf{A})))\}\\
& (\equiv\mathrm{Sym}_{2m+1}(\mathbf{W},\mathbf{A}))\\
R\quad & \mathrm{tr}\mathbf{H}\mathbf{W};\mathbf{C}:\mathrm{Sym}_{2m+1}(\mathbf{W});\\
& I_{2m}(\mathbf{W})\cup I_{2m}(\mathbf{A})\cup\{(\mathbf{W}\mathbf{n})\cdot(\overset{\circ}{\mathbf{A}}\,\mathbf{n}),\\
& (\mathbf{W}\mathbf{n})\cdot\overset{\circ}{\mathbf{A}}\,\mathbf{W}\mathbf{n},\mathbf{n}\cdot\mathbf{W}\,\overset{\circ}{\mathbf{A}}\,^2\mathbf{n}\}
\end{aligned}$$

In the above table, the skewsymmetric tensor variable $\mathbf{H} \in \mathrm{Skw}$ is assumed to be of the form $\mathbf{H} = c\mathbf{W}$, and hence only one invariant from the scalar product concerning $\mathbf{H}$ is retained. The form for $\mathbf{H}$ just given is derived from cases (c1)–(c2) for the D_{2m+1d}-irreducible set $(\mathbf{W}, \mathbf{A})$ given later and the condition (see $(3.3)_2$ in Part I)

$$\Gamma(\mathbf{W}, \mathbf{H}) \cap D_{2m+1d} \neq \Gamma(\mathbf{W}, \mathbf{A}, \mathbf{H}) \cap D_{2m+1d} \; (= S_2).$$

For the other form of $\mathbf{H}$, we have $\Gamma(\mathbf{W}, \mathbf{H}, \mathbf{A}) \cap D_{2m+1d} = \Gamma(\mathbf{W}, \mathbf{H}) \cap D_{2m+1d} = S_2$, which has been covered by (v). Moreover, the symmetric tensor variable $\mathbf{C} \in \mathrm{Sym}$ is assmued to be subjected to the condition $\mathbf{C} \in \mathrm{span}\, \mathrm{Sym}_{2m+1}(\mathbf{A})$, and hence here appear only the invariants from the scalar products of $\mathbf{C}$ and the generators in $\mathrm{Sym}_{2m+1}(\mathbf{A})$. The form for $\mathbf{C}$ just indicated is derived from cases (c1)–(c2) for the D_{2m+1d}-irreducible set $(\mathbf{W}, \mathbf{A})$ given later and the condition (see $(3.3)_2$ in Part I)

$$\Gamma(\mathbf{A}, \mathbf{C}) \cap D_{2m+1d} \neq \Gamma(\mathbf{W}, \mathbf{A}, \mathbf{C}) \cap D_{2m+1d} \; (= S_2).$$

By using cases (c1)–(c2) for the D_{2m+1d}-irreducible set $(\mathbf{W}, \mathbf{A})$ given later, we see that $\Gamma(\mathbf{A}) \cap D_{2m+1d} = 2h(\mathbf{a})$, and hence we deduce that the other form for $\mathbf{C}$ leads to

$$\Gamma(\mathbf{W}, \mathbf{A}, \mathbf{C}) \cap D_{2m+1d} = \Gamma(\mathbf{A}, \mathbf{C}) \cap D_{2m+1d} = S_2,$$

which will be covered by the next case.

We proceed to work out the D_{2m+1d}-irreducible set $(\mathbf{W}, \mathbf{A})$, which is specified by (see (3.1) in Part I)

$$\Gamma(\mathbf{W}, \mathbf{A}) \cap D_{2m+1d} \neq \Gamma(\mathbf{z}) \cap D_{2m+1d}, \; \mathbf{z} = \mathbf{W}, \; \mathbf{A}.$$

It is evident that $\Gamma(\mathbf{z}) \cap D_{2m+1d} \neq S_2, \; D_{2m+1d}$, should hold for $\mathbf{z} = \mathbf{W}, \; \mathbf{A}$. Hence, either $\mathbf{R}_{\mathbf{n}}^{2\pi/2m+1}$ or $\mathbf{R}_{\mathbf{a}}^{\pi}$ pertains to the symmetry group $\Gamma(\mathbf{z})$ for each $\mathbf{z} \in \{\mathbf{W}, \mathbf{A}\}$. The case when $\mathbf{R}_{\mathbf{n}}^{2\pi/2m+1} \in \Gamma(\mathbf{A})$ is excluded, since it results in $\mathbf{A} = x\mathbf{I} + y\mathbf{n} \otimes \mathbf{n}$ and hence $\Gamma(\mathbf{A}) \cap D_{2m+1d} = D_{2m+1d}$, in contradiction to the D_{2m+1d}-irreducibility condition for $(\mathbf{W}, \mathbf{A})$. From these facts we deduce that $\mathbf{W}$ and $\overset{\circ}{\mathbf{A}}$ take one of the forms

$$\mathbf{W} = c\mathbf{E}\mathbf{n}, \; c \neq 0; \quad \mathbf{W} = c\mathbf{E}\mathbf{a}, \; c \neq 0\,; \tag{2.9}$$

$$\overset{\circ}{\mathbf{A}} = x(\mathbf{a} \otimes \mathbf{a} - \mathbf{a}' \otimes \mathbf{a}') + y\mathbf{n} \vee \mathbf{a}', \; \mathbf{a}' = \mathbf{n} \times \mathbf{a}, \; x^2 + y^2 \neq 0\,. \tag{2.10}$$

Thus, combining the above forms and excluding the case

$$\mathbf{W} = f\mathbf{E}\mathbf{a}, \; \overset{\circ}{\mathbf{A}} = x(\mathbf{a} \otimes \mathbf{a} - \mathbf{a}' \otimes \mathbf{a}') + y\mathbf{n} \vee \mathbf{a}', \; \mathbf{a}' = \mathbf{n} \times \mathbf{a},$$

we derive the following two cases for D_{2m+1d}-irreducible set $(\mathbf{W}, \mathbf{A})$:

(c1) $\mathbf{W} = f\mathbf{E}\mathbf{n}$ and $\overset{\circ}{\mathbf{A}} = a\mathbf{D}_1 + b\mathbf{D}_4$ with $f(a^2 + b^2) \neq 0$;

(c2) $\mathbf{W} = f\mathbf{E}\mathbf{a}$ and $\overset{\circ}{\mathbf{A}} = a\mathbf{D}_1 + b\mathbf{D}_4$ with $\mathbf{a} \neq \mathbf{e}$ and $f(a^2 + b^2) \neq 0$.

For cases (c1)–(c2) we have

$$\text{rank Skw}_{2m+1}(\mathbf{W}, \mathbf{A}) \geq \begin{cases} \text{rank}\{\mathbf{W}, \mathbf{E}\pi_m(\mathbf{q}(\mathbf{A})), (\mathbf{E} : \mathbf{W}) \wedge \eta_m(\mathbf{q}(\mathbf{A}))\} \\ = 3 \ \text{ if } \ a \neq 0\,, \\ \text{rank}\{\mathbf{W}, \mathbf{E}\eta_{2m}(\overset{\circ}{\mathbf{A}}\,\mathbf{n}), \overset{\circ}{\mathbf{A}}\,\mathbf{W} + \mathbf{W}\,\overset{\circ}{\mathbf{A}}\} \\ = 3 \ \text{ if } \ a = 0, \ b \neq 0\,. \end{cases}$$

Moreover, utilizing the formula (2.4) in Part I we have

$$\begin{aligned} \text{(2.11)} \qquad \text{rank Sym}_{2m+1}(\mathbf{W}, \mathbf{A}) &= \text{rank}(\text{Sym}(C_{2h}(\mathbf{e})) \cup \{\overset{\circ}{\mathbf{A}}\,\mathbf{N} - \mathbf{N}\,\overset{\circ}{\mathbf{A}}, \\ &\qquad (-1)^m\,\overset{\circ}{\mathbf{A}}\,\mathbf{n} \vee \eta_{2m}(\overset{\circ}{\mathbf{A}}\,\mathbf{n}) + \mathbf{n} \vee \boldsymbol{\rho}_m(\mathbf{q}(\mathbf{A}))\}) \\ &= \text{rank}\{\mathbf{n} \otimes \mathbf{n}, \mathbf{e} \otimes \mathbf{e}, \mathbf{e}' \otimes \mathbf{e}', \mathbf{n} \vee \mathbf{e}', a\mathbf{e} \vee \mathbf{e}' - b\mathbf{n} \vee \mathbf{e}, \\ &\qquad b^{2m+1}\mathbf{e} \vee \mathbf{e}' + a^{2m+1}\mathbf{n} \vee \mathbf{e}\}) = 6, \end{aligned}$$

for case (c1). In deriving the second equality above, the following facts for case (c1) are used: $\psi(\mathbf{A}) = \dfrac{\pi}{2}$ for $b > 0$ or $\dfrac{3\pi}{2}$ for $b < 0$ and $\phi(\mathbf{A}) = 0$ for $a > 0$ or π for $a < 0$, and hence

$$\sin(2m-1)\psi(\mathbf{A}) = -(-1)^m, \ \cos(2m-1)\psi(\mathbf{A}) = 0,$$

$$\begin{aligned} \sin m\phi(\mathbf{A}) = \sin(m+1)\phi(\mathbf{A}) = 0, \ |a| \cos \frac{1}{2}(2m + 1 - (-1)^m)\phi(\mathbf{A}) \\ = |a| \cos \phi(\mathbf{A}) = a. \end{aligned}$$

Owing to the above facts, the last two tensors in the second equality of (2.11) are independent and hence the last equality of (2.11) holds. On the other hand, these facts explain why, in the expression of the last generator in the set $\text{Sym}_{2m+1}(\mathbf{W}, \mathbf{A})$, the factor $(-1)^m$ should appear and why the vector-valued function $\boldsymbol{\rho}_m(\mathbf{q}(\mathbf{A}))$ (see (2.4)) should take different forms for an odd number m and an even number m. Finally, by utilizing the formula (2.4) in Part I and the equality

$$\text{(2.12)} \qquad \text{span}(\text{Sym}(C_{2h}(\mathbf{e})) \cup \text{Sym}(C_{2h}(\mathbf{a})) = \text{Sym}$$

for any two vectors $\mathbf{e}$ and $\mathbf{a}$ satifying $(\mathbf{a}\cdot\mathbf{e})\mathbf{a}\times\mathbf{e}\neq\mathbf{0}$, we have

$$\operatorname{rank}\operatorname{Sym}_{2m+1}(\mathbf{W},\mathbf{A}) \geq \operatorname{rank}(\operatorname{Sym}(\Gamma(\mathbf{W})\cap D_{2m+1d})\cup\operatorname{Sym}(\Gamma(\mathbf{A})$$

$$\cup D_{2m+1d})) = \operatorname{rank}(\operatorname{Sym}(C_{2h}(\mathbf{a}))\cup\operatorname{Sym}(C_{2h}(\mathbf{e}))) = 6$$

for case (c2).

From the above facts and the criterion (2.3) in Part I we conclude that the two presented sets $\operatorname{Skw}_{2m+1}(\mathbf{W},\mathbf{A})$ and $\operatorname{Sym}_{2m+1}(\mathbf{W},\mathbf{A})$ supply a desired skewsymmetric tensor generating set and a desired symmetric tensor generating set respectively. Further, by considering the two pairs $(\mathbf{W}_1,\mathbf{A}_1)=(\mathbf{N},\mathbf{D}_1)$ and $(\mathbf{W}_2,\mathbf{A}_2)=(\mathbf{N},\mathbf{D}_4)$, we deduce that the the respective last two generators in the two sets $\operatorname{Skw}_{2m+1}(\mathbf{W},\mathbf{A})$ and $\operatorname{Sym}_{2m+1}(\mathbf{W},\mathbf{A})$ are irreducible.

Finally, with the aid of cases (c1)–(c2) it can readily be shown that a functional basis of the D_{2m+1}-irreducible set $(\mathbf{W},\mathbf{A})$ under the cylindrical group $D_{\infty h}(\mathbf{n})$ is determined by the presented set $I_{2m+1}(\mathbf{W},\mathbf{A})$ of invariants, and hence the latter supplies a desired functional basis (see the remark at the end of Sec. 4 (**vi**) in Part I).

(vii) The D_{2m+1d}-irreducible set $(\mathbf{A},\mathbf{B})$ of two symmetric tensors

Skw $\operatorname{Skw}_{2m+1}(\mathbf{A})\cup\operatorname{Skw}_{2m+1}(\mathbf{B})\cup\{\overset{\circ}{\mathbf{A}}\overset{\circ}{\mathbf{B}}-\overset{\circ}{\mathbf{B}}\overset{\circ}{\mathbf{A}},\overset{\circ}{\mathbf{A}}\,\mathbf{n}\wedge\overset{\circ}{\mathbf{B}}\overset{\circ}{\mathbf{A}}\,\mathbf{n},$
$\overset{\circ}{\mathbf{B}}\,\mathbf{n}\wedge\overset{\circ}{\mathbf{A}}\overset{\circ}{\mathbf{B}}\,\mathbf{n}\}$
$(\equiv\operatorname{Skw}_{2m+1}(\mathbf{A},\mathbf{B}))$

Sym $\operatorname{Sym}_{2m+1}(\mathbf{A})\cup\operatorname{Sym}_{2m+1}(\mathbf{B})$ $(\equiv\operatorname{Sym}_{2m+1}(\mathbf{A},\mathbf{B}))$,

R $\mathbf{H}:\operatorname{Skw}_{2m+1}(\mathbf{A}),\mathbf{H}:\operatorname{Skw}_{2m+1}(\mathbf{B})$;
$\operatorname{tr}\mathbf{H}\,\overset{\circ}{\mathbf{A}}\overset{\circ}{\mathbf{B}},(\overset{\circ}{\mathbf{A}}\,\mathbf{n})\cdot\mathbf{H}\,\overset{\circ}{\mathbf{B}}\overset{\circ}{\mathbf{A}}\,\mathbf{n},(\overset{\circ}{\mathbf{B}}\,\mathbf{n})\cdot\mathbf{H}\,\overset{\circ}{\mathbf{A}}\overset{\circ}{\mathbf{B}}\,\mathbf{n}$;
$I_{2m+1}(\mathbf{A})\cup I_{2m+1}(\mathbf{B})\cup\{\operatorname{tr}\mathbf{A}_\mathbf{n}\mathbf{B}_\mathbf{n},\operatorname{tr}\mathbf{A}_\mathbf{e}\mathbf{B}_\mathbf{e},\operatorname{tr}\overset{\circ}{\mathbf{A}}{}^2\,\overset{\circ}{\mathbf{B}},\operatorname{tr}\overset{\circ}{\mathbf{B}}{}^2\,\overset{\circ}{\mathbf{A}}\}$
$(\equiv I_{2m+1}(\mathbf{A},\mathbf{B}))$.

To prove the above results, we first work out the D_{2m+1d}-irreducible set $(\mathbf{A},\mathbf{B})$, specified by

$$\Gamma(\mathbf{A},\mathbf{B})\cap D_{2m+1d}\neq\Gamma(\mathbf{z})\cap D_{2m+1d},\ \mathbf{z}=\mathbf{A},\ \mathbf{B}.$$

Evidently, we have $\Gamma(\mathbf{z})\cap D_{2m+1d}\neq S_2,\ D_{2m+1d}$ for $\mathbf{z}=\mathbf{A},\ \mathbf{B}$. From the latter and the relevant argument given in (**vi**) we know that each $\mathbf{z}\in\{\mathbf{A},\mathbf{B}\}$ is of the form given by (2.10). Hence, the D_{2m+1d}-irreducible set $(\mathbf{A},\mathbf{B})$ is specified by

(2.13) $$\overset{\circ}{\mathbf{A}} = aD_1 + bD_4,\ \overset{\circ}{\mathbf{B}} = c(\mathbf{a}\otimes\mathbf{a} - \mathbf{a}'\otimes\mathbf{a}') + d\mathbf{n}\vee\mathbf{a}',\ \mathbf{a}\neq\mathbf{e},$$
$$(a^2+b^2)(c^2+d^2)\neq 0.$$

Consequently, we have

$$\Gamma(\mathbf{A})\cap D_{2m+1d} = C_{2h}(\mathbf{e}),\ \Gamma(\mathbf{B})\cap D_{2m+1d} = C_{2h}(\mathbf{a}).$$

Utilizing the above and Eq. (2.4) in Part I, we have

(2.14) $$\operatorname{rank}\operatorname{Skw}_{2m+1}(\mathbf{A},\mathbf{B}) = \operatorname{rank}(\operatorname{Skw}(C_{2h}(\mathbf{e}))\cup\operatorname{Skw}(C_{2h}(\mathbf{a}))$$
$$\cup\{\mathbf{G}_1,\mathbf{G}_2,\mathbf{G}_3\}) = \operatorname{rank}\{\mathbf{n}\wedge\mathbf{e}',\mathbf{n}\wedge\mathbf{a}',(bd+2ac\cos\alpha)\mathbf{N},b^2c\sin 2\alpha\mathbf{N},$$
$$d^2a\sin 2\alpha\mathbf{N}\} = 3 \text{ if } (a^2+b^2)(c^2+d^2)\neq 0,$$
$$\operatorname{rank}\operatorname{Sym}_{2m+1}(\mathbf{A},\mathbf{B}) = \operatorname{rank}(\operatorname{Sym}(C_{2h}(\mathbf{e}))\cup\operatorname{Sym}(C_{2h}(\mathbf{a}))) = 6,$$

where $\mathbf{G}_1$, $\mathbf{G}_2$ and $\mathbf{G}_3$ are used to represent the last three generators in the set $\operatorname{Skw}_{2m+1}(\mathbf{A},\mathbf{B})$, and α the angle formed by $\mathbf{e}$ and $\mathbf{a}$. Note that $\sin 2\alpha\neq 0$.

From the above results we know that the two sets $\operatorname{Skw}_{2m+1}(\mathbf{A},\mathbf{B})$ and $\operatorname{Sym}_{2m+1}(\mathbf{A},\mathbf{B})$ obey the criterion (2.3) in Part I, respectively. Hence they supply a desired skewsymmetric tensor generating set and a desired symmetric tensor generating set. Further, in (2.13) let $a=c=0$, $a=d=0$ and $b=c=0$, respectively. Then we have $\Gamma(\mathbf{A},\mathbf{B})\cap D_{2m+1d} = S_2$ for each of the three cases. From this and the second equality in (2.14) we deduce that each of the generators $\mathbf{G}_1$, $\mathbf{G}_2$ and $\mathbf{G}_3$ is irreducible.

Finally, the presented set $I_{2m+1}(\mathbf{A},\mathbf{B})$ determines a functional basis of $(\mathbf{A},\mathbf{B})$ under the cylindrical group $D_{\infty h}(\mathbf{n})$ and hence supplies a desired functional basis (see the comment at the end of Sec. 4 (**vi**) in Part I).

(viii) The D_{2m+1d}-irreducible set $(\mathbf{u},\mathbf{W})$ of a vector and a skewsymmetric tensor

V $V_{2m+1}(\mathbf{u})\cup\{\mathbf{W}\mathbf{u},\mathbf{W}^2\mathbf{u},\mathbf{u}\times\boldsymbol{\eta}_{2m}(\mathbf{W}\mathbf{n}),\mathbf{u}\times\mathbf{W}\boldsymbol{\eta}_{2m}(\overset{\circ}{\mathbf{u}})\}$
$(\equiv V_{2m+1}(\mathbf{u},\mathbf{W}))$

Skw $\operatorname{Skw}_{2m+1}(\mathbf{u})\cup Skw_{2m+1}(\mathbf{W})\cup\{(\mathbf{E}:\mathbf{W})\wedge\boldsymbol{\eta}_{2m}(\overset{\circ}{\mathbf{u}})\}$
$(\equiv \operatorname{Skw}_{2m+1}(\mathbf{u},\mathbf{W}))$

Sym $\operatorname{Sym}_{2m+1}(\mathbf{u})\cup\operatorname{Sym}_{2m+1}(\mathbf{W})\cup\{(\operatorname{tr}\mathbf{W}\mathbf{N})\overset{\circ}{\mathbf{u}}\vee(\mathbf{n}\times\overset{\circ}{\mathbf{u}}),$
$(\operatorname{tr}\mathbf{W}\mathbf{N})\mathbf{n}\vee\boldsymbol{\eta}_{2m}(\overset{\circ}{\mathbf{u}})\};(\equiv \operatorname{Sym}_{2m+1}(\mathbf{u},\mathbf{W}))$

$$R \quad \mathbf{r}\cdot V_{2m+1}(\mathbf{u});\mathbf{H}:\mathrm{Skw}_{2m+1}(\mathbf{z}),\mathbf{C}:\mathrm{Sym}_{2m+1}(\mathbf{z}),\ \mathbf{z}=\mathbf{u},\ \mathbf{W};$$

$$\mathrm{tr}\mathbf{H}\mathbf{W}(\mathbf{E}\boldsymbol{\eta}_{2m}(\overset{\circ}{\mathbf{u}}));(\mathrm{tr}\mathbf{W}\mathbf{N})[\mathbf{n},\overset{\circ}{\mathbf{u}},\overset{\circ}{\mathbf{C}}\overset{\circ}{\mathbf{u}}],(\mathrm{tr}\mathbf{W}\mathbf{N})\boldsymbol{\eta}_{2m}(\overset{\circ}{\mathbf{u}})\cdot\overset{\circ}{\mathbf{C}}\,\mathbf{n};$$

$$I_{2m+1}(\mathbf{u})\cup I_{2m+1}(\mathbf{W})\cup\{(\mathbf{u}\cdot\mathbf{n})\,\overset{\circ}{\mathbf{u}}\cdot\mathbf{W}\mathbf{n},(\overset{\circ}{\mathbf{u}}\cdot\mathbf{W}\mathbf{n})^2\}$$

$$(\equiv I_{2m+1}(\mathbf{u},\mathbf{W})).$$

In the above table and that given later, the vector variable $\mathbf{r}$ is assumed to pertain to the subspace $V(\Gamma(\mathbf{u})\cap D_{2m+1d})$, the latter being spanned by the vector generating set $V_{2m+1}(\mathbf{u})$ (see (2.4) in Part I). Owing to this fact, of the invariants from the scalar products of $\mathbf{r}$ and the vector generators in the set $V_{2m+1}(\mathbf{u},\mathbf{D})$, the invariants except $\mathbf{r}\cdot V_{2m+1}(\mathbf{u})$ are redundant and have been and will be deleted. Here $\mathbf{D}=\mathbf{W},\ \mathbf{A}$. When $\overset{\circ}{\mathbf{u}}\neq\mathbf{0}$, the foregoing condition for $\mathbf{r}$ can be derived from (see $(3.3)_2$)

$$\Gamma(\mathbf{u},\mathbf{r})\cap D_{2m+1d}\neq\Gamma(\mathbf{u},\mathbf{D},\mathbf{r})\cap D_{2m+1d}$$

for the D_{2m+1d}-irreducible set $(\mathbf{u},\mathbf{D})$. When $\overset{\circ}{\mathbf{u}}=\mathbf{0}$, i.e. $\mathbf{u}=a\mathbf{n}$, we have $\mathbf{r}=c\mathbf{n}=x\mathbf{u}$. The case when $\overset{\circ}{\mathbf{r}}\neq\mathbf{0}$ is the same as the case when $\overset{\circ}{\mathbf{u}}\neq\mathbf{0}$.

The proof for the presented results is as follows. First, we prove that the three presented sets $I_{2m+1}(\mathbf{u},\mathbf{W})$, $\mathrm{Skw}_{2m+1}(\mathbf{u},\mathbf{W})$ and $\mathrm{Sym}_{2m+1}(\mathbf{u},\mathbf{A})$ supply a desired functional basis, a desired skewsymmetric tensor generating set and a desired symmetric tensor generating set, respectively. In fact, since the central inversion $-\mathbf{I}$ is included in the group D_{2m+1d}, we infer that each scalar-valued or second order tensor-valued anisotropic function of the set $(\mathbf{u},\mathbf{W})$ under D_{2m+1d} is equivalent to a scalar-valued or second tensor-valued anisotropic function of the set $(\mathbf{W},\mathbf{u}\otimes\mathbf{u})$ under D_{2m+1d}. Evidently, the set $(\mathbf{W},\mathbf{u}\otimes\mathbf{u})$ is the particular case of the set $(\mathbf{W},\mathbf{A})$ considered in **(vi)** when $\mathbf{A}=\mathbf{u}\otimes\mathbf{u}$. Hence, by setting $\mathbf{A}=\mathbf{u}\otimes\mathbf{u}$ in the set $I_{2m+1}(\mathbf{W},\mathbf{A})$ we derive a desired functional basis. After removing some obviously redundant invariants, we know that this basis is just given by the set $I_{2m+1}(\mathbf{u},\mathbf{W})$. Similarly, a skewsymmetric tensor generating set and a symmetric tensor generating set for $(\mathbf{u}\otimes\mathbf{u},\mathbf{W})$ can be derived. By removing some redundant generators we arrive at the desired two irreducible tensor generating sets, given by $\mathrm{Skw}_{2m+1}(\mathbf{u},\mathbf{W})$ and $\mathrm{Sym}_{2m+1}(\mathbf{u},\mathbf{W})$. The proof is as follows.

From cases (c1) and (c2) given in **(vi)**, we know that the D_{2m+1d}-irreducible set $(\mathbf{W},\mathbf{u}\otimes\mathbf{u})$ is specified by

(c1) $\mathbf{W}=f\mathbf{E}\mathbf{n},\ \mathbf{u}\otimes\mathbf{u}=a\mathbf{D}_1+b\mathbf{D}_4+p\mathbf{n}\otimes\mathbf{n}+y\mathbf{I},\ f(a^2+b^2)\neq 0;$

(c2) $\mathbf{W}=f\mathbf{E}\mathbf{a},\ \mathbf{u}\otimes\mathbf{u}=a\mathbf{D}_1+b\mathbf{D}_4+p\mathbf{n}\otimes\mathbf{n}+y\mathbf{I},\ \mathbf{a}\neq\mathbf{e},\ f(a^2+b^2)\neq 0;$

Further, from the scalar products $\mathrm{tr}(\mathbf{u}\otimes\mathbf{u})\mathbf{D}_i$ for $i=1,\ 2,\ 3,\ 4$, we derive

$$2a = (\mathbf{u}\cdot\mathbf{e})^2 - (\mathbf{u}\cdot\mathbf{e}')^2,\ b = (\mathbf{u}\cdot\mathbf{n})(\mathbf{u}\cdot\mathbf{e}'),\ (\mathbf{u}\cdot\mathbf{e})(\mathbf{u}\cdot\mathbf{e}')$$
$$= (\mathbf{u}\cdot\mathbf{n})(\mathbf{u}\cdot\mathbf{e}) = 0.$$

These yield $\mathbf{u} = c\mathbf{e}$ or $\mathbf{u} = c\mathbf{e}' + d\mathbf{n}$ with $c \neq 0$.

With the above facts in mind we have

$$\text{rank Skw}_{2m+1}(\mathbf{u}, \mathbf{W}) \geq \{\mathbf{E}\boldsymbol{\eta}_{2m}(\overset{\circ}{\mathbf{u}}), \mathbf{W}, (\mathbf{E}:\mathbf{W}) \wedge \boldsymbol{\eta}_{2m}(\overset{\circ}{\mathbf{u}})\} = 3,$$

for cases (c1) and (c2), and

$$\text{rank Sym}_{2m+1}(\mathbf{u}, \mathbf{W}) \geq \text{rank}(\text{Sym}_{2m+1}(\mathbf{u}) \cup \{\overset{\circ}{\mathbf{u}} \vee (\mathbf{n}\times \overset{\circ}{\mathbf{u}}),\ \mathbf{n} \vee \boldsymbol{\eta}_{2m}(\overset{\circ}{\mathbf{u}})\})$$
$$= \{\mathbf{I}, \mathbf{n}\otimes\mathbf{n}, \mathbf{e}\otimes\mathbf{e}, \mathbf{n}\vee\mathbf{e}', \mathbf{e}\vee\mathbf{e}', \mathbf{n}\vee\mathbf{e}\} = 6$$

for case (c1), and by using the formula (2.4) in Part I we have

$$\text{rank Sym}_{2m+1}(\mathbf{u}, \mathbf{W}) \geq \text{rank}(\text{Sym}_{2m+1}(\mathbf{u}) \cup \text{Sym}_{2m+1}(\mathbf{W}))$$
$$= \text{rank}(\text{Sym}(\Gamma(\mathbf{u}) \cap D_{2m+1d}) \cup \text{Sym}(\Gamma(\mathbf{W}) \cap D_{2m+1d}))$$
$$= \text{rank}(\text{Sym}(C_{2h}(\mathbf{a}) \cup \text{Sym}(C_{2h}(\mathbf{e}))) = 6,$$

for case (c2).

From the above results we know that the two sets $\text{Skw}_{2m+1}(\mathbf{u}, \mathbf{W})$ and $\text{Sym}_{2m+1}(\mathbf{u}, \mathbf{A})$ obey the criterion (2.3) in Part I, respectively, and hence they supply a desired skewsymmetric and symmetric tensor generating sets. Further, by considering the pair $\mathbf{u}_0 = \mathbf{e}$ and $\mathbf{W}_0 = \mathbf{En}$ we infer that the last generator in the set $\text{Skw}_{2m+1}(\mathbf{u}, \mathbf{W})$ and the latter two generators in the set $\text{Sym}_{2m+1}(\mathbf{u}, \mathbf{W})$ are irreducible.

Finally, we show that the presented set $V_{2m+1}(\mathbf{u}, \mathbf{W})$ is a desired irreducible vector generating set. To this end, two cases for a nonvanishing $\mathbf{u}$ are discussed: $\overset{\circ}{\mathbf{u}} = \mathbf{0}$ and $\overset{\circ}{\mathbf{u}} \neq \mathbf{0}$. First, suppose $\overset{\circ}{\mathbf{u}} = \mathbf{0}$, i.e. $\mathbf{u} = a\mathbf{n} \neq \mathbf{0}$. Then each form-invariant vector-valued function of $(\mathbf{u}, \mathbf{W})$ under D_{2m+1d} can be extended as a vector-valued isotropic function of $(\mathbf{u}, \mathbf{W}, \mathbf{E}\boldsymbol{\eta}_{2m}(\mathbf{Wn}), \mathbf{n}\otimes\mathbf{n})$ (see XIAO [15]). Accordingly, an anisotropic vector generating set for $(\mathbf{u}, \mathbf{W})$ under D_{2m+1d} is derivable from an isotropic vector generating set for $(\mathbf{u}, \mathbf{W}, \mathbf{E}\boldsymbol{\eta}_{2m}(\mathbf{Wn}), \mathbf{n}\otimes\mathbf{n})$. By applying the related result for isotropic functions we know that the latter is given by

$$\mathbf{u}, \mathbf{Wu}, \mathbf{W}^2\mathbf{u}, (\mathbf{u}\cdot\mathbf{n})\mathbf{n}\times\boldsymbol{\eta}_{2m}(\mathbf{Wn}), (\mathbf{W}(\mathbf{E}\boldsymbol{\eta}_{2m}(\mathbf{Wn}))$$
$$-(\mathbf{E}\boldsymbol{\eta}_{2m}(\mathbf{Wn}))\mathbf{W})\mathbf{u}.$$

In deriving the above set, some obviously redundant generators have been deleted by using the equalities $\mathbf{u} = (\mathbf{u}\cdot\mathbf{n})\mathbf{n}$. Of the five generators given above, the first

four are included in the set $\mathrm{Skw}_{2m+1}(\mathbf{u}, \mathbf{W})$, and the last is redundant. The latter fact is obviously true for the case when $\mathbf{Wn} = \mathbf{0}$ and the case when the first three generators above are independent. Moreover, the other case for $\mathbf{W}$ is given by $\mathbf{W} = \mathbf{Ez}$ with $\mathbf{z}$ being a vector normal to $\mathbf{n}$. Utilizing the identity $(\mathbf{Ex})\mathbf{y} = \mathbf{y} \times \mathbf{x}$ and the equality $\mathbf{u} = (\mathbf{u} \cdot \mathbf{n})\mathbf{n}$ we deduce

$$(\mathbf{W}(\mathbf{E}\boldsymbol{\eta}_{2m}(\mathbf{Wn})) - (\mathbf{E}\boldsymbol{\eta}_{2m}(\mathbf{Wn}))\mathbf{W})\mathbf{u} = (\mathbf{u} \times \boldsymbol{\eta}_{2m}(\mathbf{Wn})) \times \mathbf{z}$$

$$+(\mathbf{u} \times \mathbf{z}) \times \boldsymbol{\eta}_{2m}(\mathbf{Wn}) = \lambda \mathbf{n},$$

i.e. the above generator is redundant.

Second, suppose $\overset{\circ}{\mathbf{u}} \neq \mathbf{0}$. Then we have

$$\Gamma(\mathbf{u}, \mathbf{W}) \cap D_{2m+1d} = \Gamma(\mathbf{u}, \mathbf{E}\boldsymbol{\eta}_{2m}(\overset{\circ}{\mathbf{u}}), \mathbf{W}), \tag{2.15}$$

for the D_{2m+1d}-irreducible set $(\mathbf{u}, \mathbf{W})$ with $\overset{\circ}{\mathbf{u}} \neq \mathbf{0}$. In fact, for $\overset{\circ}{\mathbf{u}} \neq \mathbf{0}$ we have

$$\Gamma(\mathbf{u}, \mathbf{E}\boldsymbol{\eta}_{2m}(\overset{\circ}{\mathbf{u}})) = \begin{cases} C_1 & \text{if } \alpha_{2m+1}(\overset{\circ}{\mathbf{u}})(\mathbf{u} \times \boldsymbol{\eta}_{2m}(\overset{\circ}{\mathbf{u}})) \neq \mathbf{0}, \\ C_{1h}(\mathbf{a}_k) & \text{if } \alpha_{2m+1}(\overset{\circ}{\mathbf{u}}) = 0, \\ C_\infty(\mathbf{a}_k) & \text{if } \mathbf{u} \times \boldsymbol{\eta}_{2m}(\overset{\circ}{\mathbf{u}}) = 0. \end{cases} \tag{2.16}$$

Of the above three cases for $\mathbf{u}$, the first means that the vector $\mathbf{u}$ is neither normal to nor collinear with any two-fold axis vector of D_{2m+1d}, and the other two yield $\mathbf{u} = c\mathbf{n} \times \mathbf{a}_k + d\mathbf{n}$ and $\mathbf{u} = c\mathbf{a}_k$ with $c \neq 0$, separately. Accordingly, we have $\Gamma(\mathbf{u}) \cap D_{2m+1d} = C_1, C_{1h}(\mathbf{a}_k), C_2(\mathbf{a}_k)$ for the three cases at issue respectively. The first case violates the D_{2m+1d}-irreducibility condition for $(\mathbf{u}, \mathbf{A})$ and is excluded, and (2.15) holds for the second. For the last case, i.e. $\mathbf{u} = c\mathbf{a}_k$ with $c \neq 0$, the case when $\mathbf{Wa}_k = \mathbf{0}$, i.e. $\mathbf{W} = f\mathbf{Ea}_k$, violates the D_{2m+1d}-irreducibility condition for $(\mathbf{u}, \mathbf{W})$ and is excluded. Then we have $\mathbf{Wa}_k \neq \mathbf{0}$ and, moreover, $\boldsymbol{\eta}_{2m}(\overset{\circ}{\mathbf{u}}) = f\mathbf{a}_k$. Thus, we infer that $\Gamma(\mathbf{E}\boldsymbol{\eta}_{2m}(\overset{\circ}{\mathbf{u}}, \mathbf{W}) = S_2$ and $\Gamma(\mathbf{u}, \mathbf{W}) \cap D_{2m+1d} = C_1$, and hence (2.15) also holds.

Then, from (2.15) and the criterion (2.3) in Part I, for the case at issue we deduce that an isotropic vector generating set for $(\mathbf{u}, \mathbf{E}\boldsymbol{\eta}_{2m}(\overset{\circ}{\mathbf{u}}), \mathbf{W})$ provides the desired result. The former is just given by the generators in the set $V_{2m+1}(\mathbf{u}, \mathbf{W})$ except $(\mathbf{u} \cdot \mathbf{n})\boldsymbol{\eta}_{2m}(\mathbf{Wn})$.

Thus, we conclude that the set $V_{2m+1}(\mathbf{u}, \mathbf{W})$ is a desired vector generating set. The irreducibility of the last four vector generators in this generating set can be inferred from the pairs $(\mathbf{u}, \mathbf{W})$ given below.

$\mathbf{Wu}$ and $\mathbf{u} \times \mathbf{W}\eta_{2m}(\overset{\circ}{\mathbf{u}})$: $\mathbf{u} = \mathbf{e}$, $\mathbf{W} = \mathbf{En}$;

$\mathbf{W}^2\mathbf{u}$: $\mathbf{u} = \mathbf{n}$, $\mathbf{W} = \mathbf{E}(\mathbf{n} + \mathbf{e})$;

$\mathbf{u} \times \eta_{2m}(\mathbf{Wn})$: $\mathbf{u} = \mathbf{n}$, $\mathbf{W} = \mathbf{n} \wedge \mathbf{e}$.

(ix) The D_{2m+1d}-irreducible set $(\mathbf{u}, \mathbf{A})$ of a vector and a symmetric tensor

$$V \quad V_{2m+1}(\mathbf{u}) \cup \{\overset{\circ}{\mathbf{A}}\,\mathbf{u}, \mathbf{u} \times \overset{\circ}{\mathbf{A}}\,\eta_{2m}(\overset{\circ}{\mathbf{u}}), (\mathbf{u}\cdot\mathbf{n})\mathbf{n} \times \eta_{2m}(\overset{\circ}{\mathbf{A}}\,\mathbf{n}),$$

$$(\mathbf{u}\cdot\mathbf{n})\mathbf{n} \times \eta_m(\mathbf{q}(\mathbf{A})), (\mathbf{u}\cdot\mathbf{n})\,\overset{\circ}{\mathbf{A}}\,(\mathbf{n} \times \eta_m(\mathbf{q}(\mathbf{A})))\} \ (\equiv V_{2m+1}(\mathbf{u}, \mathbf{A}))$$

$$\text{Skw} \quad \text{Skw}_{2m+1}(\mathbf{u}) \cup \text{Skw}_{2m+1}(\mathbf{A}) \cup \{\overset{\circ}{\mathbf{u}} \wedge \overset{\circ}{\mathbf{A}}\overset{\circ}{\mathbf{u}}, (\overset{\circ}{\mathbf{u}}\cdot\overset{\circ}{\mathbf{A}}\,\mathbf{n})\,\overset{\circ}{\mathbf{u}} \wedge \overset{\circ}{\mathbf{A}}\,\mathbf{n}\}$$

$$(\equiv \text{Skw}_{2m+1}(\mathbf{u}, \mathbf{A}))$$

$$\text{Sym} \quad \text{Sym}_{2m+1}(\mathbf{u}) \cup \text{Sym}_{2m+1}(\mathbf{A}) \ (\equiv \text{Sym}_{2m+1}(\mathbf{u}, \mathbf{A}))$$

$$R \quad \mathbf{r}\cdot V_{2m+1}(\mathbf{u}); \mathbf{H} : \text{Skw}_{2m+1}(\mathbf{u}), \mathbf{H} : \text{Skw}_{2m+1}(\mathbf{A}); \mathbf{C} : \text{Sym}_{2m+1}(\mathbf{u});$$

$$\overset{\circ}{\mathbf{u}}\cdot\mathbf{H}\,\overset{\circ}{\mathbf{A}}\overset{\circ}{\mathbf{u}}, (\overset{\circ}{\mathbf{u}}\cdot\overset{\circ}{\mathbf{A}}\,\mathbf{n})\,\overset{\circ}{\mathbf{u}}\cdot\mathbf{H}\,\overset{\circ}{\mathbf{A}}\,\mathbf{n};$$

$$I_{2m+1}(\mathbf{u}) \cup I_{2m+1}(\mathbf{A}) \cup \{(\mathbf{u}\cdot\mathbf{n})\,\overset{\circ}{\mathbf{u}}\cdot\overset{\circ}{\mathbf{A}}\,\mathbf{n}, \overset{\circ}{\mathbf{u}}\cdot\overset{\circ}{\mathbf{A}}\overset{\circ}{\mathbf{u}}, \overset{\circ}{\mathbf{u}}\cdot\overset{\circ}{\mathbf{A}}{}^2\,\overset{\circ}{\mathbf{u}}\}$$

$$(\equiv I_{2m+1}(\mathbf{u}, \mathbf{A}))$$

The proof for the above results is as follows. First, for each integer $r \geq 0$, each $2r$-th order tensor-valued anisotropic function of the variables $(\mathbf{u}, \mathbf{A})$ under the group D_{2m+1d} is equivalent to an anisotropic function of the variables $(\mathbf{A}, \mathbf{u} \otimes \mathbf{u})$ under the same group. As a result, setting $\mathbf{B} = \mathbf{u} \otimes \mathbf{u}$ in the corresponding results given in **(vii)**, we obtain a desired functional basis and a desired symmetric tensor generating set, as well as the related invariants from the scalar products, given by $I_{2m+1}(\mathbf{u}, \mathbf{A})$ and $\text{Sym}_{2m+1}(\mathbf{u}, \mathbf{A})$ etc.

Next, we show that the presented set $\text{Skw}_{2m+1}(\mathbf{u}, \mathbf{A})$ supplies a desired skewsymmetric tensor generating set. In fact, setting $\mathbf{B} = \mathbf{u} \otimes \mathbf{u}$ in $(2.13)_2$, we derive that the vector variable $\mathbf{u}$ takes one of the two forms $c\mathbf{a}$ with $c \neq 0$ and $c\mathbf{n} \times \mathbf{a} + d\mathbf{n}$ with $c \neq 0$ (see the relevant argument used in **(viii)**). Thus, combining the two forms and $(2.13)_1$, we derive the following two cases for the D_{2m+1d}-irreducible set $(\mathbf{A}, \mathbf{u} \otimes \mathbf{u})$:

$$(1)\mathbf{u} = c\mathbf{a},\ \overset{\circ}{\mathbf{A}} = a\mathbf{D}_1 + b\mathbf{D}_4,\ \mathbf{a} \neq \mathbf{e},\ c(a^2 + b^2) \neq 0;$$

$$(2)\mathbf{u} = c\mathbf{n} \times \mathbf{a} + d\mathbf{n},\ \overset{\circ}{\mathbf{A}} = a\mathbf{D}_1 + b\mathbf{D}_4,\ \mathbf{a} \neq \mathbf{e},\ c(a^2 + b^2) \neq 0.$$

For the above two cases we have

$$\begin{aligned}\operatorname{rank}\operatorname{Skw}_{2m+1}(\mathbf{u},\mathbf{A}) &\geq \operatorname{rank}(\operatorname{Skw}(C_{2h}(\mathbf{a}))\cup\operatorname{Skw}(C_{2h}(\mathbf{e}))\\ &\quad \cup\{\overset{\circ}{\mathbf{u}}\wedge\overset{\circ}{\mathbf{A}}\overset{\circ}{\mathbf{u}},(\overset{\circ}{\mathbf{u}}\cdot\overset{\circ}{\mathbf{A}}\,\mathbf{n})\,\overset{\circ}{\mathbf{u}}\wedge\overset{\circ}{\mathbf{A}}\,\mathbf{n}\})\\ &= \operatorname{rank}\{\mathbf{n}\wedge\mathbf{a},\mathbf{n}\wedge\mathbf{e},a\,\overset{\circ}{\mathbf{u}}\wedge\mathbf{D}_1\,\overset{\circ}{\mathbf{u}},b^2(\overset{\circ}{\mathbf{u}}\cdot\mathbf{e})\,\overset{\circ}{\mathbf{u}}\wedge\mathbf{e}\}=3\,.\end{aligned}$$

In deriving the first expression above, the formula (2.4) in Part I and the following equalities are used.

$$\Gamma(\mathbf{u}\otimes\mathbf{u})\cap D_{2m+1d}=C_{2h}(\mathbf{a}),\ \Gamma(\mathbf{A})\cap D_{2m+1d}=C_{2h}(\mathbf{e}).$$

From the above results we infer that the presented set $\operatorname{Skw}_{2m+1}(\mathbf{u},\mathbf{A})$ obeys the criterion (2.3) in Part I and hence supplies a desired skewsymmetric tensor generating set. Further, by considering the two pairs

$$\mathbf{u}_1=\mathbf{a}_1,\ \mathbf{A}_1=\mathbf{n}\vee\mathbf{e};\quad \mathbf{u}_2=\mathbf{a}_1,\ \mathbf{A}_2=\mathbf{e}\otimes\mathbf{e},$$

we deduce that the last two generators in the set $\operatorname{Skw}_{2m+1}(\mathbf{u},\mathbf{A})$ are irreducible.

Finally, we show that the presented set $V_{2m+1}(\mathbf{u},\mathbf{A})$ supplies the desired irreducible vector generating set. From the D_{2m+1d}-irreducibility condition for $(\mathbf{u},\mathbf{A})$ (see (3.1) in Part I) we deduce that $\Gamma(\mathbf{u})\cap D_{2m+1d}\neq C_1$. The latter produces the three cases for $\mathbf{u}$ (see cases (c1) – (c3) derived in **(iv)**): (c1) $\mathbf{u}=c\mathbf{n}$, (c2) $\mathbf{u}=c\mathbf{e}$ and (c3) $\mathbf{u}=c\mathbf{e}'+d\mathbf{n}$, where $c\neq 0$. In what follows we prove that the set $V_{2m+1}(\mathbf{u},\mathbf{A})$ obeys the criterion (2.3) in Part I for the just-mentioned three cases, respectively. Without losing generality we set $c=1$. First, for case (c1), i.e. $\mathbf{u}=\mathbf{n}$, we have

$$D\geq\begin{cases}\operatorname{rank}\{\mathbf{n},\overset{\circ}{\mathbf{A}}\,\mathbf{n},\mathbf{n}\times\boldsymbol{\eta}_{2m}(\overset{\circ}{\mathbf{A}}\,\mathbf{n})\}=3 \text{ if } \alpha_{2m+1}(\overset{\circ}{\mathbf{A}}\,\mathbf{n})\neq 0\,,\\ \operatorname{rank}\{\mathbf{n},\mathbf{n}\times\boldsymbol{\eta}_m(\mathbf{q}(\mathbf{A})),\overset{\circ}{\mathbf{A}}\,(\mathbf{n}\times\boldsymbol{\eta}_m(\mathbf{q}(\mathbf{A}))\}=3 \text{ if } \beta_{2m+1}(\mathbf{q}(\mathbf{A}))\neq 0\,,\\ \operatorname{rank}\{\mathbf{n},\overset{\circ}{\mathbf{A}}\,\mathbf{n},\mathbf{n}\times\boldsymbol{\eta}_m(\mathbf{q}(\mathbf{A}))\}=3 \text{ if } \alpha_{2m+1}(\overset{\circ}{\mathbf{A}}\,\mathbf{n})\\ \qquad\qquad =\beta_{2m+1}(\mathbf{q}(\mathbf{A}))=0,\ J(\mathbf{A})\neq 0\,,\\ \operatorname{rank}\{\mathbf{n},\overset{\circ}{\mathbf{A}}\,\mathbf{n},\mathbf{n}\times\boldsymbol{\eta}_m(\mathbf{q}(\mathbf{A}))\}\geq 2 \text{ if } \alpha_{2m+1}(\overset{\circ}{\mathbf{A}}\,\mathbf{n})\\ \qquad\qquad =\beta_{2m+1}(\mathbf{q}(\mathbf{A}))=J(\mathbf{A})=0\end{cases}$$

for $\overset{\circ}{\mathbf{A}}\neq\mathbf{O}$, where $D=\operatorname{rank}V_{2m+1}(\mathbf{u},\mathbf{A})$. Here and henceforth, the trivial case when $\overset{\circ}{\mathbf{A}}=\mathbf{O}$, i.e. $\overset{\circ}{\mathbf{A}}\,\mathbf{n}=\mathbf{q}(\mathbf{A})=\mathbf{0}$, is excluded. From the above facts and

$$\Gamma(\mathbf{n},\mathbf{A}) \cap D_{2m+1d} = C_{1h}(\mathbf{a}_k) \text{ if } \alpha_{2m+1}(\overset{\circ}{\mathbf{A}}\,\mathbf{n}) = \beta_{2m+1}(\mathbf{q}(\mathbf{A})) = J(\mathbf{A}) = 0,$$

as well as from Table 1 in Sec. 2 in Part I, for case (c1) we infer that the set $V_{2m+1}(\mathbf{u},\mathbf{A})$ obeys the criterion (2.3) in Part I.

Second, for case (c2), i.e. $\mathbf{u} = \mathbf{e}$, we have $\boldsymbol{\eta}_{2m}(\overset{\circ}{\mathbf{u}}) = \mathbf{e}$ and hence

$$\operatorname{rank} V_{2m+1}(\mathbf{u},\mathbf{A}) \geq \begin{cases} \operatorname{rank}\{\mathbf{e}, \overset{\circ}{\mathbf{A}}\,\mathbf{e}, \mathbf{e}\times \overset{\circ}{\mathbf{A}}\,\mathbf{e}\} \text{ if } \mathbf{e}\times \overset{\circ}{\mathbf{A}}\,\mathbf{e} \neq \mathbf{0}, \\ \operatorname{rank}\{\mathbf{e}, \overset{\circ}{\mathbf{A}}\,\mathbf{e}, \overset{\circ}{\mathbf{A}}\,\mathbf{n}\} \geq 2 \text{ if } \mathbf{e}\times \overset{\circ}{\mathbf{A}}\,\mathbf{e} = \mathbf{0}. \end{cases}$$

From the above facts and $\Gamma(\mathbf{e},\mathbf{A}) \cap D_{2m+1d} = C_2(\mathbf{e})$ when $\mathbf{e}\times \overset{\circ}{\mathbf{A}}\,\mathbf{e} = \mathbf{0}$, as well as Table 1 in Sec. 2 in Part I, for case (c2) we infer that the set $V_{2m+1}(\mathbf{u},\mathbf{A})$ obeys the criterion (2.3) in Part I. Here and below it is helpful to note the fact: A nonvanishing vector $\mathbf{z}$ normal to $\mathbf{n}$ is an eigenvector of $\mathbf{A}$ if and only if $\mathbf{z}\times \overset{\circ}{\mathbf{A}}\,\mathbf{z}$ vanishes.

Third, for case (c3), i.e. $\mathbf{u} = \mathbf{e}' + d\mathbf{n}$, we have $\boldsymbol{\eta}_{2m}(\overset{\circ}{\mathbf{u}}) = (-1)^m\mathbf{e}$ and hence

$$\operatorname{rank} V_{2m+1}(\mathbf{u},\mathbf{A}) \geq \begin{cases} \operatorname{rank}\{\mathbf{n}, \mathbf{e}', \overset{\circ}{\mathbf{A}}\,\mathbf{u}, \mathbf{u}\times \overset{\circ}{\mathbf{A}}\,\mathbf{e}\} \text{ if } \mathbf{e}\times \overset{\circ}{\mathbf{A}}\,\mathbf{e} \neq \mathbf{0}, \\ \operatorname{rank}\{\mathbf{n}, \mathbf{e}'\} \text{ if } \mathbf{e}\times \overset{\circ}{\mathbf{A}}\,\mathbf{e} = \mathbf{0}. \end{cases}$$

From the above facts and Table 1 in Sec. 2 and the equality : $\Gamma(\mathbf{u},\mathbf{A}) \cap D_{2m+1d} = C_{1h}(\mathbf{e})$ when $\mathbf{e}$ is an eigenvector of $\mathbf{A}$, as well as Table 1 in Sec. 2 in Part I, for case (c3) we infer that the set $V_{2m+1}(\mathbf{u},\mathbf{A})$ obeys the criterion (2.3) in Part I.

From the above we conclude that the presented set $V_{2m+1}(\mathbf{u},\mathbf{A})$ supplies a desired vector generating set. Further, we infer that the last five generators in this set are irreducible by considering the paris $(\mathbf{u},\mathbf{A})$ given below:

$\overset{\circ}{\mathbf{A}}\,\mathbf{u}$ and $\mathbf{u}\times \overset{\circ}{\mathbf{A}}\,\boldsymbol{\eta}_{2m}(\overset{\circ}{\mathbf{u}})$: $\mathbf{u} = \mathbf{a}_1$, $\mathbf{A} = \mathbf{e}\otimes\mathbf{e}$;

$(\mathbf{u}\cdot\mathbf{n})\mathbf{n}\times\boldsymbol{\eta}_{2m}(\overset{\circ}{\mathbf{A}}\,\mathbf{n})$: $\mathbf{u} = \mathbf{n}$, $\mathbf{A} = \mathbf{n}\vee\mathbf{e}$;

$(\mathbf{u}\cdot\mathbf{n})\mathbf{n}\times\boldsymbol{\eta}_m(\mathbf{q}(\mathbf{A}))$ and $(\mathbf{u}\cdot\mathbf{n})\,\overset{\circ}{\mathbf{A}}\,(\mathbf{n}\times\boldsymbol{\eta}_m(\mathbf{q}(\mathbf{A}))$: $\mathbf{u} = \mathbf{n}$, $\mathbf{A} = \mathbf{e}\vee\mathbf{e}'$.

2.3. D_{2m+1d}-irreducible sets of three variables

(x) Three vector variables; two vector variables and a tensor variable

Consider any set of three variables $(\mathbf{u},\mathbf{v},\mathbf{z})$ where $\mathbf{z}$ is a vector or a skewsymmetric tensor or a symmetric tensor. From the D_{2m+1d}-irreducibility condition

for $(\mathbf{u}, \mathbf{v}, \mathbf{z})$ (see (3.2) in Part I) it follows that $(\mathbf{u}, \mathbf{v})$ is a D_{2m+1d}-irreducible set, specified by cases (c1) – (c3) derived in **(iv)**. For each of cases (c1) – (c2) we have $\Gamma(\mathbf{u}, \mathbf{v}) \cap D_{2m+1d} = C_1$. The latter leads to

$$\Gamma(\mathbf{u}, \mathbf{v}, \mathbf{z}) \cap D_{2m+1d} = (\Gamma(\mathbf{u}, \mathbf{v}) \cap D_{2m+1d}) \cap \Gamma(\mathbf{z}) = C_1.$$

The above fact shows that any set $(\mathbf{u}, \mathbf{v}, \mathbf{z})$ may be reduced to the D_{2m+1d}-irreducible set $(\mathbf{u}, \mathbf{v})$, which has been covered by **(iv)**.

(xi) A vector variable and two tensor variables

Consider any set $(\mathbf{x}, \mathbf{y}, \mathbf{u})$, where $(\mathbf{x}, \mathbf{y}) \in \{(\mathbf{W}, \boldsymbol{\Omega}), (\mathbf{W}, \mathbf{A}), (\mathbf{A}, \mathbf{B})\}$. For each such set, tensor generating sets and functional bases have been covered before (see Theorem 3.2 in XIAO [19]). As a result, it suffices to supply a vector generating set. Towards the latter goal we work out the D_{2m+1d}-irreducible set $(\mathbf{x}, \mathbf{y}, \mathbf{u})$, specified by the condition (3.2) in Part I with $\mathbf{x}$ and $\mathbf{y}$ two tensors and $\mathbf{z} = \mathbf{u}$ and $g = D_{2m+1d}$. Let $\mathbf{D}$ represent any of the two tensors $\mathbf{x}$ and $\mathbf{y}$. Evidently, we have $\Gamma(\mathbf{D}) \cap D_{2m+1d} \neq S_2$. Hence, if the tensor $\mathbf{D}$ is skewsymmetric, we have (see (2.9)) $\mathbf{D} = c\mathbf{E}\mathbf{a}_r$ or $\mathbf{D} = c\mathbf{E}\mathbf{n}$, where $c \neq 0$. If $\mathbf{D}$ is symmetric, we have (2.10) with the replacement of $\mathbf{A}$ by $\mathbf{D}$ and hence $\Gamma(\mathbf{D}) \cap D_{2m+1d} = C_{2h}(\mathbf{a})$. From these facts and

$$\Gamma(\mathbf{u}, \mathbf{x}) \cap D_{2m+1d} \neq C_1, \qquad \Gamma(\mathbf{u}, \mathbf{y}) \cap D_{2m+1d} \neq C_1,$$

as well as $C_{2h}(\mathbf{a}_r) \cap C_{2h}(\mathbf{a}_s) = S_2$ for any two two-fold axis vectors $\mathbf{a}_r$ and $\mathbf{a}_s$ of the group D_{2m+1d}, we derive each D_{2m+1d}-irreducible set $(\mathbf{u}, \mathbf{x}, \mathbf{y})$ at issue taking the forms:

$(\mathbf{u}, \mathbf{W}, \boldsymbol{\Omega})$:

(c1) $\mathbf{u} = c\mathbf{n}$, $\mathbf{W} = a\mathbf{E}\mathbf{e}$, $\boldsymbol{\Omega} = b\mathbf{E}\mathbf{n}$, $abc \neq 0$;

(c2) $\mathbf{u} = c\mathbf{n}$, $\mathbf{W} = a\mathbf{E}\mathbf{e}$, $\boldsymbol{\Omega} = b\mathbf{E}\mathbf{a}$, $abc \neq 0$.

$(\mathbf{u}, \mathbf{W}, \mathbf{A})$:

(c1) $\mathbf{u} = c\mathbf{n}$, $\mathbf{W} = a\mathbf{e}$, $\overset{\circ}{\mathbf{A}} = b(\mathbf{a} \otimes \mathbf{a} - \mathbf{a}' \otimes \mathbf{a}') + d\mathbf{n} \vee \mathbf{a}'$, $ac(b^2 + d^2) \neq 0$;

(c2) $\mathbf{u} = c\mathbf{n}$, $\mathbf{W} = a\mathbf{n}$, $\overset{\circ}{\mathbf{A}} = b\mathbf{D}_1 + d\mathbf{D}_4$, $ac(b^2 + d^2) \neq 0$.

$(\mathbf{u}, \mathbf{A}, \mathbf{B})$:

$\mathbf{u} = f\mathbf{n}$, $\overset{\circ}{\mathbf{A}} = a\mathbf{D}_1 + b\mathbf{D}_4$, $\overset{\circ}{\mathbf{B}} = c(\mathbf{a} \otimes \mathbf{a} - \mathbf{a}' \otimes \mathbf{a}') + d\mathbf{n} \vee \mathbf{a}'$,
$f(a^2 + b^2)(c^2 + d^2) \neq 0$.

In the above, $\mathbf{e} \neq \mathbf{a} \in \{\mathbf{a}_1, \cdots, \mathbf{a}_{2m}\}$ and $\mathbf{a}' = \mathbf{n} \times \mathbf{a}$. Then, we construct the following table for vector generating sets.

$$
\begin{aligned}
V \quad & V_{2m+1}(\mathbf{u}, \mathbf{W}) \cup V_{2m+1}(\mathbf{u}, \boldsymbol{\Omega}) \cup \{(\mathbf{u}\cdot\mathbf{n})(\mathbf{W}\boldsymbol{\Omega} - \boldsymbol{\Omega}\mathbf{W})\mathbf{n}\} \\
V \quad & V_{2m+1}(\mathbf{u}, \mathbf{W}) \cup V_{2m+1}(\mathbf{u}, \mathbf{A}) \\
& \cup\{(\mathbf{u}\cdot\mathbf{n})(\mathrm{tr}\mathbf{W}\mathbf{N})\mathbf{n}\times \overset{\circ}{\mathbf{A}}\,\mathbf{n}, (\mathbf{u}\cdot\mathbf{n})(\mathrm{tr}\mathbf{W}\mathbf{N})\boldsymbol{\eta}_m(\mathbf{q}(\mathbf{A}))\} \\
V \quad & V_{2m+1}(\mathbf{u}, \mathbf{A}) \cup V_{2m+1}(\mathbf{u}, \mathbf{B})
\end{aligned}
$$

Applying the fact

$$\mathrm{rank}(V(C_{1h}(\mathbf{a}_r) \cup V(C_{1h}(\mathbf{a}_s)) = \dim V = 3$$

for any two two-fold axis vectors $\mathbf{a}_r$ and $\mathbf{a}_s$ of the group D_{2m+1d}, and the cases derived for each D_{2m+1d}-irreducible set $(\mathbf{u}, \mathbf{x}, \mathbf{y})$ at issue, it may easily be verified that the above three presented sets supply the desired vector generating sets. The irreducibility of the three generators $(\mathbf{u}\cdot\mathbf{n})(\mathbf{W}\boldsymbol{\Omega} - \boldsymbol{\Omega}\mathbf{W})\mathbf{n}$, $(\mathbf{u}\cdot\mathbf{n})(\mathrm{tr}\mathbf{W}\mathbf{N})\mathbf{n}\times \overset{\circ}{\mathbf{A}}\,\mathbf{n}$ and $(\mathbf{u}\cdot\mathbf{n})(\mathrm{tr}\mathbf{W}\mathbf{N})\boldsymbol{\eta}_m(\mathbf{q}(\mathbf{A}))$ can be deduced from case (c1) for $(\mathbf{u}, \mathbf{W}, \boldsymbol{\Omega})$, and case (c2) for $(\mathbf{u}, \mathbf{W}, \mathbf{A})$ with $d = 0$ and $b = 0$ separately.

2.4. The general result

THEOREM 4. *The four sets given by*

$$
\begin{aligned}
& I_{2m+1}(\mathbf{u}); I_{2m+1}(\mathbf{W}); I_{2m+1}(\mathbf{A}); (\mathbf{u}\cdot\mathbf{n})(\mathbf{v}\cdot\mathbf{n}), \mathbf{u}\cdot\mathbf{v}, [\mathbf{u}, \mathbf{v}, \boldsymbol{\eta}_{2m}(\overset{\circ}{\mathbf{u}})], \\
& [\mathbf{v}, \mathbf{u}, \boldsymbol{\eta}_{2m}(\overset{\circ}{\mathbf{u}})], \\
& \alpha_{2m+1}(\overset{\circ}{\mathbf{u}})\ \overset{\circ}{\mathbf{v}}\cdot\boldsymbol{\eta}_{2m}(\overset{\circ}{\mathbf{u}}), \alpha_{2m+1}(\overset{\circ}{\mathbf{v}})\ \overset{\circ}{\mathbf{u}}\cdot\boldsymbol{\eta}_{2m}(\overset{\circ}{\mathbf{v}}); \\
& \mathrm{tr}\mathbf{W}\boldsymbol{\Omega}, \mathrm{tr}\mathbf{W}(\mathbf{E}\boldsymbol{\eta}_{2m}(\boldsymbol{\Omega}\mathbf{n})), \mathrm{tr}\boldsymbol{\Omega}(\mathbf{E}\boldsymbol{\eta}_{2m}(\mathbf{W}\mathbf{n})), \mathrm{tr}\boldsymbol{\Omega}\mathbf{W}(\mathbf{E}\boldsymbol{\eta}_{2m}(\mathbf{W}\mathbf{n})), \\
& \mathrm{tr}\mathbf{W}\boldsymbol{\Omega}(\mathbf{E}\boldsymbol{\eta}_{2m}(\boldsymbol{\Omega}\mathbf{n})); \\
& (\overset{\circ}{\mathbf{A}}\,\mathbf{n})\cdot\overset{\circ}{\mathbf{B}}\,\mathbf{n}, \mathrm{tr}\mathbf{A}_\mathbf{e}\mathbf{B}_\mathbf{e}, \mathrm{tr}\overset{\circ}{\mathbf{A}}{}^2\,\overset{\circ}{\mathbf{B}}, \mathrm{tr}\overset{\circ}{\mathbf{A}}\overset{\circ}{\mathbf{B}}{}^2, \mathrm{tr}\mathbf{A}_\mathbf{e}(\mathbf{E}\boldsymbol{\eta}_m(\mathbf{q}(\mathbf{B})))^2, \\
& [\mathbf{n}, \overset{\circ}{\mathbf{A}}\,\mathbf{n}, \boldsymbol{\eta}_{2m}(\overset{\circ}{\mathbf{B}}\,\mathbf{n})], [\mathbf{n}, \boldsymbol{\eta}_{2m}(\overset{\circ}{\mathbf{A}}\,\mathbf{n}), \overset{\circ}{\mathbf{B}}\overset{\circ}{\mathbf{A}}\,\mathbf{n}], [\mathbf{n}, \boldsymbol{\eta}_{2m}(\overset{\circ}{\mathbf{B}}\,\mathbf{n}), \overset{\circ}{\mathbf{A}}\overset{\circ}{\mathbf{B}}\,\mathbf{n}]; \\
& (\mathbf{W}\mathbf{n})\cdot\overset{\circ}{\mathbf{A}}\,\mathbf{W}\mathbf{n}, (\mathbf{W}\mathbf{n})\cdot\overset{\circ}{\mathbf{A}}\,\mathbf{n}, (\mathbf{W}\mathbf{n})\cdot\overset{\circ}{\mathbf{A}}{}^2\mathbf{n}, \mathrm{tr}\overset{\circ}{\mathbf{A}}\,\mathbf{W}(\mathbf{E}\boldsymbol{\eta}_{2m}(\mathbf{W}\mathbf{n})), \\
& [\mathbf{n}, \boldsymbol{\eta}_{2m}(\mathbf{W}\mathbf{n}), \overset{\circ}{\mathbf{A}}\,\mathbf{W}^2\mathbf{n}], (\mathrm{tr}\mathbf{W}\mathbf{N})\boldsymbol{\beta}_{2m+1}(\mathbf{q}(\mathbf{A})), \mathrm{tr}\mathbf{W}(\mathbf{E}\boldsymbol{\pi}_m(\mathbf{q}(\mathbf{A}))), \\
& \mathrm{tr}\mathbf{W}(\mathbf{E}\boldsymbol{\eta}_{2m}(\overset{\circ}{\mathbf{A}}\,\mathbf{n})), (\mathrm{tr}\mathbf{W}\mathbf{N})J(\mathbf{A}), (\mathrm{tr}\mathbf{W}\mathbf{N})\alpha_{2m+1}(\overset{\circ}{\mathbf{A}}\,\mathbf{n}) \\
& +\mathrm{tr}\mathbf{W}(\mathbf{E}\boldsymbol{\rho}_m(\mathbf{q}(\mathbf{A})));
\end{aligned}
$$

$$(\mathbf{u}\cdot\mathbf{n})\,\overset{\circ}{\mathbf{u}}\cdot\mathbf{W}\mathbf{n},(\overset{\circ}{\mathbf{u}}\cdot\mathbf{W}\mathbf{n})^2,\mathrm{tr}\mathbf{W}(\mathbf{E}\eta_{2m}(\overset{\circ}{\mathbf{u}})),[\mathbf{u},\mathbf{W}\mathbf{u},\eta_{2m}(\overset{\circ}{\mathbf{u}})],$$

$$\alpha_{2m+1}(\overset{\circ}{\mathbf{u}})\eta_{2m}(\overset{\circ}{\mathbf{u}})\cdot\mathbf{W}\mathbf{u};$$

$$\overset{\circ}{\mathbf{u}}\cdot\overset{\circ}{\mathbf{A}}\overset{\circ}{\mathbf{u}},\overset{\circ}{\mathbf{u}}\cdot\overset{\circ}{\mathbf{A}}{}^2\,\overset{\circ}{\mathbf{u}},(\mathbf{u}\cdot\mathbf{n})\,\overset{\circ}{\mathbf{u}}\cdot\overset{\circ}{\mathbf{A}}\,\mathbf{n},[\mathbf{u},\eta_{2m}(\overset{\circ}{\mathbf{u}}),\overset{\circ}{\mathbf{A}}\overset{\circ}{\mathbf{u}}],$$

$$\alpha_{2m}(\overset{\circ}{\mathbf{u}})(\eta_{2m}(\overset{\circ}{\mathbf{u}})\cdot\overset{\circ}{\mathbf{A}}\overset{\circ}{\mathbf{u}}-(\mathbf{u}\cdot\mathbf{n})\eta_{2m}(\overset{\circ}{\mathbf{u}})\cdot\overset{\circ}{\mathbf{A}}\,\mathbf{n});[\mathbf{r},\mathbf{u},\eta_{2m}(\overset{\circ}{\mathbf{v}})],[\mathbf{r},\mathbf{v},\eta_{2m}(\overset{\circ}{\mathbf{u}})];$$

$$\mathrm{tr}\mathbf{W}\Omega\mathbf{H};\mathrm{tr}\overset{\circ}{\mathbf{A}}\overset{\circ}{\mathbf{B}}\,\mathbf{W},(\overset{\circ}{\mathbf{A}}\,\mathbf{n})\cdot\mathbf{W}\,\overset{\circ}{\mathbf{B}}\overset{\circ}{\mathbf{A}}\,\mathbf{n},(\overset{\circ}{\mathbf{B}}\,\mathbf{n})\cdot\mathbf{W}\,\overset{\circ}{\mathbf{A}}\overset{\circ}{\mathbf{B}}\,\mathbf{n};$$

$$\mathrm{tr}\mathbf{W}\Omega\,\overset{\circ}{\mathbf{A}},|\mathrm{tr}\Omega\mathbf{N}|(\mathrm{tr}\Omega\mathbf{N})[\mathbf{n},\mathbf{W}\mathbf{n},\overset{\circ}{\mathbf{A}}\,\mathbf{W}\mathbf{n}]$$

$$+|\mathrm{tr}\mathbf{W}\mathbf{N}|(\mathrm{tr}\mathbf{W}\mathbf{N})[\mathbf{n},\Omega\mathbf{n},\overset{\circ}{\mathbf{A}}\,\Omega\mathbf{n}];$$

$$\mathbf{u}\cdot\mathbf{W}\mathbf{v},(\mathbf{u}\cdot\mathbf{n})^{2m+1}[\mathbf{n},\eta_{2m}(\overset{\circ}{\mathbf{v}}),\mathbf{W}\mathbf{v}]+(\mathbf{v}\cdot\mathbf{n})^{2m+1}[\mathbf{n},\eta_{2m}(\overset{\circ}{\mathbf{u}}),\mathbf{W}\mathbf{u}];$$

$$\mathbf{u}\cdot\overset{\circ}{\mathbf{A}}\,\mathbf{v},(\mathbf{u}\cdot\mathbf{n})^{2m+1}[\mathbf{n},\eta_{2m}(\overset{\circ}{\mathbf{v}}),\overset{\circ}{\mathbf{A}}\,\mathbf{v}]+(\mathbf{v}\cdot\mathbf{n})^{2m+1}[\mathbf{n},\eta_{2m}(\overset{\circ}{\mathbf{u}}),\overset{\circ}{\mathbf{A}}\,\mathbf{u}];$$

$$\mathrm{tr}\mathbf{W}\Omega(\mathbf{E}\eta_{2m}(\overset{\circ}{\mathbf{u}}));$$

$$(\mathrm{tr}\mathbf{W}\mathbf{N})[\mathbf{n},\overset{\circ}{\mathbf{u}},\overset{\circ}{\mathbf{A}}\overset{\circ}{\mathbf{u}}],(\mathrm{tr}\mathbf{W}\mathbf{N})\eta_{2m}(\overset{\circ}{\mathbf{u}})\cdot\overset{\circ}{\mathbf{A}}\,\mathbf{n},\overset{\circ}{\mathbf{u}}\cdot\mathbf{W}\,\overset{\circ}{\mathbf{A}}\overset{\circ}{\mathbf{u}},$$

$$(\overset{\circ}{\mathbf{u}}\cdot\overset{\circ}{\mathbf{A}}\,\mathbf{n})\,\overset{\circ}{\mathbf{u}}\cdot\mathbf{W}\,\overset{\circ}{\mathbf{A}}\,\mathbf{n};$$

and

$$V_{2m+1}(\mathbf{u});\mathbf{u}\times\eta_{2m}(\overset{\circ}{\mathbf{v}}),\mathbf{v}\times\eta_{2m}(\overset{\circ}{\mathbf{u}});\mathbf{W}\mathbf{u},\mathbf{W}^2\mathbf{u},\mathbf{u}\times\eta_{2m}(\mathbf{W}\mathbf{n}),$$

$$\mathbf{u}\times\mathbf{W}\eta_{2m}(\overset{\circ}{\mathbf{u}});$$

$$\overset{\circ}{\mathbf{A}}\,\mathbf{u},\mathbf{u}\times\overset{\circ}{\mathbf{A}}\,\eta_{2m}(\overset{\circ}{\mathbf{u}}),(\mathbf{u}\cdot\mathbf{n})\mathbf{n}\times\eta_{2m}(\overset{\circ}{\mathbf{A}}\,\mathbf{n}),$$

$$(\mathbf{u}\cdot\mathbf{n})\mathbf{n}\times\eta_m(\mathbf{q}(\mathbf{A})),(\mathbf{u}\cdot\mathbf{n})\,\overset{\circ}{\mathbf{A}}\,(\mathbf{n}\times\eta_m(\mathbf{q}(\mathbf{A})));$$

$$(\mathbf{u}\cdot\mathbf{n})(\mathbf{W}\Omega-\Omega\mathbf{W})\mathbf{n};(\mathbf{u}\cdot\mathbf{n})(\mathrm{tr}\mathbf{W}\mathbf{N})\mathbf{n}\times\overset{\circ}{\mathbf{A}}\,\mathbf{n},$$

$$(\mathbf{u}\cdot\mathbf{n})(\mathrm{tr}\mathbf{W}\mathbf{N})\eta_m(\mathbf{q}(\mathbf{A}));$$

and

$$\mathrm{Skw}_{2m+1}(\mathbf{u});\mathrm{Skw}_{2m+1}(\mathbf{W});\mathrm{Skw}_{2m+1}(\mathbf{A});$$

$$\mathbf{u}\wedge\mathbf{v},(\mathbf{u}\cdot\mathbf{n})^{2m+1}\,\overset{\circ}{\mathbf{v}}\wedge(\mathbf{n}\times\eta_{2m}(\overset{\circ}{\mathbf{v}}))+(\mathbf{v}\cdot\mathbf{n})^{2m+1}\,\overset{\circ}{\mathbf{u}}\wedge(\mathbf{n}\times\eta_{2m}(\overset{\circ}{\mathbf{u}}));$$

$$\mathbf{W}\Omega-\Omega\mathbf{W};\overset{\circ}{\mathbf{A}}\overset{\circ}{\mathbf{B}}-\overset{\circ}{\mathbf{B}}\overset{\circ}{\mathbf{A}},\overset{\circ}{\mathbf{A}}\,\mathbf{n}\wedge\overset{\circ}{\mathbf{B}}\overset{\circ}{\mathbf{A}}\,\mathbf{n},\overset{\circ}{\mathbf{B}}\,\mathbf{n}\wedge\overset{\circ}{\mathbf{A}}\overset{\circ}{\mathbf{B}}\,\mathbf{n};\overset{\circ}{\mathbf{A}}\,\mathbf{W}+\mathbf{W}\,\overset{\circ}{\mathbf{A}},$$

$$(\mathbf{E}:\mathbf{W})\wedge\eta_m(\mathbf{q}(\mathbf{A}));(\mathbf{E}:\mathbf{W})\wedge\eta_{2m}(\overset{\circ}{\mathbf{u}});\overset{\circ}{\mathbf{u}}\wedge\overset{\circ}{\mathbf{A}}\overset{\circ}{\mathbf{u}},(\overset{\circ}{\mathbf{u}}\cdot\overset{\circ}{\mathbf{A}}\,\mathbf{n})\,\overset{\circ}{\mathbf{u}}\wedge\overset{\circ}{\mathbf{A}}\,\mathbf{n};$$

and

$$\mathrm{Sym}_{2m+1}(\mathbf{u}), \mathrm{Sym}_{2m+1}(\mathbf{W}), \mathrm{Sym}_{2m+1}(\mathbf{A});$$

$$\mathbf{u} \vee \mathbf{v}, (\mathbf{u}\cdot\mathbf{n})^{2m+1}\, \overset{\circ}{\mathbf{v}} \vee (\mathbf{n} \times \boldsymbol{\eta}_{2m}(\overset{\circ}{\mathbf{v}})) + (\mathbf{v}\cdot\mathbf{n})^{2m+1}\, \overset{\circ}{\mathbf{u}} \vee (\mathbf{n} \times \boldsymbol{\eta}_{2m}(\overset{\circ}{\mathbf{u}}));$$

$$\mathbf{W}\boldsymbol{\Omega} + \boldsymbol{\Omega}\mathbf{W}, |\mathrm{tr}\boldsymbol{\Omega}\mathbf{N}|(\mathrm{tr}\boldsymbol{\Omega}\mathbf{N})\mathbf{W}\mathbf{n} \vee \mathbf{N}\mathbf{W}\mathbf{n} + |\mathrm{tr}\mathbf{W}\mathbf{N}|$$

$$(\mathrm{tr}\mathbf{W}\mathbf{N})\boldsymbol{\Omega}\mathbf{n} \vee \mathbf{N}\boldsymbol{\Omega}\mathbf{n};$$

$$(\mathrm{tr}\mathbf{W}\mathbf{N})(\overset{\circ}{\mathbf{A}}\,\mathbf{N} - \mathbf{N}\,\overset{\circ}{\mathbf{A}}), (\mathrm{tr}\mathbf{W}\mathbf{N})((-1)^m\, \overset{\circ}{\mathbf{A}}\,\mathbf{n} \vee \boldsymbol{\eta}_{2m}(\overset{\circ}{\mathbf{A}}\,\mathbf{n})$$

$$+\mathbf{n} \vee \boldsymbol{\rho}_m(\mathbf{q}(\mathbf{A})));$$

$$(\mathrm{tr}\mathbf{W}\mathbf{N})\, \overset{\circ}{\mathbf{u}} \vee (\mathbf{n} \times \overset{\circ}{\mathbf{u}}), (\mathrm{tr}\mathbf{W}\mathbf{N})\mathbf{n} \vee \boldsymbol{\eta}_{2m}(\overset{\circ}{\mathbf{u}});$$

where $(\mathbf{u}, \mathbf{v}, \mathbf{r}) = (\mathbf{u}_i, \mathbf{u}_j, \mathbf{u}_k)$, $(\mathbf{W}, \boldsymbol{\Omega}, \mathbf{H}) = (\mathbf{W}_\sigma, \mathbf{W}_\tau, \mathbf{W}_\theta)$, $(\mathbf{A}, \mathbf{B}) = (\mathbf{A}_L, \mathbf{A}_M)$, $k > j > i = 1, \cdots, a$, $\theta > \tau > \sigma = 1, \cdots, b$, $M > L = 1, \cdots, c$, *supply a functional basis and irreducible generating sets for scalar-, vector-, skewsymmetric and symmetric tensor-valued anisotropic functions of the a vectors* $\mathbf{u}_1, \cdots, \mathbf{u}_a$, *the b skewsymmetric tensors* $\mathbf{W}_1, \cdots, \mathbf{W}_b$ *and the c symmetric tensors* $\mathbf{A}_1, \cdots, \mathbf{A}_c$ *under the group* D_{2m+1d} *for each* $m \geq 1$. *In the presented result,* $\mathbf{n}$ *and* $\mathbf{e}$ *are two orthonormal vectors in the directions of the principal axis and a two-fold axis of the group* D_{2m+1d}.

In the above results, the invariants depending on two symmetric tensors are cited from Theorem 3 in XIAO, BRUHNS and MEYERS [19], as mentioned earlier.

3. Crystal and quasicrystal classes D_{2m+1}

The class D_{2m+1}, which includes the crystal class D_3 as the particular case when $m = 1$, is the rotation subgroup of the centrosymmetrical subgroup D_{2m+1d}, i.e. $D_{2m+1} = D_{2m+1d} \cap \mathrm{Orth}^+$. Following the procedure indicated in Sec. 5 in Part I, from the related results given in Theorem 4 we derive the results for the classes D_{2m+1} as follows.

THEOREM 5. *The four sets given by*

$$(\mathbf{u}\cdot\mathbf{n})^2, |\, \overset{\circ}{\mathbf{u}}\,|^2, \alpha_{2m+1}(\overset{\circ}{\mathbf{u}}), (\mathbf{u}\cdot\mathbf{n})\beta_{2m+1}(\overset{\circ}{\mathbf{u}}); I_{2m+1}(\mathbf{W}); I_{2m+1}(\mathbf{A});$$

$$I_{2m+1}(\mathbf{W}, \boldsymbol{\Omega}, \mathbf{H}, \mathbf{A}, \mathbf{B});$$

$$\mathbf{u}\cdot\mathbf{v}, \overset{\circ}{\mathbf{u}}\cdot\boldsymbol{\eta}_{2m}(\overset{\circ}{\mathbf{v}}), \overset{\circ}{\mathbf{v}}\cdot\boldsymbol{\eta}_{2m}(\overset{\circ}{\mathbf{u}}), [\mathbf{u}, \mathbf{v}, \boldsymbol{\eta}_{2m}(\overset{\circ}{\mathbf{v}})], [\mathbf{v}, \mathbf{u}, \boldsymbol{\eta}_{2m}(\overset{\circ}{\mathbf{u}})]; [\mathbf{u}, \mathbf{v}, \mathbf{r}];$$

$$\mathrm{tr}\mathbf{W}(\mathbf{E}\mathbf{u}), \mathrm{tr}\mathbf{W}(\mathbf{E}\boldsymbol{\eta}_{2m}(\overset{\circ}{\mathbf{u}})), \overset{\circ}{\mathbf{u}}\cdot\boldsymbol{\eta}_{2m}(\mathbf{W}\mathbf{n}), \boldsymbol{\eta}_{2m}(\overset{\circ}{\mathbf{u}})\cdot\mathbf{W}\mathbf{u}, \boldsymbol{\eta}_{2m}(\mathbf{W}\mathbf{n})\cdot\mathbf{W}\mathbf{u};$$

$$\overset{\circ}{\mathbf{u}}\cdot\overset{\circ}{\mathbf{A}}\mathbf{u}, [\mathbf{n}, \overset{\circ}{\mathbf{u}}, \overset{\circ}{\mathbf{A}}\,\mathbf{n}], [\mathbf{n}, \overset{\circ}{\mathbf{u}}, \overset{\circ}{\mathbf{A}}{}^2\mathbf{n}], \boldsymbol{\eta}_{2m}(\overset{\circ}{\mathbf{u}})\cdot\overset{\circ}{\mathbf{A}}\,\mathbf{u}, [\mathbf{n}, \boldsymbol{\eta}_{2m}(\overset{\circ}{\mathbf{u}}),$$

$\overset{\circ}{\mathbf{A}}\ ((\mathbf{n}\times\mathbf{u})\times\mathbf{u})]$,

$(\mathbf{u}\cdot\mathbf{n})\beta_{2m+1}(\mathbf{q}(\mathbf{A})), \overset{\circ}{\mathbf{u}}\cdot\pi_m(\mathbf{q}(\mathbf{A})), \overset{\circ}{\mathbf{u}}\cdot\eta_{2m}(\overset{\circ}{\mathbf{A}}\ \mathbf{n})$,

$(\mathbf{u}\cdot\mathbf{n})J(\mathbf{A}), (\mathbf{u}\cdot\mathbf{n})\alpha_{2m+1}(\overset{\circ}{\mathbf{A}}\ \mathbf{n})+\overset{\circ}{\mathbf{u}}\cdot\rho_m(\mathbf{q}(\mathbf{A}))$;

$\mathbf{u}\cdot\mathbf{W}\mathbf{v}; \mathbf{u}\cdot\mathbf{A}\mathbf{v}, |\mathbf{u}\cdot\mathbf{n}|(\mathbf{u}\cdot\mathbf{n})[\mathbf{n}, \overset{\circ}{\mathbf{v}}, \mathbf{A}\ \overset{\circ}{\mathbf{v}}] + |\mathbf{v}\cdot\mathbf{n}|(\mathbf{v}\cdot\mathbf{n})[\mathbf{n}, \overset{\circ}{\mathbf{u}}, \mathbf{A}\ \overset{\circ}{\mathbf{u}}]$;

$\mathrm{tr}\mathbf{W}\Omega(\mathbf{E}\mathbf{u}); \mathrm{tr}\overset{\circ}{\mathbf{A}}\overset{\circ}{\mathbf{B}}\ (\mathbf{E}\mathbf{u}), [\overset{\circ}{\mathbf{u}}, \overset{\circ}{\mathbf{A}}\ \mathbf{n}, \overset{\circ}{\mathbf{B}}\overset{\circ}{\mathbf{A}}\ \mathbf{n}], [\overset{\circ}{\mathbf{u}}, \overset{\circ}{\mathbf{B}}\ \mathbf{n}, \overset{\circ}{\mathbf{A}}\overset{\circ}{\mathbf{B}}\ \mathbf{n}]$;

$\mathrm{tr}\mathbf{W}(\mathbf{E}\mathbf{u})\ \overset{\circ}{\mathbf{A}}, |\mathbf{u}\cdot\mathbf{n}|(\mathbf{u}\cdot\mathbf{n})[\mathbf{n}, \mathbf{W}\mathbf{n}, \overset{\circ}{\mathbf{A}}\ \mathbf{W}\mathbf{n}]$

$-|\mathrm{tr}\mathbf{W}\mathbf{N}|(\mathrm{tr}\mathbf{W}\mathbf{N})[\mathbf{n}, \overset{\circ}{\mathbf{u}}, \overset{\circ}{\mathbf{A}}\overset{\circ}{\mathbf{u}}]$;

and

$\mathbf{u}, \eta_{2m}(\overset{\circ}{\mathbf{u}}), \mathbf{u}\times\eta_{2m}(\overset{\circ}{\mathbf{u}}); \mathbf{E}:\mathbf{W}, \eta_{2m}(\mathbf{W}\mathbf{n}), \mathbf{W}\eta_{2m}(\mathbf{W}\mathbf{n})$;

$\beta_{2m+1}(\mathbf{q}(\mathbf{A}))\mathbf{n}, \pi_m(\mathbf{q}(\mathbf{A})), \eta_{2m}(\overset{\circ}{\mathbf{A}}\ \mathbf{n}), \overset{\circ}{\mathbf{A}}\ \mathbf{n}\times\overset{\circ}{\mathbf{A}}\ ^2\mathbf{n}$,

$\alpha_{2m+1}(\overset{\circ}{\mathbf{A}}\ \mathbf{n})\mathbf{n}+\rho_m(\mathbf{q}(\mathbf{A}))$;

$\mathbf{u}\times\mathbf{v}; \mathbf{E}:(\mathbf{W}\Omega-\Omega\mathbf{W}); \mathbf{E}:(\overset{\circ}{\mathbf{A}}\overset{\circ}{\mathbf{B}}-\overset{\circ}{\mathbf{B}}\overset{\circ}{\mathbf{A}})$,

$\overset{\circ}{\mathbf{A}}\ \mathbf{n}\times\overset{\circ}{\mathbf{B}}\overset{\circ}{\mathbf{A}}\ \mathbf{n}, \overset{\circ}{\mathbf{B}}\ \mathbf{n}\times\overset{\circ}{\mathbf{A}}\overset{\circ}{\mathbf{B}}\ \mathbf{n}$;

$\overset{\circ}{\mathbf{A}}\ (\mathbf{E}:\mathbf{W}), \mathbf{W}\eta_m(\mathbf{q}(\mathbf{A})); \mathbf{W}\mathbf{u}; \overset{\circ}{\mathbf{A}}\ \mathbf{u}, \mathbf{u}\times\eta_m(\mathbf{q}(\mathbf{A}))$;

and

$\mathbf{E}\mathbf{u}, \mathbf{E}\eta_{2m}(\overset{\circ}{\mathbf{u}}), \mathbf{u}\wedge\eta_m(\overset{\circ}{\mathbf{u}}); \mathrm{Skw}_{2m+1}(\mathbf{W}); \mathrm{Skw}_{2m+1}(\mathbf{A})$;

$\mathbf{u}\wedge\mathbf{v}; \mathbf{W}\Omega-\Omega\mathbf{W}; \overset{\circ}{\mathbf{A}}\overset{\circ}{\mathbf{B}}-\overset{\circ}{\mathbf{B}}\overset{\circ}{\mathbf{A}}, \overset{\circ}{\mathbf{A}}\ \mathbf{n}\wedge\overset{\circ}{\mathbf{B}}\overset{\circ}{\mathbf{A}}\ \mathbf{n}, \overset{\circ}{\mathbf{B}}\ \mathbf{n}\wedge\overset{\circ}{\mathbf{A}}\overset{\circ}{\mathbf{B}}\ \mathbf{n}$;

$\overset{\circ}{\mathbf{A}}\ \mathbf{W}+\mathbf{W}\ \overset{\circ}{\mathbf{A}}, (\mathbf{E}:\mathbf{W})\wedge\eta_m(\mathbf{q}(\mathbf{A})); \mathbf{E}(\mathbf{W}\mathbf{u}); \mathbf{E}(\overset{\circ}{\mathbf{A}}\ \mathbf{u}), \mathbf{u}\wedge\eta_m(\mathbf{q}(\mathbf{A}))$;

and

$\mathbf{I}, \mathbf{n}\otimes\mathbf{n}, \overset{\circ}{\mathbf{u}}\otimes\overset{\circ}{\mathbf{u}}, \mathbf{n}\vee(\mathbf{n}\times\overset{\circ}{\mathbf{u}}), \mathbf{u}\vee\eta_{2m}(\overset{\circ}{\mathbf{u}}), (\mathbf{u}\times(\mathbf{u}\times\mathbf{n}))\vee(\mathbf{n}\times\eta_{2m}(\overset{\circ}{\mathbf{u}}))$;

$\mathrm{Sym}_{2m+1}(\mathbf{W}); \mathrm{Sym}_{2m+1}(\mathbf{A}); \mathbf{u}\vee\mathbf{v}, |\mathbf{u}\cdot\mathbf{n}|(\mathbf{u}\cdot\mathbf{n})\ \overset{\circ}{\mathbf{v}}\vee(\mathbf{n}\times\overset{\circ}{\mathbf{v}})$

$+|\mathbf{v}\cdot\mathbf{n}|(\mathbf{v}\cdot\mathbf{n})\ \overset{\circ}{\mathbf{u}}\vee(\mathbf{n}\times\overset{\circ}{\mathbf{u}})$;

$\mathbf{W}\Omega+\Omega\mathbf{W}, |\mathrm{tr}\Omega\mathbf{N}|(\mathrm{tr}\Omega\mathbf{N})\mathbf{W}\mathbf{n}\vee\mathbf{N}\mathbf{W}\mathbf{n}$

$+|\mathrm{tr}\mathbf{W}\mathbf{N}|(\mathrm{tr}\mathbf{W}\mathbf{N})\Omega\mathbf{n}\vee\mathbf{N}\Omega\mathbf{n}$;

$(\mathrm{tr}\mathbf{W}\mathbf{N})(\overset{\circ}{\mathbf{A}}\ \mathbf{N}-\mathbf{N}\ \overset{\circ}{\mathbf{A}}), (\mathrm{tr}\mathbf{W}\mathbf{N})((-1)^m\ \overset{\circ}{\mathbf{A}}\ \mathbf{n}\vee\eta_{2m}(\overset{\circ}{\mathbf{A}}\ \mathbf{n})$

$$+\mathbf{n} \vee \boldsymbol{\rho}_m(\mathbf{q}(\mathbf{A})));$$

$$\mathbf{W}(\mathbf{Eu}) + (\mathbf{Eu})\mathbf{W}, |\mathbf{u}\cdot\mathbf{n}|(\mathbf{u}\cdot\mathbf{n})\mathbf{Wn} \vee \mathbf{NWn}$$

$$+|\mathrm{tr}\mathbf{WN}|(\mathrm{tr}\mathbf{WN})\overset{\circ}{\mathbf{u}} \vee (\mathbf{n}\times\overset{\circ}{\mathbf{u}});$$

$$(\mathbf{u}\cdot\mathbf{n})(\overset{\circ}{\mathbf{A}}\,\mathbf{N} - \mathbf{N}\overset{\circ}{\mathbf{A}}), (\mathbf{u}\cdot\mathbf{n})((-1)^m\overset{\circ}{\mathbf{A}}\,\mathbf{n} \vee \boldsymbol{\eta}_{2m}(\overset{\circ}{\mathbf{A}}\,\mathbf{n})$$

$$+\mathbf{n} \vee \boldsymbol{\rho}_m(\mathbf{q}(\mathbf{A})));$$

where $(\mathbf{u},\mathbf{v},\mathbf{r}) = (\mathbf{u}_i,\mathbf{u}_j,\mathbf{u}_k)$, $(\mathbf{W},\boldsymbol{\Omega},\mathbf{H}) = (\mathbf{W}_\sigma,\mathbf{W}_\tau,\mathbf{W}_\theta)$, $(\mathbf{A},\mathbf{B}) = (\mathbf{A}_L,\mathbf{A}_M)$, $k > j > i = 1,\cdots,a$, $\theta > \tau > \sigma = 1,\cdots,b$, $M > L = 1,\cdots,c$, *supply a functional basis and irreducible generating sets for scalar-, vector-, skewsymmetric and symmetric tensor-valued anisotropic functions of the a vectors* $\mathbf{u}_1,\cdots,\mathbf{u}_a$, *the b skewsymmetric tensors* $\mathbf{W}_1,\cdots,\mathbf{W}_b$ *and the c symmetric tensors* $\mathbf{A}_1,\cdots,\mathbf{A}_c$ *under the group* D_{2m+1} *for each* $m \geq 1$. *In the presented result,* $\mathbf{n}$ *and* $\mathbf{e}$ *are two orthonormal vectors in the directions of the principal axis and a two-fold axis of the group* D_{2m+1}.

Here and henceforth, $I_{2m+1}(\mathbf{W},\boldsymbol{\Omega},\mathbf{H},\mathbf{A},\mathbf{B})$ is used to represent the invariants depending on two or three second order tensor variables given in Theorem 4.

4. Crystal and quasicrystal classes C_{2m+1v}

The classes at issue are of the form

$$C_{2m+1v}(\mathbf{n},\mathbf{e}) = \{\mathbf{R}_{\mathbf{n}}^{\theta_k}, -\mathbf{R}_{\mathbf{a}_k}^{\pi} \mid \mathbf{a}_k = \mathbf{R}_{\mathbf{n}}^{\theta_k}\mathbf{e},\ \theta_k = \frac{2k\pi}{2m+1}, \quad k = 1,\cdots,2m+1\}. \tag{4.1}$$

They include the crystal classes C_{3v} as particular case when $m = 1$.

For anisotropic functions under any subgroup $g \subset C_{\infty v}$, the general cases involving any number of vector variables and tensor variables may be reduced to the cases involving not more than two variables (see Theorem 2.3 in XIAO [18]). As a result, the third step in the procedure outlined in Sec. 3 in Part I can be omitted. Further reduction is possible. Let X_0 represent any of the sets of variables, $\mathbf{W}$, $\mathbf{A}$, $(\mathbf{W},\boldsymbol{\Omega})$, $(\mathbf{W},\mathbf{A})$ and $(\mathbf{A},\mathbf{B})$. Then each scalar-valued or tensor-valued anisotropic function of X_0 under the group $C_{2mv}(\mathbf{n},\mathbf{e})$ is a scalar-valued or tensor-valued anisotropic function of X_0 under the larger group $D_{2m+1d}(\mathbf{n},\mathbf{e})$ $(\supset C_{2m+1v}(\mathbf{n},\mathbf{e}))$. Thus, in the general results for the group C_{2m+1v} (Theorem 6 below), we can directly cite the invariants and the tensor generators depending on skewsymmetric and/or symmetric tensor variables in Theorem 4. Moreover, for the foregoing sets of variables, vector generating sets under the group C_{2m+1v}

and related invariants from the scalar products, can be derived by setting $\mathbf{u} = \mathbf{n}$ in the corresponding results in the tables given in Sec. 2 **(viii)**, **(ix)**, **(xi)**, since each anisotropic function of any set Y_0 of vectors and tensors under the group C_{2m+1v} is an anisotropic function of the set $(Y_0, \mathbf{n})$ under the larger group D_{2m+1d} $(\supset C_{2m+1v})$.

There remain four sets of variables that are not covered in the above, including $(\mathbf{u})$, $(\mathbf{u}, \mathbf{v})$, $(\mathbf{u}, \mathbf{W})$ and $(\mathbf{u}, \mathbf{A})$. In what follows the four sets of variables will be treated separately.

(i) A single vector $\mathbf{u}$

Results for a single vector variable $\mathbf{u}$ under the group C_{2m+1v} can be derived by setting $\mathbf{v} = \mathbf{n}$ in the table given in Sec. 2 **(iv)**. However, the results thus obtained include redundant invariants and generators. The desired irreducible functional basis and irreducible generating sets can be derived by removing some redundant invariants and generators. This can easily be done by means of the fact: when $\alpha_{2m+1}(\overset{\circ}{\mathbf{u}}) \neq 0$, $\overset{\circ}{\mathbf{u}}$ and $\mathbf{n} \times \boldsymbol{\eta}_{2m}(\overset{\circ}{\mathbf{u}})$ yield two independent vectors on the $\mathbf{n}$-plane and hence $\boldsymbol{\eta}_{2m}(\overset{\circ}{\mathbf{u}}) = x\,\overset{\circ}{\mathbf{u}} + y\mathbf{n} \times \boldsymbol{\eta}_{2m}(\overset{\circ}{\mathbf{u}})$. The results are as follows.

$$
\begin{aligned}
V \quad & \{\mathbf{n}, \overset{\circ}{\mathbf{u}}, \mathbf{n} \times \boldsymbol{\eta}_{2m}(\overset{\circ}{\mathbf{u}})\} \ (\equiv V^0_{2m+1}(\mathbf{u})) \\
\text{Skw} \quad & \{\alpha_{2m+1}(\overset{\circ}{\mathbf{u}})\mathbf{N}, \mathbf{n} \wedge \overset{\circ}{\mathbf{u}}, \mathbf{E}\boldsymbol{\eta}_{2m}(\overset{\circ}{\mathbf{u}})\} \ (\equiv \mathrm{Skw}^0_{2m+1}(\mathbf{u})) \\
\text{Sym} \quad & \{\mathbf{I}, \mathbf{n} \otimes \mathbf{n}, \overset{\circ}{\mathbf{u}} \otimes \overset{\circ}{\mathbf{u}}, \mathbf{n} \vee \overset{\circ}{\mathbf{u}}, \mathbf{n} \vee (\mathbf{n} \times \boldsymbol{\eta}_{2m}(\overset{\circ}{\mathbf{u}})), \overset{\circ}{\mathbf{u}} \vee (\mathbf{n} \times \boldsymbol{\eta}_{2m}(\overset{\circ}{\mathbf{u}}))\} \\
& (\equiv \mathrm{Sym}^0_{2m+1}(\mathbf{u})) \\
R \quad & \mathbf{n} \cdot \mathbf{r}, \overset{\circ}{\mathbf{r}} \cdot \overset{\circ}{\mathbf{u}}, [\mathbf{n}, \overset{\circ}{\mathbf{r}}, \boldsymbol{\eta}_{2m}(\overset{\circ}{\mathbf{u}})]; (\mathrm{tr}\mathbf{HN})\alpha_{2m+1}(\overset{\circ}{\mathbf{u}}), \overset{\circ}{\mathbf{u}} \cdot \mathbf{Hn}, \\
& \mathrm{tr}\mathbf{H}(\mathbf{E}\boldsymbol{\eta}_{2m}(\overset{\circ}{\mathbf{u}})); \\
& \mathrm{tr}\mathbf{C}, \mathbf{n} \cdot \mathbf{Cn}, \overset{\circ}{\mathbf{u}} \cdot \overset{\circ}{\mathbf{C}}\overset{\circ}{\mathbf{u}}, \overset{\circ}{\mathbf{u}} \cdot \overset{\circ}{\mathbf{C}}\,\mathbf{n}, [\mathbf{n}, \overset{\circ}{\mathbf{C}}\,\mathbf{n}, \boldsymbol{\eta}_{2m}(\overset{\circ}{\mathbf{u}})], [\mathbf{n}, \overset{\circ}{\mathbf{C}}\overset{\circ}{\mathbf{u}}, \boldsymbol{\eta}_{2m}(\overset{\circ}{\mathbf{u}})]; \\
& \{\mathbf{u} \cdot \mathbf{n}, |\,\overset{\circ}{\mathbf{u}}\,|^2, \beta_{2m+1}(\overset{\circ}{\mathbf{u}})\} \ (\equiv I^0_{2m+1}(\mathbf{u})).
\end{aligned}
$$

(ii) The C_{2m+1v}-irreducible set $(\mathbf{u}, \mathbf{v})$ of two vectors

The C_{2m+1v}-irreducibility condition for $(\mathbf{u}, \mathbf{v})$, i.e. (3.1) with $(\mathbf{x}, \mathbf{y}) = (\mathbf{u}, \mathbf{v})$ and $g = C_{2m+1v}$, yields $\Gamma(\mathbf{z}) \cap C_{2m+1v} \neq C_1$, C_{2m+1v}, $\mathbf{z} = \mathbf{u}$, $\mathbf{v}$. The latter means that $-\mathbf{R}^{\pi}_{\mathbf{a}}$ pertains to the symmetry group $\Gamma(\mathbf{z})$ for $\mathbf{z} = \mathbf{u}$, $\mathbf{v}$, i.e. $\mathbf{z} = c\mathbf{n} \times \mathbf{a} + d\mathbf{n}$ with $c \neq 0$. Thus, the C_{2m+1v}-irreducible set $(\mathbf{u}, \mathbf{v})$ is specified by $\mathbf{u} = a\mathbf{n} \times \mathbf{e} + b\mathbf{n}$ and $\mathbf{v} = c\mathbf{n} \times \mathbf{a} + d\mathbf{n}$ with $\mathbf{a} \neq \mathbf{e}$ and $ac \neq 0$. Here and henceforth, $\mathbf{a}$ is used to represent a two-fold axis vector of the group C_{2m+1v}.

With the aid of the latter we construct the following table.

$$
\begin{aligned}
V \quad & V^0_{2m+1}(\mathbf{u}) \cup V^0_{2m+1}(\mathbf{v}) \\
\text{Skw} \quad & \{\mathbf{n}\wedge \overset{\circ}{\mathbf{u}}, \mathbf{n}\wedge \overset{\circ}{\mathbf{v}}, \overset{\circ}{\mathbf{u}} \wedge \overset{\circ}{\mathbf{v}}\} \\
\text{Sym} \quad & \mathrm{Sym}^0_{2m+1}(\mathbf{u}) \cup \mathrm{Sym}^0_{2m+1}(\mathbf{v}) \\
R \quad & \mathbf{r} \cdot V^0_{2m+1}(\mathbf{z}), \mathbf{C} : \mathrm{Sym}^0_{2m+1}(\mathbf{z}),\ \overset{\circ}{\mathbf{z}} \cdot \mathbf{Hn},\ \mathbf{z} = \mathbf{u},\ \mathbf{v}; \overset{\circ}{\mathbf{u}} \cdot \mathbf{H}\, \overset{\circ}{\mathbf{v}}; \\
& I^0_{2m+1}(\mathbf{u}) \cup I^0_{2m+1}(\mathbf{v}) \cup \{\overset{\circ}{\mathbf{u}} \cdot \overset{\circ}{\mathbf{v}}\}.
\end{aligned}
$$

(iii) The C_{2m+1v}-irreducible set $(\mathbf{u}, \mathbf{A})$ of a vector and a symmetric tensor

The C_{2m+1v}-irreducibility condition for $(\mathbf{u}, \mathbf{A})$, i.e. (3.1) with $(\mathbf{x}, \mathbf{y})=(\mathbf{u}, \mathbf{A})$ and $g = C_{2m+1v}$, produces $\Gamma(\mathbf{u}) \cap C_{2m+1v} \neq C_1$, C_{2m+1v} and $\Gamma(\mathbf{A}) \cap C_{2m+1v} \neq C_1$. These mean that $-\mathbf{R}^{\pi}_{\mathbf{a}}$ pertains to the symmetry group $\Gamma(\mathbf{z})$ for $\mathbf{z} = \mathbf{u},\ \mathbf{A}$. Hence we deduce that the C_{2m+1v}-irreducible set $(\mathbf{u}, \mathbf{A})$ is specified by

$$
\mathbf{u} = a\mathbf{e}' + b\mathbf{n},\ \overset{\circ}{\mathbf{A}} = c(\mathbf{a} \otimes \mathbf{a} - \mathbf{a}' \otimes \mathbf{a}') + d\mathbf{n} \vee \mathbf{a}',\ \mathbf{a}' = \mathbf{n} \times \mathbf{a},\ \mathbf{a} \neq \mathbf{e}, \tag{4.2}
$$

$$
a(c^2 + d^2) \neq 0\,.
$$

Thus, we construct the following table.

$$
\begin{aligned}
V \quad & V^0_{2m+1}(\mathbf{u}) \cup V^0_{2m+1}(\mathbf{A})\ (\equiv V^0_{2m+1}(\mathbf{u}, \mathbf{A})) \\
\text{Skw} \quad & \mathrm{Skw}_{2m+1}(\mathbf{A}) \cup \{\mathbf{n}\wedge \overset{\circ}{\mathbf{u}}, \overset{\circ}{\mathbf{u}} \wedge \overset{\circ}{\mathbf{A}}\, \mathbf{n}, \overset{\circ}{\mathbf{u}} \wedge \overset{\circ}{\mathbf{A}}\overset{\circ}{\mathbf{u}}\} \\
\text{Sym} \quad & \mathrm{Sym}^0_{2m+1}(\mathbf{u}) \cup \mathrm{Sym}_{2m+1}(\mathbf{A}) \\
R \quad & \mathbf{r} \cdot V^0_{2m+1}(\mathbf{u}); \mathbf{H} : \mathrm{Skw}_{2m+1}(\mathbf{A}); \mathbf{C} : \mathrm{Sym}^0_{2m+1}(\mathbf{u}); \\
& \overset{\circ}{\mathbf{u}} \cdot \mathbf{H}\, \overset{\circ}{\mathbf{A}}\, \mathbf{n}, \overset{\circ}{\mathbf{u}} \cdot \mathbf{H}\, \overset{\circ}{\mathbf{A}}\overset{\circ}{\mathbf{u}}; \\
& I^0_{2m+1}(\mathbf{u}) \cup I_{2m+1}(\mathbf{A}) \cup \{\overset{\circ}{\mathbf{u}} \cdot \overset{\circ}{\mathbf{A}}\, \mathbf{n}, \overset{\circ}{\mathbf{u}} \cdot \overset{\circ}{\mathbf{A}}{}^2 \mathbf{n}, \overset{\circ}{\mathbf{u}} \cdot \overset{\circ}{\mathbf{A}}\overset{\circ}{\mathbf{u}}\} \\
& (\equiv I^0_{2m+1}(\mathbf{u}, \mathbf{A})).
\end{aligned}
$$

Here and henceforth, $V^0_{2m+1}(\mathbf{A})$ is used to designate the vector generating set for a symmetric tensor $\mathbf{A}$ under C_{2m+1v}, given by

$$
V^0_{2m+1}(\mathbf{A}) = V_{2m+1}(\mathbf{n}, \mathbf{A}) = \{\mathbf{n}, \overset{\circ}{\mathbf{A}}\, \mathbf{n}, \mathbf{n} \times \boldsymbol{\eta}_{2m}(\overset{\circ}{\mathbf{A}}\, \mathbf{n}), \mathbf{n} \times \boldsymbol{\eta}_m(\mathbf{q}(\mathbf{A})), \tag{4.3}
$$

$$
\overset{\circ}{\mathbf{A}}\, (\mathbf{n} \times \boldsymbol{\eta}_{2m}(\overset{\circ}{\mathbf{A}}\, \mathbf{n}))\}\,.
$$

In the above table and the table that will be given in (**iv**), the vector variable $\mathbf{r}$ pertains to the subspace $V(\Gamma(\mathbf{u}) \cap C_{2m+1v})$, the latter being spanned by the

vector generating set $V^0_{2m+1}(\mathbf{u})$. Owing to this fact, of the invariants from the scalar products of $\mathbf{r}$ and the vector generators in the set $V^0_{2m+1}(\mathbf{u}, \mathbf{D})$, where $\mathbf{D} = \mathbf{A}, \mathbf{W}$, the invariants except $\mathbf{r} \cdot V^0_{2m+1}(\mathbf{u})$ are redundant and can be deleted, as has been and will be done. The foregoing condition for $\mathbf{r}$ is derived from (see $(3.3)_2$ in Part I)

$$\Gamma(\mathbf{u}, \mathbf{r}) \cap C_{2m+1v} \neq \Gamma(\mathbf{u}, \mathbf{D}, \mathbf{r}) \cap C_{2m+1v} \ (= C_1).$$

The other case for $\mathbf{r}$, i.e. $\mathbf{r} \notin V(\Gamma(\mathbf{u}) \cap C_{2m+1v})$, has been covered by (**ii**) in this section.

By virtue of (4.2), it can easily be shown that the three presented sets of generators obey the criterion (2.3) in Part I, respectively, and hence they supply the desired vector, skewsymmetric and symmetric tensor generating sets. Moreover, we prove that the presented set $I^0_{2m+1}(\mathbf{u}, \mathbf{A})$ supplies a functional basis for the C_{2m+1v}-irreducible set $(\mathbf{u}, \mathbf{A})$ under the group C_{2m+1v}. Towards this goal it suffices to show that the set $I^0_{2m+1}(\mathbf{u}, \mathbf{A})$ determines a functional basis for the C_{2m+1v}-irreducible set $(\mathbf{u}, \mathbf{A})$ under the transverse isotropy group $C_{\infty v}(\mathbf{n})$ (see the comment at the end of Sec. 4 (**vi**) in Part I). In fact, the latter is obtainable from an isotropic functional basis for $(\overset{\circ}{\mathbf{u}}, \overset{\circ}{\mathbf{A}}, \mathbf{n})$, plus the three $C_{\infty v}$-invariants $\mathbf{u} \cdot \mathbf{n}$, $\mathbf{n} \cdot \mathbf{An}$ and $\mathrm{tr}\mathbf{A}$. The just-mentioned isotropic functional basis is given by $I_1 = \overset{\circ}{\mathbf{u}} \cdot \overset{\circ}{\mathbf{A}}\,\mathbf{n}$, $I_2 = \overset{\circ}{\mathbf{u}} \cdot \overset{\circ}{\mathbf{A}}{}^2\mathbf{n}$, $I_3 = \overset{\circ}{\mathbf{u}} \cdot \overset{\circ}{\mathbf{A}}\overset{\circ}{\mathbf{u}}$, $I_4 = \overset{\circ}{\mathbf{u}} \cdot \overset{\circ}{\mathbf{A}}{}^2\overset{\circ}{\mathbf{u}}$, as well as certain invariants of a single variable $\mathbf{u}$ or $\mathbf{A}$, each of the latter being covered or determined by the basis $I^0_{2m+1}(\mathbf{u})$ or $I_{2m+1}(\mathbf{A})$. Moreover, using (4.2) we have

$$I_1 = ad\cos\theta, \ I_4 = a^2(c^2 + d^2\cos^2\theta),$$

where $\theta = \mathbf{a} \cdot \mathbf{e}$. It is evident that I_4 is redundant, since we have $a^2 = |\overset{\circ}{\mathbf{u}}|^2$, $c^2 = |\mathbf{q}(\mathbf{A})|^2$ and $d^2 = |\overset{\circ}{\mathbf{A}}\,\mathbf{n}|^2$ for the C_{2m+1v}-irreducible set $(\mathbf{u}, \mathbf{A})$ (see (4.2)).

(**iv**) The C_{2m+1v}-irreducible set $(\mathbf{u}, \mathbf{W})$ of a vector and a skewsymmetric tensor

The C_{2m+1v}-irreducibility condition for $(\mathbf{u}, \mathbf{W})$, i.e. (3.1) with $(\mathbf{x}, \mathbf{y}) = (\mathbf{u}, \mathbf{W})$ and $g = C_{2m+1v}$, produces $\Gamma(\mathbf{u}) \cap C_{2m+1v} \neq C_1$, C_{2m+1v} and $\Gamma(\mathbf{W}) \cap C_{2m+1v} \neq C_1$. These mean that $-\mathbf{R}^{\pi}_{\mathbf{a}}$ pertains to the symmetry group $\Gamma(\mathbf{z})$ for $\mathbf{z} = \mathbf{u}, \mathbf{W}$. Hence we deduce that the C_{2m+1v}-irreducible set $(\mathbf{u}, \mathbf{W})$ is specified by the two cases

(c1) $\mathbf{u} = a\mathbf{e}' + b\mathbf{n}$ and $\mathbf{W} = c\mathbf{En}$ with $ac \neq 0$,

(c2) $\mathbf{u} = a\mathbf{e}' + b\mathbf{n}$ and $\mathbf{W} = c\mathbf{Ea}$ with $\mathbf{a} \neq \mathbf{e}$ and $ac \neq 0$.

Thus, we construct the following table.

$$
\begin{aligned}
V \quad & V^0_{2m+1}(\mathbf{u}) \cup \{\mathbf{Wn}, (\mathrm{tr}\mathbf{WN})\mathbf{n}\times \overset{\circ}{\mathbf{u}}\} \ (\equiv V^0_{2m+1}(\mathbf{u}, \mathbf{W})) \\
\mathrm{Skw} \quad & \{\mathbf{n}\wedge \overset{\circ}{\mathbf{u}}, \mathbf{W}, (\mathbf{E} : \mathbf{W}) \wedge \boldsymbol{\eta}_{2m}(\overset{\circ}{\mathbf{u}})\} \\
\mathrm{Sym} \quad & \mathrm{Sym}^0_{2m+1}(\mathbf{u}) \cup \mathrm{Sym}_{2m+1}(\mathbf{W}) \cup \{(\mathrm{tr}\mathbf{WN})\overset{\circ}{\mathbf{u}} \vee (\mathbf{n}\times \overset{\circ}{\mathbf{u}}), \\
& (\mathrm{tr}\mathbf{WN})\mathbf{n} \vee \boldsymbol{\eta}_{2m}(\overset{\circ}{\mathbf{u}})\} (\equiv \mathrm{Sym}^0_{2m+1}(\mathbf{u}, \mathbf{W})) \\
R \quad & \mathbf{r} \cdot V^0_{2m+1}(\mathbf{u}); \mathbf{C} : \mathrm{Sym}^0_{2m+1}(\mathbf{u}); \overset{\circ}{\mathbf{u}} \cdot \mathbf{Hn}, \mathrm{tr}\mathbf{HW}, \\
& \mathrm{tr}\mathbf{HW}(\mathbf{E}\boldsymbol{\eta}_{2m}(\overset{\circ}{\mathbf{u}})); \\
& I^0_{2m+1}(\mathbf{u}) \cup I_{2m+1}(\mathbf{W}) \cup \{\overset{\circ}{\mathbf{u}} \cdot \mathbf{Wn}\}.
\end{aligned}
$$

In the above table, the symmetric tensor variable $\mathbf{C}$ pertains to the subspace $\mathrm{Sym}(\Gamma(\mathbf{u}) \cap C_{2m+1v})$, the latter being spanned by the generating set $\mathrm{Sym}_{2m+1}(\mathbf{u})$. Owing to this fact, of the invariants from the scalar products of $\mathbf{C}$ and the symmetric tensor generators in the set $\mathrm{Sym}^0_{2m+1}(\mathbf{u}, \mathbf{W})$, those except $\mathbf{C} \cdot V^0_{2m+1}(\mathbf{u})$ are redundant and can be deleted, as has been done. The foregoing condition for $\mathbf{C}$ is derived from the condition (see $(3.3)_2$ in Part I)

$$\Gamma(\mathbf{u}, \mathbf{C}) \cap C_{2m+1v} \neq \Gamma(\mathbf{u}, \mathbf{W}, \mathbf{C}) \ (= C_1).$$

The other case for $\mathbf{C}$, i.e. $\mathbf{C} \notin \mathrm{Sym}(\Gamma(\mathbf{u}) \cap C_{2m+1v})$, has been covered before by **(iii)**.

With cases (c1) and (c2) for the C_{2m+1v}-irreducible set $(\mathbf{u}, \mathbf{W})$, it can easily be shown that the three presented sets of generators obey the criterion (2.3) in Part I, respectively, and hence they supply the desired vector, skewsymmetric and symmetric tensor generating sets. Moreover, we prove that the presented set $I^0_{2m+1}(\mathbf{u}, \mathbf{W})$ supplies a functional basis for the C_{2m+1v}-irreducible set $(\mathbf{u}, \mathbf{W})$ under the group C_{2m+1v}. Towards this goal it suffices to show that the set $I^0_{2m+1}(\mathbf{u}, \mathbf{W})$ determines a functional basis for the C_{2m+1v}-irreducible set $(\mathbf{u}, \mathbf{W})$ under the transverse isotropy group $C_{\infty v}(\mathbf{n})$ (see the comment at the end of Sec. 4 **(vii)** in Part I). In fact, the latter is obtainable from an isotropic functional basis for $(\overset{\circ}{\mathbf{u}}, \mathbf{W}, \mathbf{n})$, plus the $C_{\infty v}$-invariant $\mathbf{u}\cdot\mathbf{n}$. The just-mentioned isotropic functional basis is given by

$$I_1 = \overset{\circ}{\mathbf{u}} \cdot \mathbf{Wn}, \ I_2 = \overset{\circ}{\mathbf{u}} \cdot \mathbf{W}^2\mathbf{n}, \ I_3 = \overset{\circ}{\mathbf{u}} \cdot \mathbf{W}^2 \overset{\circ}{\mathbf{u}},$$

as well as certain invariants of a single variable $\mathbf{u}$ or $\mathbf{W}$, each of the latter being covered or determined by the basis $I^0_{2m+1}(\mathbf{u})$ or $I_{2m+1}(\mathbf{W})$. The two invariants I_2 and I_3 are redundant for cases (c1) and (c2) derived before. This fact is obviously true for case (c1), and it is also true for case (c2), since for case (c2) we have $I_2 = 0, \ I_3 = -a^2c^2(\mathbf{a} \cdot \mathbf{e})^2 = -(I_1)^2$.

Combining the above results, we arrive at the general result as follows.

THEOREM 6. *The four sets given by*

$$I^0_{2m+1}(\mathbf{u}); I_{2m+1}(\mathbf{W}); I_{2m+1}(\mathbf{A}); I_{2m+1}(\mathbf{W},\boldsymbol{\Omega},\mathbf{H},\mathbf{A},\mathbf{B});$$

$$\overset{\circ}{\mathbf{u}}\cdot\overset{\circ}{\mathbf{v}}, [\mathbf{n},\overset{\circ}{\mathbf{u}},\boldsymbol{\eta}_{2m}(\overset{\circ}{\mathbf{v}})], [\mathbf{n},\overset{\circ}{\mathbf{v}},\boldsymbol{\eta}_{2m}(\overset{\circ}{\mathbf{u}})];$$

$$\overset{\circ}{\mathbf{u}}\cdot\mathbf{W}\mathbf{n}, \mathrm{tr}\mathbf{W}(\mathbf{E}\boldsymbol{\eta}_{2m}(\overset{\circ}{\mathbf{u}})), (\mathrm{tr}\mathbf{W}\mathbf{N})\alpha_{2m+1}(\overset{\circ}{\mathbf{u}});$$

$$\overset{\circ}{\mathbf{u}}\cdot\overset{\circ}{\mathbf{A}}\,\mathbf{n}, \overset{\circ}{\mathbf{u}}\cdot\overset{\circ}{\mathbf{A}}\overset{\circ}{\mathbf{u}}, \overset{\circ}{\mathbf{u}}\cdot\overset{\circ}{\mathbf{A}}{}^2\mathbf{n}, [\mathbf{n},\boldsymbol{\eta}_{2m}(\overset{\circ}{\mathbf{u}}),\overset{\circ}{\mathbf{A}}\,\mathbf{n}], [\mathbf{n},\boldsymbol{\eta}_{2m}(\overset{\circ}{\mathbf{u}}),\overset{\circ}{\mathbf{A}}\overset{\circ}{\mathbf{u}}];$$

$$\overset{\circ}{\mathbf{u}}\cdot\mathbf{W}\overset{\circ}{\mathbf{v}}; \mathrm{tr}\mathbf{W}\boldsymbol{\Omega}(\mathbf{E}\boldsymbol{\eta}_{2m}(\overset{\circ}{\mathbf{u}})); \overset{\circ}{\mathbf{u}}\cdot\mathbf{W}\overset{\circ}{\mathbf{A}}\,\mathbf{n}, \overset{\circ}{\mathbf{u}}\cdot\mathbf{W}\overset{\circ}{\mathbf{A}}\overset{\circ}{\mathbf{u}};$$

and

$$V^0_{2m+1}(\mathbf{u}); V^0_{2m+1}(\mathbf{A}); \mathbf{W}\mathbf{n}, \mathbf{W}^2\mathbf{n}, \mathbf{n}\times\boldsymbol{\eta}_{2m}(\mathbf{W}\mathbf{n}); (\mathrm{tr}\mathbf{W}\mathbf{N})\mathbf{n}\times\overset{\circ}{\mathbf{u}};$$
$$(\mathbf{W}\boldsymbol{\Omega}-\boldsymbol{\Omega}\mathbf{W})\mathbf{n}; (\mathrm{tr}\mathbf{W}\mathbf{N})\mathbf{n}\times\overset{\circ}{\mathbf{A}}\,\mathbf{n}, (\mathrm{tr}\mathbf{W}\mathbf{N})\boldsymbol{\eta}_m(\mathbf{q}(\mathbf{A}));$$

and

$$\mathrm{Skw}^0_{2m+1}(\mathbf{u}); \mathrm{Skw}_{2m+1}(\mathbf{W}); \mathrm{Skw}_{2m+1}(\mathbf{A}); \overset{\circ}{\mathbf{u}}\wedge\overset{\circ}{\mathbf{v}};$$

$$\mathbf{W}\boldsymbol{\Omega}-\boldsymbol{\Omega}\mathbf{W}; \overset{\circ}{\mathbf{A}}\overset{\circ}{\mathbf{B}}-\overset{\circ}{\mathbf{B}}\overset{\circ}{\mathbf{A}}, \overset{\circ}{\mathbf{A}}\,\mathbf{n}\wedge\overset{\circ}{\mathbf{B}}\overset{\circ}{\mathbf{A}}\,\mathbf{n}, \overset{\circ}{\mathbf{B}}\,\mathbf{n}\wedge\overset{\circ}{\mathbf{A}}\overset{\circ}{\mathbf{B}}\,\mathbf{n};$$

$$\overset{\circ}{\mathbf{A}}\,\mathbf{W}+\mathbf{W}\overset{\circ}{\mathbf{A}}, (\mathbf{E}:\mathbf{W})\wedge\boldsymbol{\eta}_m(\mathbf{q}(\mathbf{A})); (\mathbf{E}:\mathbf{W})\wedge\boldsymbol{\eta}_{2m}(\overset{\circ}{\mathbf{u}});$$

$$\overset{\circ}{\mathbf{u}}\wedge\overset{\circ}{\mathbf{A}}\,\mathbf{n}, \overset{\circ}{\mathbf{u}}\wedge\overset{\circ}{\mathbf{A}}\overset{\circ}{\mathbf{u}};$$

and

$$\mathbf{I}, \mathbf{n}\otimes\mathbf{n}, \overset{\circ}{\mathbf{u}}\otimes\overset{\circ}{\mathbf{u}}, \mathbf{n}\vee\overset{\circ}{\mathbf{u}}, \mathbf{n}\vee(\mathbf{n}\times\boldsymbol{\eta}_{2m}(\overset{\circ}{\mathbf{u}})), \overset{\circ}{\mathbf{u}}\vee(\mathbf{n}\times\boldsymbol{\eta}_{2m}(\overset{\circ}{\mathbf{u}}));$$

$$\mathrm{Sym}_{2m+1}(\mathbf{W}); \mathrm{Sym}_{2m+1}(\mathbf{A});$$

$$\mathbf{W}\boldsymbol{\Omega}+\boldsymbol{\Omega}\mathbf{W}, |\mathrm{tr}\boldsymbol{\Omega}\mathbf{N}|(\mathrm{tr}\boldsymbol{\Omega}\mathbf{N})\mathbf{W}\mathbf{n}\vee\mathbf{N}\mathbf{W}\mathbf{n}$$

$$+|\mathrm{tr}\mathbf{W}\mathbf{N}|(\mathrm{tr}\mathbf{W}\mathbf{N})\boldsymbol{\Omega}\mathbf{n}\vee\mathbf{N}\boldsymbol{\Omega}\mathbf{n};$$

$$(\mathrm{tr}\mathbf{W}\mathbf{N})(\overset{\circ}{\mathbf{A}}\,\mathbf{N}-\mathbf{N}\overset{\circ}{\mathbf{A}}), (\mathrm{tr}\mathbf{W}\mathbf{N})((-1)^m\overset{\circ}{\mathbf{A}}\,\mathbf{n}\vee\boldsymbol{\eta}_{2m}(\overset{\circ}{\mathbf{A}}\,\mathbf{n})$$

$$+\mathbf{n}\vee\boldsymbol{\rho}_m(\mathbf{q}(\mathbf{A})));$$

$$(\mathrm{tr}\mathbf{W}\mathbf{N})\overset{\circ}{\mathbf{u}}\vee(\mathbf{n}\times\overset{\circ}{\mathbf{u}}), (\mathrm{tr}\mathbf{W}\mathbf{N})\mathbf{n}\vee\boldsymbol{\eta}_{2m}(\overset{\circ}{\mathbf{u}});$$

where $(\mathbf{u},\mathbf{v}) = (\mathbf{u}_i,\mathbf{u}_j)$, $(\mathbf{W},\boldsymbol{\Omega},\mathbf{H}) = (\mathbf{W}_\sigma,\mathbf{W}_\tau,\mathbf{W}_\theta)$, $(\mathbf{A},\mathbf{B}) = (\mathbf{A}_L,\mathbf{A}_M)$, $j>i=1,\cdots,a$, $\theta>\tau>\sigma=1,\cdots,b$, $M>L=1,\cdots,c$, *supply a functional basis and irreducible generating sets for scalar-, vector-, skewsymmetric*

and symmetric tensor-valued anisotropic functions of the a vectors $\mathbf{u}_1, \cdots, \mathbf{u}_a$, *the b skewsymmetric tensors* $\mathbf{W}_1, \cdots, \mathbf{W}_b$ *and the c symmetric tensors* $\mathbf{A}_1, \cdots, \mathbf{A}_c$ *under the group* C_{2m+1v} *for each* $m \geq 1$. *In the presented result,* $\mathbf{n}$ *and* $\mathbf{e}$ *are two orthonormal vectors in the directions of the principal axis and a two-fold axis of the group* C_{2m+1v}.

Acknowledgment

This research was completed under the finiancial support from Deutsche Forschungsgemeinschaft (DFG) (Contract No.: Br 580/26-1) and Alexander von Humboldt-Stiftung. This support is gratefully acknowledged. Moreover, the authors are very grateful to the reviewer for the careful examination and the constructive and helpful comments on the early version of ths work.

References

1. J. BETTEN, *Recent advances in applications of tensor functions in solid mechanics*, Advances in Mech., **14**, 1, 79–109, 1991.
2. J. BETTEN, *Kontinuumsmecnik: Elasto-, Plasto- und Kriechmechanik*, Springer, Berlin 1993.
3. J.P. BOEHLER, *A simple derivation of non-polynomial representations for constitutive equations in some cases of anisotropy*, Zeits. Angew. Math. Mech., **59**, 157–167, 1979.
4. J.P. BOEHLER [Ed.], *Applications of tensor functions in solid mechanics*, CISM Courses and Lectures no. 292, Springer-Verlag, New York, Wien 1987.
5. A.C. ERINGEN and G.A. MAUGIN, *Electrodynamics of continua I. Foundations and solid media*. Springer-Verlag, Berlin, New York 1989.
6. E. KIRAL and A.C. ERINGEN, *Constitutive equations of electromagnetic-elastic crystals*, Springer-Verlag, Berlin, New York, etc. 1990.
7. J. RYCHLEWSKI, *Symmetry of causes and effects*, SIAMM Research Report no. 8706, Shanghai Institute of Applied Mathematics and Mechanics, Shanghai 1987; also: Wydawnictwo Naukowe PWN, Warsaw 1991.
8. J. RYCHLEWSKI and J.M. ZHANG, *On representations of tensor functions: A review*, Advances in Mech., **14**, 4, 75–94, 1991.
9. G.F. SMITH, *Constitutive equations for anisotropic and isotropic materials*, Elsevier, New York 1994.
10. A.J.M. SPENCER, *Theory of invariants*, In *Continuum physics*, Vol. I, A.C. ERINGEN [Ed.], Academic Press, pp. 239–353, New York 1971.
11. C. TRUESDELL and W. NOLL, *The nonlinear field theories of mechanics*, In *Handbuch der Physik*, Vol. III/3, S. FLÜGGE [Ed.], Springer-Verlag, Berlin, New York, etc. 1965.
12. C.C. WANG, *A new representation theorem for isotropic functions, Part I and II*, Arch. Rat. Mech. Anal., **36**, 166–223, 1970; *Corrigendum*, ibid, **43**, 392–395, 1971.

13. H. XIAO, *Two general representation theorems for arbitrary-order-tensor-valued isotropic and anisotropic tensor functions of vectors and second order tensors*, Zeits. Angew. Math. Mech., **76**, 151–162, 1996.

14. H. XIAO, *On isotropic extension of anisotropic tensor functions*, Zeits. Angew. Math. Mech., **76**, 205–214, 1996.

15. H. XIAO, *A unified theory of representations for scalar-, vector- and second order tensor-valued anisotropic functions of vectors and second order tensors*, Arch. Mech., **50**, 275–313, 1997.

16. H. XIAO, *On constitutive equations of Cauchy elastic solids: All kinds of crystals and quasicrystals*, J. Elasticity, **48**, 241–283, 1997.

17. H. XIAO, *On anisotropic invariants of a symmetric tensor: crystal classes, quasicrystal classes and others*, Proc. Roy. Soc. London, A**454**, 1217–1240, 1998.

18. H. XIAO, *Further results on general representation theorems for arbitrary-order-tensor-valued isotropic and anisotropic tensor functions of vectors and second order tensors*, Zeits. Angew. Math. Mech., 1999 (to appear).

19. H. XIAO, O.T. BRUHNS and A. MEYERS, *On anisotropic invariants of N symmetric second order tensors: all crystal and quasicrystal classes as subgroups of the cylindrical group $D_{\infty h}$*, Proc. Roy. Soc. London A, **455**, 1993–2020, 1999.

20. H. XIAO, O.T. BRUHNS and A. MEYERS, *Irreducible representations for constitutive equations of anisotropic solids I: crystal and quasicrystal classes D_{2mh}, D_{2m} and C_{2mv}*, Arch. Mech., **51**, 559–603, 1999.

21. Q.S. ZHENG, *Theory of representations for tensor functions: A unified invariant approach to constitutive equations*, Appl. Mech. Rev., **47**, 545–587, 1994.

Received November 25, 1998; revised version August 5, 1999.

Arch. Mech., **52**, 1, pp. 89–102, Warszawa 2000

Stress distribution in the muscles of the diaphragm [1)]

M. ANGELILLO (*), A. FORTUNATO (*) and T. A. WILSON (**)

(*) *Department of Civil Engineering*
University of Salerno, Italy

(**) *Department of Aerospace Engineering and Mechanics,*
University of Minnesota, Minnesota

THE DIAPHRAGM is treated as a membrane subject to a uniform pressure. The muscle action is modeled as a uniaxial active stress in the direction of muscle bundles. In the present paper we look for the generalized stress distribution in the membrane. The shape of the active diaphragm is approximated by a surface know as a cyclide. For this simplified shape, a closed form solution of the equilibrium equations is obtained.

1. Introduction

THE DIAPHRAGM, by virtue of its curved shape, converts muscle tension to transdiaphragmatic pressure and muscle shortening to volume displacement. During breathing, the displacement of the diaphragm is large (see [1, 2]); for example in dogs, in quiet spontaneous breathing, muscle bundles shorten on average to 75% of their original length [1].

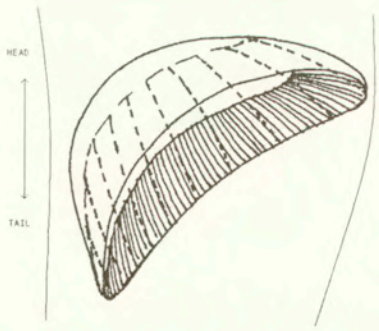

FIG. 1.a) Typical dog diaphragm displacement during breathing.

[1)] The paper was presented at the 32nd Solid Mechanics Conference: SolMec'98, held in Zakopane, September 1–5, 1998.

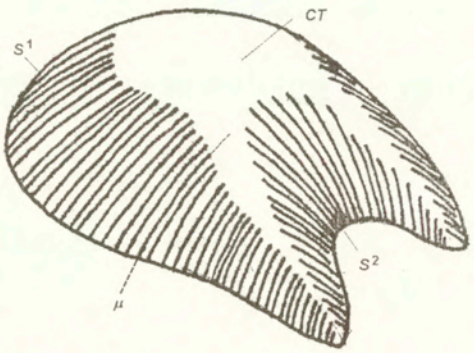

FIG. 1. b) Schematic view showing central tendon (CT), costal diaphragm (S^1) and crural diaphragm (S^2).

The diaphragm is a rather complex muscular structure. Some features of the diaphragm common to many mammals, such as humans and dogs, can be recognized:

a) The muscle bundles extend from the chest wall to a tendinous island known as the central tendon.

b) The muscle bundles and the central tendon form a curved sheet that separates the abdominal from the thoracic cavities.

c) The muscle bundles are connected transversely by fibers of connective tissue.

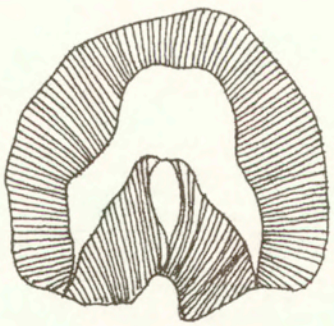

FIG. 2. a) Upper view of a typical dog diaphragm laid flat on a plane.

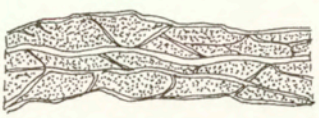

FIG. 2. b) Section of diaphragm tissue transverse to muscle fibers, showing collagen fibers.

The complex geometry and mechanics of the diaphragm, which are crucial to its function, have not been thoroughly described. As a result, the relations between muscle tension and transdiaphragmatic pressure are poorly understood.

The description of the geometry and of the state of stress of the active diaphragm, that is of equilibrium configurations at end of inspiration, is the scope of the research we are currently conducting in collaboration with scientists from the Baylor College of Medicine of Houston. In this paper the more mechanical results of this research, regarding the stress analysis of an active membrane modeling the canine diaphragm, are presented.

The central tendon consists of connective tissue and is effectively inextensible under physiological stress. The muscle layer is bounded by membranes consisting of connective tissue and contains connective tissue. At physiological level of stress, it is effectively inextensible in the direction transverse to muscle fibers. Therefore we picture the stress along the muscle bundles in the active diaphragm as being primarily the results of the active stress in the muscle and the stress in the transverse direction as being carried by connective tissue. Considering the small resistance to bending of the diaphragm, its structure is treated as a membrane with no bending stiffness. Due to its curved shape, the diaphragm converts this stress into a pressure difference across the surface, balanced by the recoil of the lungs. Each muscle bundle, when activated, exerts a force per unit length in the direction of the curvature vector of the surface. Such force is proportional to the curvature.

In recent papers BORIEK *et al.* [5] reported data on the shape of muscle bundles and the shape of the surface in the mid-costal region of the canine diaphragm. The data were obtained by attaching radio-opaque markers along muscle bundles on the peritoneal surface of the diaphragm in this region, and then determining the three-dimensional locations of the markers from biplane videofluoroscopic images recorded during passive lung inflation and spontaneous breathing. They found that, in this region, the surface of the diaphragm has approximately the shape of a right circular cylinder with the muscle bundles forming circular arcs that lie in planes orthogonal to the surface.

ANGELILLO *et al.* proposed a theory of the structure and shape of the diaphragm [6]. The theory was based on the assumptions that muscles of the diaphragm lie along lines that are both lines of maximum curvature and geodesics of the surface. These assumptions were shown to be equivalent to the assumption that muscle bundles lie in planes that are orthogonal to the surface. Thus the theory was based on the hypothesis that the relations between muscle bundles and surface geometry observed in the mid-costal region are in fact universal relations that can be obtained everywhere.

If muscle lines satisfy this assumption they are, in a sense, optimal since their energy consumption in deforming the surface is minimal: if the muscle lines are

lines of principal, maximum curvature, the contribution of the muscle force to create pressure difference is maximal; if the muscle lines are geodesics, no energy is lost in deforming the surface since the curvature vectors of these lines are orthogonal to the surface.

The class of surfaces with these properties was determined. It is a restricted class. In a surface of this class all the muscle lines must have the same shape, the orientation of the muscle lines is restricted. A special collection of surfaces belonging to this class is that of surfaces spanned by circular arcs of constant radius. Surfaces formed by circular arcs that are both principal and geodesics are known as cyclides (see HILBERT [7]). In a recent work, [8], an example of fitting of the costal and crural dog diaphragm by two cyclides having different radii and meeting smoothly at an interface is presented.

Neglecting inertia effects, we are interested in the equilibrium configuration of the diaphragm in its active state. Since the diaphragm is in contact with the lungs and the abdominal organs through a fluid interface, as a first approximation we consider the diaphragm acted on by a uniform pressure p normal to the surface, representing the transdiaphragmatic pressure. Therefore we study the equilibrium of a membrane surface having the form of a cyclide of radius ρ and subject to a given uniform pressure.

Using physical stress components $(\sigma_{11}, \sigma_{22}, \sigma_{12})$ in the curvilinear coordinates of principal curvature of the surface (as a result of the optimality assumptions one family of these lines coincides with the muscle lines), the equilibrium equations of the membrane subject to a uniform pressure can be solved, imposing sufficient stress boundary conditions. The problem, with convenient boundary conditions, admits a closed-form solution with the shear stress $\sigma_{12} = 0$ everywhere, that is with the fibers of connective tissue orthogonal to the muscle lines.

2. Diaphragm theory

2.1. Preliminaries

The geometry of the surface in its actual configuration (*Eulerian* description), is described, in the *Euclidean* three-space, by the position vector

$$\mathbf{x} = \mathbf{x}(t^1, t^2), \tag{2.1}$$

depending on two curvilinear coordinates ranging in an open, connected domain Ω of $\mathcal{R}^2$ (see Fig. 3).

We assume that the surface is smooth in the sense that $\mathbf{x}(t^1, t^2)$ belongs to $C^3(\Omega)$. The natural base vectors associated to the curvilinear coordinates t^1, t^2

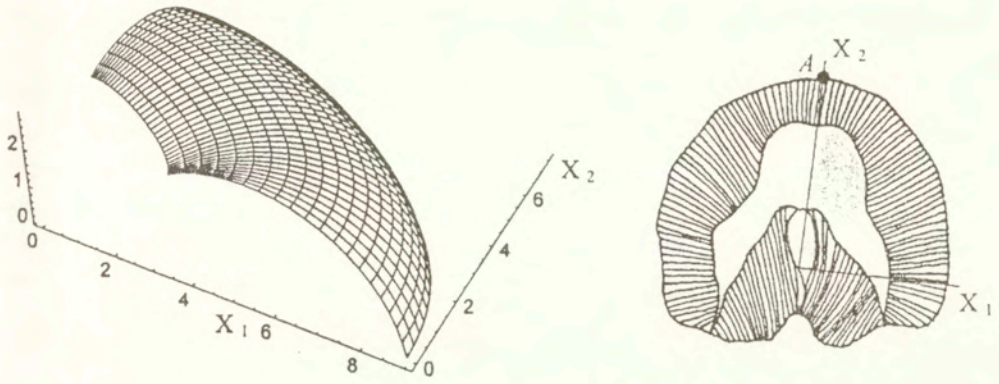

FIG. 3. Shape of diaphragm surface used for stress analysis. In the right-hand picture the top schematic view of the portion modeled is shown.

are denoted

$$\mathbf{g}_1 = \frac{\partial \mathbf{x}}{\partial t^1}, \qquad \mathbf{g}_2 = \frac{\partial \mathbf{x}}{\partial t^2}. \tag{2.2}$$

The controvariant base vectors $\mathbf{g}^k$ are defined through the relation

$$\mathbf{g}^\alpha \cdot \mathbf{g}_\beta = \delta^\alpha_\beta, \qquad \alpha, \beta = 1, 2. \tag{2.3}$$

δ^α_β being the Kronecker delta. $\mathbf{g}_3$ is the unit normal to the surface, defined by the relation

$$\mathbf{g}_3 = \frac{\mathbf{g}_1 \times \mathbf{g}_2}{|\mathbf{g}_1 \times \mathbf{g}_2|}. \tag{2.4}$$

Taking into account that the element of area $da = J dt^1 dt^2$ is

$$da = |\mathbf{g}_1 \times \mathbf{g}_2| dt^1 dt^2, \tag{2.5}$$

we can write

$$\mathbf{g}_3 = \frac{\mathbf{g}_1 \times \mathbf{g}_2}{J}. \tag{2.6}$$

The covariant components of the second fundamental form ϱ of $\mathcal{S}$ are denoted

$$\rho_{\alpha\beta} = \frac{\partial \mathbf{g}_\alpha}{\partial t^\beta} \cdot \mathbf{g}_3 = \frac{\partial \mathbf{x}}{\partial t^\alpha \partial t^\beta} \cdot \mathbf{g}_3. \tag{2.7}$$

2.2. Forces and equilibrium equations

The muscle fibers are arranged in bundles that span the diaphragm surface. In our continuum model we model the muscle bundles as a family of curves, say

μ, on $\mathcal{S}$ and consider the coordinate lines t^2 directed as the μ lines (Fig. 1b, Fig. 3).

The material restriction on the generalized *Cauchy* stress $\mathbf{T}$ (force per unit length)

$$\mathbf{T} = T^{\alpha\beta}\mathbf{g}_\alpha \otimes \mathbf{g}_\beta, \tag{2.8}$$

define $\mathcal{S}$ as a membrane.

Therefore the equilibrium equations of the diaphragm in its active state are

$$\frac{\partial \mathbf{T}}{\partial t^\gamma}\mathbf{g}^\gamma + p\mathbf{g}_3 = \mathbf{0}, \tag{2.9}$$

and in component form

$$T^{\mu\gamma}_{,\gamma} + T^{\alpha\gamma}\mathbf{g}^\mu \cdot \mathbf{g}_{\alpha\gamma} + T^{\mu\beta}\mathbf{g}^\gamma \cdot \mathbf{g}_{\beta\gamma} = 0, \tag{2.10}$$

$$T^{\alpha\beta}\rho_{\alpha\beta} + p = 0, \tag{2.11}$$

where a comma followed by an index denotes differentiation with respect to that index.

2.3. Constitutive assumptions

We model the high number of discrete internal forces exerted by muscle fibers as a uniaxial active stress. Then it is assumed that the stress can be decomposed in the following form

$$\mathbf{T} = \mathbf{T}^a + \mathbf{T}^p, \tag{2.12}$$

where $\mathbf{T}^p$ is the passive stress, and

$$\mathbf{T}^a = \sigma^a \mathbf{g}_2 \otimes \mathbf{g}_2, \tag{2.13}$$

is the active stress.

Considering that both the shear stiffness of the muscle tissue, and the elastic component of the muscle fiber itself is low, as a first approximation we can assume that the stress $\mathbf{T}$ consists of a uniaxial active stress in the direction of the muscle fibers and a uniaxial passive stress in the direction of the collagen fibers

$$\mathbf{T} = \sigma^p \mathbf{b}_1 \otimes \mathbf{b}_1 + \sigma^a \mathbf{g}_2 \otimes \mathbf{g}_2, \tag{2.14}$$

$\mathbf{b}_1$ being a unit vector in the direction of the collagen fibers.

Therefore, introducing these simplification, the diaphragm, in its active state, behaves essentially as a net.

For what concerns the passive stress-strain behavior in the $\mathbf{b}_1$ direction, as pointed out in the Introduction, in the transverse direction muscle tissue exhibits a sort of locking behavior at stretches of about 1.1.

Our idea, based on the experimental observation that the diaphragm results pre-stressed in the rest physiological position, is that, in the functional state, the initial strain in the $\mathbf{b}_1$ direction is large enough to come up against the stop in that direction, that the transverse fibers displace at 1.1 of their natural length during normal breathing, and that the muscle tissue behaves essentially as inextensible along $\mathbf{b}_1$. The passive stress σ^p becomes a reactive stress taking any value that is required for equilibrium.

3. Diaphragm shape

In [6] ANGELILLO *et al.* propose a theory on the structure of the diaphragm based on two assumptions:

1. Muscle lines are geodesics of $\mathcal{S}$;
2. Muscle lines are lines of principal (maximum) curvature of $\mathcal{S}$.

As a consequence of these assumptions, it is shown in [6] that the shape of the μ-lines and of the surface $\mathcal{S}$ itself are severely restricted.

In fact, it can be shown that

i) the μ-lines are plane;

ii) the μ-lines are universal curves on $\mathcal{S}$;

iii) the orientation of the μ-lines is restricted.

A particular simple class of surfaces satisfying all of the above implications is represented by the so-called cyclides, that is surfaces spanned by circular arcs of constant radius that are both principal and geodesics.

We model the diaphragm surface as a cyclide of radius ρ (or eventually as a composite cyclide, see [8]) with the muscle line μ directed along the circles. Such a surface can be also described as formed by circles lying in planes that are perpendicular to an arbitrary line Γ^c, with their centers on Γ^c. Since Γ^c is arbitrary, the cyclide is a flexible surface with a variety of shapes.

To describe the surface $\mathcal{S}$ we identify t^1 as the arc-length along Γ^c:

$$\Gamma^c = \{\mathbf{x}^c = \mathbf{x}^c(t^1), \quad t^1 \in \mathbf{I}\}. \tag{3.1}$$

We assume that Γ^c is a plane curve and call $R(s)$ the radius of curvature of Γ^c. This assumption is crucial to get a simple form of the equilibrium equations.

Let us introduce the Frenèt triad along Γ^c; tangent, normal, binormal: $\mathbf{k}_1, \mathbf{k}_2, \mathbf{k}_3$.

Since Γ^c is plane then

$$\mathbf{k}_1' = \frac{1}{R}\mathbf{k}_2, \quad \mathbf{k}_2' = -\frac{1}{R}\mathbf{k}_1 + \tau\mathbf{k}_3 = -\frac{1}{R}\mathbf{k}_1, \quad \mathbf{k}_3' = -\tau\mathbf{k}_2 = 0, \tag{3.2}$$

where $(\cdot)'$ denotes differentiation with respect to t^1.

On introducing the vector

$$\mathbf{z}(t^2) = \rho\left(\cos\frac{t^2}{\rho}\mathbf{k}_2 + \sin\frac{t^2}{\rho}\mathbf{k}_3\right), \tag{3.3}$$

we describe the cyclide surface $\mathcal{S}$ in the following way

$$\mathcal{S} = \left\{\mathbf{x} = \mathbf{x}^c(t^1) + \mathbf{z}(t^2), \quad (t^1, t^2) \in \Omega \subset \mathcal{R}^2\right\}, \tag{3.4}$$

t^2 being the arc length along the muscles.

Notice that if $\mathcal{S}$ is a cyclide, with this choice of the curvilinear coordinates (t^1, t^2), whether or not Γ^c be plane, then the natural base vectors $\mathbf{g}_1, \mathbf{g}_2$ tangent to the curvilinear lines t^1, t^2 are orthogonal and principal.

In particular it results

$$\mathbf{g}_1 = \frac{\partial \mathbf{x}}{\partial t^1} = \left(1 + \frac{\rho}{R}\cos\frac{t^2}{\rho}\right)\mathbf{k}_1, \tag{3.5}$$

$$\mathbf{g}_2 = \frac{\partial \mathbf{x}}{\partial t^2} = \sin\frac{t^2}{\rho}\mathbf{k}_2 + \cos\frac{t^2}{\rho}\mathbf{k}_3, \tag{3.6}$$

and $\mathbf{g}_2$ is a unit vector. Notice that R, representing the curvature of the line of centers, is a function of t^1.

Calling

$$f = \left(1 + \frac{\rho}{R}\cos\frac{t^2}{\rho}\right), \tag{3.7}$$

we have

$$\mathbf{g}_1 = f\mathbf{k}_1. \tag{3.8}$$

Notice that $\mathbf{g}_1$ is parallel to $\mathbf{k}_1$.

Observing that $f > 0$, since muscle lines do not intersect each other, we also have

$$|\mathbf{g}_1| = f. \tag{3.9}$$

The unit normal to the surface is now

$$\mathbf{g}_3 = \frac{\mathbf{g}_1 \times \mathbf{g}_2}{|\mathbf{g}_1||\mathbf{g}_2|} = \frac{\mathbf{g}_1 \times \mathbf{g}_2}{f} = \sin\frac{t^2}{\rho}\mathbf{k}_3 + \cos\frac{t^2}{\rho}\mathbf{k}_2 = \frac{\mathbf{z}}{\rho}. \tag{3.10}$$

The contravariant base vectors $\mathbf{g}^i$ defined by the conditions (2.3) are in this case

$$\mathbf{g}^1 = \frac{1}{f}\mathbf{k}_1, \tag{3.11}$$

$$\mathbf{g}^2 = \mathbf{g}_2 = \sin\frac{t^2}{\rho}\mathbf{k}_2 + \cos\frac{t^2}{\rho}\mathbf{g}_3, \tag{3.12}$$

$$\mathbf{g}^3 = \mathbf{g}_3 = -\cos\frac{t^2}{\rho}\mathbf{k}_2 + \sin\frac{t^2}{\rho}\mathbf{k}_3. \tag{3.13}$$

4. Stress in the mid-costal diaphragm

We can write

$$p_\tau = p(\tau), \qquad \tau \in [0, \overline{\tau}] \tag{4.1}$$

for the pressure at any stage of spontaneous breathing.

To simplify notations we take $p = p_{\overline{\tau}}$. Neglecting inertia effects, the Cauchy stress must be balanced by the pressure p. Locally (recall (2.9), (2.10) and (2.11)):

$$\frac{\partial \mathbf{T}}{\partial t^\alpha}\mathbf{g}^\alpha + p\mathbf{g}_3 = 0, \tag{4.2}$$

where

$$\mathbf{T} = \sigma^p \mathbf{b}_1 \otimes \mathbf{b}_1 + \sigma^a \mathbf{g}_2 \otimes \mathbf{g}_2. \tag{4.3}$$

By rewriting $\mathbf{T}$ in physical components $\sigma_{\alpha\beta}$

$$\mathbf{T} = \sigma_{\alpha\beta}\hat{\mathbf{g}}_\alpha \otimes \hat{\mathbf{g}}_\beta, \qquad \alpha, \beta = 1, 2, \tag{4.4}$$

$\{\hat{\mathbf{g}}_1, \hat{\mathbf{g}}_2, \hat{\mathbf{g}}_3\}$ being the orthonormal triad directed as the natural base vectors $\{\mathbf{g}_1, \mathbf{g}_2, \mathbf{g}_3\}$:

$$\hat{\mathbf{g}}_1 = \mathbf{g}_2/|\mathbf{g}_1|, \quad \hat{\mathbf{g}}_2 = \mathbf{g}_2, \quad \hat{\mathbf{g}}_3 = \mathbf{g}_3 = \mathbf{g}^3, \tag{4.5}$$

the following relation between the physical component of $\mathbf{T}$ and the active and passive stresses are easily found:

$$\sigma_{11} = \sigma^p \cos^2\omega, \quad \sigma_{12} = \sigma^p \sin\omega\cos\omega, \tag{4.6}$$

$$\sigma_{22} = \sigma^a + \sigma^p \sin^2\omega, \tag{4.7}$$

$$\mathrm{tg}\omega = \frac{\sigma_{12}}{\sigma_{11}}. \tag{4.8}$$

Here ω is the *net angle*, that is the angle between the direction $\mathbf{b}_1$ of the fibers of connective tissue and the base vector $\mathbf{g}_1$, orthogonal to the muscle direction.

If the deformed shape is known, the equilibrium equations can be solved in terms of stresses if sufficient boundary conditions on the stress are given. We

consider in particular the case in which the boundary is the line $t^2 = 0$ and restrict to the case of "determined" boundary conditions. An example of such determined boundary conditions is

$$\mathbf{g}_1^0 \cdot \mathbf{T}\mathbf{g}_2^0 = \varphi(t^1), \tag{4.9}$$

where $\mathbf{g}_1^0$, $\mathbf{g}_2^0$ are the natural base vectors at $t^2 = 0$, and $\varphi(t^1)$ is a given scalar function of t^1.

In the costal part of the diaphragm the surface is well approximated by a cyclide of constant radius ρ whose line of centers Γ^c is a plane curve, as the surface shown in Fig. 3. A particular approximation of the costal diaphragm of a dog at end of inspiration obtained by ANGELILLO *et al.* in [8] is show in Fig. 3.

Substituting (4.4) into equilibrium Eq. (4.2) and recalling (3.11 – 3.13) and (4.5), we have

$$\frac{\partial}{\partial t^1}(\sigma_{\alpha\beta}\hat{\mathbf{g}}_\alpha \otimes \hat{\mathbf{g}}_\beta)\frac{\hat{\mathbf{g}}_1}{f} + \frac{\partial}{\partial t^2}(\sigma_{\alpha\beta}\hat{\mathbf{g}}_\alpha \otimes \hat{\mathbf{g}}_\beta)\hat{\mathbf{g}}_2 + p\hat{\mathbf{g}}_3 = 0. \tag{4.10}$$

Expanding the sums in (4.10):

$$\begin{aligned}\frac{\partial}{\partial t^1}(\sigma_{11}\hat{\mathbf{g}}_1 \otimes \hat{\mathbf{g}}_1 + \sigma_{12}\hat{\mathbf{g}}_1 \otimes \hat{\mathbf{g}}_2 + \sigma_{21}\hat{\mathbf{g}}_2 \otimes \hat{\mathbf{g}}_1 + \sigma_{22}\hat{\mathbf{g}}_2 \otimes \hat{\mathbf{g}}_2)\frac{\hat{\mathbf{g}}^1}{f} \\ + \frac{\partial}{\partial t^2}(\sigma_{11}\hat{\mathbf{g}}_1 \otimes \hat{\mathbf{g}}_1 + \sigma_{12}\hat{\mathbf{g}}_1 \otimes \hat{\mathbf{g}}_2 + \sigma_{21}\hat{\mathbf{g}}_2 \otimes \hat{\mathbf{g}}_1 + \sigma_{22}\hat{\mathbf{g}}_2 \otimes \hat{\mathbf{g}}_2)\hat{\mathbf{g}}^2 \\ + p\hat{\mathbf{g}}^3 = 0,\end{aligned} \tag{4.11}$$

and taking the derivatives, we are left with

$$\begin{aligned}d\frac{1}{f}\sigma_{11,1}\hat{\mathbf{g}}_1 + \frac{1}{f}\sigma_{11}\hat{\mathbf{g}}_{1,1} + \frac{1}{f}\sigma_{12}\hat{\mathbf{g}}_1(\hat{\mathbf{g}}_{2,1}\cdot\hat{\mathbf{g}}_1) + \frac{1}{f}\sigma_{21,1}\hat{\mathbf{g}}_2 + \frac{1}{f}\sigma_{21}\hat{\mathbf{g}}_{2,1} \\ + \frac{1}{f}\sigma_{22}\hat{\mathbf{g}}_2(\hat{\mathbf{g}}_{2,1}\cdot\hat{\mathbf{g}}_1) + \sigma_{12,2}\hat{\mathbf{g}}_1 + \sigma_{22,2}\hat{\mathbf{g}}_2 + \sigma_{22}\hat{\mathbf{g}}_{2,2} + p\hat{\mathbf{g}}_3 = 0,\end{aligned} \tag{4.12}$$

where an index, say i, preceded by a comma stands for differentiation with respect to t^i.

Recalling (3.2), (3.5), (3.6), (3.11 – 3.13) and (4.5) we have

$$\begin{aligned}(4.13)\qquad &\frac{1}{f}\sigma_{11,1}\hat{\mathbf{g}}_1+\frac{1}{Rf}\sigma_{11}\left(\sin\frac{t^2}{\rho}\hat{\mathbf{g}}_2-\cos\frac{t^2}{\rho}\hat{\mathbf{g}}_3\right)+\frac{1}{Rf}\sigma_{12}\sin\frac{t^2}{\rho}\hat{\mathbf{g}}_1\\ &+\frac{1}{f}\sigma_{21,1}\hat{\mathbf{g}}_2-\frac{1}{Rf}\sigma_{21}\sin\frac{t^2}{\rho}\hat{\mathbf{g}}_1-\frac{1}{Rf}\sigma_{22}\sin\frac{t^2}{\rho}\hat{\mathbf{g}}_2+\sigma_{12,2}\hat{\mathbf{g}}_1+\sigma_{22,2}\hat{\mathbf{g}}_2\\ &-\frac{1}{\rho}\sigma_{22}\hat{\mathbf{g}}_3+p\hat{\mathbf{g}}_3=0.\end{aligned}$$

In components in the local Cartesian frame $\{\hat{\mathbf{g}}_1,\hat{\mathbf{g}}_2,\hat{\mathbf{g}}_3\}$

$$\begin{aligned}&\frac{1}{f}\sigma_{11,1}+\sigma_{12,2}-\frac{2}{Rf}\sigma_{12}\sin\frac{t^2}{\rho}=0,\\ (4.14)\qquad &\frac{1}{f}\sigma_{21,1}+\sigma_{22,2}+\frac{1}{Rf}\sigma_{11}\sin\frac{t^2}{\rho}-\frac{1}{Rf}\sigma_{22}\sin\frac{t^2}{\rho}=0,\\ &-\frac{1}{Rf}\sigma_{11}\cos\frac{t^2}{\rho}-\frac{1}{\rho}\sigma_{22}+p=0.\end{aligned}$$

Or, since $f=1+\rho/R\cos(t^2/\rho)$, $Rf=R+\rho\cos(t^2/\rho)$,

$$\begin{aligned}&\frac{1}{1+\dfrac{\rho}{R}\cos\dfrac{t^2}{\rho}}\sigma_{11,1}+\sigma_{12,2}-\frac{2}{R+\rho\cos\dfrac{t^2}{\rho}}\sigma_{12}\sin\frac{t^2}{\rho}=0,\\ (4.15)\qquad &\frac{1}{1+\dfrac{\rho}{R}\cos\dfrac{t^2}{\rho}}\sigma_{21,1}+\sigma_{22,2}+\frac{1}{R+\rho\cos\dfrac{t^2}{\rho}}(\sigma_{11}-\sigma_{22})\sin\frac{t^2}{\rho}=0,\\ &\sigma_{11}\frac{\cos\dfrac{t^2}{\rho}}{R+\rho\cos\dfrac{t^2}{\rho}}+\frac{1}{\rho}\sigma_{22}=p.\end{aligned}$$

By multiplying the second equation by $Rf=R+\rho\cos(t^2/\rho)$, it can be written in the form

$$(4.16)\qquad R\sigma_{21,1}+\frac{\partial}{\partial t^2}\left(\sigma_{22}\left(R+\rho\cos\frac{t^2}{\rho}\right)\right)+\sigma_{11}\sin\frac{t^2}{\rho}=0.$$

The differential system (4.15) can be solved if proper conditions are given at the boundary. To any of these boundary conditions it corresponds, through (4.8), a particular distribution of the net angle ω. We look for solutions of (4.15) compatible with the conditions $\omega = 0$ (or, what is the same, $\sigma_{12} = 0$), corresponding to an orthogonal net.

Indeed, on assuming $\sigma_{12} = 0$ at the boundary (this corresponds to considering the boundary condition (4.9) with $\varphi(t^1) = 0$, the stress field

$$\sigma_{11} = -\frac{B}{\rho \cos^2 \dfrac{t^2}{\rho}} + \frac{\rho p}{2},$$

$$\sigma_{22} = \frac{B}{\cos \dfrac{t^2}{\rho}\left(R + \rho \cos \dfrac{t^2}{\rho}\right)} + \rho p \frac{R + \dfrac{\rho}{2} \cos \dfrac{t^2}{\rho}}{R + \rho \cos \dfrac{t^2}{\rho}}, \tag{4.17}$$

$$\sigma_{12} = 0,$$

solve (4.34). To avoid that the normal stress σ_{11} blow up at $t^2 = \rho\pi/2$, we assume $B = 0$ and consider the solution:

$$\sigma_{11} = \frac{\rho p}{2}, \qquad \sigma_{22} = \rho p \frac{R + \dfrac{\rho}{2} \cos \dfrac{t^2}{\rho}}{R + \rho \cos \dfrac{t^2}{\rho}}, \qquad \sigma_{12} = 0. \tag{4.18}$$

This stress field appears as the generalization of the stress distribution for a toroidal surfaces to cyclides generated by plane, but otherwise arbitrary, line of centers (see, for example, [9] p. 213).

In [10], EVANS and SKALAK, in dealing with cell membranes, consider the mechanics of membranes and give the equilibrium equations for axisymmetric surfaces. A torus is axisymmetric, but here we have shown that the corresponding stress distribution can be generalized to cyclides generated by plane line of centers, a set of surfaces that are not axisymmetric.

According to (4.8), if the net angle ω vanishes, then the fibers of connective tissue are orthogonal to the muscle lines, $\sigma_{11} = \sigma^p$, $\sigma_{22} = \sigma^a$. The normal stress σ_{11} along the fibers of connective tissue is constant and the normal stress σ_{22} along the muscle fibers depends on t^1 through R.

The graph of σ_{22} for the particular cyclide $\mathcal{S}$, depicted in Fig. 3, approximating the costal diaphragm of a dog and generated by a plane line of centers Γ^c, is shown in Fig. 4. Notice that the points $(t^1, 0)$ describe the line of attachment

of the diaphragm along the chest wall and the point $(t^1, t^2) = (0, 0)$ corresponds to point A in Fig. 3. The value taken for the pressure is $p = 0.2$, the radius $\rho = 4$ cm and the expression for R is

$$R = 8.05 - 0.67 \cos\left(\frac{1}{4}t^1\right) + 0.22 \cos\left(\frac{1}{2}t^1\right).$$

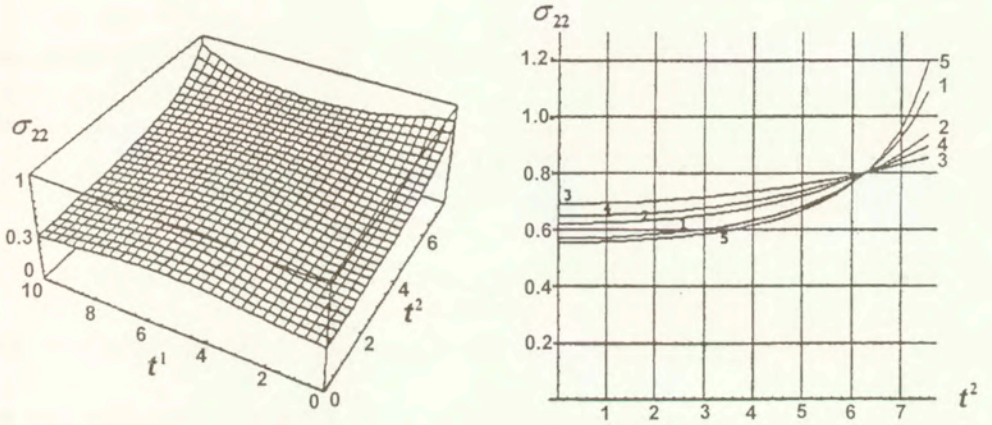

FIG. 4. 3D Plot and stress profiles at: $t^1 = 0(1)$, $t^1 = 2.5(2)$, $t^1 = 5(3)$, $t^1 = 7.5(4)$, $t^1 = 10(5)$, of the stress component σ_{22}.

Summing up, we can draw some conclusions.

Solution (4.18) generalizes to cyclides the stress distributions for a pressurized torus.

The solution we picked for the stress is compatible with the assumption that the fibers of connective tissue are orthogonal to the muscle lines in the active diaphragm configuration. As a consequence of (4.18), the active and passive stresses are principal stresses over the surface.

The stress along the fibers of connective tissue is constant.

The variation of active stress in between the lines of attachment, from chest wall to central tendon, suggest that the thickness of the diaphragm should be larger close to the central tendon. This is consistent with some physiological observations that the diaphragm is thicker at the central tendon end [11].

Acknowledgments

The original idea for the solution of the equilibrium equations (4.34) is due to Dr. Mark HILL, to which we are greatly indebted. This work was supported in part by Grant HL 46230 from the USPHS.

References

1. J. SPRUNG, C. DESCHAMPS, R. D. HUBMAYR, B. J. WALTERS, J. R. RODARTE, *In vivo regional diaphragm functions in dogs,* J. Appl. Physiol., **67**, 655–662, 1989.
2. N. PETTIAUX, M. CASSART, M. PAIVA, M. ESTENNE, *Three-dimensional reconstruction of human diaphragm with use of spiral computed tomography,* J. Appl. Physiol., **78**, 998–1002, 1997.
3. D. J. AIDLEY, *Physiology of excitable cells*, Cambridge University Press, 1990.
4. T. MC MAHON, *Muscles, reflexes and locomotion*, Princeton University Press, 1984.
5. A. BORIEK, S. LIU, J. R. RODARTE, *Costal diaphragm curvature in the dog,* J.Appl.Physiol., **75**, 527–533, 1993.
6. M. ANGELLILLO, A. BORIEK, J. R. RODARTE, T. A. WILSON, *Theory of diaphragm structure and shape*, J.Appl. Physiol., **83**, 1486–1491, 1997.
7. D. HILBERT, *Geometry and the Imagination*, Chelsea Pub Co., 2nd ed. 1952.
8. M. ANGELLILLO, A. BORIEK, J. R. RODARTE, T. A. WILSON, *Shape of the canine diaphragm*, to appear on J. Appl. Physiol.
9. F. I. NIORDSON, Shell theory, North Holland, 1985.
10. E. A. EVANS, R. SKALAK, *Mechanics and thermodynamics of biomembranes*, CRC Press, 1980.
11. A. M. BORIEK, J. R. RODARTE, *Inferences on passive diaphragm mechanics from gross anatomy*, J. Appl. Physiol., **77**, 2065–2070, 1994.

Received December 08, 1998.

Arch. Mech., **52**, 1, pp. 103–125, Warszawa 2000

A new approach to the analysis of polycrystal plasticity

X. PENG and J. FAN

Department of Engineering Mechanics, Chongqing University, Chongqing, 400044, P. R. China

When a polycrystal is subjected to inelastic deformation, there inevitably exist residual microstress fields in a *polycrystalline material* due to its nonhomogeneous morphology. The energy stored in these microstress fields may partly be released and influence the material behavior during subsequent inelastic deformation. Correspondingly, a simple mechanical model is introduced to formulate the constitutive equation for a slip system and the hardening law for single crystal. The corresponding approach for the analysis of polycrystalline materials is obtained based on KBW's self-consistent theory. The proposed approach employs no yield criterion and the corresponding numerical analysis is greatly simplified because it involves no additional process for determination of the activation of slip systems and slip direction. A mixed averaging approach is used in polycrystalline plasticity analysis. The response of 316 stainless steel subjected to typical biaxial nonproportional plastic strain cycling is described and the validity of the proposed approach is demonstrated by the satisfactory agreement between the calculated result and experimental observation.

Key words: Crystal plasticity, Hardening law, Nonproportional cyclic plasticity of Polycrystal

1. Introduction

The research on crystal plasticity can be dated back to 1930's [1]. Since Hill [2], Hill and Rice [3] built up a complete system of the geometry and kinetics of crystal plasticity, it becomes more and more attractive.

The conventional constitutive relation of a slip system was derived within the framework of the conventional theory of plasticity, i.e., taking the existence of a yield shear stress as its basic premise. Suppose a single crystal is subjected to the stress σ_c, the activation of its ith slip system is determined by [4]

$$\gamma^{(1)} \begin{cases} \geq & \text{if} \quad \sigma_c : \mathbf{a}^{(1)} = \tau^{(1)} \quad \text{and} \quad \sigma_c : \alpha^{(1)} = \dot{\tau}^{(1)}, \\ = 0 & \text{if} \quad \sigma_c : \alpha^{(1)} < \tau^{(1)} \text{ or } \sigma_c : \alpha^{(1)} = \tau^{(1)} \\ & \qquad\qquad\qquad\qquad \text{while } \sigma_c : \alpha^{(1)} < \dot{\tau}^{(1)}, \end{cases} \tag{1.1}$$

where

$$\alpha^{(1)} = \frac{1}{2}\left(\mathbf{n}^{(1)} \otimes \mathbf{s}^{(1)} + \mathbf{s}^{(1)} \otimes \mathbf{n}^{(1)}\right) \tag{1.2}$$

denotes the orientation tensor of the slip system, $\mathbf{n}^{(i)}$ and $\mathbf{s}^{(i)}$ are the unit vectors directed along respectively along the outer normal of the slip plane and in the slip direction. In general, the hardening law of a single crystal can be expressed as

$$\dot{\tau}^{(1)} = \sum_{j=1}^{N} h_{ij}\dot{\gamma}^{(1)} \tag{1.3}$$

where h_{ij} denotes the hardening coefficient. Some kinds of h_{ij} have been proposed on the basis of different kinds of hardening mechanisms [5 – 10].

In the existing literature analyzing polycrystalline response, additional iterations were usually introduced to determine the activation of slip systems and slip direction because of the existence of a critical shear stress and the corresponding slip criterion (see Eq. (1.1)). This not only increases the complexity, but also affects the efficiency and accuracy in the corresponding computational process. In the analysis under a plastic strain controlled process, the computation becomes more complicated.

A constitutive equation for a slip system is derived on the basis of on a simple mechanical model, which enables to obtain the hardening law for a single crystal and the corresponding analysis for polycrystalline response based on KBW's self-consistent theory. Since the proposed model employs no yield criterion so that no additional iteration is used for the determination of the activation of slip systems and the direction of slip, great convenience is experienced in the analysis of polycrystalline plasticity. The response of 316 stainless steel subjected to plastic strain cycling along typical paths in biaxial plastic strain plane is analyzed and the validity of the proposed approach is demonstrated by the satisfactory agreement between the theoretical and the experimental results [11].

2. Constitutive equation for single crystal

In polycrystalline materials, the deformation of any single crystal is inevitably constrained by the neighboring crystals due to the nonhomogeneous morphology of the materials, which may lead to residual microstress fields when plastic deformation occurs. On the other hand, when plastic deformation occurs in a single crystal, there also exist residual microstress fields in the stochastic microstructures due to the nonhomogeneous nature and the respective pattern of lattice defects, for instance, residual distortion, dislocation and its substructures, etc.

[12]. The energy stored in these microstress fields may partly be released under certain condition, which reduces the external energy needed for further plastic deformation of the crystals. Correspondingly, a simple mechanical model (see Fig. 1) is introduced to describe the constitutive behavior of a slip system, the similar concept of which was also used in other papers [13 – 15].

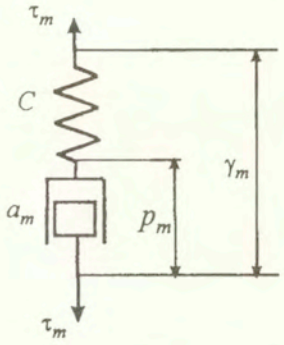

FIG. 1. A simple mechanical model for the constitutive relation of a slip system.

It is seen in Fig. 1 that the dissipated mechanism of the mth slip system is described by a dashpot-like block a_m (with plastic damping coefficient a_m) and a spring C (with stiffness C). The latter is related to the stochastic internal structure, and the energy stored in the spring C represents the energy stored in various kinds of the residual microstress fields. The deformation of the spring C represents the part of plastic deformation (slip) that may recover under some condition and does not make any contribution to the macroscopic elastic property. $p^{(m)}$, the deformation of a_m, is an internal variable that represents the irreversible part of the deformation on the mth slip system. The behavior of the spring is described by

$$\tau^{(m)} = C\left(\gamma^{(m)} - p^{(m)}\right) \qquad m = 1, 2, ..., N, \tag{2.1}$$

where $\gamma^{(m)}$ and $\tau^{(m)}$ denote the strain and the shear stress on the mth slip system, N is the number of the independent ones. The change of $p^{(m)}$ and the corresponding $\tau^{(m)}$ should satisfy the dissipation inequality $\tau^{(m)} dp^{(m)} \geq 0$ (m not summed). By introducing a generalized time $\zeta^{(m)}$ defined by

$$d\zeta^{(m)} = \left| d\gamma^{(m)} \right|. \tag{2.2}$$

$\tau^{(m)}$ can be assumed to satisfy the following phenomenological relation:

$$\tau^{(m)} = a_m \frac{dp^{(m)}}{d\zeta^{(m)}}, \quad (m \text{ not summed}), \tag{2.3}$$

where $a_m > 0$ so that the dissipation inequality can be satisfied in any case. During irreversible deformation, obstacles formed by the pile-ups and tangles of dislocations increase the resistance to active dislocations and result in macroscopic hardening. The hardening of the mth slip system can phenomenologically be described by the change of a_m. Suppose the hardening can be separated into instantaneous hardening and cross-hardening related respectively to the slip on a single slip system and the interaction between the slips on different slip systems [10], which are represented respectively by f_m and H_m, and assuming

$$a_m = a_0 f_m H_m \qquad dz^{(m)} = \frac{d\zeta^{(m)}}{f_m H_m} \quad (m \text{ not summed}), \tag{2.4}$$

Eq. (2.3) can be rewritten as

$$\tau^{(m)} = a_0 \frac{dp^{(m)}}{dz^{(m)}} \quad (m \text{ not summed}), \tag{2.5}$$

in which a_0 is the initial plastic damping coefficient and $z^{(m)}$ is the generalized time scale of the mth slip system. By combining Eqs. (2.1), (2.3) and (2.4), one obtains

$$d\tau^{(m)} = C d\gamma^{(m)} - \alpha \tau^{(m)} dz^{(m)} \quad (m \text{ not summed}) \tag{2.6}$$

in which $\alpha = \dfrac{C}{a_0}$. If $C \to \infty$, then $p^{(m)} = \gamma^{(m)}$ (see Fig. 1), and one obtains immediately the following result from Eqs. (2.5) and (2.6)

$$\tau^{(m)} = \pm a_0 f_m H_m \quad (m \text{ not summed}). \tag{2.7}$$

It is just the critical condition in the constitutive relation of the conventional crystal plasticity, in which a_0 is the initial critical shear stress. It should be stressed that the component C (see Fig. 1) is related to stochastic internal microstructure and makes no contribution to the macroscopic elastic shear modulus G (see Sec. 4). Eq. (2.6) is, therefore, a relation to describe the slip (instead of overall elastoplastic deformation) on the mth slip system. The form of Eq. (2.6) is similar to a single term in the endochronic model [16], the back stress proposed by CHABOCHE [17] and some other constitutive equations. The proposed model does not use a yield criterion, but it can include the conventional relation with a yield criterion as its special case (see Eq. (2.7)). It can also be proved that there exists a limit in stress when slip fully develops [18]. The introduction of the stored energy may, on the one hand, make the slip model more realistic, and on the other hand, make the analysis for polycrystalline response much more convenient.

For easier application to crystal plasticity, Eq. (2.6) can further be expressed as

$$\dot{\tau}^{(m)} = T_m \dot{\gamma}^{(m)} \quad (m \text{ not summed}), \tag{2.8}$$

where

$$T_m = C - \frac{\alpha \Gamma_m}{f_m H_m}, \qquad \Gamma_m = \frac{d\gamma^{(m)}}{d\zeta^{(m)}} \quad (m \text{ not summed}), \tag{2.9}$$

By defining the following hardening coefficient

$$h_{mn} = T_m \delta_{mn} \quad (m \text{ not summed}), \tag{2.10}$$

one obtains the hardening law for a single crystal

$$\dot{\tau}^{(m)} = \sum_{n=1}^{N} h_{mn} \dot{\gamma}^{(n)} \quad (m = 1, 2, ..., N). \tag{2.11}$$

It is easily found that for non-softening materials, h_{mn} is positive definite, which guarantees the existence and uniqueness of the solution. The above relations will be used in the following analysis for the nonproportional cyclic plasticity of 316 stainless steel.

It should be mentioned that although the form of the definition of h_{mn} in Eq. (2.10) is similar to Koiter's postulate of independent hardening [19], the interactive hardening can be considered through H_m. Bassani once mentioned that the least well-characterized aspect of the constitutive framework for either time-dependent or independent behavior is the set of instantaneous hardening moduli h_{mn} that relate the rate of hardening on each slip system to the plastic slip-rate on all systems [10]. If H_m is assumed in the following form

$$H_m^{-1} = \sum_{n=1}^{N} g_{mn} \frac{\dot{\zeta}^{(n)}}{\dot{\zeta}^{(m)}}, \tag{2.12}$$

one obtains the hardening coefficients (see Eq. (2.11)) as follows:

$$h_{mn} = C\delta_{mn} - \frac{\alpha \tau^{(m)}}{f_m} g_{mn} \Gamma, \quad (m, n \text{ not summed}), \tag{2.13}$$

where δ_{mn} denotes the Kronecker symbol and g_{mn} is a set of material-, geometry-, temperature- and plastic deformation history-dependent parameters. The form of the obtained relation is similar to that taking into account the latent hardening. It is easily found that for non-softening materials, a conservative result is that if g_{mn} is selected so that $f_m H_m$ is non-decreasing during any plastic deformation process, h_{mn} will be positive definite, which guarantees the existence and uniqueness of the solution. If $g_{mn} = 0$ for $m \neq n$ then the h_{mn} in Eq. (2.13) reduces to that in Eq. (2.10).

3. Physically based hardening functions

In Eq. (2.4) the hardening functions f_m and H_m are introduced to describe respectively the hardening related to single slip and cross-hardening related to the interaction between the slips on different slip systems.

Although the hardening mechanisms may be complicated during the plastic deformation process, dislocation pile-ups and tangles are considered to be the two dominant ones.

Dislocation pile-ups form obstacles against active dislocations. The associated long-range microstress fields are directional and thus kinematic, which can account to some extent for the Bauschinger effect. The hardening of a slip system induced by dislocation pile-ups should be determined by the superimposition of the effects of the corresponding residual microstress fields caused by the dislocations pile-ups in all slip systems.

The hardening induced by dislocation tangles is attributed to the interaction between the active dislocations and dislocation forests. The associated residual microstress field is short-ranged and less directional. This type of hardening strongly depends on the slip histories and the current states of dislocations at all slip systems. The interaction between dislocations on different slip systems may result in different hardening effects. The corresponding description should, therefore, be able to express its history-dependence and the different effect caused by the interaction between different slip systems.

The hardening behavior of materials strongly depends on the current microstructure of the materials, but macroscopically described by the hardening functions. Suppose f_m possesses a saturated value corresponding to the saturated state of dislocation when plastic deformation fully develops, the evolution of f_m can be determined by

$$\frac{df_m}{dz^{(m)}} = \beta_1(d_1 - f_m), \tag{3.1}$$

where d_1 and β_1 are two material-dependent parameters representing respectively the saturation value of f_m and the rate for f_m to approach d_1.

BASSANI [10] proposed a hardening law that can well describe cross-hardening based on a detailed analysis. This law is directly adopted to be the cross-hardening function H_m as follows

$$H_m = 1 + \sum_{k \neq m} f_{mk} \mathrm{th}(2\beta_s \zeta^{(k)}) \quad (m = 1, 2, ..., N), \tag{3.2}$$

in which $\zeta^{(k)}$ denotes the accumulated slip at the kth slip system, β_s is a material parameter representing the rate for H_m to approach to its saturation value, and f_{mk} denote coupled hardening coefficients connecting the relative orientation of

the considered two slip systems m and k, which can take into account the contribution of the accumulated slip of the kth slip system to the hardening of the mth slip system.

It can be seen that there exist saturated values d_1 and $1 + \sum_{k \neq m} f_{mk}$ for f_m and H_m, respectively. It is easily shown that there exists a saturated value for the shear stress on a slip system when plastic deformation fully develops, and the hardening modulus T_m tends to vanish as the shear stress tends to this saturated value.

4. Application and verification

4.1. Incremental form of the proposed constitutive relation

It has been pointed out by PENG and FAN [20] that when α is very large, rewriting Eq. (2.6) directly in an incremental form will induce a very large error in numerical analysis and even affect the convergence of the solution. To avoid this situation, the integral of Eq. (2.6) is introduced and the following incremental constitutive equation is derived [20]:

$$\Delta\tau^{(m)} = A_m \Delta\gamma^{(m)} + B_m \Delta z^{(m)} \quad (m \text{ not summed}), \tag{4.1}$$

in which

$$A_m = k_m C, \qquad B_m = -k_m \alpha \tau^{(m)}(z_n^{(m)}), \quad z^{(m)} = z_n^{(m)} + \Delta z^{(m)} \quad (m \text{ not summed}), \tag{4.2}$$

$$k_m = \frac{1 - e^{-\alpha \Delta z^{(m)}}}{\alpha \Delta z^{(m)}}, \quad \Delta z^{(m)} = \frac{\Delta\zeta^{(m)}}{f_m H_m}, \qquad \Delta\zeta^{(m)} = \left|\Delta\gamma^{(m)}\right|$$

$z_n^{(m)}$ and $\tau^{(m)}(z_n^{(m)})$ denote respectively the generalized time scale and the shear stress of the mth slip system after nth incremental loading, with which Eq. (2.8) can be expressed as

$$\Delta\tau^{(m)} = T_m \Delta\gamma^{(m)}, \quad T_m = A_m + \frac{\Gamma_m B_m}{f_m H_m}, \quad \Gamma_m = \frac{\Delta\gamma^{(m)}}{\Delta\zeta^{(m)}} \quad (m \text{ not summed}). \tag{4.3}$$

The constitutive relation for a single crystal can then be expressed in the following incremental form

$$\Delta\tau^{(m)} = \sum_{n=1}^{N} h_{mn} \Delta\gamma^{(n)}. \tag{4.4}$$

4.2. Polycrystalline analysis based on KBW's self-consistent theory

Suppose the considered crystals and polycrystals are plastically incompressible, in the case of isothermal and small deformation, KBW's self-consistent model gives [5, 21]

$$\Delta\sigma_c - \Delta\overline{\sigma} = -2G(1-\beta)(\Delta\varepsilon_c^p - \Delta\overline{\varepsilon}^p), \tag{4.5}$$

where $\Delta\sigma_c$ and $\Delta\varepsilon_c^p$ denote respectively the increments of stress and plastic strain in a single crystal, $\Delta\overline{\sigma}$ and $\Delta\overline{\varepsilon}^p$ the increments of averaging stress and plastic strain of the polycrystal, G elastic shear modulus of the material, and β satisfies

$$2G(1-\beta) = \frac{2(7-5v)}{15(1-v)}G, \tag{4.6}$$

in which v denotes Poisson's ratio. It is easily obtained from Eq. (4.5) that

$$(\Delta\sigma_c)_{kk} = \Delta\overline{\sigma}_{kk}, \qquad \Delta\mathbf{s}_c - \Delta\overline{\mathbf{s}} = -2G(\Delta\varepsilon_c^p - \Delta\overline{\varepsilon}_c^p - \Delta\overline{\varepsilon}^p), \tag{4.7}$$

where $\Delta\mathbf{s}_c$ and $\Delta\overline{\mathbf{s}}$ are, respectively, the incremental deviatoric stresses of single crystal and polycrystal, respectively. By defining $\Delta\mathbf{q}$ as follows

$$\Delta\mathbf{q} = \Delta\overline{\mathbf{s}} + \frac{2(7-5v)}{15(1-v)}G\Delta\overline{\varepsilon}^p = \Delta\mathbf{s}_c + \frac{2(7-5v)}{15(1-v)}G\Delta\varepsilon_c^p \tag{4.8}$$

and using

$$\Delta\varepsilon_c^p = \sum_{m=1}^{N} \boldsymbol{\alpha}^m \Delta\gamma^{(m)}, \qquad \Delta\tau^{(m)} = \boldsymbol{\alpha}^{(m)} : \Delta\mathbf{s}_c, \tag{4.9}$$

one obtains

$$\sum_{m=1}^{N} A_{nm}\Delta\gamma^{(m)} = b_n, \qquad (n = 1, 2, ..., N), \tag{4.10}$$

in which

$$A_{nm} = h_{nm} + \frac{2(7-5v)}{15(1-v)}G\boldsymbol{\alpha}^{(n)} : \boldsymbol{\alpha}^{(m)}, \qquad b_n = \Delta\mathbf{q} : \boldsymbol{\alpha}^{(n)}. \tag{4.11}$$

In the above equations the macroscopic plastic strain increment $\Delta\overline{\varepsilon}^p$ is related to the plastic strain increment of each crystal $\Delta\varepsilon_c^p$ by a certain averaging procedure, i.e.,

$$\Delta\overline{\varepsilon}^p = \{\Delta\varepsilon_c^p\} \tag{4.12}$$

and the increment of stress can then be calculated by

$$\Delta\overline{\mathbf{s}} = 2G\,(\Delta\overline{\mathbf{e}} - \Delta\overline{\boldsymbol{\varepsilon}}^{p})\,, \qquad \Delta\overline{\sigma}_{kk} = 3K\Delta\overline{\varepsilon}_{kk}, \tag{4.13}$$

in which $\Delta\overline{\mathbf{e}}$ is the deviatoric strain increment of the material, and K is the elastic volumetric modulus.

4.3 Averaging procedure

In general, Eq. (4.12) can be specified as follows

$$\Delta\overline{\boldsymbol{\varepsilon}}^{p} = \frac{1}{V}\sum_{i=1}^{N}\Delta\boldsymbol{\varepsilon}_{c}^{p(i)}V_{i} \tag{4.14}$$

in which $\Delta\boldsymbol{\varepsilon}_{c}^{p(i)}$ and V_i represent respectively the plastic strain increment and the volume of the ith single crystal, and V is the volume of the polycrystal. If one further assumes that the volume of crystals are identical, i.e., $V = N'V_i$, then Eq. (4.14) can be rewritten as

$$\Delta\overline{\boldsymbol{\varepsilon}}^{p} = \frac{1}{N'}\sum_{i=1}^{N'}\Delta\boldsymbol{\varepsilon}_{c}^{p(i)}. \tag{4.15}$$

In analysis, polycrystal is usually considered as an aggregate of numerous single crystals with randomly distributed orientations. With this assumption, Eq. (4.15) can be expressed as an integral and then calculated with Gaussian quadrature approach [22]. This method, in substance, determines approximately the response of a polycrystal through the single crystals with some specific orientations by weight factors, and can hardly guarantee that the chosen orientations are spatially uniformly distributed, especially in the directions of θ and ϕ (see Fig. 2). To overcome this shortcoming, a mixed averaging approach is used in polycrystalline analysis, which is based on an icosahedron: the outer normal directions of the 20 faces determine 20 spatially uniformly distributed orientations and are represented by 20 sets of θ_i and ϕ_i $(i = 1, 2, ..., 20)$, and in each face it is assumed that there are numerous single crystals with randomly distributed orientations, i.e., ω varies continuously (see Fig. 2). If the arithmetic averaging procedure is used for θ_i and ϕ_i $(i = 1, 2, ..., 20)$ and integral averaging for ω, Eq. (4.15) can be rewritten as

$$\Delta\overline{\boldsymbol{\varepsilon}}^{p} = \frac{1}{20}\sum_{i=1}^{20}\frac{1}{2\pi}\int_{0}^{2\pi}\Delta\boldsymbol{\varepsilon}_{c}^{p}(\theta_i, \phi_i, \omega)d\omega. \tag{4.16}$$

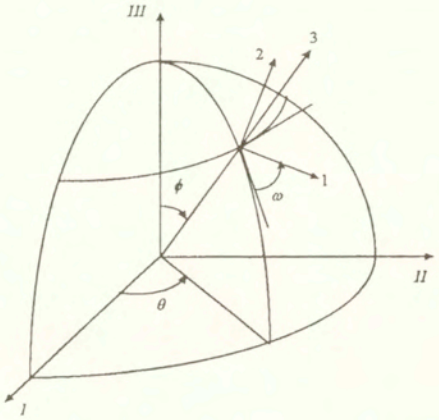

FIG. 2. Global and local coordinate systems.

It is found that: (1) the 20 faces of an icosahedron can be separated into 10 sets, in each of which the two faces are parallel to each other; and (2) the integral range of ω can be reduced to $[0, \pi/2]$ due to symmetry. The above equation can, therefore, be rewritten as

$$\Delta\overline{\varepsilon}^p = \frac{1}{10}\sum_{i=1}^{10}\frac{2}{\pi}\int_0^{\frac{\pi}{2}}\Delta\varepsilon_c^p(\theta_i,\phi_i,\omega)d\omega. \tag{4.17}$$

Further applying the Gaussian quadrature to Eq. (4.17), one obtains

$$\Delta\overline{\varepsilon}^p = \frac{1}{20}\sum_{i=1}^{10}\sum_{j=1}^{4}A_j^{\omega}\Delta\varepsilon_c^p(\theta_i,\phi_i,\omega_j), \tag{4.18}$$

where the coordinates of the Gaussian integration points ω_j and the corresponding weighted coefficients A_j^{ω} are listed in Table 1 (see Appendix), and the values of the 10 sets of independent θ_i and $\phi_i (i = 1, 2, ..., 10)$ are listed in Table 2.

The above averaging procedure involves the response of 40 single crystals with different orientations even if the improvement by the Gaussian weighed coefficients is not considered. It should be stressed that the distribution of the orientations determined by the chosen θ_i and ϕ_i are spatially uniform.

Table 1. The coordinates of Gaussian points ω_j and the corresponding weighted coefficients A_j^{ω}.

j	1	2	3	4
ω_j (rad)	0.1090633	0.5183777	1.052419	1.461733
A_j^{ω}	0.3478548	0.6521452	0.6521452	0.3478548

Table 2. Values of the independent 10 sets of θ_i and ϕ_i.

j	1	2	3	4	5	6	7	8	9	10
$\theta_j(^\circ)$	0	72	144	216	288	288	216	144	72	0
$\phi_j(^\circ)$	37.38	37.38	37.38	37.38	37.38	142.62	142.62	142.62	142.62	142.62

4.4. Application and verification

The cyclic plasticity of 316 stainless steel subjected to some typical biaxial nonproportional plastic strain paths is analyzed. The material has a face-centered-cubic (FCC) crystal lattice. In the local coordinate systems the **n** and **s** of the 12 independent slip systems are listed sequentially in Table 3.

Table 3. 12 sets of independent n and s of FCC crystal.

	1	2	3	4	5	6	7	8	9	10	11	12
n	$(11\bar{1})$	$(11\bar{1})$	$(11\bar{1}1)$	$(1\bar{1}1)$	$(1\bar{1}1)$	$(1\bar{1}1)$	$(1\bar{1}\,\bar{1})$	$(1\bar{1}\,\bar{1})$	$(1\bar{1}\,\bar{1})$	(111)	(111)	(111)
s	[101]	[011]	$[1\bar{1}0]$	[110]	[011]	$[10\bar{1}]$	[101]	[110]	$[01\bar{1}]$	$[10\bar{1}]$	$[0\bar{1}1]$	$[1\bar{1}0]$

Following BASSANI'S consideration [10], the coupled hardening coefficients f_{mn} can be expressed in the form of a matrix as follows in terms of the sequence of the independent slip systems (see Table 3)

$$[f_{mn}] = \begin{bmatrix} 0 & C_1 & C_1 & C_3 & C_2 & C_1 & C_1 & C_2 & C_2 & C_1 & C_3 & C_2 \\ & 0 & C_1 & C_2 & C_1 & C_2 & C_1 & C_3 & C_1 & C_3 & C_1 & C_2 \\ & & 0 & C_1 & C_2 & C_3 & C_2 & C_1 & C_3 & C_2 & C_2 & C_1 \\ & & & 0 & C_1 & C_1 & C_2 & C_1 & C_2 & C_2 & C_3 & C_1 \\ & & & & 0 & C_1 & C_3 & C_2 & C_1 & C_2 & C_1 & C_3 \\ & & & & & 0 & C_1 & C_2 & C_3 & C_1 & C_2 & C_2 \\ & & & & & & 0 & C_1 & C_1 & C_1 & C_2 & C_3 \\ & & & & & & & 0 & C_1 & C_3 & C_2 & C_1 \\ & & & & & & & & 0 & C_2 & C_1 & C_2 \\ & & & \text{sym.} & & & & & & 0 & C_1 & C_1 \\ & & & & & & & & & & 0 & C_1 \\ & & & & & & & & & & & 0 \end{bmatrix}$$

A procedure for the analysis of the stress (or strain) response of polycrystalline materials subjected to a strain (or stress) history was suggested by PENG *et al.* [23], where no additional iteration is used for the determination of the activation of slip systems and the direction of slip. It greatly simplifies the numerical process. The stress response of 316 stainless steel subjected to nonproportional strain cycling was analyzed and experimentally verified [23].

When deformation is controlled by plastic strain, the numerical process becomes more complicated. The macroscopic stress increment $\Delta\bar{\mathbf{s}}$ and the stress increment $\Delta\mathbf{s}_c$ of each crystal can not be known before the shear stress of each slip system, $\Delta\tau^{(m)}$, is obtained, so that $\Delta\mathbf{s}_c$ has to be determined by solving the following equation:

$$\boldsymbol{\alpha}^{(m)} : \Delta\mathbf{s}_c = \Delta\tau^{(m)} \qquad (m = 1, 2, ..., N). \tag{4.19}$$

There are 12 equations in Eq. (4.18) for FCC crystal and it can be shown that there are five independent ones among them. It should be emphasized that in the framework of the employed constitutive model, no yield criterion is used and the relation between slip and the corresponding shear stress is smooth and continuous. Slip occurs at extremely low rate at the onset of loading and unloading but increases and speeds up as $\tau^{(m)}$ increases. At any stage of deformation, $\Delta\tau^{(m)}$ can uniquely be determined by the given $\Delta\gamma^{(m)}$ (see Eq. (4.4)), and inversely, $\Delta\gamma^{(m)}$ can also be uniquely determined by the given $\Delta\tau^{(m)}$. This feature greatly simplifies the numerical process, in which one can simply select and fix five independent slip systems *a priori* without considering if slip occurs on each system or not. Given a set of $\Delta\tau^{(m)}$, the five components of the corresponding $\Delta\mathbf{s}_c$ can be obtained by solving Eq. (4.19). The increment of the polycrystalline stress $\Delta\bar{\mathbf{s}}$ is then related to $\Delta\mathbf{s}_c$ of each crystal by some averaging procedure, i.e.,

$$\Delta\bar{\mathbf{s}} = \{\Delta\mathbf{s}_c\}. \tag{4.20}$$

The following averaging procedure similar to Eq. (4.17) can be derived from Eqs. (4.7), (4.12) and (4.18)

$$\Delta\bar{\mathbf{s}} = \frac{1}{20}\sum_{i=1}^{10}\sum_{j=1}^{4} A_j^{\omega}\,\Delta\mathbf{s}_c(\theta_i, \phi_i, \omega_j). \tag{4.21}$$

In the conventional theory of crystal plasticity, no slip occurs in a slip system if the shear stress is less than the critical shear stress. In other words, the relation between stress and slip is not unique before slip occurs. When solving $\Delta\mathbf{s}_c$ from Eq. (4.19), one can hardly select and fix 5 independent equations from the 12 ones *a priori*. For nonproportional loading, searching for this kind of 5 independent equations is tedious and needs some additional principle such as the

principle of maximum plastic work proposed by BISHOP and HILL [24] to reduce the computational difficulty.

A numerical procedure for the analysis of the elastoplastic behavior of a polycrystalline material subjected to nonproportional plastic strain histories is proposed as follows: with the result obtained in the kth iteration of the nth increment of loading, such as $\Delta\bar{\mathbf{s}}_{(n)}^{(k)}$ of the material, $\Delta\boldsymbol{\varepsilon}_{c(n)}^{p(k)}$ and $\Delta\mathbf{s}_{c(n)}^{(k)}$ of each single crystal and $\{\Delta\gamma^{(m)}\}_{(n)}^{(k)}$, $\{\Delta\zeta^{(m)}\}_{(n)}^{(k)}$, $\{\Delta z^{(m)}\}_{(n)}^{(k)}$ of each slip system, one can calculate $[h_{ij}]_{(n)}^{(k)}$ with Eqs. (4.2), (4.3) and (2.10). Given an increment of plastic strain $\Delta\boldsymbol{\varepsilon}_{(n)}^{p}$, $\Delta\mathbf{q}_{(n)}^{(k+1)}$ can be calculated with Eq. (4.8) and then $[A_{ij}]_{(n)}^{(k)}$, $\{b_j\}_{(n)}^{(k)}$ with Eq. (4.11), $\{\Delta\gamma^{(m)}\}_{(n)}^{(k+1)}$ by solving Eq. (4.10) and $\{\Delta\tau^{(m)}\}_{(n)}^{(k+1)}$ by Eq. (4.4). $\Delta\mathbf{s}_{c(n)}^{(k+1)}$ of each crystal can be obtained by solving Eq. (4.19) and $\Delta\bar{\mathbf{s}}_{(n)}^{(k+1)}$ by Eq. (4.21). The iterative process continues until the following inequality is satisfied

$$\delta = \max_{j=1}^{N'} \frac{||\Delta\mathbf{q}_{(n)}^{(k+1)} - \Delta\mathbf{q}_{(n)}^{(k)}||}{||\Delta\mathbf{q}_{(n)}^{(k+1)}||} \leq \delta_0, \tag{4.22}$$

where N' is the total number of the single crystals used in the calculation, δ and δ_0 are respectively the maximum relative error and the tolerant error. The value of δ_0 is chosen as 1% in the calculation. Then the obtained incremental results are added respectively to the corresponding results up to the $(n-1)$th increment of loading and one, therefore, obtains $\mathbf{s}_{(n)}$ of the polycrystalline material, $\{\boldsymbol{\varepsilon}_c^p\}_{(n)}$ of each single crystal, $\{\tau^{(m)}\}_{(n)}$, $\{\zeta^{(m)}\}_{(n)}$, $\{z^{(m)}\}_{(n)}$, $\{f_m\}_{(n)}$, $\{H_m\}_{(n)}$ of each slip system, and starts the calculation of the next increment of loading.

The response of 316 stainless steel subjected to biaxial nonproportional plastic strain cycling at room temperature is analyzed with the proposed approach. The material is considered as an aggregate of single crystals with FCC lattice structure. The material constants are determined as follows from the experimental result [11]:

$$G = 78 \text{ GPa}, \quad \nu = 0.23,$$

$$C = 2.92 * 10^3 \text{ GPa}, \quad \alpha = 3.2 * 10^4, \quad d_c = 1.0,$$

$$C_1 = 0.04, \quad C_2 = 0.30, \quad C_3 = 0.50, \quad \beta_s = 15.$$

The constitutive behavior of a slip system during loading-unloading and reloading determined by the constitutive model is shown in Fig. 3 without taking into account the cross-hardening. The solid line corresponds to the determined C, α and d_c; while the dashed line corresponds to the same d_c but both C and α are reduced to 10 percent of the determined values. It is seen that when α is

sufficiently large, the constitutive behavior of a slip system is quite close to that using the slip model containing a yield criterion, and an appropriate choice of α can describe to some extent the Bauschinger effect. For biaxial analysis, we define the following stress and strain vectors:

$$\vec{\sigma} = \sigma \mathbf{n}_1 + \sqrt{3}\tau \mathbf{n}_2, \qquad \vec{\varepsilon}^p = \varepsilon^p \mathbf{n}_1 + \frac{1}{\sqrt{3}}\gamma^p \mathbf{n}_2 \tag{4.23}$$

in which σ and τ denote the tensile and shear stress, respectively, ε^p and γ^p the tensile and shear plastic strain, $\mathbf{n}_1$ and $\mathbf{n}_2$ are two unit vectors perpendicular to each other. We also define the equivalent stress, equivalent plastic strain and the accumulative plastic strain as follows:

$$\sigma_e = |\vec{\sigma}| = \sqrt{\sigma^2 + 3\tau^3}, \qquad \varepsilon_e^p = |\vec{\varepsilon}^p| = \sqrt{(\varepsilon^p)^2 + \frac{1}{3}(\gamma^p)^2}, \tag{4.24}$$

$$\zeta^p = \int |d\vec{\varepsilon}^p|.$$

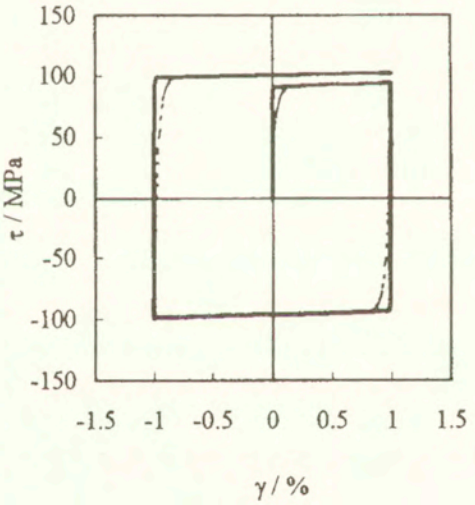

FIG. 3. The loading-unloading and reloading behavior of a slip system without considering cross-hardening.

The calculated $\sigma - \varepsilon^p$ curve of the material subjected to symmetrically tensile-compressive plastic strain cycling with a fixed equivalent plastic strain amplitude $\varepsilon_a^p = 0.2\%$ is shown in Fig. 4. And the relation between $\sqrt{3}\tau$ and $\frac{1}{\sqrt{3}}\gamma^p$ of the material subjected to symmetrically plastic shear strain cycling with the same equivalent plastic strain amplitude is shown in Fig. 5. Both are in satisfactory agreement with the experimental result [11]. It is seen by comparing Fig. 4 with

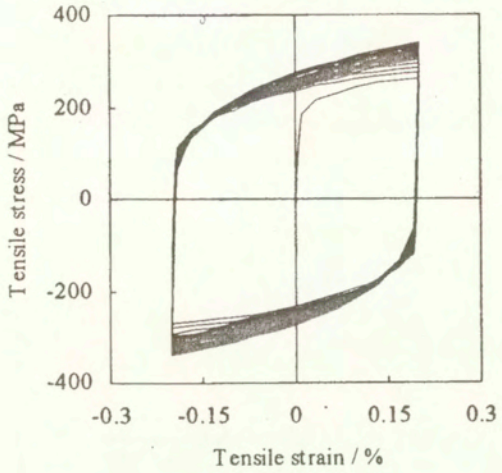

FIG. 4. Calculated $\sigma - \varepsilon^p$ curve corresponding to symmetrically tensile-compressive plastic strain cycling with $\varepsilon_a^p = 0.2\%$.

Fig. 5 that besides the minor difference between the hysteresis loops, the calculated equivalent stress amplitude corresponding to plastic shear strain cycling are distinctly less than that corresponding to tensile-compressive plastic strain cycling (also see Fig. 8) although the equivalent plastic strain amplitudes are identical. This phenomenon also coincides with the experimental observation and can mainly be attributed to the difference of the activation of slip systems under these two kinds of loading conditions, which can not be well described by simply using the Mises equivalent rule.

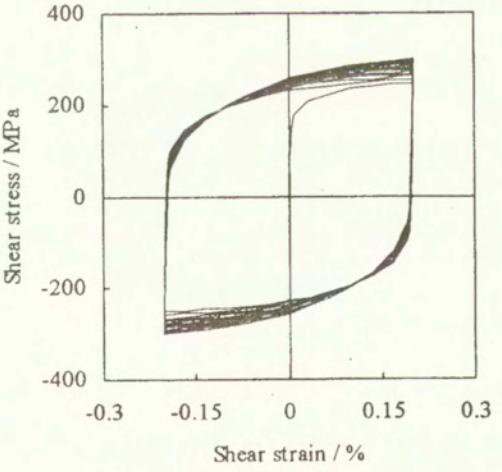

FIG. 5. Calculated $\sqrt{3}\tau - \gamma^p/\sqrt{3}$ curve corresponding to symmetrically plastic shear strain cycling with $\gamma_a^p/\sqrt{3} = 0.2\%$.

In the analysis of the response of materials subjected to nonproportional plastic strain cycling, one usually defines the radius of the minimal super-sphere surrounding the cyclic plastic strain path as equivalent plastic strain amplitude ε_a^p. Figure 6(a) and (b) show respectively the calculated and experimental [11] biaxial stress trajectories corresponding to the square path with $\varepsilon_a^p = 0.2\%$ in $\varepsilon^p - \gamma^p/\sqrt{3}$ plane (the coordinates of the four corners are $(0.2\%, 0)$, $(0, 0.2\%)$, $(-0.2\%, 0)$ and $(0, -0.2\%)$, sequentially), and Fig. 7(a) and (b) the calculated and experimental [11] stress trajectories corresponding to the 90° out-of-phase

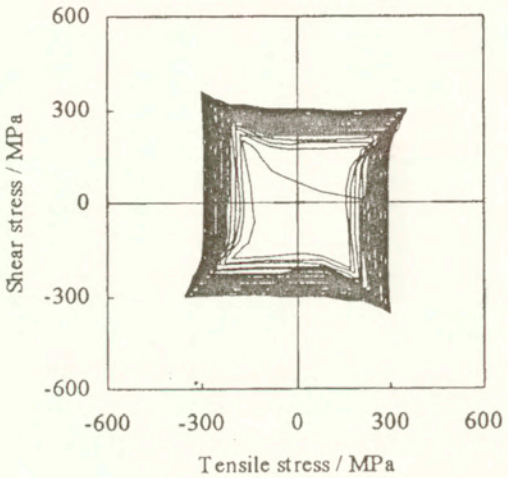

FIG. 6. a) Calculated stress trajectory in $\sigma - \sqrt{3}\tau$ plane corresponding to the cyclic square path in $\varepsilon^p - \gamma^p/\sqrt{3}$ plane.

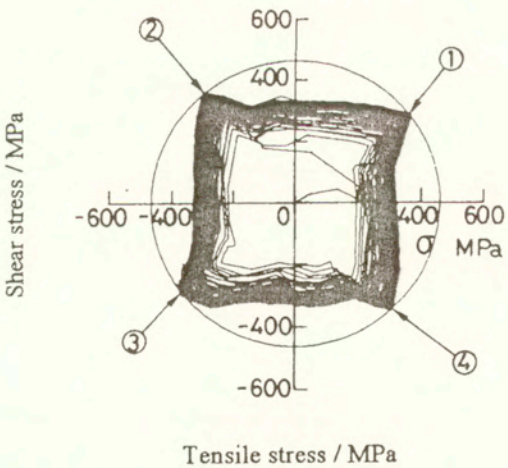

FIG. 6. b) Experimental stress trajectory in $\sigma - \sqrt{3}\tau$ plane corresponding to the cyclic square path in $\varepsilon^p - \gamma^p/\sqrt{3}$ plane.

(circular) path with $\varepsilon_a^p = 0.2\%$, respectively. The comparison between the calculated and experimental results shows reasonable agreement. Compared with the results corresponding to the proportional paths (see Figs. 4 and 5), the stress amplitudes in Figs. 6 and 7 increase about 50% (see Fig. 8). This marked difference can be attributed to the cross-hardening caused by the intersection between the moving dislocations and the dislocation forests, the dislocation tangle and

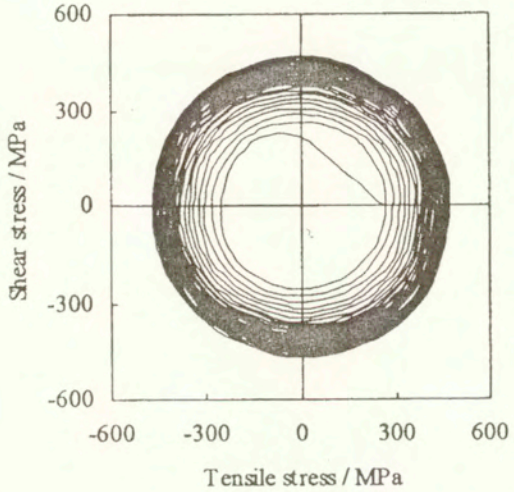

FIG. 7. a) Calculated stress trajectory in $\sigma - \sqrt{3}\tau$ plane corresponding to the cyclic circular path in $\varepsilon^p - \gamma^p/\sqrt{3}$ plane.

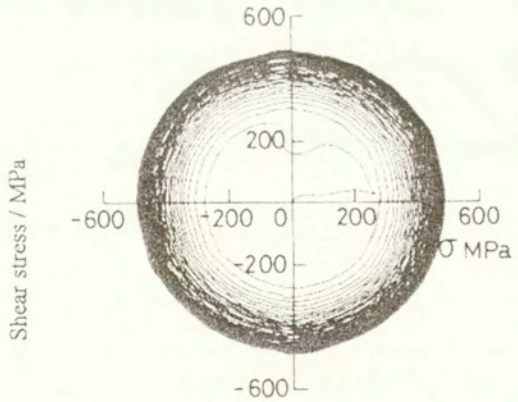

FIG. 7. b) Experimental stress trajectory in $\sigma - \sqrt{3}\tau$ plane corresponding to the cyclic circular path in $\varepsilon^p - \gamma^p/\sqrt{3}$ plane.

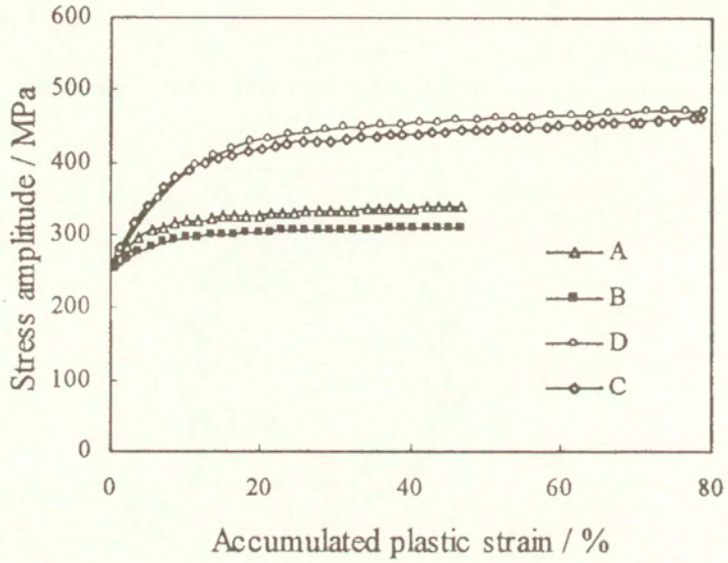

FIG. 8. a) Calculated relation between equivalent stress amplitudes and accumulated plastic strain along different plastic strain paths.

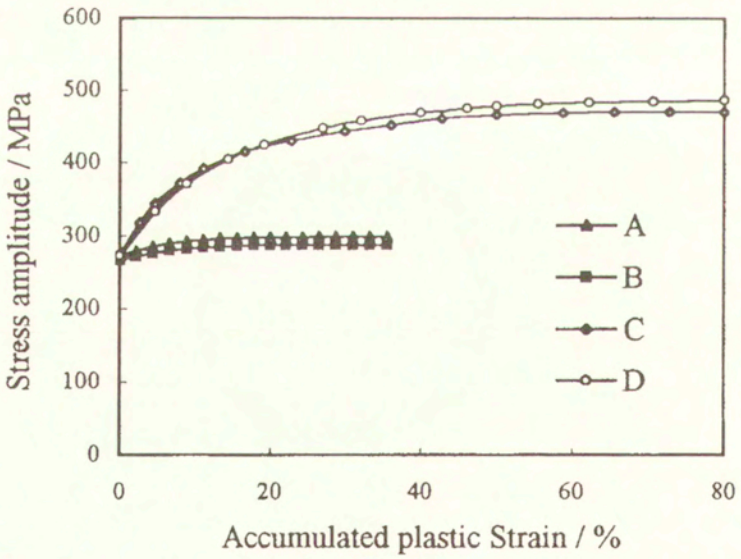

FIG. 8. b) Experimental relation between equivalent stress amplitudes and accumulated plastic strain along different plastic strain paths.

the corresponding substructures induced by which may greatly increase the resistance to dislocation glide. In phenomenological analysis, such kind of increase is usually attributed to the nonproportionality of the plastic strain path and is considered by introducing an appropriate measure of nonproportionality and the corresponding hardening laws [13, 23, 25]. In the proposed approach, the response is satisfactorily described by considering the interaction of dislocations along different slip systems. The variation of the equivalent stress amplitude σ_a against the accumulative plastic strain ζ^p along the above four typical paths in $\varepsilon^p - \gamma^p/\sqrt{3}$ plane with a constant strain amplitude $\varepsilon_a^p = 0.2\%$ is shown in Fig. 8. These plastic strain paths can be classified to proportional ones (cyclic tension-compression and cyclic torsion, respectively) and nonproportional ones (square path and circular path). Calculation shows that, for the proportional plastic strain cycling the equivalent stress amplitudes are relatively small, but for the cycling along nonproportional plastic strain paths, the equivalent stress amplitudes greatly increase. The qualitative and quantitative agreement between the calculated and experimental results [11] demonstrates the validity of the proposed approach in the analysis of plastic strain controlled nonproportional cyclic crystalline plasticity.

5. Discussion and conclusion

During inelastic deformation process, a part of energy can be stored in the substructure of materials in the form of residual microstress fields and this part of energy can be released under some condition so that the external energy to activate and motivate dislocations can be reduced. With this viewpoint, a constitutive relation for a slip system is derived based on a simple mechanical model consisting of a spring and a plastic dashpot-like block. The corresponding hardening law for single crystal and the approach based on KBW's self-consistent theory for polycrystalline analysis is then obtained. The constitutive model contains no yield criterion and the corresponding numerical analysis is greatly simplified.

A mixed averaging approach is used to analyze the response of polycrystalline materials. It is based on 20 sets of θ_i and ϕ_i representing 20 spatially uniformly distributed orientations, and in each face with a set of θ_i and ϕ_i as its normal it is assumed that there are numerous single crystals with randomly distributed orientations. An arithmetic averaging procedure is used for θ_i and $\phi_i (i = 1, 2, ..., 20)$ and Gaussian quadrature averaging procedure is used for ω.

A valuable discussion on the crystal orientation distribution was given in [26], in which the volume of FCC crystal orientation space was shown and the minimal size of the orientation regions for crystals was suggested. In the present analysis, it seems from Eq. (4.17), Tables 1 and 2 that the orientation region for crystals is

$(0 \leq \theta < 2\pi, 0 \leq \phi < \pi/2, 0 \leq \omega < \pi/2)$. The values of θ used in the analysis are $(0°, 72°, 144°, 216°, 288°)$. Calculation shows that if the values of θ were replaced by $(0°, 72°, 144°, 36°, 108°)$, i.e., the region of θ was reduced to $[0, \pi)$, identical results for all the given plastic strain paths would be obtained. But if they were further replaced by $(0°, 72°, 54°, 36°, 18°)$, i.e., the region of θ was reduced to $[0, \pi/2)$, a marked difference was detected. It indicates that the adopted orientation region for crystals may further reduce to $(0 \leq \theta < \pi, 0 \leq \phi < \pi/2, 0 \leq \omega < \pi/2)$ and a conservative estimation for the volume of the orientation space is

$$\Omega = \int_0^{\pi} d\theta \int_0^{\frac{\pi}{2}} d\omega \int_0^{\frac{\pi}{2}} \sin\phi d\phi = \frac{\pi^2}{2},$$

which is a little larger than the volume of FCC crystal orientation space [26] and may result in some equivalent orientations when the number of the used orientations is large.

The cyclic plasticity of 316 stainless steel subjected to four typical biaxial nonproportional plastic strain paths was analyzed and experimentally verified. Calculation also showed that the corresponding numerical algorithm is of good convergence and efficiency.

Appendix

Gaussian quadrature can be expressed as

$$\int_{-1}^{1} f(x)dx = \sum_{k=1}^{n} A_k f(x_k). \tag{A.1}$$

Suppose the orientation region for crystals is $(a_1 \leq \theta < a_2, b_1 \leq \phi < b_2, c_1 \leq \omega < c_2)$, the averaging of s is given as

$$< \mathbf{s} >= \frac{1}{\Omega} \int_{a_1}^{a_2} d\theta \int_{c_1}^{c_2} d\omega \int_{b_1}^{b_2} \mathbf{s}(\theta, \phi, \omega) \sin\varphi d\varphi, \tag{A.2}$$

where

$$\Omega = \int_{a_1}^{a_2} d\theta \int_{c_1}^{c_2} d\omega \int_{b_1}^{b_2} \sin\phi d\phi. \tag{A.3}$$

If the θ, ω and ϕ are replaced respectively with $\frac{1}{2}[(a_2 - a_1)x + (a_2 + a_1)]$, $\frac{1}{2}[(c_2 - c_1)y + (c_2 + c_1)]$, and $\arccos\left\{\frac{1}{2}[(\cos b_1 - \cos b_2)z + (\cos b_1 + \cos b_2)]\right\}$, Eq. (A.2) can be rewritten as follows by using Eq. (A.3)

$$< \mathbf{s} >= \frac{1}{8}\int_{-1}^{1} dx \int_{-1}^{1} dy \int_{-1}^{1} \mathbf{s} dz, \tag{A.4}$$

where

$$\mathbf{s} = \mathbf{s}\left(\frac{1}{2}[(a_2 - a_1)x + (a_2 + a_1)], \quad \frac{1}{2}[(c_2 - c_1)y + (c_2 + c_1)], \right.$$
$$\left. \arccos\left\{\frac{1}{2}[(\cos b_1 - \cos b_2)z + (\cos b_1 + \cos b_2)]\right\}\right).$$

Eq. (A.4) can then be numerically calculated by

$$< \mathbf{s} >= \frac{1}{8}\sum_{i=1}^{N_i}\sum_{j=1}^{N_j}\sum_{k=1}^{N_k} A_i^{\theta} A_j^{\omega} A_k^{\varphi} \mathbf{s}(\theta_i, \omega_j \phi_k), \tag{A.5}$$

where N_i, N_j, N_k and A_i^{θ}, A_j^{ω}, A_k^{φ} denote the number of integration points and the weight coefficients.

If the orientation region consists of n subregions $\Omega_i (I = 1, ..., n)$, the averaging of s can be calculated with

$$< \mathbf{s} >= \frac{1}{\Omega}\sum_{i=1}^{n}\int_{\Omega_i} \mathbf{s} d\Omega = \sum_{i=1}^{n}\frac{\Omega_i}{\Omega}\frac{1}{\Omega_i}\int_{\Omega_i} \mathbf{s} d\Omega = \sum_{i=1}^{n} V_i < \mathbf{s} >_i \tag{A.6}$$

in which V_i and $< \mathbf{s} >_i$ denote respectively the volume fraction and the averaging of s of the ith subregion.

At the given range of orientation region for crystals and the number of Gaussian integration points, one can find the coordinates of the integration points and the corresponding weight coefficients. For example, for $0 \leq \omega < \pi/2$, and using four integral points, one can find that the coordinates of the Gaussian integration points are $y_{1,2} = \pm 0.3399810$ and $y_{3,4} = \pm 0.8611363$, which corresponds to $\omega_{1,2,3,4} = 0.5183777$, 1.052419, 0.1090633, 1.461733 (rad), the corresponding weight coefficients are $A_1^{\omega} = A_2^{\omega} = 0.6521452$ and $A_3^{\omega} = A_4^{\omega} = 0.3478548$ which are the values given in Table 1.

Acknowledgment

Financuially supported by WSFC and the Education Ministry of China.

References

1. G. I. TAYLOR, *Plastic strain in metals*, J. Inst. Metals, **62**, 307–324, 1938.
2. R. HILL, *Generalized constitutive relations for incremental deformation of metals and crystals multislip*, J. Mech. Phys. Solids, **14**, 95–102, 1966.
3. R. HILL and J.R. RICE, *Constitutive analysis of elastic-plastic crystals at arbitrary strain*, J. Mech. Phys. Solids, **20**, 401–413, 1972.
4. E. SCHMID and W. BOAS, *Kristallplastizität*, Springer-Verlag, Berlin 1950.
5. B. BUDIANSKY and T.T. WU, *Theoretical prediction of plastic strain of polycrystals*, Proc 4th US national Congr. Appl. Mech., 1175–1185, 1962.
6. J. W. HUTCHINSON, *Elastic-plastic behavior of polycrystalline metals and composites*, Proc Roy Soc London, A., **319**, 247–272, 1970.
7. G. J. WENG, *Kinematic hardening rule in single crystals*, Int. J. Solids & Struct., **15**, 861–875, 1979.
8. G. J. WENG, *Dislocation theories of work hardening and yield surfaces of single crystals*, Acta Mech., **37**, 217–228, 1980.
9. R. J. ASARO, *Crystal plasticity*, J. Appl. Mech., **50**, 921–934, 1983.
10. J. L. BASSANI, *Single crystal hardening*, Appl. Mech. Rev., **43**(5), 320–327, 1990.
11. E. TANAKA, S. MURAKAMI and M. OOKA, *Effect of strain path shape on nonproportional cyclic plasticity*, J. Mech. Phys. Solids, **33**, 559–575, 1985.
12. Z. R. SONG, *The physics of metals*, Vol II, High Education Press, Beijing 1992.
13. J. FAN and X. PENG, *A physically based constitutive description for nonproportional cyclic plasticity*, J. Engng. Mat. Tech., **113**, 254–262, 1991.
14. X. PENG and A.R.S. PONTER, *A constitutive law for two-phase materials with experimental verification*, Int. J. Solids & Struct., **31**, 8, 1099–1111, 1994.
15. X. PENG, C. MEYER and L. FANG, *A thermomechanically consistent continuum damage model for concrete meterials*, ASCE, J. Engng. Mech., **123**, 1, 60–69, 1997.
16. K. C. VALANIS, *Fundamental consequences of new intrinsic time measure plasticity as a limit of the endochronic theory*, Arch. Mech., **23**, 171–190, 1980.
17. J. L. CHABOCHE and G. ROUSSELIER, *On plastic and viscoplastic constitutive equations*, J. Pressure Vessel Tach., **105**, 153–164, 1983.
18. H. MURAKAMI and H.E. READ, *Endochronic plasticity: some basic properties of plastic flow and failure*, Int. J. Solids & Struct., **23**, 133–151, 1987.
19. W. KOITER, *Stress-strain relation, uniqueness and variational theorems for elastic-plastic materials with singular yield surface*, Quert. Appl. Math., **11**, 350–359, 1953.
20. X. PENG and J. FAN, *A new numerical approach for nonclassical plasticity*, Computers and Structures, **47**, 2, 313–320, 1993.
21. E. KRÖNER, *Zur plastichen verformung des vielkristalls*, Acta Metall., **9**, 155–165, 1961.

22. K. HWANG and S. SUN, *Micromechanical modeling of cyclic plasticity*, Advances in Engineering Plasticity: 41–48, Proc. Second Asia-Pacific Symposium on Advances in Engineering Plasticity and Its Applications, Edited by B Xu and W Yang, International Academic Publishers, Beijing 1994.

23. X. PENG, X. ZENG and J. FAN, *On a nonclassical constitutive theory of crystal plasticity*, Mechanics Research Communication, **24**, 6, 631–638, 1997.

24. J. F. W. BISHOP and R. HILL, *A theoretical derivation of the plastic properties of a polycrystalline face centered metal*, Philos. Mag., **42**, 414–427, 1951.

25. A. BENALLEL and D. MARQUIS, *Constitutive equation for nonproportional cyclic plasticity*, J. Engng. Mat. Tech., **109**, 326–336, 1987.

26. P. H. DŁUŻEWSKI, *Crystal orientation spaces and remarks on the modeling of polycrystal anisotropy*, J. Mech. Phys. Solids, **39**, 5, 651–661, 1991.

Received March 10, 1999; new version September 24, 1999.

Arch. Mech., **52**, 1, pp. 127–142, Warszawa 2000

Nonlinearity and memory effects in low temperature heat propagation

K. SAXTON ([1]) and R. SAXTON ([2])

([1]) *Department of Mathematics and Computer Science*
Loyola University, New Orleans
LA 70118 USA
e-mail: saxton@loyono.edu

([2]) *Department of Mathematics University of New Orleans*
New Orleans LA 70148 USA
e-mail: rsaxton@math.uno.edu

IN ORDER TO ACCOUNT for low temperature heat propagation phenomena in crystals of sodium fluoride and bismuth, we employ a thermodynamic model for rigid materials involving a vector-field internal state variable. The model is either wavelike or diffusive, depending on the temperature regime considered.

1. Introduction

IN THIS PAPER we continue an investigation ([12, 21]) of the effects of nonlinearity and memory on the propagation of heat waves through crystalline materials at low temperatures. The work is intended to extend the interpretation of the experimental results of [5, 6, 15] and [18] in the context of thermodynamics with internal state parameters. These experimental results gave evidence, as had been seen previously in ^{3}He ([1]), that there existed second sound in crystals of sodium fluoride and bismuth at temperatures below where the materials reached their peak thermal conductivity (approximately 18.5 K and 4.5 K respectively). There was an absence of any such wavelike thermal phenomena at higher temperatures, where only diffusive heat propagation was observed. The speed, U_E, of small-amplitude waves tended to zero as the temperature approached the temperature of peak conductivity from below, while appearing, at least in the case of bismuth, to tend to a finite limit as the temperature fell towards 0 K (no useful measurements could be made below 10 K in sodium fluoride because of interference from transverse and longitudinal mechanical waves). This material-dependent temperature of peak thermal conductivity, or *critical* temperature, is denoted by ϑ_λ.

Our present approach is different from our earlier results, which were built on the ideas in [11, 13]. The internal variable[1] responsible for the effective memory in heat propagation will here be a vector field, $\mathbf{p}$, rather than the *semi-empirical* temperature, β, a scalar field. The advantage of this setting is that mathematically, the system of equations derived for a rigid conductor becomes a first order hyperbolic system, a balance law in $\mathbf{p}$ and ϑ, which reduces to a nonlinearly damped two by two (rather than three by three) system in the one-dimensional case. Physically, it also becomes more straightforward to apply experimental data (the observed speed of second sound waves and heat conductivity as functions of temperature) to constitutive equations, avoiding the necessity of integration and making invertibility assumptions, which further resolves a difficulty at zero kelvin where the use of simple algebraic constitutive functions could lead to an unphysical singularity, and lets us extend our analysis to bismuth.

The method of describing thermal wave phenomena in inelastic bodies using vector-valued internal state variables was introduced by KOSIŃSKI [9], and one of the authors, [22]. Related ideas were also introduced in [4] and [16] (see [14]). Here we employ this approach in order to propose physically motivated constitutive equations for bismuth and sodium fluoride which depend on ϑ_λ and investigate the relation between ϑ_λ and a further temperature ϑ_m where the system loses genuine nonlinearity. Corresponding results have been obtained in [12, 21] for sodium fluoride, using the scalar-valued internal state variable, β. Loss of genuine nonlinearity has also been found in the setting of extended thermodynamics ([19, 20]). In that context, it was speculated that the temperature at which this occurs plays a role in solids analogous to the lambda point in liquid helium at which the speed of second sound vanishes. The analysis based on our constitutive equations shows that these temperatures are however different.

We now attempt to motivate the ideas contained in the derivation, which will be presented fully in Sec. 2. Consider the classical constitutive equation for heat flux, $\mathbf{q} = -k_0 \nabla \vartheta$, where $\mathbf{q}$ denotes heat flux, k_0 the conductivity and ϑ the absolute temperature. One approach for allowing $\mathbf{q}$ to become dependent the on effect of memory is to consider if as a functional of the history of the temperature gradient,

$$\mathbf{q} = -\frac{k_0}{\tau} \int_{-\infty}^{t} e^{-\frac{1}{\tau}(t-s)} \nabla \vartheta(\mathbf{x}, s) ds, \tag{1.1}$$

where τ denotes a relaxation time. An extensive discussion of this and more modern ideas can be found in [7] and [8]. It follows easily from (1.1) that one

[1]) Internal parameters were introduced to constitutive models for thermodynamics of solids by COLEMAN and GURTIN, [2].

obtains the well-known Maxwell-Cattaneo equation

$$\tau \mathbf{q}_t + \mathbf{q} = -k_0 \nabla \vartheta. \tag{1.2}$$

In order to extend the idea behind (1.1), define

$$\mathbf{p} = \frac{1}{\tau} \int_{-\infty}^{t} e^{-\frac{1}{\tau}(t-s)} \nabla \vartheta(\mathbf{x}, s) ds, \tag{1.3}$$

so that (1.1) is equivalent to

$$q = -k_0 \mathbf{p}, \tag{1.4}$$

$$\mathbf{p}_t = -\frac{1}{\tau}\mathbf{p} + \frac{1}{\tau}\nabla \vartheta \tag{1.5}$$

which in the steady-state case, $\mathbf{p}_t = \mathbf{0}$, implies the classical relation

$$\mathbf{q} = -k_0 \nabla \vartheta. \tag{1.6}$$

Next consider the more general relations

$$\begin{aligned} \mathbf{q} &= -\alpha(\vartheta) \int_{-\infty}^{t} e^{-b(t-s)} \nabla f_1(\vartheta)(\mathbf{x}, s) ds, \\ \mathbf{p} &= \int_{-\infty}^{t} e^{-b(t-s)} \nabla f_1(\vartheta)(\mathbf{x}, s) ds, \end{aligned} \tag{1.7}$$

with $b > 0$, which are equivalent to

$$\mathbf{q} = -\alpha(\vartheta)\mathbf{p}, \tag{1.8}$$

$$\mathbf{p}_t = -b\mathbf{p} + g_1(\vartheta)\nabla \vartheta, \tag{1.9}$$

where $f_1'(\vartheta) = g_1(\vartheta)$ and, for $\mathbf{p}_t = \mathbf{0}$,

$$\mathbf{q} = -\frac{\alpha(\vartheta) g_1(\vartheta)}{b} \nabla \vartheta \equiv -\mathcal{K}(\vartheta) \nabla \vartheta. \tag{1.10}$$

It will be seen in the next section that there is a thermodynamic relationship, (2.18), showing that

$$\alpha(\vartheta) = \psi_{20} \vartheta^2 g_1(\vartheta), \tag{1.11}$$

where ψ_{20} is a constant coming from the Helmholtz free energy function ψ,

$$\psi = \psi_1(\vartheta) + \frac{1}{2}\psi_{20}\vartheta|\mathbf{p}|^2. \tag{1.12}$$

Using (1.10) and (1.11), the steady-state thermal conductivity coefficient $\mathcal{K}(\vartheta)$ is given by

$$\mathcal{K}(\vartheta) = \frac{\psi_{20}}{b}\,(\vartheta g_1(\vartheta))^2, \tag{1.13}$$

and, as will be seen in the next section, the speed of second sound satisfies

$$U_E^2 = \psi_{20}\,\frac{(g_1(\vartheta))^2}{c_0\vartheta}, \tag{1.14}$$

where c_0 is a constant, cf. (2.26), (2.27). Recalling the critical temperature ϑ_λ,

$$U_E^2 \to 0 \text{ as } \vartheta \to \vartheta_\lambda -, \tag{1.15}$$

(1.14) implies that $g_1(\vartheta) \to 0$ as $\vartheta \to \vartheta_\lambda -$, from which (1.13) gives

$$\mathcal{K}(\vartheta) \to 0 \text{ as } \vartheta \to \vartheta_\lambda - . \tag{1.16}$$

Unfortunately, (1.16) is incompatible with experimental evidence ([5]) which shows a large peak in thermal conductivity at ϑ_λ, and a further generalization of either (1.7), or of (1.8) and (1.9) is needed in order to account for this fact. We replace (1.8) and (1.9) with

$$\mathbf{q} = -\alpha(\vartheta)\mathbf{p}, \tag{1.17}$$

$$\mathbf{p}_t = g_1(\vartheta)\nabla\vartheta + g_2(\vartheta)\mathbf{p}. \tag{1.18}$$

If, in addition, we wish to take into account the "effective", Fourier conductivity $k(\vartheta)$, [7], which is considered as part of the heat flux law in Jeffrey's type materials, where

$$\mathbf{q} = -k(\vartheta)\nabla\vartheta - \alpha_0 \int_{-\infty}^{t} e^{-b(t-s)}\nabla\vartheta(\mathbf{x}, s)ds, \quad \alpha_0 = \text{constant}, \tag{1.19}$$

we can replace the second term on the right in (1.19) by the right side of the expression for $\mathbf{q}$ in (1.7), and the constitutive equation for $\mathbf{q}$ becomes

$$\mathbf{q} = -k(\vartheta)\nabla\vartheta - \alpha(\vartheta)\mathbf{p}. \tag{1.20}$$

Equations (1.18) and (1.20) make it possible to account for small diffusive effects such as the broadening which can be seen in travelling pulses of second sound as the temperature increases towards ϑ_λ.

The approach introduced here, based on (1.20) and (1.18), is equivalent to that in [12] and [21] only if $\mathbf{p}$ is a gradient field, $\mathbf{p} = \nabla\beta$ for the scalar field β representing a *semi-empirical* temperature. This is however possible only if the evolution equation for $\mathbf{p}$ is of the form (1.9), when (1.20) and (1.18) reduce to

$$\mathbf{q} = -k(\vartheta)\nabla\vartheta - \alpha(\vartheta)\nabla\beta, \tag{1.21}$$

$$\beta_t = f_1(\vartheta) - b\beta. \tag{1.22}$$

In our case however, and in general, the models are distinct.

We present the general framework of the model in the next section and provide examples of constitutive functions which we relate to experimental data in Sec. 3. In the final Section, we will use these functions in examining three-dimensional weakly discontinuous plane waves propagating through crystals.

2. The governing system of equations

In the following section there are parallels to the derivation of [21] concerning the thermodynamics of materials which allow the propagation of low temperature heat pulses. For clarity, we will give a derivation of the present model and note differences where they occur, and refer the reader to that paper for more detailed information.

As in [21], we let ϑ_λ be the critical temperature below which second sound is observed. The vector field, $\mathbf{p}$, as defined in the Introduction, is related to the absolute temperature, ϑ, and its gradient through the initial value problem (1.18) together with appropriate initial data. That is (see [22]),

$$\mathbf{p}_t = g_1(\vartheta)\nabla\vartheta + g_2(\vartheta)\mathbf{p}, \tag{2.1}$$

$$\mathbf{p}(\mathbf{x}, 0) = \mathbf{p}_0(\mathbf{x}). \tag{2.2}$$

The free energy per unit volume, ψ, entropy density, η, and heat flux, $\mathbf{q}$, are related by

$$\psi(\vartheta, \mathbf{p}) = \psi_1(\vartheta) + \frac{1}{2}\psi_2(\vartheta)|\mathbf{p}|^2, \tag{2.3}$$

$$\mathbf{q} = -k(\vartheta)\nabla\vartheta - \alpha(\vartheta)\mathbf{p}, \tag{2.4}$$

and

$$\eta = -\partial_\vartheta\psi(\vartheta, \mathbf{p}). \tag{2.5}$$

The free energy is connected to the internal energy per unit volume, ε, by

$$\psi = \varepsilon - \eta\vartheta. \tag{2.6}$$

Balance of energy and the second law of thermodynamics imply

$$\varepsilon_t + \nabla \cdot \mathbf{q} = r, \tag{2.7}$$

and

$$\eta_t + \nabla \cdot \left(\frac{\mathbf{q}}{\vartheta}\right) \geq \frac{r}{\vartheta}, \tag{2.8}$$

where r is the body heat supply per unit volume.

Using (2.1), (2.3) – (2.6) and (2.8) as in [21], we find

$$\psi_2(\vartheta)g_2(\vartheta)|\mathbf{p}|^2 + \left(\psi_2(\vartheta)g_1(\vartheta) - \frac{\alpha(\vartheta)}{\vartheta}\right)\nabla\vartheta \cdot \mathbf{p} - \frac{1}{\vartheta}k(\vartheta)|\nabla\vartheta|^2 \leq 0. \tag{2.9}$$

This inequality is satisfied for arbitrary choices of $\nabla\vartheta$ and $\mathbf{p}$ if and only if

$$\psi_2(\vartheta)g_2(\vartheta) \leq 0, \quad k(\vartheta) \geq 0 \tag{2.10}$$

and

$$\left(\psi_2(\vartheta)g_1(\vartheta) - \frac{\alpha(\vartheta)}{\vartheta}\right)^2 \leq -4\,\frac{k(\vartheta)}{\vartheta}\psi_2(\vartheta)g_2(\vartheta). \tag{2.11}$$

By setting

$$\alpha(\vartheta) = \vartheta\psi_2(\vartheta)g_1(\vartheta), \tag{2.12}$$

(2.11) is satisfied for arbitrary choices of admissible $k(\vartheta)$ including $k(\vartheta) = 0$

As in [21], we adopt a particular form, (1.12), for (2.3),

$$\psi_2(\vartheta) = \psi_{20}\vartheta, \quad \psi_{20} > 0. \tag{2.13}$$

For this choice of ψ, the internal energy ε is related to ψ_1 by

$$\varepsilon(\vartheta) = \psi_1(\vartheta) - \psi_1'(\vartheta)\vartheta. \tag{2.14}$$

and the specific heat $c_v > 0$ in terms of ϑ by

$$c_v(\vartheta) = \varepsilon'(\vartheta). \tag{2.15}$$

Finally, in the absence of a body heat supply, Eqs. (2.7), (2.4), (2.15), and (2.1) give

$$c_v(\vartheta)\vartheta_t - \nabla \cdot (k(\vartheta)\nabla\vartheta + \alpha(\vartheta)\mathbf{p}) = 0, \tag{2.16}$$

$$\mathbf{p}_t = g_1(\vartheta)\nabla\vartheta + g_2(\vartheta)\mathbf{p}, \tag{2.17}$$

where by (2.10), (2.11) and (2.13),

$$\alpha(\vartheta) = \psi_{20}\vartheta^2 g_1(\vartheta), \tag{2.18}$$

$$k(\vartheta) \geq 0 \quad \text{and} \quad g_2(\vartheta) \leq 0. \tag{2.19}$$

By letting $\mathbf{p}_t = 0$ in (2.17),

$$g_1(\vartheta)\nabla\vartheta = -g_2(\vartheta)\mathbf{p}, \tag{2.20}$$

and taking $\mathbf{p}$ and $\nabla\vartheta$ to point in the same direction in this case, implies

$$g_1(\vartheta) \geq 0 \tag{2.21}$$

from (2.19). The steady-state conductivity coefficient, $\mathcal{K}(\vartheta)$ (in contrast with (1.10), (1.13)) for (2.4) becomes

$$\mathbf{q}(\vartheta) = -\left(k(\vartheta) - \frac{\psi_{20}\vartheta^2 g_1^2(\vartheta)}{g_2(\vartheta)}\right)\nabla\vartheta = -\mathcal{K}(\vartheta)\nabla\vartheta. \tag{2.22}$$

In order for the equations derived above to hold over the critical temperature ϑ_λ, as well as under, it is sufficient to make the following assumption concerning the constitutive functions, $g_1, g_2 \in C(\mathbb{R}_+)$,

$$\lim_{\vartheta\to\vartheta_\lambda-} \frac{g_1^2(\vartheta)}{g_2(\vartheta)} > 0 \quad \text{and} \quad g_i(\vartheta) = 0, \ \ i = 1, 2, \ \ \vartheta \geq \vartheta_\lambda. \tag{2.23}$$

This ensures both the required Fourier conductivity above ϑ_λ (see (2.4), with $\alpha(\vartheta) = 0$ by (2.8)), and from (2.22), a conductivity peak as $\vartheta \to \vartheta_\lambda-$.[2] For $\vartheta \geq \vartheta_\lambda$, Eqs. (2.16) and (2.17) reduce to

$$c_v(\vartheta)\vartheta_t - \nabla\cdot(k(\vartheta)\nabla\vartheta) = 0, \tag{2.24}$$

and

$$\mathbf{p}_t = 0. \tag{2.25}$$

Thus the vector field $\mathbf{p}$ no longer possesses any time dependence and decouples from the field equation for temperature. In the absence of viscosity, $k(\vartheta)$, and the transition temperature, ϑ_λ, the system (2.16), (2.17) in ϑ and $\mathbf{p}$ is equivalent to that obtained in terms of ϑ and $\mathbf{q}$ by MORRO and RUGGERI ([17]).

For $\vartheta < \vartheta_\lambda$, neglecting the influence of $k(\vartheta)$ in (2.4) (the inviscid limit), the system (2.16), (2.17) is a hyperbolic balance law. The expression for the second

[2]) It may be useful in certain situations to modify (2.23) with a transition layer $(\vartheta_\lambda, \vartheta_\lambda + \varepsilon)$ over which $\frac{g_1^2(\vartheta)}{g_2(\vartheta)}$ decays to zero smoothly.

sound speed U_E is the nonzero characteristic speed λ in (4.20), which provides the speed of weakly discontinuous waves propagating into a state for which $\mathbf{q} = 0$,

$$U_E^2 = \frac{\alpha(\vartheta) g_1(\vartheta)}{c_v(\vartheta)} = \frac{\psi_{20} \vartheta^2 g_1(\vartheta)^2}{c_v(\vartheta)}, \tag{2.26}$$

where we have used relation (2.18).

Specific constitutive functions may be derived from experimental data ([5, 6, 15] and [18]). Data for U_E give the function $g_1(\vartheta)$, while data for the steady-state conductivity $\mathcal{K}(\vartheta)$ give $g_2(\vartheta)$, (cf. (2.22) with $k(\vartheta) = 0$). For the heat capacity we will use Debye's law,

$$c_v(\vartheta) = c_0 \vartheta^3, \quad c_0 > 0. \tag{2.27}$$

We note, in particular, that (2.22) and (2.26) provide very simple connections between the constitutive functions g_1, g_2, and the steady-state conductivity and second sound speed (cf. [12, 21]).

3. Constitutive functions

In order to derive a specific example for $g_1(\vartheta)$, we will use an empirical relation employed to interpolate experimental data for NaF and Bi ([3]),

$$U_E(\vartheta)^{-2} = A + B\vartheta^n, \tag{3.1}$$

where, for ϑ measured in degrees kelvin, and U_E in cm/sec,

$$n = 3.10, \ A = 9.09 \times 10^{-12}, \ B = 2.22 \times 10^{-15}, \ 10 \text{ K} \leq \vartheta \leq 18 \text{ K}, \tag{3.2}$$

for NaF, and

$$n = 3.75, \ A = 9.07 \times 10^{-11}, \ B = 7.58 \times 10^{-13}, \ 1 \text{ K} \leq \vartheta \leq 4 \text{ K}, \tag{3.3}$$

for Bi.

Equation (3.1) fits the available experimental data ([5, 6, 15] and [18]) for the range of temperatures where second sound is detected, that is, for a set of temperatures below ϑ_λ. For high purity crystals of Bi and NaF, we take the values of ϑ_λ to be 4.5K and 18.5K, respectively. We will take, for $\vartheta < \vartheta_\lambda$,

$$g_1(\vartheta) = g_{10}(\vartheta)(\vartheta_\lambda - \vartheta)_+^{r_1}, \ g_{10}(\vartheta) > 0, \ g_{10}(\vartheta_\lambda) \neq 0, \tag{3.4}$$

and

$$g_2(\vartheta) = g_{20}(\vartheta)(\vartheta_\lambda - \vartheta)_+^{r_2}, \ g_{20}(\vartheta) < 0, \ g_{20}(\vartheta_\lambda) \neq 0, \tag{3.5}$$

subject to (2.23), where $z_+^r \equiv z^r H(z)$ and $H(z)$ denotes the Heaviside step function.

In this case we obtain the following formulae for U_E (see (2.26)) and the conductivity $\mathcal{K}(\vartheta)$ with $k(\vartheta) = 0$ (see (2.22)) using (2.27),

$$U_E(\vartheta)^2 = \psi_{20} \frac{g_{10}(\vartheta)^2}{c_0 \vartheta} (\vartheta_\lambda - \vartheta)_+^{2r_1}, \tag{3.6}$$

and

$$\mathcal{K}(\vartheta) = -\psi_{20} \frac{\vartheta^2 g_{10}(\vartheta)^2}{g_{20}(\vartheta)} (\vartheta_\lambda - \vartheta)_+^{2r_1 - r_2}. \tag{3.7}$$

Here the case $2r_1 = r_2$ admits a finite peak in conductivity at $\vartheta = \vartheta_\lambda$, while for $2r_1 < r_2$ the peak is infinite. Observation of second sound in bismuth as $\vartheta \to 0$ ([18]) indicates that U_E reaches a finite, nonzero limit there. We reflect this by choosing

$$g_{10}(\vartheta) = a\vartheta^{\frac{1}{2}}, \quad a > 0, \tag{3.8}$$

for both Bi and NaF, even though the data appear unavailable at temperatures below about 10K for NaF because of interference by mechanical waves. Then (3.6) reduces to

$$U_E(\vartheta)^2 = \frac{\psi_{20}\, a^2}{c_0} (\vartheta_\lambda - \vartheta)_+^{2r_1}. \tag{3.9}$$

We can now use the experimental data contained in (3.1) to obtain values for the parameters in (3.9). For NaF, we choose $r_1 = 1/5$ and

$$U_E = 0.186((18.5 - \vartheta)_+^{1/5} \tag{3.10}$$

where here U_E is measured in cm/μsec and $\vartheta_\lambda = 18.5$K. A comparison of (3.10) with (3.1) and (3.2) is given in Fig. 1.

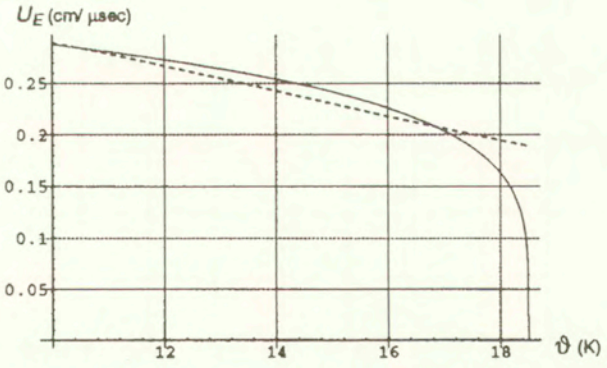

FIG. 1. NaF, second sound speed (solid curve), $U_E = 0.186(18.5 - \vartheta)_+^{1/5}$, together with data (dotted curve), $U_E = (9.09 + 0.00222\vartheta^{3.1})^{-1/2}$, (COLEMAN and NEWMAN, [3]).

For Bi, we take $r_1 = 1/4, \vartheta_\lambda = 4.5$ and

$$U_E = 0.078(4.5 - \vartheta)_+^{1/4}. \tag{3.11}$$

Equation (3.11) with (3.1) and (3.3) illustrates Fig. 2.

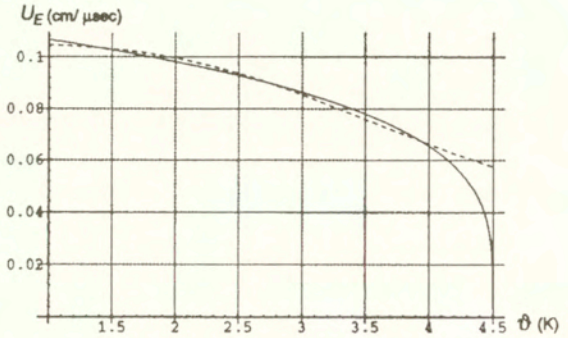

FIG. 2. Bi, second sound speed (solid curve), $U_E = 0.078(4.5 - \vartheta)_+^{1/4}$, together with data (dotted curve), $U_E = (90.7 + 0.758\vartheta^{3.75})^{-1/2}$, (COLEMAN and NEWMAN, [3]).

These simple power law constitutive functions lead to reasonable approximations to the data for second sound. The drops close to the critical temperatures reflect the vanishing of the speed of second sound at these temperatures, while the empirical data-interpolation functions become invalid above ϑ_λ.

Next we obtain $g_{20}(\vartheta)$ in the case of NaF. Having $g_{10}(\vartheta)$ by (3.8), and $r_1 = 1/5$ for NaF, one can obtain $g_{20}(\vartheta)$ with $r_2 = 2/5$ by using experimental data for heat conductivity together with (3.7). Since crystalline materials are known to have cubic temperature dependence close to zero kelvin (see [6] for NaF), we take

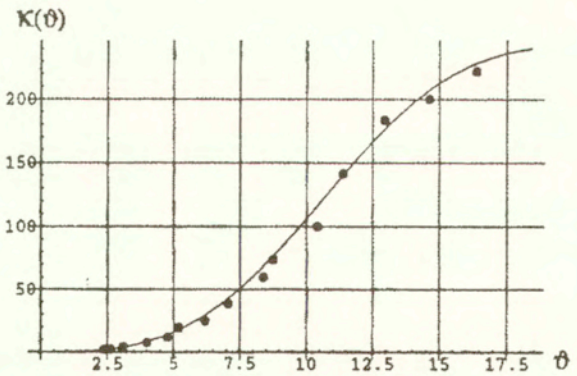

FIG. 3. NaF, conductivity $\mathcal{K}(\vartheta) = 0.127\,\vartheta^3(1 + 0.00002\vartheta^4)^{-1}\,\mathrm{watt\,K^{-1}cm^{-1}}$, and experimental data after [6].

$$g_{20}(\vartheta) = -b(1 + \epsilon\vartheta^4), \quad b > 0, \quad |\epsilon| << 1, \tag{3.12}$$

and (3.7) gives

$$\mathcal{K}(\vartheta) = \frac{\psi_{20}\, a^2 \vartheta^3}{b(1 + \epsilon\vartheta^4)}\,. \tag{3.13}$$

Figure 3 illustrates Eq. (3.13) together with data of thermal conductivity against temperature for NaF, for $\psi_{20}\, a^2/b = 0.127$ and $\epsilon = 2.10^{-5}$.

4. Weakly discontinuous plane waves

In this section, we will consider the system of four Eqs. (2.16), (2.17), with $k(\vartheta) = 0$ and $\vartheta < \vartheta_\lambda$,

$$\vartheta_t - \frac{\alpha'(\vartheta)}{c_v(\vartheta)}\, \mathbf{p} \cdot \nabla\vartheta - \frac{\alpha(\vartheta)}{c_v(\vartheta)}\, \nabla \cdot \mathbf{p} = 0, \tag{4.1}$$

$$\mathbf{p}_t - g_1(\vartheta)\nabla\vartheta = g_2(\vartheta)\mathbf{p}, \tag{4.2}$$

where $\mathbf{p} = (p^1, p^2, p^3)$, and ϑ are continuous in $(\mathbf{x}, t)$.

We represent a three-dimensional characteristic surface $\mathcal{S}(t)$ in implicit form by

$$\mathcal{S}(t) = \{\mathbf{x} \in \mathbb{R}^3 : \mathcal{G}(\mathbf{x}, t) = 0\}, \tag{4.3}$$

where the unit normal $\mathbf{n}$ and normal speed λ are given by

$$\mathbf{n} = \frac{\nabla\mathcal{G}}{|\nabla\mathcal{G}|}, \quad \lambda = -\frac{\mathcal{G}_t}{|\nabla\mathcal{G}|}. \tag{4.4}$$

Across $\mathcal{S}(t)$, $\mathbf{p}$ and ϑ are continuous,

$$[\![\mathbf{p}]\!] = \mathbf{0}, \quad [\![\vartheta]\!] = 0, \tag{4.5}$$

but their derivatives experience a jump discontinuity. Evaluating (4.1) and (4.2) across $\mathcal{S}(t)$ gives

$$[\![\vartheta_t]\!] - \frac{\alpha'(\vartheta^+)}{c_v(\vartheta^+)}\, \mathbf{p}^+ \cdot [\![\nabla\vartheta]\!] - \frac{\alpha(\vartheta^+)}{c_v(\vartheta^+)}\, [\![\nabla \cdot \mathbf{p}]\!] = 0, \tag{4.6}$$

$$[\![\mathbf{p}_t]\!] - g_1(\vartheta^+)[\![\nabla\vartheta]\!] = 0, \tag{4.7}$$

where ϑ^+ and $\mathbf{p}^+$ are the values of ϑ and $\mathbf{p}$ ahead of the wave.

Next we define the directional derivative of a vector field $\mathbf{U}$ by

$$\frac{d}{dt}[\![\mathbf{U}]\!] = [\![\mathbf{U}_t]\!] + \lambda n^k [\![\mathbf{U}_{,k}]\!], \tag{4.8}$$

where $\mathbf{U}_{,k} = \dfrac{\partial}{\partial x^k}$, $k = 1, 2, 3$, with $\mathbf{n}$ and λ from (4.4). For $\mathbf{U}$ continuous across $\mathcal{S}(t)$, we therefore have

$$[\![\mathbf{U}_t]\!] = -\lambda n^k [\![\mathbf{U}_{,k}]\!]. \tag{4.9}$$

Let $\mathbf{a}$ denote the jump of derivatives $\mathbf{U}_{,k}$ across $\mathcal{S}(t)$ via

$$[\![\mathbf{U}_{,k}]\!] = \mathbf{a}\, n_k. \tag{4.10}$$

Taking $\mathbf{U} = (\vartheta, p^1, p^2, p^3)$ and $\mathbf{a} = (r_0, r^1, r^2, r^3)$, (4.10) can be expressed as

$$[\![\nabla\vartheta]\!] = r_0\mathbf{n}, \tag{4.11}$$

$$[\![\nabla\mathbf{p}]\!] = \mathbf{r} \otimes \mathbf{n}, \quad \mathbf{r} = (r^1, r^2, r^3). \tag{4.12}$$

By combining the compatibility condition (4.9) with (4.7) for ϑ and $\mathbf{p}$, we can relate r_0 to $\mathbf{r}$,

$$\mathbf{r} = -r_0 \frac{g_1(\vartheta^+)}{\lambda}\, \mathbf{n}. \tag{4.13}$$

This allows us to represent the jumps of the first derivatives of ϑ and $\mathbf{p}$ in terms of r_0 ,

$$[\![\vartheta_t]\!] = -\lambda r_0\,, \tag{4.14}$$

$$[\![\nabla\vartheta]\!] = r_0\mathbf{n}\,, \tag{4.15}$$

$$[\![\mathbf{p}_t]\!] = r_0 g_1^+ \mathbf{n}\,, \tag{4.16}$$

$$[\![\nabla\mathbf{p}]\!] = -r_0 \frac{g_1^+}{\lambda}\mathbf{n} \otimes \mathbf{n}\,, \tag{4.17}$$

where we abbreviate $g_1(\vartheta^+)$ with g_1^+, and will continue similarly for any functions of ϑ evaluated across $\mathcal{S}(t)$. Substituting (4.14) – (4.17) into (4.6) and (4.7) gives the following equation for λ when $r_0 \neq 0$,

$$\lambda^2 + \lambda \frac{\alpha'^+}{c_v^+}\, \mathbf{p}^+ \cdot \mathbf{n} - \frac{\alpha^+ g_1^+}{c_v^+} = 0. \tag{4.18}$$

From (2.18), (2.19) and (2.21) we therefore have real characteristic speeds, depending on the state $(\vartheta^+, \mathbf{p}^+)$ ahead of the wave, and the normal $\mathbf{n}$ to the wavefront. If $\vartheta^+ < \vartheta_\lambda$ is constant, the evolution Eq. (4.2) implies that $\mathbf{p}^+$ satisfies

$$\mathbf{p}^+ = \mathbf{p}_0 e^{g_2^+ t} \tag{4.19}$$

with $g_2^+ < 0$. We take $\mathbf{p}_0 = \mathbf{0}$, which leads to $\lambda = \lambda(\vartheta^+)$,

$$\lambda^2 = \frac{\alpha^+ g_1^+}{c_v^+}. \tag{4.20}$$

For the remainder of this section we consider plane waves propagating into an equilibrium state,

$$\vartheta^+ = \text{constant}, \quad \mathbf{p}^+ = \mathbf{0}, \quad \mathbf{n} = \text{constant}. \tag{4.21}$$

To derive an equation for the amplitude, r_0, we differentiate (4.1), (4.2) with respect to t and then compute the jump across $\mathcal{S}(t)$. Using the relation

$$[\![\vartheta_{tt}]\!] = -\lambda \frac{dr_0}{dt} - \lambda \mathbf{n} \cdot [\![\nabla \vartheta_t]\!] \tag{4.22}$$

and

$$[\![\mathbf{p}_{tt}]\!] = g_1^+ \mathbf{n} \frac{dr_0}{dt} - \lambda \mathbf{n} \cdot [\![\nabla \mathbf{p}_t]\!] \tag{4.23}$$

which come from (4.8) and (4.14) – (4.17), we obtain

$$-\lambda c_v \frac{dr_0}{dt} + r_0^2 (c_v' \lambda^2 - 2\alpha' g_1) - \lambda c_v \mathbf{n} \cdot [\![\nabla \vartheta_t]\!] - \alpha [\![\nabla \cdot \mathbf{p}_t]\!] = 0, \tag{4.24}$$

$$g_1 \mathbf{n} \frac{dr_0}{dt} - \lambda \mathbf{n} \cdot [\![\nabla \mathbf{p}_t]\!] + \lambda g_1' r_0^2 \mathbf{n} - g_1 [\![\nabla \vartheta_t]\!] = g_1 g_2 r_0 \mathbf{n}. \tag{4.25}$$

For simplicity of notation, we have omitted the symbol "+" in the coefficients above. Taking the scalar product of (4.25) with $\dfrac{1}{g_1}\mathbf{n}$, we calculate

$$\mathbf{n} \cdot [\![\nabla \vartheta_t]\!] = \frac{dr_0}{dt} - \frac{\lambda}{g_1} \mathbf{n} \otimes \mathbf{n} \cdot [\![\nabla \mathbf{p}_t]\!] + \frac{\lambda g_1'}{g_1} r_0^2 - g_2 r_0. \tag{4.26}$$

Using (4.26) in (4.24) gives

$$-2\lambda c_v \frac{dr_0}{dt} + r_0^2 \left(c_v' \lambda^2 - 2\alpha' g_1 - \lambda^2 c_v \frac{g_1'}{g_1} \right) + \lambda c_v g_2 r_0 + \lambda^2 c_v \frac{1}{g_1} \mathbf{n} \otimes \mathbf{n} \cdot [\![\nabla \mathbf{p}_t]\!] - \alpha [\![\nabla \cdot \mathbf{p}_t]\!] = 0. \tag{4.27}$$

The final two terms in (4.27) reduce to

$$\alpha \mathbf{n} \otimes \mathbf{n} \cdot [\![\nabla \mathbf{p}_t]\!] - \alpha [\![\nabla \cdot \mathbf{p}_t]\!], \tag{4.28}$$

after applying relation (4.20) for λ^2. Arguing as in [10] (Chapter 2.6), one finds that

$$\mathbf{n} \otimes \mathbf{n} \cdot [\![\nabla \mathbf{p}_t]\!] = \mathbf{n} \cdot \left(\frac{d}{dt} \left[\!\left[\frac{\partial \mathbf{p}}{\partial n} \right]\!\right] - \left[\!\left[\lambda \frac{\partial^2 \mathbf{p}}{\partial n^2} \right]\!\right] \right) = [\![\nabla \cdot \mathbf{p}_t]\!]. \tag{4.29}$$

As a result, (4.27) can be written in terms of $[\![\vartheta_t]\!]$, using (4.14) and (4.20),

$$\frac{d}{dt}[\![\vartheta_t]\!] + \mathcal{A}[\![\vartheta_t]\!]^2 + \mathcal{B}[\![\vartheta_t]\!] = 0 \tag{4.30}$$

where the coefficients $\mathcal{A}$ and $\mathcal{B}$ are given (see (2.18), (2.19) and (2.21)) by

$$\mathcal{A} = \frac{1}{2}\left(\frac{c_v'}{c_v} - \frac{4}{\vartheta^+} - \frac{3g_1'}{g_1}\right), \tag{4.31}$$

$$\mathcal{B} = -\frac{1}{2}g_2 > 0. \tag{4.32}$$

Finally we examine (4.31) for the special case (2.27), (3.4) with $g_{10} = a\vartheta^{1/2}$. This gives

$$\mathcal{A} = \frac{1}{2}\left(\frac{3r_1}{\vartheta_\lambda - \vartheta^+} - \frac{5}{2\vartheta^+}\right). \tag{4.33}$$

As in [21], we obtain a temperature $\vartheta^+ = \vartheta_m$ at which $\mathcal{A} = 0$, here

$$\vartheta_m = \frac{5\vartheta_\lambda}{6r_1 + 5}. \tag{4.34}$$

Since $\mathcal{B} > 0$, the solutions $[\![\vartheta_t]\!]$ of (4.30) tend to infinity in finite time whenever $\mathcal{A}[\![\vartheta_t]\!]_0 + \mathcal{B} < 0$, with initial condition $[\![\vartheta_t]\!]_0 = \vartheta_t^-(0)$. We now have an analogous result on the finite time blowup of three-dimensional plane temperature-rate waves to the one-dimensional case in [21], with a *hot* temperature-rate wave having $\vartheta_t^-(0) > 0$, and a *cold* temperature-rate wave having $\vartheta_t^-(0) < 0$.

THEOREM *Let $\vartheta^+ < \vartheta_\lambda$ be the temperature in front of the temperature-rate wave, and let $[\![\vartheta_t]\!]_0 = \vartheta_t^-(0)$. Then,*

1. *For $\vartheta_m < \vartheta^+ < \vartheta_\lambda$ (i.e. $\mathcal{A} > 0$), the amplitude $[\![\vartheta_t]\!]$ blows up in finite time if $\vartheta_t^-(0) < -\frac{B}{A} < 0$ (cold temperature-rate wave);*

2. *For $0 < \vartheta^+ < \vartheta_m$ (i.e. $\mathcal{A} < 0$), the amplitude $[\![\vartheta_t]\!]$ blows up in finite time if $\vartheta_t^-(0) > -\frac{B}{A} > 0$ (hot temperature-rate wave);*

3. *For $\vartheta^+ = \vartheta_m$ (i.e. $\mathcal{A} = 0$), the amplitude $[\![\vartheta_t]\!]$ is a decreasing function of time, and blow-up does not occur.*

We remark that at ϑ_m, the system (4.1), (4.2) loses genuine nonlinearity. Such a temperature has also been found by RUGGERI *et al.* ([19, 20]), whose derivation is based on (3.1) for U_E and so does not reflect the fact that second sound is not observed above certain temperatures. As a result, they do not obtain a relationship of the type (4.34) since there is no analogue of the temperature ϑ_λ playing the part, in solids, of the lambda point for liquid helium.

As in [21], one may also show that no one-dimensional shocks can propagate into equilibrium states for which $\vartheta^+ = \vartheta_m$. From (3.10) and (3.11) respectively, ϑ_m is found to be 14.9 K for sodium fluoride and 3.46 K for bismuth.

References

1. C. C. ACKERMAN, B. BERTMAN, H.A. FAIRBANK and R.A. GUYER, *Second sound in solid helium*, Phys. Rev. Letters, **16**, 789–791, 1966.
2. B. D. COLEMAN and M.E. GURTIN, *Thermodynamics with internal state variables*, J. Chem. Phys., **47**, 597–613, 1967.
3. B. D. COLEMAN and D.C. NEUMANN, *Implication of a nonlinearity in the theory of second sound in solids*, Phys. Rev. B, **32**, 1492–1498, 1988.
4. B. D. COLEMAN, M. FRABIZIO and D. OWEN, *On the thermodynamics of second sound in dielectric crystals*, Arch. Rational Mech. Anal., **80**, 135–158, 1982.
5. H. E. JACKSON, C. T. WALKER and T.F. MCNELLY, *Second sound in NaF*, Phys. Rev. Letters, **25** (1), 26–28, 1970.
6. H.E. JACKSON and C.T. WALKER, *Thermal conductivity, second sound, and phonon-phonon interactions in NaF*, Physical Review B, **3**, 4, 1428–1439, 1971.
7. D. D. JOSEPH and L. PREZIOSI, *Heat waves*, Rev. Mod. Phys., **61**, 41, 1–62, 1989.
8. D. D. JOSEPH and L. PREZIOSI, *Addendum to the paper "Heat Waves"*, Rev. Mod. Phys., **61**, 41 1989, Rev. Mod. Phys., **62**, 2, 375–392, 1990.
9. W. KOSIŃSKI, *Thermal waves in inelastic bodies*, Arch. Mech., **27**, 5–6, 733–748, 1975.
10. W. KOSIŃSKI, *Field singularities and wave analysis in continuum mechanics*, Ellis Horwood Limited Publishers, Chichester 1986.
11. W. KOSIŃSKI, *Elastic waves in the presence of a new temperature scale*, [in:] Elastic Wave Propagation, M.F.McCarthy and M.Hayes, [Eds.], Elsevier Science (North Holland), 1989, 629–634.
12. W. KOSIŃSKI, K. SAXTON and R. SAXTON, *Second sound speed in a crystal of NaF at low temperature*, Arch. Mech., **49**, 1, 189–196, 1997.
13. W. KOSIŃSKI and W. WOJNO, *Gradient generalization to internal state variable approach*, Arch. Mech., **47**, 3, 523–536, 1995.
14. W. LARECKI, *Symmetric forms of the equations of heat transport in a rigid conductor of heat with internal state variables I. Analysis of the model and thermodynamic restrictions via the main dependency relation*, Arch. Mech., **50**, 2, 143–173, 1998.
15. T.F. MCNELLY, S.J. ROGERS, D.J. CHAMIN, R.J. ROLLEFSON, W.M. GOUBAU, G.E. SCHMIDT, J.A. KRUMHANSI and R.O. POHL, *Heat pulses in NaF: onset of second sound*, Phys. Rev. Letters, **24**, 3, 100–102, 1970.
16. A. MORRO and T. RUGGERI, *Second sound and internal energy in solids*, Int. J. Nonlinear Mech., **22**, 1, 27–36, 1987.
17. A. MORRO and T. RUGGERI, *Non-equilibrium properties of solids obtained from second-sound measurements*, J. Phys. C, **21**, 1743–1752, 1988.
18. V. NARAYANAMURTI and R.C. DYNES, *Observation of second sound in bismuth*, Phys. Rev. Letters, **28**, 22, 1461–1465, 1972.
19. T. RUGGERI, A. MURACCHINI and L. SECCIA, *Shock waves and second sound in a rigid heat conductor: a critical temperature for NaF and Bi*, Phys. Rev. Letters, **64**, 22, 2640–2643, 1990.
20. T. RUGGERI, A. MURACCHINI and L. SECCIA, *Continuum approach to phonon gas and shape changes of second sound via shock waves theory*, Il Nuovo Cimento, **16** D, 1, 15–44, 1994.

21. K. SAXTON, R. SAXTON and W. KOSIŃSKI, *On second sound at the critical temperature*, Quart. Appl. Math., **57**, 723–740, 1999.

22. K. WOŁOSZYŃSKA, *On coupling acceleration waves in a thermoviscoplastic medium I. Symmetry and hyperbolicity conditions*, Arch. Mech., **33**, 2, 261–272, 1981.

Received March 12, 1999; new version October 21, 1999.

Arch. Mech., **52**, 1, pp. 143–158, Warszawa 2000

Deflection relationships between the homogeneous Kirchhoff plate theory and different functionally graded plate theories

Z-Q. CHENG ([1]) and R. C. BATRA ([2])

([1]) *Department of Modern Mechanics*
University of Science and Technology of China
Hefei, Anhui 230026, P. R. China
Currently, Visiting Research Associate
Virginia Polytechnic Institute and State University

([2]) *Department of Engineering Science and Mechanics, M/C 0219*
Virginia Polytechnic Institute and State University
Blacksburg, VA 24061, USA

We derive field equations for a functionally graded plate whose deformations are governed by either the first-order shear deformation theory or the third-order shear-deformation theory. These equations are further simplified for a simply supported polygonal plate. An exact relationship is established between the deflection of the functionally graded plate and that of an equivalent homogeneous Kirchhoff plate. This relationship is used to explicitly express the displacements of a plate particle according to the first-order shear deformation theory in terms of the deflection of a homogeneous Kirchhoff plate. These relationships can readily be used to obtain similar correspondences between the deflections of a transversely isotropic laminated plate and a homogeneous Kirchhoff plate.

Key Words: deflection relationship, functionally graded plate, laminated plate.

1. Introduction

Laminated composite materials are commonly used in engineering structures. A sudden change in material properties at the interfaces can result in locally large deformations which may trigger the initiation and propagation of a microcrack in a lamina. One way to overcome this is to use functionally graded materials in which material properties vary continuously. This is achieved by gradually changing the volume fraction of the constituent materials usually only in one (the thickness) direction to obtain a smooth variation of material properties and an optimum response to external thermomechanical loads (Reddy and Chin [12], Praveen and Reddy [9]).

An interesting issue for plates made of functionally gradient materials is the determination of relationships between their deflections predicted by various shear deformation plate theories and that given by the classical Kirchhoff plate theory. Such relationships have been found for sandwich plates (HU [2], LIU and CHENG [7], WANG [13]), single-layer homogeneous plates (WANG and ALWIS [15], REDDY and WANG [13] and laminated plates materially and geometrically symmetric about the midplane (CHENG and KITIPORNCHAI [1]). For plates symmetric about the midsurface, the stretching and bending deformation modes are uncoupled and hence can be separately analyzed. This, however, is not the case for functionally graded plates whose material properties are generally not symmetric about the midsurface. Here we study deformations of a thin plate made of a functionally graded material and seek relationships between its deflections predicted by two shear deformation theories and that given by the classical Kirchhoff plate theory.

2. Field equations

Consider an undeformed plate of uniform thickness h. We use a rectangular Cartesian coordinate system $\{x_i\}(i = 1, 2, 3)$, with the plane $x_3 = 0$ coincident with the mid-surface of the plate. Hereafter, a comma followed by a subscript i denotes the partial derivative with respect to x_i, and a repeated index implies summation over the range of the index with Latin indices ranging from 1 to 3 and Greek indices from 1 to 2.

The displacement field in the third-order plate theory (HSDT) proposed by REDDY [10], the first-order shear deformation plate theory (FSDT) and the classical laminated plate theory (CLT) can be written as

$$v_\alpha(x_i) = u_\alpha - x_3 u_{3,\alpha} + g\varphi_\alpha, \quad v_3(x_i) = u_3, \tag{2.1}$$

where u_α, u_3 and φ_α are independent of x_3 and

$$g(x_3) = x_3\left(1 - \frac{4x_3^2}{3h^2}\right). \tag{2.2}$$

Note that the hypothesis (2.1) is a special case of that proposed by KĄCZKOWSKI [4]; the reader is also referred to the survey article by JEMIELITA [3]. Substitution from (2.2) into (2.1) gives the displacement field for the HSDT and the choices $g(x_3) = x_3$ and $g(x_3) = 0$ give, respectively, the displacement fields for the FSDT and the CLT.

For the linear bending problem of a functionally graded plate subjected to an arbitrary distributed normal load $q(x_\alpha)$ on its surface, the field equations are

$$N_{\alpha\beta,\beta} = 0, \quad M_{\alpha\beta,\alpha\beta} + q = 0, \quad P_{\alpha\beta,\beta} - R_\alpha = 0, \tag{2.3}$$

where

$$[N_{\alpha\beta},\ M_{\alpha\beta},\ P_{\alpha\beta}] = \int_{-h/2}^{h/2} \sigma_{\alpha\beta}[1,\ x_3,\ g]dx_3, \quad R_\alpha = \int_{-h/2}^{h/2} \sigma_{\alpha 3} g_{,3} dx_3, \tag{2.4}$$

$$\sigma_{\alpha\beta} = H_{\alpha\beta\omega\rho} e_{\omega\rho}, \quad \sigma_{\alpha 3} = 2E_{\alpha 3\omega 3} e_{\omega 3}, \tag{2.5}$$

$$e_{ij} = \frac{1}{2}(v_{i,j} + v_{j,i}). \tag{2.6}$$

Here σ_{33} is assumed to be negligible. For an isotropic material (LIBRESCU [5])

$$H_{\alpha\beta\omega\rho} = \frac{\nu E}{1-\nu^2}\delta_{\alpha\beta}\delta_{\omega\rho} + \frac{E}{2(1+\nu)}(\delta_{\alpha\omega}\delta_{\beta\rho} + \delta_{\alpha\rho}\delta_{\beta\omega}), \quad E_{\alpha 3\omega 3} = \bar{\mu}\delta_{\alpha\omega}, \tag{2.7}$$

where δ_{ij} is the Kronecker delta, E, ν and $\bar{\mu}$ denote respectively, Young's modulus, Poisson's ratio, and the shear modulus. Here we have purposely not set $\bar{\mu} = E/2(1+\nu)$ so that the results may be applicable to a transversely isotropic plate. For the functionally graded plate, the material properties are assumed to vary in the thickness direction only,

$$E = E(x_3), \quad \nu = \nu(x_3), \quad \bar{\mu} = \bar{\mu}(x_3). \tag{2.8}$$

For a plate made of different isotropic laminae, the material moduli are piecewise constant functions of x_3. Using Eqs. (2.1), (2.5) and (2.6), Eq. (2.4) may alternatively be written as

$$\begin{bmatrix} N_{\alpha\beta} \\ M_{\alpha\beta} \\ P_{\alpha\beta} \end{bmatrix} = (\mathbf{a} - \mathbf{b}) \begin{bmatrix} u_{\omega,\omega} \\ -u_{3,\omega\omega} \\ \varphi_{\omega,\omega} \end{bmatrix} \delta_{\alpha\beta} + \mathbf{b} \begin{bmatrix} \frac{1}{2}(u_{\alpha,\beta} + u_{\beta,\alpha}) \\ -u_{3,\alpha\beta} \\ \frac{1}{2}(\varphi_{\alpha,\beta} + \varphi_{\beta,\alpha}) \end{bmatrix}, \tag{2.9}$$

$$R_\alpha = c\varphi_\alpha,$$

where

$$\mathbf{a} = \int_{-h/2}^{h/2} \mathbf{F}\frac{E}{1-\nu^2}dx_3, \quad \mathbf{b} = \int_{-h/2}^{h/2} \mathbf{F}\frac{E}{1+\nu}dx_3, \quad c = \int_{-h/2}^{h/2} (g_{,3})^2 \bar{\mu} dx_3,$$

$$\mathbf{a} = \begin{bmatrix} a_0 & a_4 & a_5 \\ a_4 & a_1 & a_2 \\ a_5 & a_2 & a_3 \end{bmatrix}, \quad \mathbf{b} = \begin{bmatrix} b_0 & b_4 & b_5 \\ b_4 & b_1 & b_2 \\ b_5 & b_2 & b_3 \end{bmatrix}, \quad \mathbf{F} = \begin{bmatrix} 1 & x_3 & g \\ x_3 & x_3^2 & x_3 g \\ g & x_3 g & g^2 \end{bmatrix}. \tag{2.10}$$

Note that a_4, a_5, b_4 and b_5 vanish for a plate materially and geometrically symmetric about its midsurface. Substitution from (2.9) into (2.3) results in the following field equations in terms of the five displacement functions u_α, u_3 and φ_α:

$$\frac{1}{2}b_0u_{\alpha,\beta\beta}+(a_0-\frac{1}{2}b_0)u_{\beta,\beta\alpha}-a_4u_{3,\alpha\beta\beta}+\frac{1}{2}b_5\varphi_{\alpha,\beta\beta}+\left(a_5-\frac{1}{2}b_5\right)\varphi_{\beta,\beta\alpha}=0, \tag{2.11}$$

$$a_4u_{\alpha,\alpha\beta\beta}-a_1u_{3,\alpha\alpha\beta\beta}+a_2\varphi_{\alpha,\alpha\beta\beta}+q=0, \tag{2.12}$$

$$\frac{1}{2}b_5u_{\alpha,\beta\beta}+(a_5-\frac{1}{2}b_5)u_{\beta,\beta\alpha}-a_2u_{3,\alpha\beta\beta}+\frac{1}{2}b_3\varphi_{\alpha,\beta\beta}+(a_3-\frac{1}{2}b_3)\varphi_{\beta,\beta\alpha}-c\varphi_\alpha=0. \tag{2.13}$$

Furthermore, substitution for $u_{\alpha,\beta\beta}$ from (2.11) into (2.12) and (2.13) yields

$$(a_4^2-a_0a_1)u_{3,\alpha\alpha\beta\beta}+(a_0a_2-a_4a_5)\varphi_{\alpha,\alpha\beta\beta}+a_0q=0, \tag{2.14}$$

$$(a_5b_0-a_0b_5)u_{\beta,\beta\alpha}+(a_4b_5-a_2b_0)u_{3,\alpha\beta\beta}+\frac{1}{2}(b_0b_3-b_5^2)\varphi_{\alpha,\beta\beta}+(a_3b_0-a_5b_5+\frac{1}{2}b_5^2-\frac{1}{2}b_0b_3)\varphi_{\beta,\beta\alpha}-b_0c\varphi_\alpha=0. \tag{2.15}$$

To simplify the field equations, two new potential functions, w and f, are introduced such that

$$\varphi_\alpha=(u_3+w)_{,\alpha}+\epsilon_{\alpha\omega}f_{,\omega}, \tag{2.16}$$

where $\epsilon_{\alpha\omega}$ is the two-dimensional permutation tensor. Even though Eq. (2.16) uniquely defines φ_α, however, w and f are not uniquely determined from it. This is because the Cauchy-Riemann equation

$$(u_3^*+w^*)_{,\alpha}+\epsilon_{\alpha\omega}f^*_{,\omega}=0 \tag{2.17}$$

always has a solution $[f^*+i(u_3^*+w^*)]$ which is an analytic function of the complex variable (x_1+ix_2). The expression (2.16) for φ_α remains unchanged when (u_3+w) and f are simultaneously incremented by $(u_3^*+w^*)$ and f^* respectively.

Substituting for φ_α from Eq. (2.16) into Eqs. (2.11), (2.14) and (2.15) we obtain

$$\frac{1}{2}b_0u_{\alpha,\beta\beta}+(a_0-\frac{1}{2}b_0)u_{\beta,\beta\alpha}-a_4u_{3,\alpha\beta\beta}+a_5(u_3+w)_{,\alpha\beta\beta}+\frac{1}{2}b_5\epsilon_{\alpha\omega}f_{,\omega\beta\beta}=0, \tag{2.18}$$

$$[(a_4^2 - a_0a_1 + a_0a_2 - a_4a_5)u_3 + (a_0a_2 - a_4a_5)w]_{,\alpha\alpha\beta\beta} + a_0q = 0, \tag{2.19}$$

$$[(a_5b_0 - a_0b_5)u_{\beta,\beta} + (a_4b_5 - a_2b_0)u_{3,\beta\beta} + (a_3b_0 - a_5b_5)(u_3 + w)_{,\beta\beta} - b_0c(u_3 + w)]_{,\alpha} + \epsilon_{\alpha\omega}[\frac{1}{2}(b_0b_3 - b_5^2)f_{,\beta\beta} - b_0cf]_{,\omega} = 0. \tag{2.20}$$

Equation (2.20) is the Cauchy-Riemann equation, which can equivalently be written as

$$\frac{1}{2}(b_0b_3 - b_5^2)f_{,\beta\beta} - b_0cf + i[(a_5b_0 - a_0b_5)u_{\beta,\beta} + (a_4b_5 - a_2b_0 + a_3b_0 - a_5b_5)u_{3,\beta\beta} - b_0cu_3 + (a_3b_0 - a_5b_5)w_{,\beta\beta} - b_0cw] = H(x_1 + ix_2), \tag{2.21}$$

where $H(x_1 + ix_2)$ is an analytic function. Furthermore, viewing Eq. (2.21) as a nonhomogeneous partial differential equation for unknowns (u_α, u_3, w, f), its solution is the sum of a homogeneous general solution and a particular solution. Since both the real and imaginary parts of $H(x_1 + ix_2)$ are harmonic functions, the particular solution (u_α^*, u_3^*, w^*, f^*) can be taken as

$$u_\alpha^* = 0,\ u_3^* = 0,\ -b_0c(f^* + iw^*) = H(x_1 + ix_2), \tag{2.22}$$

which satisfies the Cauchy-Riemann condition (2.17). We note that the particular solution makes trivial contributions to u_α, u_3 and φ_α, and hence to displacements and stresses of the functionally graded plate. Consequently, it is discarded. The homogeneous part of Eq. (2.21) gives

$$(a_5b_0 - a_0b_5)u_{\beta,\beta} + (a_4b_5 - a_2b_0 + a_3b_0 - a_5b_5)u_{3,\beta\beta} - b_0cu_3 + (a_3b_0 - a_5b_5)w_{,\beta\beta} - b_0cw = 0, \tag{2.23}$$

$$\frac{1}{2}(b_0b_3 - b_5^2)f_{,\beta\beta} - b_0cf = 0. \tag{2.24}$$

Let

$$\hat{u}_\alpha = u_\alpha + \frac{1}{a_0}[(a_5 - a_4)u_3 + a_5w]_{,\alpha} + \frac{b_5}{b_0}\epsilon_{\alpha\omega}f_{,\omega}, \tag{2.25}$$

and using it to eliminate u_α from Eqs. (2.18) and (2.23), we rewrite Eqs. (2.18), (2.19), (2.23) and (2.24) as

$$\frac{1}{2}b_0\hat{u}_{\alpha,\beta\beta} + (a_0 - \frac{1}{2}b_0)\hat{u}_{\beta,\beta\alpha} = 0, \tag{2.26}$$

$$[(\bar{a}_2 - \bar{a}_1)u_3 + \bar{a}_2 w]_{,\alpha\alpha\beta\beta} + q = 0, \tag{2.27}$$

$$(a_5 - \frac{a_0 b_5}{b_0})\hat{u}_{\beta,\beta} + (\bar{a}_3 - \bar{a}_2)u_{3,\beta\beta} - cu_3 + \bar{a}_3 w_{,\beta\beta} - cw = 0, \tag{2.28}$$

$$\frac{1}{2}\bar{b}_3 f_{,\beta\beta} - cf = 0, \tag{2.29}$$

where

$$\bar{a}_1 = a_1 - \frac{a_4^2}{a_0}, \quad \bar{a}_2 = a_2 - \frac{a_4 a_5}{a_0}, \quad \bar{a}_3 = a_3 - \frac{a_5^2}{a_0}, \quad \bar{b}_3 = b_3 - \frac{b_5^2}{b_0}. \tag{2.30}$$

It follows from Eqs. (2.10) and the usual assumptions, $E > 0$, $-1 < \nu < \frac{1}{2}$ that $a_0 > 0$, $b_0 > 0$. This form of field equations is convenient for seeking fundamental solutions. Note that the unknown function f has been uncoupled from the other four unknowns $\hat{u}_\alpha$, u_3 and w in the field Eqs. (2.26) – (2.29), but is still coupled with them in Eq. (2.25) and hence in most of boundary conditions. However, as shown below, for simply supported functionally graded polygonal plates, the unknown f can be totally decoupled and hence separately determined.

3. Simply supported rectilinear edges

We now consider a simply supported polygonal plate, and express boundary conditions as

$$N_{NN} = 0, \quad M_{NN} = 0, \quad P_{NN} = 0, \tag{3.1}$$

$$u_3 = 0, \quad u_T = 0, \quad \varphi_T = 0, \tag{3.2}$$

where the upper case subscripts N and T denote, respectively, the normal and tangential directions on the boundary. No implicit summation applies to the repeated upper case subscripts. Also, note that $u_3 = 0$ implies $u_{3,T} = 0$, and

$$\begin{bmatrix} N_{NN} \\ M_{NN} \\ P_{NN} \end{bmatrix} = \begin{bmatrix} 0 \\ 0 \\ 0 \end{bmatrix} \Rightarrow \mathbf{a} \begin{bmatrix} u_{N,N} \\ -u_{3,NN} \\ \varphi_{N,N} \end{bmatrix} = \begin{bmatrix} 0 \\ 0 \\ 0 \end{bmatrix}. \tag{3.3}$$

We recall Gram's inequality (MITRINOVIC and VASIC [8])

$$\det(\mathbf{G}) \geq 0, \tag{3.4}$$

where $\mathbf{G} = (G_{ij})$ is a $n \times n$ matrix with elements defined by

$$G_{ij} = \int_a^b f_i f_j dx_3, \tag{3.5}$$

and the equality in (3.4) holds if and only if the real and integrable functions $f_i(x_3)$ $(x_3 \in [a,b];\ i = 1,\ldots,n)$ are linearly dependent. The Gram theorem implies that

$$\det(\mathbf{a}) > 0, \tag{3.6}$$

for the HSDT. Therefore, Eq. (3.3) gives

$$u_{N,N} = 0, \quad u_{3,NN} = 0, \quad \varphi_{N,N} = 0. \tag{3.7}$$

Using Eqs. (2.16) and (2.23), Eqs. (3.1) and (3.7) can be written as

$$u_3 = 0, \quad u_{3,NN} = 0, \quad w = 0, \quad w_{,NN} = 0, \quad f_{,N} = 0, \quad u_T = 0, \quad u_{N,N} = 0, \tag{3.8}$$

where only three of the first four and the last three of Eqs. (3.8) are necessary for finding a solution of the bending problem. Note that the unknowns u_α, u_3, w and f are uncoupled in the boundary condition for a simply supported polygonal plate.

4. Deflection relations between different theories

The solution of Eq. (2.29) under the boundary condition $(3.8)_5$ is

$$f = 0. \tag{4.1}$$

Note that Eq. (2.29) has the null solution (3.9) only when the polygonal plate is simply supported. Thus for the bending problem of a simply supported functionally graded polygonal plate, only four functions u_α, u_3 and w need to be determined.

Recalling Eqs. (2.5) and (3.8), the boundary conditions associated with the field Eq. (2.6) for a simply supported polygonal plate are

$$\hat{u}_T = 0, \quad \hat{u}_{N,N} = 0, \tag{4.2}$$

and the solution of this boundary value problem is $\hat{u}_\alpha = 0$, i.e.,

$$u_\alpha = -[(a_5 - a_4)u_3 + a_5 w]_{,\alpha}/a_0. \tag{4.3}$$

The field equations for u_3 and w are the biharmonic Eq. (2.27) and the second-order Eq. (2.28). Equation (2.28) upon using $\hat{u}_\alpha = 0$ yields

$$(\bar{a}_3 - \bar{a}_2)u_{3,\beta\beta} - cu_3 + \bar{a}_3 w_{,\beta\beta} - cw = 0; \tag{4.4}$$

and the associated boundary conditions are three of the Eqs. $(3.8)_{1-4}$.

Note that the field Eqs. (2.27) and (4.4) have the same forms as those for a plate (CHENG and KITIPORNCHAI [1]) symmetric about its mid-plane and thus can be regarded as equations for such an equivalent plate with parameters given by Eq. (2.30). The over-barred quantities $\bar{a}_1$, $\bar{a}_2$ and $\bar{a}_3$ defined by (2.30) are the constants of a functionally graded plate equivalent to those of a plate symmetric about the midsurface because $a_4 = a_5 = 0$ for such a plate. This implies that a solution of the bending problem for a simply supported and polygonal functionally graded plate can be equivalently obtained from the solution of the corresponding problem for an identical plate symmetric about the midsurface. The in-plane displacements are then obtained from Eq. (4.3).

We now consider the classical Kirchhoff theory for functionally graded plates. Setting $g(x_3) = 0$ in Eq. (2.10) yields

$$a_2 = a_3 = a_5 = c = 0, \tag{4.5}$$

or

$$\bar{a}_2 = \bar{a}_3 = c = 0, \tag{4.6}$$

and Eq. (4.4) is trivially satisfied. We conclude from Eq. (4.3) that the in-plane displacements are given by

$$u_\alpha^K = \frac{a_4}{a_0} u_{3,\alpha}^K, \tag{4.7}$$

and Eq. (2.27) reduces to

$$-\bar{a}_1 u_{3,\alpha\alpha\beta\beta}^K + q = 0. \tag{4.8}$$

This is the Kirchhoff field equation for the bending deformation of the functionally graded plate with simply supported rectilinear edges. The superscript K on a variable signifies its value for the Kirchhoff plate theory. The boundary conditions on simply supported rectilinear edges are

$$u_3^K = 0, \quad u_{3,NN}^K = 0. \tag{4.9}$$

Based on the uniqueness of the solution of the boundary-value problem defined by Eqs. (4.8) and (4.9), and the analogy between the field Eqs. (2.27) and (4.8) and between the boundary conditions $(3.8)_{1-4}$ and (4.9), it can be concluded that

$$(\bar{a}_2 - \bar{a}_1) u_3 + \bar{a}_2 w = -\bar{a}_1 u_3^K. \tag{4.10}$$

Eliminating the function w from Eqs. (4.4) and (4.10), we obtain

$$(\bar{a}_1 \bar{a}_3 - \bar{a}_2^2) u_{3,\alpha\alpha} - c\bar{a}_1 u_3 = \bar{a}_1 \bar{a}_3 u_{3,\alpha\alpha}^K - c\bar{a}_1 u_3^K. \tag{4.11}$$

This is an exact relationship between the deflections of the HSDT and the Kirchhoff theories for simply supported polygonal plates made of functionally graded

materials. If the deflection u_3^K for the Kirchhoff theory is known, the deflection u_3 of the HSDT can be computed from the second-order Eq. (4.11) and the boundary condition $(3.8)_1$. Other unknown functions w and u_α are then simply obtained from Eqs. (4.10) and (4.3).

Furthermore, it is seen that the form of Eq. (4.8) is precisely the same as that of the equation governing the bending deformations of a homogeneous Kirchhoff thin plate with bending rigidity $\bar{a}_1$ and subjected to the normal pressure q. Thus the deflection of the functionally graded plate using the HSDT has been connected with the deflection of a homogeneous Kirchhoff thin plate. As there are solutions available for a classical homogeneous thin plate, the calculation of the deflection of the functionally graded plate using the relatively more sophisticated HSDT reduces to solving the second-order differential Eq. (4.11), which is a much easier task than solving the original problem.

The aforestated calculation is even further simplified if one uses the FSDT for the functionally graded plate. In this case, taking $g(x_3) = x_3$ in Eq. (2.10) we get

$$a_1 = a_2 = a_3, \quad a_4 = a_5, \tag{4.12}$$

or

$$\bar{a}_1 = \bar{a}_2 = \bar{a}_3. \tag{4.13}$$

Explicit expressions for u_3^F, w^F and u_α^F in terms of the Kirchhoff deflection u_3^K obtained from Eqs. (4.11), (4.10) and (4.3) are

$$u_3^F = u_3^K - \frac{\bar{a}_1}{c^F} u_{3,\alpha\alpha}^K, \quad w^F = -u_3^K, \quad u_\alpha^F = \frac{a_4}{a_0} u_{3,\alpha}^K, \tag{4.14}$$

where

$$c^F = \kappa \int_{-h/2}^{h/2} \bar{\mu} dx_3, \tag{4.15}$$

and κ is the shear correction factor. Therefore, once the deflection of the homogeneous Kirchhoff plate of rigidity $\bar{a}_1$ is known, the solution of the FSDT is readily obtained through simple algebraic and differential manipulations of the deflection of the Kirchhoff plate. It should be noted that unless $q = 0$, Eq. $(3.8)_2$ is not an essential boundary condition for simply supported edges in the FSDT for which $\det(\mathbf{a}) = 0$. The proof of this statement is omitted.

Our results also apply to a plate made of a transversely isotropic material because we have not required that $\bar{\mu} = E/2(1+\nu)$. For a transversely isotropic plate with its plane of isotropy parallel to the mid-plane, E and ν are designated, respectively, as Young's modulus and Poisson's ratio in the plane of isotropy and $\bar{\mu}$ as the transverse shear modulus. A typical example is a laminated composite

plate with transversely isotropic laminae. Such composite laminates are widely used in missiles and re-entry vehicles because their special thermomecianical properties provide thermal protection and high flexibility in transverse shear (LIBRESCU and STEIN [6]).

For laminated plates made of transversely isotropic materials and symmetric about their midsurfaces, CHENG and KITIPORNCHAI [1] have established relationships between the deflections of a plate according to the HSDT, FSIT and the classical plate theory. Equations (4.11), (4.10), (4.3) and (4.14) represent generalizations of such relationships to a plate that is not symmetric about its mid-plane.

5. An example

Consider a functionally graded rectangular plate simply supported at edges $x_1 = 0, a$ and $x_2 = 0, b$. Under the action of the normal pressure

$$q = Q \sin \frac{\pi x_1}{a} \sin \frac{\pi x_2}{b}, \tag{5.1}$$

the deflection due to the bending deformations of the functionally graded plate according to the HSDT and the Kirchhoff plate theory is assumed to be given by

$$[u_3 \; u_3^K] = [U_3 \; U_3^K] \sin \frac{\pi x_1}{a} \sin \frac{\pi x_2}{b}, \tag{5.2}$$

where U_3 and U_3^K are respectively, the central deflections of the plate in the HSDT and classical theory. In view of the relation (4.11) between the deflections of the two theories, we have

$$u_3 = (1 + \beta) U_3^K \sin \frac{\pi x_1}{a} \sin \frac{\pi x_2}{b}, \tag{5.3}$$

where

$$\beta = \frac{\bar{a}_2^2 (a^2 + b^2) \pi^2}{(\bar{a}_1 \bar{a}_3 - \bar{a}_2^2)(a^2 + b^2)\pi^2 + c \bar{a}_1 a^2 b^2} \tag{5.4}$$

characterizes the difference in the two deflections. This parameter depends only on the geometry and the material properties of the functionally graded plate. The through-thickness in-plane displacements of the HSDT are given by

$$v_1 = \frac{\gamma \pi}{a} U_3^K \cos \frac{\pi x_1}{a} \sin \frac{\pi x_2}{b}, \quad v_2 = \frac{\gamma \pi}{b} U_3^K \sin \frac{\pi x_1}{a} \cos \frac{\pi x_2}{b}, \tag{5.5}$$

where

$$\gamma(x_3) = \left(\frac{a_4}{a_0} - x_3 \right) (1 + \beta) + \left(g - \frac{a_5}{a_0} \right) \frac{\bar{a}_1}{\bar{a}_2} \beta \tag{5.6}$$

is a function of x_3 and characterizes the through-thickness variation of the in-plane displacements. For the FSDT parameters β and γ are given by

$$\beta^F = \frac{\bar{a}_1\pi^2}{c^F}\left(\frac{1}{a^2}+\frac{1}{b^2}\right), \quad \gamma^F(x_3) = \frac{a_4}{a_0} - x_3. \tag{5.7}$$

It can be shown that γ for the Kirchhoff plate theory is the same as that for the FSDT. Since there is no interlayer between two different materials in a functionally graded plate, computation of the out-of-plane shear stresses $\sigma_{\alpha 3}$ and the normal stress σ_{33} is not important which, compared with the longitudinal stresses, are of small orders of magnitude. The longitudinal stresses are given by

$$\begin{aligned}
\sigma_{11} &= -\frac{\gamma E\pi^2}{1-\nu^2}\left(\frac{1}{a^2}+\frac{\nu}{b^2}\right)U_3^K \sin\frac{\pi x_1}{a}\sin\frac{\pi x_2}{b},\\
\sigma_{22} &= -\frac{\gamma E\pi^2}{1-\nu^2}\left(\frac{\nu}{a^2}+\frac{1}{b^2}\right)U_3^K \sin\frac{\pi x_1}{a}\sin\frac{\pi x_2}{b},\\
\sigma_{12} &= \frac{\gamma E\pi^2}{(1+\nu)ab}U_3^K \cos\frac{\pi x_1}{a}\cos\frac{\pi x_2}{b}.
\end{aligned} \tag{5.8}$$

The functionally graded materials are usually made by mixing two distinct material phases, such as a metal and a ceramic. The effective material properties can be obtained from the "rule of mixture"

$$P_{\text{eff}}V = P_mV_m + P_cV_c, \quad V_m + V_c = 1, \tag{5.9}$$

where P stands for the material property, V for the volume fraction, and subscripts m, c and eff stand, respectively, for the metal, ceramic and the effective. A more accurate determination of the macroscopic material properties requires a better understanding of the microstructure and deformation of the constituents. The relation $(5.9)_1$ is exact for the mass density.

The volume fraction of the ceramic phase is assumed to be given by

$$V_c = \left(\frac{h+2x_3}{2h}\right)^n. \tag{5.10}$$

Figure 1 shows the through-thickness variation of the volume fraction of the ceramic for $n = 0.2,\ 0.5,\ 1,\ 2,\ 5$. Note that the bottom surface of the plate is metal-rich and the top surface ceramic-rich.

The dimensionless through-thickness in-plane displacement and the longitudinal stress are defined by

$$\bar{v}_1 = \frac{v_1(0,b/2,x_3)}{U_3^K}, \qquad \bar{\sigma}_{11} = \frac{a\sigma_{11}(a/2,b/2,x_3)}{E^*U_3^K}, \tag{5.11}$$

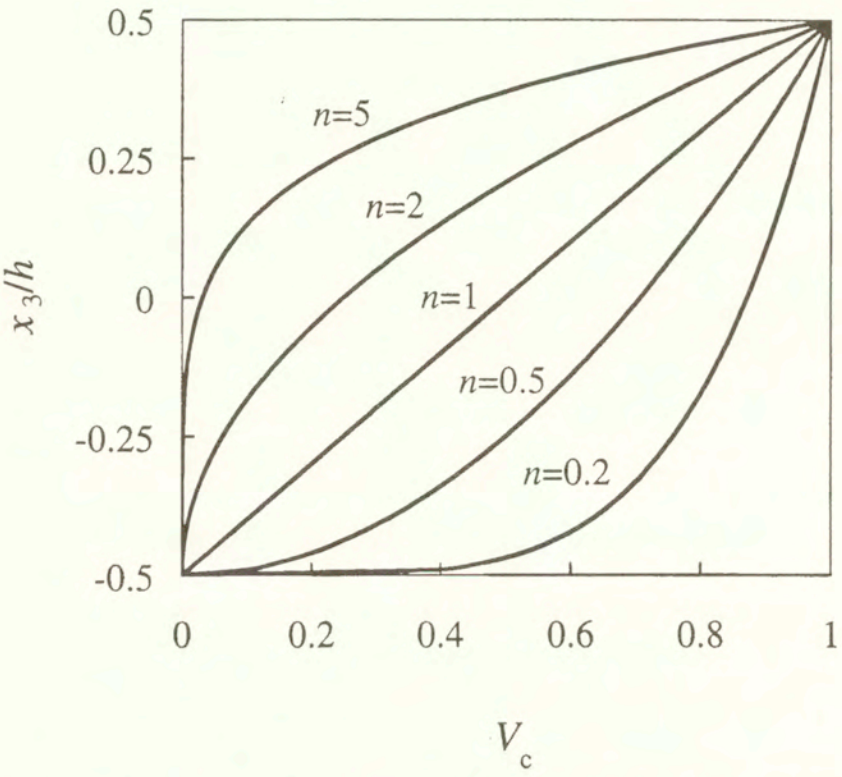

FIG. 1. Through-the-thickness distribution of the volume fraction of the ceramic phase in the functionally gradient plate.

where E^* is set equal to 1 GPa. We take the shear correction factor $\kappa = 5/6$ in the FSDT. Note that the value 5/6 of the shear correction factor was proposed for a homogeneous and isotropic plate; its use in a functionally graded plate may not be very realistic. The functionally graded material is a mixture of aluminum and zirconia (PRAVEEN and REDDY [9]), and we take

(5.12) $\quad E_m = 70\text{GPa}, \quad E_c = 151\text{GPa}, \quad \nu_m = \nu_c = 0.3, \quad a = b = 10h.$

For simplicity, Poisson's ratio for both aluminum and zirconia is assigned the same value; it is equivalent to the assumption that the effective value of the shear modulus is also derived from Eq. (5.9).

Table 1 lists values of U_3/U_3^K and U_3^F/U_3^K for $n = 0$, 0.2, 0.5, 1, 2 and 5. Here U_3^F equals the central deflection according to the FSDT. Figures 2 and 3 show the through-thickness distributions of the non-dimensional in-plane displacement $\bar{v}_1$ and the longitudinal stress $\bar{\sigma}_{11}$ obtained by using (a) the HSDT and (b) the FSDT. These variables are nondimensionalized (e.g. see Eq. (5.11)) so once the central deflection of the effective homogeneous Kirchhoff plate is known, the displacements and stresses of the functionally graded plate can be determined.

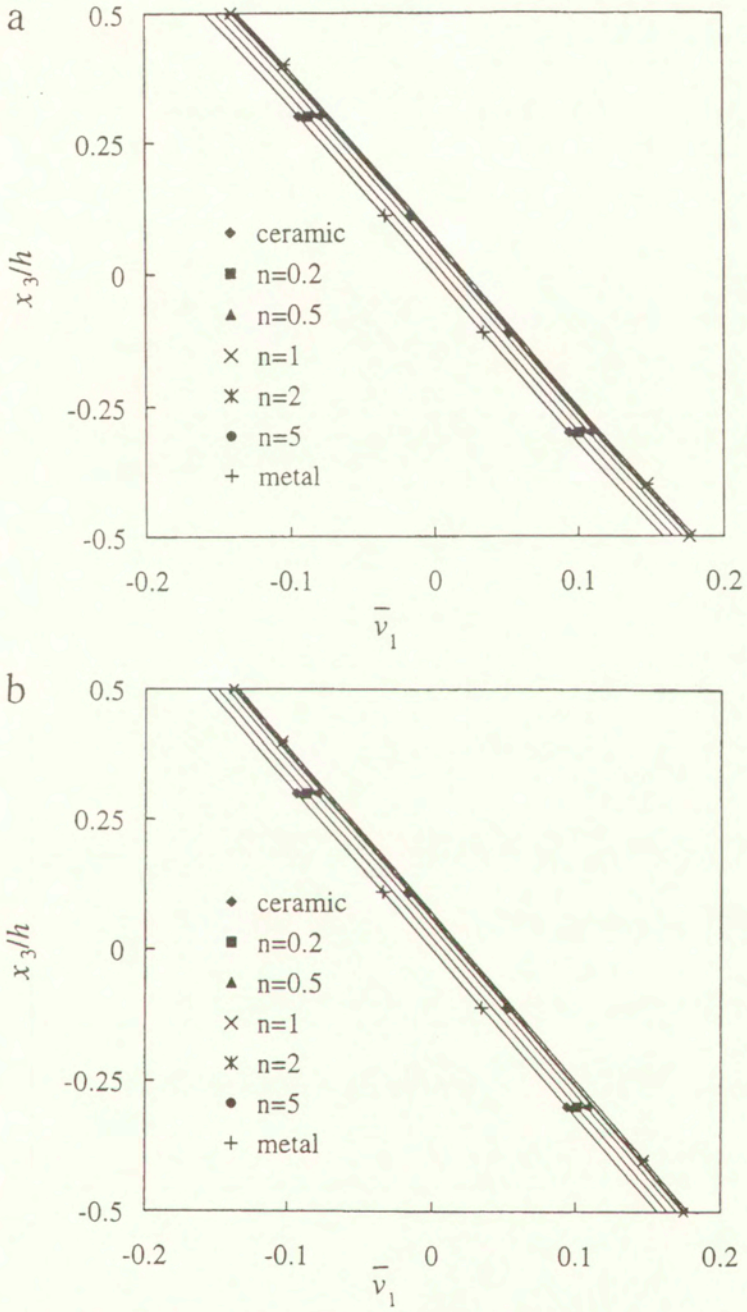

FIG. 2. Through-the-thickness distribution of the dimensionless in-plane displacement of the functionally graded square plate ($a = 10h$) using (a) the third-order plate theory and (b) the first-order plate theory.

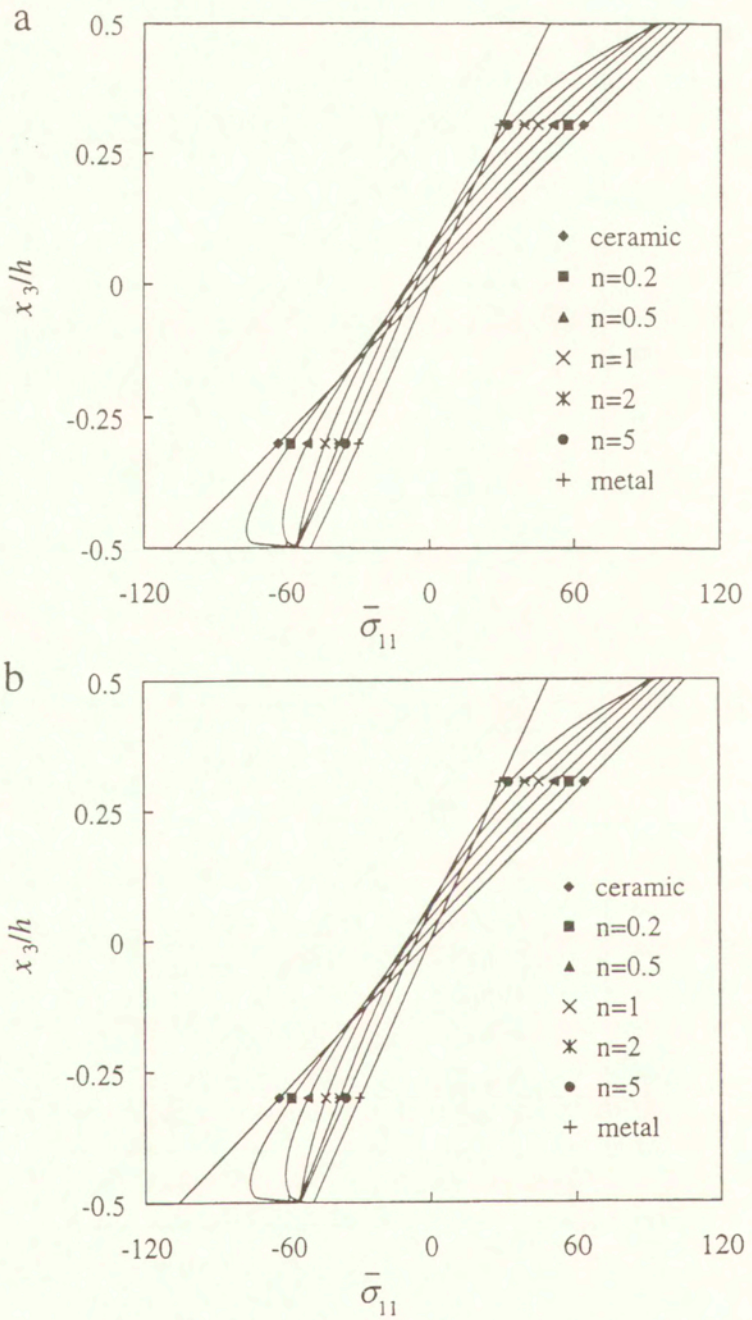

FIG. 3. Through-the-thickness distribution of the dimensionless longitudinal stress of the functionally graded square plate ($a = 10h$) using (a) the third-order plate theory and (b) the first-order plate theory.

Table 1. Central deflection of a functionally gradient square plate according to the three theories.

n	0	0.2	0.5	1	2	5
U_3/U_3^K	1.056360	1.054326	1.053157	1.053836	1.057850	1.064430
U_3^F/U_3^K	1.056398	1.054802	1.053711	1.053872	1.056260	1.060650

It is clear from the values listed in Table 1 that for each value of n, the classical Kirchhoff plate theory underestimates the central deflection of the plate by about 5.5% as compared to that given by either one of the other two plate theories studied herein. Results plotted in Figs. 2 and 3 reveal that the in-plane displacement $\bar{v}_1$ and the stress $\bar{\sigma}_{11}$ calculated from the two theories essentially coincide with each other. Thus for the problem studied herein results predicted by the FSDT are accurate enough for all practical purposes. This is because the through-thickness distribution of the in-plane displacement for the HSDT is nearly affine and agrees with that assumed in the FSDT. The FSDT obviates the need to solve the second-order differential Eq. (4.11).

The curves depicting the through-thickness distributions of the in-plane displacement $\bar{v}_1$ are parallel to each other for all values of the volume fraction V_c of the ceramic. The largest deviation between the values of $\bar{v}_1$ for an equivalent homogeneous plate and a functionally gradient plate occurs for $n = 2$. The maximum value of $|\bar{\sigma}_{11}|$ depends upon V_c. For $n = 0.2$ and 0.5, the magnitude of the compressive $\bar{\sigma}_{11}$ is maximum at a point a little above the lower surface of the plate. However, for other values of n, the magnitude of $\bar{\sigma}_{11}$ is maximum at a point on the top and bottom surfaces of the plate, as is the case for a homogeneous plate.

6. Conclusions

Two potential functions have been used to derive a set of equations that govern the deformations of a functionally graded plate. The deflections of a simply supported functionally graded polygonal plate given by the first-order shear deformation theory (FSDT) and the higher-order shear deformation theory (HSDT) have been related to that of an equivalent homogeneous Kirchhoff plate. These relationships are valid for a laminated plate that is not necessarily symmetric about its midsurface, and have been used to compute results for a simply supported square metal-ceramic plate.

Acknowledgements

This work was partially supported by the NSF grant CMS9713453 and ARO grant DAAG55-98-1-0030 to Virginia Polytechnic Institute and State University. We thank the anonymous reviewer for bringing to our attention Kączkowski's and Jemielita's papers.

References

1. Z. Q. CHENG, S. KITIPORNCHAI, *Exact connection between deflections of the classical and shear deformation laminated plate theories*, J. Appl. Mech., **66**, 260–262, 1999.
2. H. C. HU, *On some problems of the antisymmetrical small deflection of isotropic sandwich plates* (in Chinese), Acta Mechanica Sinica, **6**, 53–60, 1963.
3. G. JEMIELITA, *On kinematical assumptions of refined theories of plates: A survey*, J. Appl. Mech., **57**, 1088–1091, 1990.
4. Z. KĄCZKOWSKI, *Plate: static analysis*, Arkady, Warszawa 1968. p. 73.
5. L. LIBRESCU, *Elastostatics and kinetics of anisotropic and heterogeneous shell-type structures*, Netherlands: Noordhoff, Leyden 1975.
6. L. LIBRESCU, M. STEIN, *Postbuckling of shear deformable composite flat panels taking into account geometrical imperfections*, AIAA J., **30**, 1352–1360, 1992.
7. R. H. LIU, Z. Q. CHENG, *Nonlinear bending of simply supported rectangular sandwich pates*, Appl. Math. Mech., **14**, 217–234, 1993.
8. D. S. MITRINOVIC, P. M. VASIC, *Analytic inequalities*, Springer-Verlag, Berlin 1970.
9. G. N. PRAVEEN, J. N. REDDY, *Nonlinear transient thermoelastic analysis of functionally graded ceramic-metal plates*, Int. J. Solids Struct., **35**, 4457–4476, 1998.
10. J. N. REDDY, *A simple higher-order theory for laminated composite plates*, J. Appl. Mech., **51**, 745–752, 1984.
11. J. N. REDDY, *Mechanics of laminated composite plates: theory and analysis*, CRC Press, Boca Raton, Florida 1997.
12. J. N. REDDY, C. D. CHIN, *Thermomechanical analysis of functionally graded cylinders and plates*, J. Thermal Stresses, **21**, 593–626, 1998.
13. J. N. REDDY, C. M. WANG, *Deflection relationships between classical and third-order plate theories*, Acta Mechanica, **130**, 199–208, 1998.
14. C. M. WANG, *Deflection of sandwich plates in terms of corresponding Kirchhoff plate solutions*, Archives Appl. Mech., **65**, 408–414, 1995.
15. C. M. WANG, W. A. M. ALWIS, *Simply supported polygonal Mindlin plate deflections using Kirchhoff plates*, J. Engng. Mech., **121**, 1383–1385, 1995.

Received June 14, 1999; new version November 18, 1999.

Arch. Mech., **52**, pp. 159–178, Warszawa 2000

Nanomaterial clusters as macroscopically small size-effect bodies. Part I

A. TRZĘSOWSKI

Polish Academy of Sciences
Institute of Fundamental Technological Research
Świętokrzyska 21, 00-049 Warsawa, Poland

ONE OF UNUSUAL FEATURES of macroscopically small three-dimensional nanocrystalline clusters is the dependence of their properties on the grain size as well as on the cluster size. Consequently, such clusters are ensembles of atoms or particles where the size effect becomes apparent. A phenomenological model of the description of thermomechanical properties of macroscopically small nanomaterial clusters is proposed. The model is based on the concept of size-effect bodies, the thermomechanical properties, dynamics and thermodynamics of which are referred to one whole body, not an infinite system of subbodies. It is pointed out that the proposed model of the size effect leads to an analogy with the theory of capillarity. A class of size-effect bodies generalizing this analogy is introduced and discussed. Particularly, it is stated that the heat capacity reveals not only the size effect but, contrary to the elastic properties, should depend also on the topological invariant of the compact and connected cluster.

1. Introduction

THE MACROSCOPIC PROPERTIES and effects of usual materials (e.g. moduli of elasticity and their temperature-sensitivity) are essentially the same on the micrometer ($1\ \mu m = 10^4$ Å $= 10^{-3}$ mm) and on the millimeter observation level scale. So, from the macroscopic point of view, both observation level scales are physically equivalent [1]. It can be continued for various mesoscale observation levels, say down to the order 100 nm (1 nm $= 10$ Å $= 10^{-6}$ mm); the atomic-size observation level scale is taken equal to 1Å – diameter of the hydrogen atom in the ground state. Grains of usual polycrystalline materials have diameters of the order of 1 μm to 1 mm, and thus they reach the macroscopic observation level scale. It is known that in the case of usual well-annealed pure metals, the mean distance between dislocations is of the order of 1 μm [2]. Thus, the crystal with many dislocations can be considered, on a mesoscale observation level that lies in the range of $10 - 100$ nm, as a part of an ideal crystal [2]. If the macroscopic properties of a crystalline solid body with many dislocations are considered, then a continuous limit approximation can be defined by means of the condition that,

at each point of the body, a characteristic mesoscale length, say of the order of 10 nm, can be approximately replaced with the local infinitesimal length [3, 4]. Consequently, according to such phenomenological approximation, the crystal with many dislocations can be identified with a locally homogeneous crystalline solid body. Thereby, the macroscopic physical equivalence of various observation level scales enables to introduce the local approximation of macroscopic material properties of crystalline bodies (homogeneous as well as with defects) that is independent of the body shape and size. For example, in this approximation, rotational symmetries of a crystalline structure are preserved (at least locally) but its translational symmetries are lost [3].

However, there exist nanocrystalline solids, both metallic and ceramic, that are built up by the same atoms as their commonly occurring counterparts, but with the grain size of the order of $1 - 10$ nm [5, 6]. For example, usual pure metals are used to produce almost spherical clusters of nanostructured metals, and size of these clusters varies from 1 nm to 100 nm according to the production process and the initial metal that has been used [5]. It is observed that if the nanostructure size becomes smaller than the critical length associated with a certain physical property, then this property changes [5, 6]. For example, it is known that nanocrystalline grains as well as clusters do not contain dislocations or they are not numerous and unstable [5]. Consequently, nanocrystalline metals reveal higher strength than their usual counterparts, and the strength increases if the size of the nanocrystalline ensemble of atoms decreases [5, 6]. Most of the unique features of three-dimensional nanostructures arise, owing to their macroscopically small size, from the very high ratio of the number of surface atoms to the total number of atoms in the cluster [7]. The fullerene C_{60} particles with all carbon atoms located in vertices of a truncated icosahedron [8, 9] provides an extreme example of such atomic structures. These particles are approximately spherical with the diameter slightly greater than 1 nm [9]. C_{60} particles crystallize, at room temperature, in solid clusters with close-packed face-centered-cubic structure [8]. The molecular dynamics simulations indicate that for some particular sizes of small C_{60} clusters these would exhibit a coexistence of solid and liquid states within a finite range of temperature. It concerns also small clusters that consist of nanometer-sized small particles built up by some other chemical elements [8]. This makes small clusters different from the bulk systems whose solid and liquid phases coexist only at a single point of temperature, the melting point [8]. Note that generally, in the nanometer regime, we have to deal with chemical bonds and no longer with bulk properties. Forces are extremely small - down to 10^{-12} N, yet strains and pressures can be very high, e.g. pressures up to 10^{12} Pa [1]. For example, computations have shown that C_{60} crystals would reveal elasticity in compression, and compressed to 70 percent of the initial volume would be harder than diamond [9].

It is observed that the production process of nanocrystalline materials can lead to clusters of a fractal structure built up by particles of the diameter 35Å [10]. In this case, the total mass m of a three-dimensional cluster of the size L_0 depends on this size according to the following formula [10]:

$$m = m_p(L_0/l_p)^D, \tag{1.1}$$

where $D < 3$ is the mass fractal dimension, m_p is the mass of particles constituting the cluster, and l_p is the size of these particles. The mass density ρ_0 of the cluster depends also on L_0 according to a power law of the fractal type:

$$\rho_0 = \rho_p(L_0/l_p)^{D-3}, \tag{1.2}$$

where ρ_p is the mass density of particles constituting the cluster. In the case of close-packed particles $D = 3$. The fractal materials differ from the general case of nanomaterials because fractals are objects that exhibit similar structures over the range of length-scales for which one can define a noninteger dimension. Consequently, if l is the size of a part of the three-dimensional fractal cluster, then it follows from the self-similarity that the elastic modulus $E(l)$ of this part should reveal the following property [10]:

$$E(\lambda l) = \lambda^{-d}E(l), \tag{1.3}$$

if l and λl belong to the self-similarity interval. The exponent d depends on the fractal structure of the cluster as well as on the forces acting between elements of this structure.

If macroscopically small clusters are considered, then their deformation and temperature can be treated as these approximated to uniform state variables of the cluster. It means, from the microscopic point of view, that the collective modes are considered [11]. Thus, owing to this phenomenological approximation, we are in the framework of classical thermodynamics which refers to one whole system, not an infinite family of subsystems [12]. Consequently, the dynamics of a macroscopically small cluster should have also a global character referable to one whole body only. It suggests us to formulate a description of macroscopically small nanomaterial clusters in the framework of the phenomenological theory of size effect that has been originally formulated as a theory which is not associated with an observation level scale [13, 14, 15]. The paper extends the contents of this theory, especially from the point of view of nanostructures revealing the existence of relations between the shape and size of a cluster and the observed properties of the condensed material of this cluster.

2. Size-effect body

Continuum mechanics is a phenomenological theory dealing with the macroscopic properties of material deformable bodies and based on an assumption that

these properties have essentially a local character independent of the change of the observation level scale (see Sec. 1). It concerns the notion of material (formalized in the framework of the theory of simple materials [16]) as well as the dynamics (the reduction of dynamics to local balance laws [16]). The same approach is applied to the description of thermodynamic processes [16] and to the description of the material structure evolution (e.g. the plasticity theory [17]). Unfortunately, in the case of nanomaterials the concept of localization can not be applied to the description of thermomechanical properties of these materials because of their sensibility to the size of nanostructures (Sec. 1). Moreover, the concept of local equilibrium states (dynamical or thermodynamical) of a body neglects the size and shape effects occurring in the case of macroscopically small bodies (cf. Sec. 1). However, the macroscopically small size of nanostructures offers a possibility for treating nanomaterial clusters, in the sense of phenomenological approximation used here (Sec. 1), as macroscopically small "*affinely rigid bodies*" with dynamics being a generalization of the rigid body dynamics which is not associated with an observation level scale [11].

If the equations of dynamics of these homogeneously deformed bodies are considered as balance laws [11, 15], then they can be extended to the balance laws of *classical thermodynamics* [13] dealing with the so-called *homogeneous thermodynamic processes* [12, 16] considered as being dependent on the body size and shape [13].

Therefore, we will deal with a homogeneous nanomaterial body of immovable center of mass, homogeneously deformed and endowed with an uniform absolute temperature. Spatial configurations of such a body can be identified with the subsets $\mathcal{B}$ of the three-dimensional Euclidean vector space E^3 (the physical space in this case) that have the form $\mathcal{B} = l(\mathbf{F})(\mathcal{B}_0)$, where $\mathcal{B}_0 \subset E^3$ is a distinguished spatial configuration and $l(\mathbf{F})$ denotes the following linear mapping in E^3:

$$
\begin{aligned}
& l(\mathbf{F})(\mathbf{X}) = \mathbf{F}\mathbf{X}, \qquad \mathbf{F} \in GL^+(E^3), \quad \mathbf{X} \in E^3, \\
& GL^+(E^3) = \{\mathbf{F} \in L(E^3) : \det \mathbf{F} > 0\}, \qquad L(E^3) = E^3 \otimes E^3.
\end{aligned} \tag{2.1}
$$

This distinguished spatial configuration of the body is called its *reference configuration* and can be identified with the body itself. The spatial configurations $\mathcal{B}$ are called *deformed configurations* of $\mathcal{B}_0$. Further on, we will consider three-dimensional compact and connected bodies $\mathcal{B}_0$. The uniform state variables of the body $\mathcal{B}_0$ (Sec. 1) are defined by the finite number of parameters $\mu = (\mathbf{F}, \theta) \in GL^+(E^3) \times I$, where $I \subset R^+$ is a certain interval of absolute temperature, and constitute a *thermodynamic configuration* of the body. The mass m of the body $\mathcal{B}_0$ is the same for all its deformed spatial configurations $\mathcal{B}$, and the volumetric mass density ρ of these configurations is defined by:

$$
\begin{aligned}
m &= \rho_0 V(\mathcal{B}_0) = \rho V(\mathcal{B}), \\
V(\mathcal{B}) &= J(\mathbf{F}) V(\mathcal{B}_0), \qquad J(\mathbf{F}) = \det \mathbf{F},
\end{aligned}
\tag{2.2}
$$

where $V(\mathcal{B})$ denotes the volume of $\mathcal{B}$. Note that if the particles constituting a cluster $\mathcal{B}_0$ are close-packed, then the mass density ρ_0 of the body $\mathcal{B}_0$ is approximated by the mass density ρ_p of these particles. Further on, we restrict the considered cluster dynamics to the case of close-packed nanomaterial clusters the total mass of which admits the approximate representation of the size effect by Eq. (2.2). It can be e.g. the case of fullerene C_{60} clusters (Sec. 1) but, according to Eqs. (1.1) and (1.2), it is not the case of fractal clusters.

Let $\Psi = \Psi(\mathcal{B}_0; \mu)$, $E = E(\mathcal{B}_0; \mu)$, and $S = S(\mathcal{B}_0, \mu)$ denote the total Helmholtz free energy, the total internal energy, and the total entropy, respectively. The dependence of these functions on the figure $\mathcal{B}_0$ represents the shape and size effects that reveal macroscopically small nanomaterial clusters. This can be presented, for instance, by the dependence of these functions on such global geometrical characteristics as: the volume of $\mathcal{B}_0$, the surface field and (or) the total mean curvature of the boundary surface $\partial\mathcal{B}_0$, and also by the dependence on topological invariants of $\mathcal{B}_0$ as well as $\partial\mathcal{B}_0$ (e.g. the Euler characteristic). Consequently, the way in which these functions depend on homogeneous deformations can be dependent on the considered geometrical characteristics of $\mathcal{B}_0$ (see Sec. 4). To simplify latter statements, we will call a body $\mathcal{B}_0$ endowed with the above defined thermodynamic functions, the *size-effect body*.

The thermodynamic functions are related by the Legendre transformation:

$$
\Psi = E - \theta S \tag{2.3}
$$

and, as the functions describing physical properties of a nanomaterial body, would by the so-called *objective scalars*, that is functions $f = f(\mathcal{B}_0; \cdot)$ of class C^k, $k \geq 2$, such that for each $(\mathbf{F}, \theta) \in GL^+(E^3) \times I$, the following condition is fulfilled:

$$
\forall \mathbf{Q} \in SO(E^3), \qquad f(\mathcal{B}_0; \mathbf{QF}, \theta) = f(\mathcal{B}_0; \mathbf{F}, \theta), \tag{2.4}
$$

where $SO(E^3) \subset GL^+(E^3)$ denotes the proper orthogonal group on E^3.

Thermomechanical properties of the size-effect body $\mathcal{B}_0$ are represented, at each instant $\tau \in R^+$, by the net working $W = W(\mathcal{B}_0; \tau)$ such that for each curve $\tau \to \mu(\tau) = (\mathbf{F}(\tau), \theta(\tau))$ in the space $GL^+(E^3) \times I$ of thermodynamic configurations, the following relation holds:

$$
\forall \tau \in R^+ \; \exists \mathbf{N}(\mathcal{B}_0; \tau) \in L(E^3), \quad W(\mathcal{B}_0; \tau) = -\mathbf{N}(\mathcal{B}_0; \tau) \cdot \dot{\mathbf{F}}(\tau), \tag{2.5}
$$

where $\mathbf{A} \cdot \mathbf{B} = \mathrm{tr}(\mathbf{A}\mathbf{B}^T)$ for $\mathbf{AB} \in L(E^3)$, $\mathbf{B}^T$ denotes a transpose of $\mathbf{B}$, and $\dot{\mathbf{F}}(\tau) = d\mathbf{F}(\tau)/d\tau$. $\mathbf{N}(\mathcal{B}_0; \tau)$ is a *generalized force* representing a thermomechanical response of the size-effect body $\mathcal{B}_0$ at the instant $\tau \in R^+$. The balance

equation of the total internal energy is given by:

$$\forall \tau \in R^+, \quad \dot{E}(\mathcal{B}_0; \mu(\tau)) = W(\mathcal{B}_0; \tau) + Q(\mathcal{B}_0; \tau), \tag{2.6}$$

where $Q(\mathcal{B}_0; \tau)$ is the heat production at the instant $\tau \in R^+$, and $\dot{E}$ denotes the time-derivative of E taken along the curve $\tau \to \mu(\tau)$ of thermodynamic configurations. Moreover, the following Planck's dissipation inequality should be fulfilled [16]:

$$\forall \tau \in R^+, \quad \delta(\mathcal{B}_0; \tau) = \theta(\tau)\dot{S}(\mathcal{B}_0; \mu(\tau)) - Q(\mathcal{B}_0; \tau) \geq 0. \tag{2.7}$$

Let us assume that for each curve $\tau \to \mu(\tau)$ of thermodynamic configurations:

$$\mathbf{N}(\mathcal{B}_0; \tau) = \mathbf{N}(\mathcal{B}_0; \mu(\tau), \dot{\mu}(\tau)) \tag{2.8}$$

where $\dot{\mu}(\tau) = d\mu(\tau)/d\tau$, and let us denote:

$$\begin{aligned} \hat{\mathbf{T}} &= V(\mathcal{B}_0)^{-1}\partial_{\mathbf{F}}\Psi, \qquad \mathbf{T} = J(\mathbf{F})^{-1}\hat{\mathbf{T}}\mathbf{F}^T, \\ \mathbf{T}_D &= -V(\mathcal{B})^{-1}\mathbf{N}\mathbf{F}^T, \qquad J(\mathbf{F}) = \det\mathbf{F}, \end{aligned} \tag{2.9}$$

where Eq. (2.2) was taken into account. It can be shown [16] that *thermodynamically admissible* are e.g. such thermodynamic configurations $\mu \in GL^+(E^3) \times I$ for which

$$S = -\partial_\theta \Psi, \tag{2.10}$$

and the mapping $(\mu, \dot{\mu}) \to \mathbf{T}_D(\mathcal{B}_0; \mu, \dot{\mu})$, where $\dot{\mu} \in L(E^3) \times R$ is a tangent element to the space of thermodynamic configurations $GL^+(E^3) \times I$ at the point μ, is a symmetric and objective tensor field of the form:

$$\begin{aligned} &\mathbf{T}_D(\mathcal{B}_0; \mu, \dot{\mu}) = \mathbf{T}_D(\mathcal{B}_0; \mathbf{F}, \theta, \mathbf{L}), \quad \mathbf{L} = \dot{\mathbf{F}}\mathbf{F}^{-1} \in L(E^3), \\ &\mathbf{T}_D(\mathcal{B}_0; \mathbf{F}, \theta, \mathbf{L}) = \mathbf{T}(\mathcal{B}_0; \mathbf{F}, \theta) + \mathbf{h}_D(\mathcal{B}_0; \mathbf{F}, \theta, \mathbf{L}), \quad \mathbf{T}_D = \mathbf{T}_D^T, \\ &\forall \mathbf{Q} \in SO(E^3), \quad \mathbf{T}_D(\mathcal{B}_0; \mathbf{QF}, \theta, \mathbf{QLQ}^T) = \mathbf{Q}\mathbf{T}_D(\mathcal{B}_0; \mathbf{F}, \theta, \mathbf{L})\mathbf{Q}^T, \end{aligned} \tag{2.11}$$

and the Planck's dissipation inequality reduces to the following condition:

$$\mathrm{tr}(\mathbf{h}_D\mathbf{D}) \geq 0, \qquad h_D(\mathcal{B}_0; F, \theta, \mathbf{O}) = \mathbf{O}, \quad \mathbf{D} = \frac{1}{2}\left(\mathbf{L} + \mathbf{L}^T\right). \tag{2.12}$$

Moreover, it follows from the objectivity condition (2.4) and from the notations of Eq. (2.9) that the mapping $\mathbf{F} \to \mathbf{T}(\mathcal{B}_0; \mathbf{F}, \theta)$ should be, at each temperature

$\theta \in I$, a symmetric and objective tensor function that can be written in the following form:

$$\begin{aligned} \mathbf{T}(\mathcal{B}_0;\mathbf{F},\theta) &= \mathbf{R}\mathbf{h}(\mathcal{B}_0;\mathbf{U},\theta)\mathbf{R}^T, \\ \mathbf{h}(\mathcal{B}_0;\mathbf{U},\theta) &= V(\mathcal{B})^{-1}\partial_{\mathbf{U}}\Psi(\mathcal{B}_0;\mathbf{U},\theta)\mathbf{U}, \\ \mathbf{F} &= \mathbf{R}\mathbf{U}, \quad \mathbf{R}\in SO(E^3), \quad \mathbf{U}=\mathbf{U}^T, \quad V(\mathcal{B}) = V(\mathcal{B}_0)\det\mathbf{U}. \end{aligned} \tag{2.13}$$

The symmetric tensor fields $\mathbf{T}$ and $\mathbf{h}_D$ of Eq. (2.11) are isothermal counterparts, assigned to one whole body $\mathcal{B}_0$, of the Cauchy stress tensor for simple materials: thermoelastic and differential of complexity 1, respectively [16]. Note that, contrary to thermoelastic simple materials for which the dissipation coming from heat conduction appears, for a *thermoelastic size-effect body* the only thermodynamically admissible processes are the reversible ones ($\delta = 0$ in Eq.(2.7)). Therefore, thermoelastic size-effect bodies can be treated as these being *elastic within a certain range of temperature*. Let us introduce, imitating the theory of simple elastic materials, the *response insensibility group* $G_\theta(\mathcal{B}_0)$ at the temperature $\theta \in I$ of an (thermo)elastic size-effect body $\mathcal{B}_0$:

$$\begin{aligned} G_\theta(\mathcal{B}_0) = \{\mathbf{H}\in SL(E^3) : \forall \mathbf{F}\in GL^+(E^3),\ \mathbf{T}(\mathcal{B}_0;\mathbf{F}\mathbf{H},\theta), \\ = \mathbf{T}(\mathcal{B}_0;\mathbf{F},\theta)\} \end{aligned} \tag{2.14}$$

$$SL(E^3) = \{\mathbf{F}\in GL^+(E^3) : \det\mathbf{F} = 1\},$$

where $SL(E^3)$ is the so-called unimodular group defining, according to Eqs. (2.1) and (2.2), all deformed spatial configurations of $\mathcal{B}_0$ of the same volume equal to $V(\mathcal{B}_0)$. So, $G_\theta(\mathcal{B}_0)$ is the group of homogeneous deformations of $\mathcal{B}_0$ preserving, at the temperature $\theta \in I$, the volumetric mass density ρ_0 and the generalized Cauchy stress tensor $\mathbf{T}$ of the size-effect body $\mathcal{B}_0$. It follows from Eqs. (2.9) and (2.14) that $\mathbf{H}\in G_\theta(\mathcal{B}_0)$ iff [16]:

$$\begin{aligned} \forall \mathbf{F}\in GL^+(E^3), \quad \Psi(\mathcal{B}_0;\mathbf{F},\theta) = \Psi(\mathcal{B}_0;\mathbf{F}\mathbf{H},\theta) + \Psi(\mathcal{B}_0;\mathbf{I},\theta) \\ -\Psi(\mathcal{B}_0;\mathbf{H},\theta), \end{aligned} \tag{2.15}$$

where $\mathbf{I}\in GL^+(E^3)$ is the unit tensor. Let us consider the set $g_\theta(\mathcal{B}_0)\subset GL^+(E^3)$ of homogeneous deformations of $\mathcal{B}_0$ describing the *size-effect insensibility* of the free energy at the temperature $\theta \in I$:

$$\begin{aligned} g_\theta(\mathcal{B}_0) &= \{\mathbf{P}\in GL^+(E^3) : \forall \mathbf{F}\in GL^+(E^3), \\ \Psi(\mathcal{B}_\mathbf{P};\mathbf{F},\theta) &= \Psi(\mathcal{B}_0;\mathbf{F},\theta)\} \\ \mathcal{B}_\mathbf{P} &= l(\mathbf{P})(\mathcal{B}_0), \end{aligned} \tag{2.16}$$

where the linear mapping $l(\mathbf{P})$ is defined by Eq. (2.1). It easy to see that for each $\mathbf{P} \in g_\theta(\mathcal{B}_0)$:

$$\mathbf{T}(\mathcal{B}_\mathbf{P}; \mathbf{F}, \theta) = J(\mathbf{P})^{-1}\mathbf{T}(\mathcal{B}_0; \mathbf{F}, \theta) \tag{2.17}$$

and thus

$$\forall \mathbf{P} \in g_\theta(\mathcal{B}_0), \qquad G_\theta(\mathcal{B}_\mathbf{P}) = G_\theta(\mathcal{B}_0). \tag{2.18}$$

Moreover, it follows from Eq. (2.17) that for $\mathbf{P} \in g_\theta(\mathcal{B}_0) \cap SL(E^3)$ the elastic response of the size-effect body $\mathcal{B}_0$ (represented by the generalized Cauchy stress) is preserved. Therefore, let us consider the *size-effect insensibility group* $g_\theta(\mathcal{B}_0) \subset SL(E^3)$ at the temperature $\theta \in I$. If $g_\theta(\mathcal{B}_0) = SL(E^3)$ for each $\theta \in I$, then the size effect can be reduced to the dependence of elastic response and thermodynamic functions on the body volume $V(\mathcal{B}_0)$. If $g_\theta(\mathcal{B}_0) = SO(E^3)$ for each $\theta \in I$, then the size effect is independent of the body orientation.

Let us assume the existence of a homogeneous deformation $\mathbf{P} \in GL^+(E^3)$ such that the following formula, analogous to the local one appearing in the theory of simple materials, is valid (cf. [16]):

$$\forall \mathbf{F} \in GL^+(E^3), \quad \mathbf{T}(\mathcal{B}_\mathbf{P}; \mathbf{F}, \theta) = \mathbf{T}(\mathcal{B}_0; \mathbf{FP}, \theta). \tag{2.19}$$

Then [16]

$$G_\theta(\mathcal{B}_\mathbf{P}) = \mathbf{P}G_\theta(\mathcal{B}_0)\mathbf{P}^{-1}. \tag{2.20}$$

For example, if

$$\forall \theta \in I, \qquad g_\theta(\mathcal{B}_0) = G_\theta(\mathcal{B}_0), \tag{2.21}$$

then for each $\mathbf{P} \in g_\theta(\mathcal{B}_0)$ the conditions (2.19) and (2.20) become identities (see Eqs. (2.17) and (2.18)), and the elastic size-effect body will be called *quasi-simple* (within the range I of temperature).

In ordinary experience we commonly think of a body as being "solid" if, within a certain range of temperature, after changing its form (under a nonorthogonal transformation), we can observe a difference in the way it responds to further deformation [16]. If the elastic size-effect body $\mathcal{B}_0$ is quasi-simple, then the above observation can be expressed, according to Eq. (2.19), by the following counterpart of the definition of simple elastic solid materials (cf. [16]):

$$\forall \theta \in I, \qquad G_\theta(\mathcal{B}_0) \subset SO(E^3). \tag{2.22}$$

The quasi-simple elastic size-effect body will then be called *elastic quasi-solid*. If $\mathcal{B}_0$ is an elastic size-effect body fulfilling the condition (2.22), then we will say that this body reveals the *quasi-solid response* within the range I of temperature. The spatial configuration $\mathcal{B}_0$ will then be called *undistorted*. Since from the objectivity condition (2.4) it follows that for each $\theta \in I$:

$$\forall \mathbf{Q} \in SO(E^3), \qquad \Psi(\mathcal{B}_0; \mathbf{Q}, \theta) = \Psi(\mathcal{B}_0; \mathbf{I}, \theta), \tag{2.23}$$

we obtain from Eq. (2.15) that in the case (2.22) it should be:

$$G_\theta(\mathcal{B}_0) = \{\mathbf{Q} \in SO(E^3) : \forall \mathbf{F} \in GL^+(E^3), \quad \Psi(\mathcal{B}_0; [\mathbf{FQ}, \theta) = \Psi(\mathcal{B}_0; \mathbf{F}, \theta)\}. \tag{2.24}$$

If

$$\forall \theta \in I, \qquad G_\theta(\mathcal{B}_0) = SO(E^3), \tag{2.25}$$

then the quasi-solid response is called *isotropic*.

In practical applications concerning solid bodies, the existence of an unstressed spatial configuration of the body [16] is usually assumed. In our case such configurations should exist within the range I of temperature, that is it should be:

$$\begin{aligned} &\forall \theta \in I \quad \exists \mathbf{P}_\theta \in GL^+(E^3), \quad \mathbf{T}(\mathcal{B}_0(\theta); \mathbf{1}, \theta) = \mathbf{O}, \\ &\mathcal{B}_0(\theta) = l(\mathbf{P}_\theta)(\mathcal{B}_0), \end{aligned} \tag{2.26}$$

where $\mathcal{B}_0$ is an elastic size-effect body. Let us consider, in order to intrinsically relate the size-effect body $\mathcal{B}_0$ with its deformed unstressed spatial configurations $\mathcal{B}_0(\theta)$ of Eq. (2.26), the following condition (cf. Eq. (2.20) and (2.22)):

$$\forall \theta \in I, \quad G_\theta(\mathcal{B}_0(\theta)) = \mathbf{P}_\theta G_\theta(\mathcal{B}_0) \mathbf{P}_\theta^{-1} \subset SO(E^3). \tag{2.27}$$

The elastic size-effect body $\mathcal{B}_0$ fulfilling the conditions (2.26) and (2.27) will be called *solid within the range I of temperature*. Further on, we will restrict ourselves to the case of nanomaterial clusters being solid bodies in the above sense. The undistorted and unstressed spatial configurations $\mathcal{B}_0(\theta)$, $\theta \in I$, will be called then *natural* configurations of the elastic size-effect solid body $\mathcal{B}_0$. If, additionally, the spatial configuration $\mathcal{B}_0$ is undistorted, then it follows from Eqs. (2.22) and (2.27) that should be [16]:

$$\begin{aligned} &\forall \theta \in I, \quad G_\theta(\mathcal{B}_0(\theta)) = \mathbf{R}(\theta) G_\theta(\mathcal{B}_0) \mathbf{R}(\theta)^T, \\ &\mathbf{P}_\theta = \mathbf{R}(\theta)\mathbf{U}(\theta), \quad \mathbf{R}(\theta) \in SO(E^3), \quad \mathbf{U}(\theta) = \mathbf{U}(\theta)^T, \\ &\forall \mathbf{Q} \in G_\theta(\mathcal{B}_0), \quad \mathbf{Q}^T \mathbf{U}(\theta) \mathbf{Q} = \mathbf{U}(\theta). \end{aligned} \tag{2.28}$$

If the quasi-solid response is isotropic, then the size-effect solid body $\mathcal{B}_0$ will be called an *isotropic solid*.

The formulae of Eq. (2.28) reduce then to:

$$\begin{aligned} &\forall \theta \in I, \quad G_\theta(\mathcal{B}_0(\theta)) = G_\theta(\mathcal{B}_0) = SO(E^3), \\ &\mathbf{P}_\theta = \eta(\theta)\mathbf{R}(\theta), \quad \eta(\theta) > 0, \quad \mathbf{R}(\theta) \in SO(E^3). \end{aligned} \tag{2.29}$$

Thus, in this case, each natural configuration $\mathcal{B}_0(\theta)$ of $\mathcal{B}_0$ takes its shape.

If

$$\forall \theta \in I, \qquad G_\theta(\mathcal{B}_0) = SL(E^3), \tag{2.30}$$

then the generalized Cauchy stress tensor $\mathbf{T}$ reduces to [16]:

$$\begin{aligned} \mathbf{T}(\mathcal{B}_0; \mathbf{F}, \theta) &= -p(\mathcal{B}_0; J(\mathbf{F}), \theta)\mathbf{1}, \\ J(\mathbf{F}) &= \det\mathbf{F}. \end{aligned} \tag{2.31}$$

We will say then that the elastic size-effect body $\mathcal{B}_0$ reveals the *quasi-fluid response* within the range I of temperature. The quasi-fluid response has, for an elastic quasi-simple size-effect body $\mathcal{B}_0$, the following form:

$$p(\mathcal{B}_0; J(\mathbf{F}), \theta) = p(V(\mathcal{B}_0); J(\mathbf{F}), \theta). \tag{2.32}$$

Note that a fluid is commonly regarded as a material having "no preferred configuration" [16], what means that should be:

$$\begin{aligned} p(V(\mathcal{B}_0; J(\mathbf{F}), \theta) &= p(V(\mathcal{B}), \theta), \\ V(\mathcal{B}) &= J(\mathbf{F})V(\mathcal{B}_0). \end{aligned} \tag{2.33}$$

However, since the response function $p = p(V, \theta)$ can describe not only a fluid but also a solid or gas, in hydrodynamics it is customary to impose the condition $p = p(V, \theta) > 0$ for $V > 0, \theta \in I$, [16].

3. Dynamics of size-effect bodies

Let $\mathcal{B}_0 \subset E^3$ be the spatial configuration of a size-effect body identified with the body itself, and let $\mathbf{F} : R^+ \to GL^+(E^3)$ be a homogeneous deformation process. Let us assume that on the body act, at each instant $\tau \in R^+$, external force fields: the body force field $\mathbf{b}(\mathbf{X}, \tau)$, $\mathbf{X} \in \mathrm{Int}\mathcal{B}_0$, and the surface force field $\mathbf{s}(\mathbf{X}, \tau), \mathbf{X} \in \partial\mathcal{B}_0$, where $\mathrm{Int}\mathcal{B}_0$ and $\partial\mathcal{B}_0$ denote the body $\mathcal{B}_0$ interior and its boundary, respectively. The volumetric kinetic energy $K(\mathcal{B}_0; \tau)$ of the body (cf. the approximate representation of the mass size-effect by Eq. (2.2)) and the power $P(\mathcal{B}_0; \tau)$ of external forces acting on the body are given by

$$\begin{aligned} K(\mathcal{B}_0; \tau) &= \frac{1}{2}\int_{\mathcal{B}_0} |\mathbf{v}(\mathbf{X}, \tau)|^2 dm(\mathbf{X}), \\ P(\mathcal{B}_0; \tau) &= \int_{\mathcal{B}_0} \mathbf{b}(\mathbf{X}, \tau) \cdot \mathbf{v}(\mathbf{X}) dV(\mathbf{X}) + \int_{\partial\mathcal{B}_0} \mathbf{s}(\mathbf{X}, \tau) \cdot \mathbf{v}(\mathbf{X}, \tau) dF(\mathbf{X}), \end{aligned} \tag{3.1}$$

where we have denoted

$$\mathbf{v}(\mathbf{X},\tau) = \frac{d}{d\tau} l(\mathbf{F}(\tau)(\mathbf{X}) = \dot{\mathbf{F}}(\tau)\mathbf{X}, \quad |\mathbf{v}|^2 = \mathbf{v}\cdot\mathbf{v},$$

(3.2)

$$dm(\mathbf{X}) = \rho_0 dV(\mathbf{X}), \quad \rho_0 = m/V(\mathcal{B}_0).$$

The volumetric net working $W(\mathcal{B}_0;\tau)$ at the instant $\tau \in R^+$ has in an inertial frame of reference the following form [16]:

$$W(\mathcal{B}_0;\tau) = P(\mathcal{B}_0;\tau) - \dot{K}(\mathcal{B}_0;\tau). \tag{3.3}$$

It follows from Eqs. (3.1) – (3.3) that for the net working of Eq. (2.5) should be:

$$\left[\mathbf{M}_{\text{ext}}(\mathcal{B}_0;\tau)^T - \ddot{\mathbf{F}}(\tau)\mathbf{J}(\mathcal{B}_0) + \mathbf{N}(\mathcal{B}_0;\tau)\right]\cdot\dot{\mathbf{F}}(\tau) = 0, \tag{3.4}$$

where $\mathbf{M}_{\text{ext}}(\mathcal{B}_0;\tau)$ denotes the dipole moment of external forces:

$$\mathbf{M}_{\text{ext}}(\mathcal{B}_0;\tau) = \int_{\mathcal{B}_0} \mathbf{X}\otimes\mathbf{b}(\mathbf{X},\tau)dV(\mathbf{X}) + \int_{\partial\mathcal{B}_0} \mathbf{X}\otimes\mathbf{s}(\mathbf{X},\tau)dF(\mathbf{X}), \tag{3.5}$$

and $\mathbf{J}(\mathcal{B}_0)$ is the body inertia tensor determined with respect to its mass center $\mathbf{X} = \mathbf{O}$:

$$\mathbf{J}(\mathcal{B}_0) = \int_{\mathcal{B}_0} \mathbf{X}\otimes\mathbf{X}dm(\mathbf{X}). \tag{3.6}$$

The equation (3.4) will be fulfilled by a class of homogeneous thermodynamic processes such that

$$\mathbf{J}(\mathcal{B}_0)\ddot{\mathbf{F}}(\tau)^T = \mathbf{N}(\mathcal{B}_0;\tau)^T + \mathbf{M}_{\text{ext}}(\mathcal{B}_0;\tau). \tag{3.7}$$

The equation (3.7) generalizes the equation of dynamics of affinely rigid bodies. Particularly, for thermodynamically admissible processes defined by Eqs. (2.8) – (2.12), where $\mu = (\mathbf{F},\theta) \in GL^+(E^3)\times I$, we have:

$$\mathbf{N}(\mathcal{B}_0;\tau)^T = -V(\mathcal{B}_0)J(\mathbf{F})(\tau)\mathbf{F}(\tau)^{-1}\mathbf{T}_D(\mathcal{B}_0;\mathbf{F},\theta,\mathbf{L})(\tau),$$

(3.8)

$$\mathbf{L}(\tau) = \dot{\mathbf{F}}(\tau)\mathbf{F}(\tau)^{-1}.$$

Note that introducing the dipole moment $\mathbf{M}_{\text{int}}(\mathcal{B}_0;\tau)$ of internal surface forces acting on the body boundary $\partial\mathcal{B}_0$:

$$\mathbf{M}_{\text{int}}(\mathcal{B}_0;\tau) = \int_{\partial\mathcal{B}_0} \mathbf{X}\otimes\mathbf{t}_D(\mathcal{B}_0;\mathbf{X},\tau)dF(\mathbf{X})$$

$$\mathbf{t}_D(\mathcal{B}_0;\mathbf{X},\tau) = -\hat{\mathbf{T}}_D(\mathcal{B}_0;\tau)\mathbf{n}(\mathbf{X}) \tag{3.9}$$

$$\hat{\mathbf{T}}_D(\mathcal{B}_0;\tau) = J(\mathbf{F})(\tau)\mathbf{T}_D(\mathcal{B}_0;\mathbf{F},\theta,\mathbf{L})(\tau)\mathbf{F}^*(\tau), \quad \mathbf{F}^* = (\mathbf{F}^{-1})^T,$$

where $\hat{\mathbf{T}}_D(\mathcal{B}_0;\tau)$ is the counterpart of the Piola-Kirchhoff stress tensor (cf. [16]) and $\mathbf{n}$ is the outward normal versor, we obtain the following interpretation rule of the generalized force $\mathbf{N}(\mathcal{B}_0;\tau)$ [13]:

$$\mathbf{N}(\mathcal{B}_0;\tau)^T = \mathbf{M}_{\text{int}}(\mathcal{B}_0;\tau). \tag{3.10}$$

The condition of immobility of the mass center means that the total external force acting on the body $\mathcal{B}_0$ should vanish:

$$\forall \tau \in R^+, \quad \int_{\mathcal{B}_0} \mathbf{b}(\mathbf{X},\tau)dV(\mathbf{X}) + \int_{\partial\mathcal{B}_0} \mathbf{s}(\mathbf{X},\tau)dF(\mathbf{X}) = \mathbf{O}. \tag{3.11}$$

If the considered size-effect body is thermoelastic, then the generalized Cauchy stress tensor $\mathbf{T}_D$ of Eq. (2.11) reduces to its part $\mathbf{T}$ (represented in the form (2.13)), and the thermodynamic processes become reversible ($\delta = 0$ in Eq. (2.7)). In this case, Eq. (2.6) can be written in the form of the following temperature evolution equation [13]:

$$\begin{aligned} K_{\mathbf{F}}\dot{\theta} &= V(\mathcal{B}_0)\theta\partial_\theta\hat{\mathbf{T}}\cdot\dot{\mathbf{F}} + Q, \\ \hat{\mathbf{T}} &= V(\mathcal{B}_0)^{-1}\partial_{\mathbf{F}}\Psi, \quad \theta \in I, \end{aligned} \tag{3.12}$$

where $K_{\mathbf{F}} = K_{\mathbf{F}}(\mathcal{B}_0;\theta)$ is the heat capacity at a constant deformation $\mathbf{F}$ deined by:

$$K_{\mathbf{F}} = \partial_\theta E = \theta\partial_\theta S = -\theta(\partial^2\Psi/\partial\theta^2)_{\mathbf{F}}, \tag{3.13}$$

and the heating $Q = Q(\mathcal{B}_0;\theta)$ is given by:

$$\begin{aligned} Q(\mathcal{B}_0;\theta) &= \theta(\tau)\dot{S}(\mathcal{B}_0;\theta), \quad S = -\partial_\theta\Psi, \\ \dot{S}(\mathcal{B}_0;\theta) &= \frac{d}{d\tau}S(\mathcal{B}_0;\mathbf{F}(\tau),\theta(\tau)). \end{aligned} \tag{3.14}$$

Note that the following relation holds [13]:

$$V(\mathcal{B}_0)\partial_\theta\hat{\mathbf{T}}\cdot\dot{\mathbf{F}} = V(\mathcal{B})\partial_\theta\mathbf{T}\cdot\mathbf{D}, \quad V(\mathcal{B}) = J(\mathbf{F})V(\mathcal{B}_0), \tag{3.15}$$

$$\mathbf{D} = \frac{1}{2}\left(\mathbf{L} + \mathbf{L}^T\right), \quad \mathbf{L} = \dot{\mathbf{F}}\mathbf{F}^{-1}.$$

We see that the above formulated dynamics as well as the considered thermodynamics refer to only one whole body, not to an infinite system of subbodies as it occurs in a field theory (local or nonlocal) or in a thermodynamics oflocal (equilibrium or nonequilibrium) body states.

4. Liquid-like response

The notions discussed in Sec. 2 concerning materials of size-effect bodies are inspired by the continuum mechanics approach represented by the theory of simple materials [16]. Let us consider, in order to introduce a class of (homogeneous and elastic) size-effect bodies based on a different approach, the theory of capillarity. In this theory, a finite free energy density is attributed not only to the volume but also to the surface measure, and the body should be defined in such a way that in the limiting case of a thin film (infinitely thin in the sense of phenomenological approximation used in the theory of capillarity) should be also considered as a body [18]. Thus, in line with the classical capillarity theory, we can endow a body $\mathcal{B}_0$ with the total free energy of the form [18]:

$$\begin{aligned} &\Psi(\mathcal{B}_0; \mathbf{F}, \theta) = \varepsilon(\theta) V(\mathcal{B}) + \gamma(\theta) F(\mathcal{B}), \\ &\mathcal{B} = l(\mathbf{F})(\mathcal{B}_0), \quad \mathbf{F} \in GL^+(E^3), \quad \theta \in I, \end{aligned} \tag{4.1}$$

where θ is uniform temperature, $V(\mathcal{B})$ and $F(\mathcal{B})$ denote the volume of the deformed body and the surface field of its boundary, respectively. The constants (at the given temperature $\theta \in I$) $\varepsilon(\theta)$ and $\gamma(\theta)$ denote the free energy densities needed to change the body volume unit and the boundary surface field unit, respectively. The formula (4.1) means that the capillarity theory enables us to define a particular case of the size-effect body endowed with the such total free energy function that can be transformed into a form independent of the choice of a preferred spatial configuration of the body. Note that Eqs. (2.31) – (2.33) can be considered as these corresponding to a total free energy of the same property but represented in the form

$$\Psi(\mathcal{B}_0; \mathbf{F}, \theta) = \varphi(V(\mathcal{B}), \theta), \tag{4.2}$$

where $\mathcal{B}$ is defined by Eq. (4.1). We will say, generalizing the formulae (4.1) and (4.2) and taking into account the analogy with fluids regarded as materials having no preferred spatial configuration, that an elastic size-effect body $\mathcal{B}_0$ has the *liquid-like response* if its total free energy function Ψ fulfills the following condition:

$$\begin{aligned} &\Psi(\mathcal{B}_0; \mathbf{F}, \theta) = \Phi_\theta(l(\mathbf{F})(\mathcal{B}_0)), \quad \theta \in I, \\ &\forall \mathbf{Q} \in SO(E^3), \qquad \Phi_\theta(l(\mathbf{Q})(\mathcal{B})) = \Phi_\theta(\mathcal{B}), \end{aligned} \tag{4.3}$$

where the objectivity condition (2.4) was taken into account.

It can be shown (basing on the Hadwiger integral theorem – [14, 19]) that an additive (in the sense $\Phi(\mathcal{B}_1 \cup \mathcal{B}_2) = \Phi(\mathcal{B}_1) + \Phi(\mathcal{B}_2) - \Phi(\mathcal{B}_1 \cap \mathcal{B}_2)$), continuous

and invariant with respect to the action of isometry group in E^3, functional $\mathcal{B} \to \Phi_\theta(\mathcal{B})$ defined on the set of all compact and convex three-dimensional bodies in E^3 endowed with the Hausdorff metric for sets, can be represented in the following general form:

$$\Phi_\theta(\mathcal{B}) = a(\theta)V(\mathcal{B}) + b(\theta)F(\mathcal{B}) + c(\theta)M(\mathcal{B}) + d(\theta)\chi(\mathcal{B}), \tag{4.4}$$

where $a(\theta), b(\theta), c(\theta), d(\theta)$ are arbitrary constants assumed here to be functions of class C^2 of the temperature parameter $\theta \in I$. $V(\mathcal{B})$, $F(\mathcal{B})$, $M(\mathcal{B})$, and $\chi(\mathcal{B})$ denote the volume of the domain $\mathcal{B}$, the surface field of its boundary $\partial\mathcal{B}$, the total mean curvature of $\partial\mathcal{B}$, and the Euler characteristic of $\mathcal{B}$, respectively. The formula (4.4) admits the case of convex bodies with a piecewise smooth boundaries, i.e. containing some edges and cornes [19, 20]. Note that it can hardly be supposed that the free energy functional of Eq. (4.4) suffers drastic changes on the transition from convex bodies to other shapes. It enables us to generalize the formula (4.4) by the extension of functionals Φ_θ, $\theta \in I$, of this form to all compact and connected spatial sets $\mathcal{B} \subset E^3$ with oriented regular boundary surface of class C^2 [18]. For compact and connected bodies [21]:

$$\chi(\mathcal{B}) = 1 - n, \tag{4.5}$$

where n is the number of holes inside the body $\mathcal{B}$. Particularly, $\chi(\mathcal{B}) = 1$ for convex bodies. The geometric functionals of Eq. (4.4) have, for the assumed class of boundary surfaces, the following representations [20, 22]:

$$V(\mathcal{B}) = \int_{\mathcal{B}} dV, \qquad F(\mathcal{B}) = \int_{\partial\mathcal{B}} dF, \qquad M(\mathcal{B}) = \int_{\partial\mathcal{B}} H dF, \tag{4.6}$$

$$\chi(\mathcal{B}) = \frac{1}{4\pi}\int_{\partial\mathcal{B}} K dF,$$

where H and K denote the mean and Gaussian curvatures of $\partial\mathcal{B}$, respectively. If R_1 and R_2 are principal radii of curvature of $\partial\mathcal{B}$, then

$$H = \frac{1}{2}\left(\frac{1}{R_1} + \frac{1}{R_2}\right), \qquad K = \frac{1}{R_1 R_2}. \tag{4.7}$$

It follows from Eq. (4.5) that

$$\begin{aligned} &\forall \mathbf{P} \in GL^+(E^3), \qquad \chi(\mathcal{B}_\mathbf{P}) = \chi(\mathcal{B}_0), \\ &\mathcal{B}_\mathbf{P} = l(\mathbf{P})(\mathcal{B}_0). \end{aligned} \tag{4.8}$$

Thus, the last term of the total free energy function Ψ defined by Eqs. (4.3) – (4.6) is equal to $d(\theta)\chi(\mathcal{B}_0)$. Consequently, this term does not influence elastic properties of the size-effect body $\mathcal{B}_0$ but influences, according to Eq. (3.13), its heat capacity. Moreover, it follows from Eqs. (4.3), (4.4) and (4.8) that the change of topological connection of the size-effect body $\mathcal{B}_0$ needs a finite discontinuous jump of the total free energy term $d(\theta)\chi(\mathcal{B}_0)$. It means that this term is conditioned by the mathematical as well as the physical connectedness of the body. Therefore, we can recognize the coefficient $d(\theta)$ as the one conditioned by forces of connectedness of nanomaterial clusters.

Let us write Eqs. (4.4) and (4.6) in the form:

$$\Phi_\theta(\mathcal{B}) = a(\theta)V(\mathcal{B}) + \Phi_{s,\theta}(\mathcal{B}),$$

(4.9)

$$\Phi_{s,\theta}(\mathcal{B}) = \int_{\partial\mathcal{B}} w_\theta(H,K)dF,$$

where it has been denoted

$$w_\theta(H,K) = b(\theta) + c(\theta)H + (d(\theta)/4\pi)K. \tag{4.10}$$

The total surface free energy density $w_\theta(H,K)$ of Eq. (4.10) depends on the definition of the boundary surface $\partial\mathcal{B}$. In the case of solid bodies for which their size is much greater than the effective size of the boundary layer, the influence of both curvatures on the total surface free energy $\Phi_{s,\theta}(\mathcal{B})$ of Eq. (4.9) can be neglected [2] (that is $c(\theta) = 0$ and $d(\theta) = 0$ in Eq. (4.10)) and Eq. (4.9) reduces then to Eq. (4.1). Therefore, the constant $b(\theta)$ of Eq. (4.10) can be identified, up to its sign, with the so-called *surface tension* $\gamma(\theta)$ [2, 23] being the free energy density needed to change the boundary surface field unit. The density $\gamma(\theta)$ is conditioned by the interactions of atoms located on the boundary solid surface [2, 23] and it is a positive quantity at the considered temperature lower than the melting temperature [23]. However, we consider macroscopically small bodies and consequently, taking into account that the term $d(\theta)\chi(\theta)$ of Eq. (4.4) characterizes the physical connectedness of these bodies, we assume that the constant $d(\theta)$ of Eq. (4.10) is a nonvanishing quantity. Thus, we obtain

$$\varepsilon(\theta) = |a(\theta)| \geq 0, \quad \gamma(\theta) = |b(\theta)| > 0, \quad \omega(\theta) = |c(\theta)| \geq 0, \tag{4.11}$$

$$\delta(\theta) = |d(\theta)|/4\pi > 0.$$

The quantity $M(\mathcal{B})/2\pi$, known in rock analysis and in stereographic metallography, is interpreted as the mean grain width [18, 20]. Therefore, according to Eqs. (4.3), (4.4) and (4.11), $\omega(\theta)/2\pi$ can be interpreted as the free energy density

needed to change the body mean width $M(\mathcal{B})/2\pi$ unit. On the other hand, the mean curvature H of Eqs. (4.9) – (4.11) is a relative geometric quantity depending on the Euclidean geometry of the ambient physical space in which the boundary surface is embedded. Consequently, the quantity $\omega(\theta)$ should be considered as the one conditioned by interactions between the boundary surface atoms and the bulk atoms located in a boundary layer. For the sake of simplicity we will call $\gamma(\theta)$ as well as $\omega(\theta)$ the *surface free energy densities*.

The generalized Cauchy stress $\mathbf{T}$ defined by Eqs. (2.9), (2.13), (4.3) – (4.5), and (4.8) – (4.11) takes the following form:

$$
\begin{aligned}
\mathbf{T}(\mathcal{B}_0;\mathbf{F},\theta) &= a(\theta)\mathbf{1} + \mathbf{T}_s(\mathcal{B}_0;\mathbf{F},\theta),\\
\mathbf{T}_s(\mathcal{B}_0;\mathbf{F},\theta) &= \mathbf{R}\mathbf{T}_s(\mathcal{B}_0;\mathbf{U},\theta)\mathbf{R}^T,\\
\mathbf{T}_s(\mathcal{B}_0;\mathbf{U},\theta) &= V(\mathcal{B}_\mathbf{U})^{-1}\partial_\mathbf{U}\Phi_{s,\theta}(\mathcal{B}_\mathbf{U})\mathbf{U},\\
\mathbf{F} &= \mathbf{R}\mathbf{U},\ \mathbf{R}\in SO(E^3),\ \mathbf{U}=\mathbf{U}^T,\\
\Phi_{s,\theta}(\mathcal{B}_\mathbf{U}) &= b(\theta)F(\mathcal{B}_\mathbf{U}) + c(\theta)M(\mathcal{B}_\mathbf{U}) + d(\theta)\chi(\mathcal{B}_\mathbf{U}),\\
\mathcal{B}_\mathbf{U} &= l(\mathbf{U})(\mathcal{B}_0),\quad V(\mathcal{B}_\mathbf{U}) = V(\mathcal{B}_0)\det\mathbf{U}.
\end{aligned}
\tag{4.12}
$$

Further on we assume that, within the range I of temperature, the surface free energy density ω is either positive or vanishes identically. It follows from Eqs. (2.24), (4.3) – (4.5) and (4.8) that if the elastic generalized stress response of Eq. (4.12) is quasi-solid within the range I of temperature (Sec. 2), then its insensibility groups $G_\theta(\mathcal{B}_0)$, $\theta\in I$, are given by

$$
G_\theta(\mathcal{B}_0) = g_\theta(\mathcal{B}_0)\cap SO(E^3) \tag{4.13}
$$

where, in the considered case, the size-effect insensibility group $g_\theta(\mathcal{B}_0)$ (Sec. 2) has the following representation:

$$
g_\theta(\mathcal{B}_0) = \{\mathbf{P}\in SL(E^3) : \forall\mathbf{F}\in GL^+(E^3),\ \ \Phi_{s,\theta}(\mathcal{B}_{\mathbf{FP}}) = \Phi_{s,\theta}(\mathcal{B}_\mathbf{F})\}. \tag{4.14}
$$

It follows from Eqs. (4.12) – (4.14) that would be:

$$
\begin{aligned}
&\forall\theta\in I,\quad g_\theta(\mathcal{B}_0) = g(\mathcal{B}_0),\quad G_\theta(\mathcal{B}_0) = G(\mathcal{B}_0),\\
&G(\mathcal{B}_0) = g(\mathcal{B}_0)\cap SO(E^3) = h(\mathcal{B}_0),\\
&h(\mathcal{B}_0) = \{\mathbf{Q}\in SO(E^3) : l(\mathbf{Q})(\mathcal{B}_0) = \mathcal{B}_0\},
\end{aligned}
\tag{4.15}
$$

where $g(\mathcal{B}_0)$ is a subgroup of the unimodular group $SL(E^3)$, and $h(\mathcal{B}_0)$ denotes the group of rotational symmetries of $\mathcal{B}_0$; if the body $\mathcal{B}_0$ has no rotational symmetries, then $h(\mathcal{B}_0) = \{\mathbf{1}\}$. The condition (2.26) defining the unstressed spatial configurations $\mathcal{B}_0(\theta)$, $\theta \in I$, takes, according to Eq. (4.12), the following form:

$$
\begin{aligned}
&a(\theta)V_0(\theta)\mathbf{1} + \partial_{\mathbf{U}}\Phi_{s,\theta}(\mathcal{B}_{\mathbf{U}}(\theta))|_{\mathbf{U}=\mathbf{1}} = \mathbf{0},\\
&\mathcal{B}_{\mathbf{U}}(\theta) = l(\mathbf{U})(\mathcal{B}_0(\theta)), \quad \mathcal{B}_0(\theta) = l(\mathbf{P}_\theta)(\mathcal{B}_0), \quad V_0(\theta) = V(\mathcal{B}_0(\theta)).
\end{aligned}
\tag{4.16}
$$

The considered elastic size-effect body $\mathcal{B}_0$ with the quasi-solid liquid-like response is, within the range I of temperature, an elastic size-effect solid body (Sec. 2) if the conditions (2.28) and (4.16) are fulfilled. The condition (2.28) is, according to Eqs. (2.24) and (4.13) – (4.15), fulfilled and takes the form:

$$
\begin{aligned}
&\forall\theta \in I, \quad G_\theta(\mathcal{B}_0(\theta)) = G(\mathcal{B}_0(\theta)) = \mathbf{R}(\theta)G(\mathcal{B}_0)\mathbf{R}(\theta)^T,\\
&\mathbf{P}_\theta = \mathbf{R}(\theta)\mathbf{U}(\theta), \quad \mathbf{R}(\theta) \in SO(E^3), \quad \mathbf{U}(\theta) = \mathbf{U}(\theta)^T,\\
&\forall\mathbf{Q} \in G(\mathcal{B}_0), \quad \mathbf{Q}^T\mathbf{U}(\theta)\mathbf{Q} = \mathbf{U}(\theta).
\end{aligned}
\tag{4.17}
$$

It is an isotropic elastic size-effect solid body iff $G(\mathcal{B}_0) = SO(E^3)$. In this case $\mathbf{P} \in GL^+(E^3)$ has the form given by Eq. (2.29) and $\mathcal{B}_0$ is a *ball*. Conversely, if $\mathcal{B}_0$ is a ball then $h(\mathcal{B}_0) = SO(E^3)$ and, according to Eq. (4.15), the elastic spherical size-effect solid body with the liquid-like response should be *isotropic*. The spatial natural configurations $\mathcal{B}_0(\theta)$ of Eq. (4.16) are then spherical of the radius $R_0(\theta)$, $\theta \in I$ and (cf. Eq. (2.29)):

$$
R_0(\theta) = \eta(\theta)R_0, \quad V_0(\theta) = \eta(\theta)^3V(\mathcal{B}_0), \quad V(\mathcal{B}_0) = (4/3)\pi R_0^3.
\tag{4.18}
$$

Let us take as $\mathcal{B}_0$ an *oblong ellipsoid of revolution* with the axis of revolution parallel to a versor $\mathbf{n}$, and let R_0 and r_0, $R_0 > r_0$, denote the length of ellipsoid semiaxes in the $\mathbf{n}$-direction and in the directions perpendicular to this direction, respectively. The group $G(\mathbf{n})$ of all rotations about the axis of revolution describes rotational symmetries of the body $\mathcal{B}_0$ and

$$
h(\mathcal{B}_0) = G(\mathcal{B}_0) = G(\mathbf{n}).
\tag{4.19}
$$

Then, the condition (4.17) with

$$
\begin{aligned}
G(\mathcal{B}_0(\theta)) &= G(\mathbf{n}_\theta), \quad \mathbf{n}_\theta = \mathbf{R}(\theta)\mathbf{n},\\
\mathbf{U}(\theta) &= \eta(\theta)\mathbf{1} + \eta_n(\theta)\mathbf{n}\otimes\mathbf{n}, \quad \eta(\theta) > 0, \quad \eta_n(\theta) \geq 0,
\end{aligned}
\tag{4.20}
$$

is fulfilled. Thus, $\mathcal{B}_0(\theta)$, $\theta \in I$, is then the oblong ellipsoid of revolution with the axis of revolution parallel to the versor $\mathbf{n}_\theta$ of Eq. (4.20), and with the semiaxes

$R_0(\theta)$ and $r_0(\theta)$ in the $\mathbf{n}_\theta$-direction and in the directions perpendicular to $\mathbf{n}_\theta$, respectively, where:

$$\begin{aligned} R_0(\theta) &= \eta_1(\theta)R_0, \quad r_0(\theta) = \eta(\theta)r_0, \quad R_0(\theta) > r_0(\theta), \\ V_0(\theta) &= \eta_1(\theta)\eta(\theta)^2 V(\mathcal{B}_0), \quad \eta_1(\theta) = \eta(\theta) + \eta_n(\theta), \\ V(\mathcal{B}_0) &= (4/3)\pi R_0 r_0^2. \end{aligned} \tag{4.21}$$

So, we have defined, within the range I of temperature, the *transversally isotropic* elastic oblong size-effect solid body $\mathcal{B}_0$ with the liquid-like response.

We see that, for the considered size-effect solid body with the liquid-like response, rotational symmetries of an undistorted spatial configuration $\mathcal{B}_0$ of the size-effect body define its *material symmetries* described by the response insensibility group $G(\mathcal{B}_0)$. Particularly, the spherical shape means that the size-effect solid body with the liquid-like response should be isotropic, and the oblong spheroidal shape means that this size-effect body should reveal transverse isotropy (cf. Eq. (4.15)). It is consistent with the essential feature of macroscopically small nanomaterial clusters: properties of these clusters (particularly - their thermomechanical properties) can not be separated from their size as well as the shape. The sphericity and oblongness of the cage shape of fullerene particles C_{60} and C_{70}, respectively [8], provide, on the nanometer observation scale, significant examples of particles whose total mass as well as shape are their intrinsic and correlated properties. Therefore, let $\mathcal{B}_0$ be an undistorted spatial configuration, and $\mathbf{P} \in GL^+(E^3)$ such that (cf. Eqs. (4.15) and (4.17)):

$$\begin{aligned} G(\mathcal{B}_\mathbf{P}) &= \mathbf{P}G(\mathcal{B}_0)\mathbf{P}^{-1} \subset SO(E^3), \\ \mathcal{B}_\mathbf{P} &= l(\mathbf{P})(\mathcal{B}_0), \quad G(\mathcal{B}_0) \subset SO(E^3). \end{aligned} \tag{4.22}$$

Then [16]:

$$\begin{aligned} &\mathbf{P} = \mathbf{RU}, \quad \mathbf{R} \in SO(E^3), \quad \mathbf{U} = \mathbf{U}^T, \\ &\forall \mathbf{Q} \in G(\mathcal{B}_0), \quad \mathbf{Q}^T\mathbf{U}\mathbf{Q} = \mathbf{U}, \end{aligned} \tag{4.23}$$

and

$$G(\mathcal{B}_\mathbf{P}) = \mathbf{R}G(\mathcal{B}_0)\mathbf{R}^T. \tag{4.24}$$

It follows from Eqs. (4.15), (4.23), and (4.24) that

$$G(\mathcal{B}_\mathbf{U}) = G(\mathcal{B}_0) \tag{4.25}$$

and the right stretch tensors $\mathbf{U}$ of Eq. (4.23) constitute a subgroup $U(\mathcal{B}_0) \subset GL^+(E^3)$. Note that if $G(\mathcal{B}_0)$ is a Lie group, then $G(\mathcal{B}_0) = SO(E^3)$ or $G(\mathcal{B}_0) = G(\mathbf{n})$, and the property

$$h(\mathcal{B}_0) = G(\mathcal{B}_0) \tag{4.26}$$

means then that the body boundary $\partial\mathcal{B}_0$ should be a sphere or a surface of revolution with the axis of revolution parallel to the versor $\mathbf{n}$. If $\mathcal{B}_0$ is a compact convex body and $G(\mathcal{B}_0)$ is a finite group of rotations, then Eq. (4.26) means that $\partial\mathcal{B}_0$ should be a piecewise smooth surface (see remarks following Eq. (4.4)). Therefore, since the group $U(\mathcal{B}_0)$ of right stretches of $\mathcal{B}_0$ defines undistorted spatial configurations of the same shape and of the same response insensibility group, deformations $\mathbf{U} \in U(\mathcal{B}_0)$ enable us to separate the shape variation effect from the size effect, and thus to describe the latter effect in a more clear manner. Particularly, the homothetic deformation

$$\mathbf{U} = \lambda\mathbf{1}, \quad \lambda > 0 \tag{4.27}$$

appears as the universal homogeneous deformation preserving the body shape and the body material symmetries. In a second part of the paper, an isotropic elastic spherical size-effect solid body for which homothetic deformations are the general ones preserving its shape, will be considered. For these deformations:

$$\mathbf{T}_\infty(\theta) = \lim_{\lambda\to\infty} \mathbf{T}(\mathcal{B}_0; \lambda\mathbf{1}, \theta) = a(\theta)\mathbf{1} \tag{4.28}$$

and $\mathbf{T}_\infty(\theta)$ defines an asymptotic uniform tension if (cf. (4.11)):

$$\varepsilon(\theta) = a(\theta) \geq 0. \tag{4.29}$$

The constant $a(\theta)$, $\theta \in I$, can be interpreted then as a quantity depending on the bulk interatomic interactions.

References

1. H. ROHRER, *Limits and possibilities of miniaturization*, Jpn. J. Appl. Phys., **32**, 1335–1341, 1993.
2. J. CHRISTIAN, *Transformation in metals and alloys*, Part I, Pergamon Press, Oxford 1975.
3. A. TRZĘSOWSKI, *Geometrical and physical gauging in the theory of dislocations*, Rep. Math. Phys., **32**, 71–98, 1993.
4. A. TRZĘSOWSKI, *On the geometry of diffusion processes in continuized dislocated crystals*, Fortschr. Phys., **43**, 565-584, 1995.
5. R. W. SIEGEL, *Creating nanophase materials*, Sci. Am., **275**, 42–47, 1996.

6. L. I. TRUSOW and V. G. GRYANOW, *Highly dispersed systems and nanocrystals*, Nanostruct. Mat., **1**, 251–254, 1992.

7. J. M. MONTEJANO-CARRIZALIVES and J. L. MORÁN-LOPEZ, *Geometrical characteristcs of compact nanoclusters*, Nanostruct. Mat., **1**, 397–409, 1992.

8. K. SATTLER, C_{60} *and beyond: from magic numbers to new materials*, Jpn. J. Appl. Phys., **32**, 1428–1432, 1993.

9. R. F. CURL and R. E. SMALLEY, *Fullerens*, Sci. Am., **265**, 54–64, 1991.

10. V. V. ZASIMOV and L. M. LJAMŠEV, *Fractals in wave processes* [in Russian], Usp Fiz. Nauk, **165**, 361–402, 1995.

11. J. SŁAWIANOWSKI, *Analytical mechanics* [in Polish], PWN, Warsaw 1982.

12. C. TRUESDELL, *Rational thermodynamics*, McGraw-Hill, New York 1969.

13. A. TRZĘSOWSKI, *The size effect*, Bull. Acad. Polon. Sci., Serie Sci. Techn., **XXVII**, 255-267, 1979.

14. A. TRZĘSOWSKI, *On the liquid-like response of the size-effect body*, Bull. Acad. Polon. Sci., Serie Sci. Techn., **XXVII**, 127–133, 1980.

15. A. TRZĘSOWSKI, *On constrained size-effect bodies*, Arch. Mech., **36**, 185–193, 1984.

16. C. TRUESDELL, *A first course in rational continuum mechanics*, John Hopkins University Press, Baltimore 1972.

17. P. PERZYNA, *Thermodynamics of inelastic materials* [in Polish], PWN, Warsaw 1972

18. A. BLINOWSKI and A. TRZĘSOWSKI, *Surface energy in liquids and the Hadwiger integral theorem*, Arch. Mech., **33**, 133–146, 1981.

19. H. HADWIGER, *Altes und neues über konvexe Körper*, Birkhaser, Basel 1955.

20. J. BODZIONY, *A characteristic of spatial structure of crystalline materials* [in Polish] [in:] Geometrical methods in physics and technology, P. Kucharczyk [Ed.], WNT, Warsaw 1968.

21. A. H. WALLACE, *Differential topology*, W. A. Benjamin, New York 1968.

22. N. J. HICKS, *Notes on differential geometry*, D. Van Nostrand Company, Princeton 965.

23. A. COTTREL, *The mechanical properties of matter*, John Willey and Sons, New York 1964.

Received June 18, 1999; revised version November 19, 1999.

Arch. Mech., **52**, pp. 179–197, Warszawa 2000

Nanomaterial clusters as macroscopically small size-effect bodies. Part II

A. TRZĘSOWSKI

Polish Academy of Sciences
Institute of fundamental Technological Research
Świętokrzyska 21, 00–049 Warszawa, Poland

AN ISOTROPIC ELASTIC SPHERICAL size-effect solid body is proposed as a phenomenological model for the description of thermomechanical properties of macroscopically small nanomaterial spherical clusters subjected to a uniform pressure. Nanomaterial clusters being mechanically stable as well as those being mechanically stable of lower order are investigated. It is shown, among others, that the isothermal bulk modulus reveals the size effect due to the influence of surface tension of the cluster boundary solid surface.

1. Introduction

INVESTIGATION OF COMPRESSIBILITY of crystalline solid bodies subjected to a uniform pressure is, independently of the grain size, of considerable importance for determining their elastic properties. This is connected with the fact that under conditions of uniform pressure, it is possible to determine experimentally the elastic response of the body to the homothetic deformation

$$\mathbf{F} = \lambda \mathbf{1}, \quad \lambda > 0, \tag{1.1}$$

without producing any plastic deformations due to the lattice defects [1]. As a result, the body elastic response to the homothetic deformation, determined by measuring the volume variation due to pressure changes, is more closely connected with the elastic character of interatomic interactions in ideal crystals than the elastic response to the other types of deformations. This statement is confirmed, for example, by fairly good experimental verification of a formula for the macroscopic bulk modulus K of usual metals determined within the framework of free-electron approximation [2]. This approximation of bulk modulus is formulated for a macroscopic metal sample such that surface atoms have a negligible contribution to bulk properties of the crystal, and as a result we obtain [2]:

$$K = \left(\frac{61.2}{r_e/a_0} \right)^5 \text{N/cm}^2, \tag{1.2}$$

where r_e is the effective radius of an electron gas and a_0 – Bohr's radius of a hydrogen atom.

We see that the macroscopic observation level scale of the free electron approximation enables a description of the macroscopic bulk modulus in terms of atomic-sized quantities (cf. [3], Sec. 1). However, for a macroscopically small sample, the influence of surface atoms makes impossible an approximation of bulk properties of a condensed material based on atomic-sized quantities only. It is observed e.g. as the dependence of elastic properties of nanostructures on the observation level scale. It suggests to consider the nanostructures as macroscopically small size-effect bodies [3]. A more detailed introduction to the topic is provided in [3], where also the general homogeneous deformations are considered. This part of the paper is a modification and extension, stimulated by properties of nanocrystalline clusters, of the paper [4] (Secs. 2 and 3). The phenomenological models introduced in Secs. 4, 5, idealizing the properties of metallic and fullerene C_{60} crystalline nanomaterials (see [3], Sec. 1), are discussed in Sec. 6.

2. Elastic compressibility of a spherical size-effect solid body

Let us consider a homogeneous and isotropic elastic size-effect spherical body $\mathcal{B}_0$ subjected to a uniform pressure ([3], Sec. 2). The body deformation has then the form (1.1). Since this deformation preserves the spherical shape of the spatial configuration $\mathcal{B}_0$, we will refer to a *spherical size-effect body* identified with its reference spatial configuration $\mathcal{B}_0$ (cf. remarks at the very end of [3], Sec. 4). The spherical body $\mathcal{B}_0$ can be treated, under these conditions, as a thermodynamic system described by thermodynamic configurations of the form $(\lambda, \theta) \in R^+ \times I$, thermodynamic functions Ψ (total free energy), E (total internal energy), S (total entropy), and the generalized force $\mathbf{N}$ depending on the radius R_0 of $\mathcal{B}_0$ as a parameter. The thermodynamic functions are related by formulae (2.3) and (2.10) of [3], and the generalized force has the form:

$$\begin{aligned} \mathbf{N}(\mathcal{B}_0; \mathbf{F}, \theta) &= N(R_0; \lambda, \theta)\mathbf{1}, \\ N(R_0; \lambda, \theta) &= -\partial_\lambda \Psi(R_0; \lambda, \theta). \end{aligned} \tag{2.1}$$

The corresponding generalized Cauchy stress tensor is given by:

$$\begin{aligned} \mathbf{T}(\mathcal{B}_0; \mathbf{F}, \theta) &= -V(\mathcal{B})^{-1}\mathbf{N}(\mathcal{B}_0; \mathbf{F}, \theta)\mathbf{F}^T = t(R_0; \lambda, \theta)\mathbf{1}, \\ t(R_0; \lambda, \theta) &= V(R_0)^{-1}\lambda^{-2}\partial_\lambda \Psi(R_0; \lambda, \theta), \\ V(\mathcal{B}) &= V(R) = (4/3)\pi R^3 = \lambda^3 V(R_0), \quad R = \lambda R_0, \end{aligned} \tag{2.2}$$

where R denotes the radius of a deformed spatial configuration $\mathcal{B}$ of $\mathcal{B}_0$. Since the natural spatial configurations $\mathcal{B}_0(\theta)$, $\theta \in I$, are here spherical of the radius $R_0(\theta)$, the condition (2.26) of [3] takes, according to Eq. (2.2), the following form:

$$\forall \theta \in I \ \exists R_0(\theta) > 0, \quad t(R_0(\theta); 1, \theta) = 0, \tag{2.3}$$

defining the considered isotropic elastic spherical size-effect body as a solid body ([3], Sec. 2). Let us denote by $t_\theta(\lambda)$ the isothermal generalized stress due to the deformation λ of a natural spatial configuration $\mathcal{B}_0(\theta)$:

$$t_\theta(\lambda) = t(R_0(\theta); \lambda, \theta), \quad t_\theta(1) = 0. \tag{2.4}$$

The behaviour of real solid bodies implies the following *postulate of compressibility* (cf. [5]): in the deformation process of Eq. (1.1) of a natural spatial configuration $\mathcal{B}_0(\theta)$, increasing of its volume $V_0(\theta)$ requires uniform tensile stresses, and decreasing of this volume - uniform compressive stresses. This postulate means that should be:

$$\forall \theta \in I, \quad \forall 0 < \lambda \neq 1, \quad t_\theta(\lambda)(\lambda - 1) > 0. \tag{2.5}$$

Let $R = \lambda R_0$ be the radius of a deformed spatial configuration $\mathcal{B}$ of the body $\mathcal{B}_0$ of the radius R_0, and let $V = V(\lambda)$ and $V = V_0$ denote the volume of the deformed and undeformed configurations, respectively. Let us denote

$$d\kappa = \frac{dV}{V}, \quad V(1) = V_0 \tag{2.6}$$

or, equivalently

$$\kappa = \ln(V/V_0) = 3\varepsilon, \quad \varepsilon = \ln \lambda. \tag{2.7}$$

Denoting

$$\begin{aligned} &\sigma(R_0; \kappa, \theta) = t(R_0; e^{\kappa/3}, \theta), \\ &K_\theta(R_0; \lambda) = \frac{\partial \sigma}{\partial \kappa}(R_0; \kappa, \theta)\,|_{\kappa = 3 \ln \lambda}, \end{aligned} \tag{2.8}$$

we obtain:

$$K_\theta(R_0; \lambda) = \frac{\lambda}{3} \partial_\lambda t(R_0; \lambda, \theta). \tag{2.9}$$

The function $\lambda \in R^+ \to K_\theta(R_0; \lambda)$ defines the *isothermal compressibility* at a constant temperature θ of the spatial configuration $\mathcal{B}_0$ of the isotropic elastic spherical size-effect solid body. If $\mathcal{B}_0 = \mathcal{B}_0(\theta)$ is a natural spatial configuration of

the body, $R_0 = R_0(\theta)$ – its radius, Δ is a small relative variation of the volume $V_0 = V_0(\theta)$ of this configuration:

$$\Delta = \frac{V(R) - V_0(\theta)}{V_0(\theta)}, \quad |\Delta| \ll 1,$$

$$R = \lambda R_0(\theta), \quad V_0(\theta) = V(R_0(\theta)), \tag{2.10}$$

and

$$\sigma_\theta(\kappa) = t_\theta(e^{\kappa/3}), \tag{2.11}$$

then we obtain, taking into account the postulate of compressibility (Eq. (25)), that

$$\sigma_\theta(\kappa) = K(\theta)\kappa + o(\kappa),$$

$$\kappa = \Delta + o(\Delta), \tag{2.12}$$

where $o(x)/x \to 0$ for $x \to 0$, and it was denoted:

$$K(\theta) = \partial_\kappa \sigma_\theta(\kappa)|_{\kappa=0} = K_\theta(R_0(\theta), 1) > 0. \tag{2.13}$$

Thus, the scalar $K(\theta)$, $\theta \in I$, can be identified with the isothermal bulk modulus of the natural spatial configuration $\mathcal{B}_0(\theta)$. If the natural configuration is uniquely defined at each temperature $\theta \in I$, then $K(\theta)$ is a well-defined physical quantity and can be considered as the *isothermal bulk modulus* of the spherical size-effect solid body. Thereby, the existence of such isothermal bulk modulus imposes a condition on the total free energy function (see e.g. Sec. 3).

Let $\mathcal{B}_0$ be an arbitrary reference configuration of the spherical size-effect solid body. The *heat capacity* function $\theta \in I \to K_\lambda(R_0; \theta)$ at the constant deformation λ is defined by

$$K_\lambda = \partial_\theta E = \theta \partial_\theta S = -\theta(\partial^2 \Psi / \partial \theta^2)_\lambda. \tag{2.14}$$

The condition of *thermal stability* at the constant deformation λ:

$$\forall \theta \in I, \qquad K_\lambda(R_0; \theta) > 0 \tag{2.15}$$

and the condition of *mechanical stability* at the constant temperature θ:

$$\forall \lambda > 0, \qquad K_\theta(R_0; \lambda) > 0, \tag{2.16}$$

define the *thermodynamical stability* of an undeformed spatial configuration $\mathcal{B}_0$ of the radius R_0 of the spherical size-effect solid body. The state of matter is stable (in the spatial configuration $\mathcal{B}_0$) iff both the stability conditions are fulfilled [6, 7]. Otherwise, the mater becomes unstable and shows a tendency to break up

into separate phases [6]. Let us assume the existence of a curve $(\theta, \lambda_{\rm cr}(\theta))$, $\theta \in I$, in R^2 along which the so-called *mechanical stability of lower order* [8] occurs, that is:

$$\forall \theta \in I, \qquad K_\theta(R_0; \lambda_{\rm cr}(\theta)) = 0. \tag{2.17}$$

According to this definition, the *critical thermodynamic configurations* separate the stable and unstable isothermal states of matter [6]. The critical deformations $\lambda_{\rm cr}(\theta)$, $\theta \in I$, can be equivalently defined as stationary points of the isothermal generalized Cauchy stress function (see Eq. (2.9)):

$$(\partial t/\partial \lambda)_\theta = 0 \quad \text{for} \quad \lambda = \lambda_{\rm cr}(\theta). \tag{2.18}$$

If $t \in C^2$ and there exists a temperature $\theta_p \in I$ such that (see Eqs. (2.7) – (2.9) and (2.18)):

$$(\partial^2 t/\partial \lambda^2)_\theta = 0 \quad \text{for} \quad \lambda = \lambda_{\rm cr}(\theta_p), \tag{2.19}$$

then the conditions (2.18) (with $\theta = \theta_p$) and (2.19) define the so-called *critical point* $(\theta_p, t_p(R_0)$ of a phase transition, where

$$t_p(R_0) = t\left(R_0; \lambda_{\rm cr}(\theta_p), \theta_p\right). \tag{2.20}$$

The existence of critical points has been experimentally confirmed [8]. Further on (Secs. 3 and 5), we consider critical thermodynamic configurations within the range I of temperature, but such that the condition (2.19) of existence of a critical point is not fulfilled.

Let us consider the generalized force $\mathbf{N}$ of Eq. (2.1) defining an elastic response of the spherical size-effect solid body to homogeneous deformations of the form (1.1) of a distinguished spatial configuration $\mathcal{B}_0$ (identified with the body itself). Assuming that

$$\begin{aligned} &\mathbf{s}(\mathbf{X}, \tau) = p_s(\tau)\mathbf{n}(\mathbf{X}), \quad \mathbf{n}(\mathbf{X}) \cdot \mathbf{n}(\mathbf{X}) = 1 \quad \text{for } \mathbf{X} \in \partial\mathcal{B}_0, \\ &\mathbf{b}(\mathbf{X}, \tau) = 0 \quad \text{for } \mathbf{X} \in \mathrm{Int}\mathcal{B}_0; \quad \mathbf{X} = R_0\mathbf{n}(\mathbf{X}) \quad \text{for } \mathbf{X} \in \partial\mathcal{B}_0, \end{aligned} \tag{2.21}$$

where $\mathbf{n}$ is the unit outward normal to the sphere $\partial\mathcal{B}_0$ of the radius R_0, and taking into account Eqs. (2.5) and (3.1) – (3.3) of [3], we obtain the following equation of the spherical size-effect body dynamics [4]:

$$\begin{aligned} J_0\ddot{\lambda} &= N(R_0; \lambda, \theta) + 3V_0 p_s, \\ N(R_0; \lambda, \theta) &= -\partial_\lambda \Psi(R_0; \lambda, \theta), \quad \lambda(0) = 1, \\ J_0 &= (3/5)mR_0^2, \quad V_0 = V(R_0) = (4/3)\pi R_0^3, \end{aligned} \tag{2.22}$$

where $\ddot{\lambda} = d^2\lambda/d\tau^2$, $J_0\mathbf{1}$ is the body $\mathcal{B}_0$ inertia tensor, and $p_s = p_s(\tau)$ is a uniform external pressure (tension or compression) acting on the body boundary at the instant $\tau \geq o$. If the radius R_0 is not dependent on the temperature (i.e. we exclude natural spatial configurations $\mathcal{B}_0(\theta)$), then nonisothermal reversible processes of time-dependent thermodynamic configurations of the body are described by the Eq. (2.22) and by the following temperature evolution equation [4] (cf. Eq. (3.12) of [3]):

$$K_\lambda(R_0;\theta)\dot{\theta} = -\theta\partial_\theta N(R_0;\lambda,\theta)\dot{\lambda} + Q(R_0;\tau),$$
$$Q(R_0;\tau) = \theta(\tau)\dot{S}(R_0;\lambda(\tau),\theta(\tau)), \quad S = -\partial_\theta\Psi, \tag{2.23}$$

where Q is the heat production, and $\dot{S}$ denotes the time derivative of the total entropy S along a curve of thermodynamic configurations.

If we deal with irreversible processes, then the generalized force $N(R_0;\lambda,\theta)$ of Eq. (2.22) should be replaced e.g. by (cf. Eqs. (2.9) – (2.12) of [3], and (2.1) – (2.3)):

$$N_D(R_0;\lambda,\dot{\lambda},\theta) = -V_0\lambda^2 t_D(R_0;\lambda,\dot{\lambda},\theta) = N(R_0;\lambda,\theta) + H_D(R_0;\lambda,\dot{\lambda},\theta)$$
$$H_D(R_0;\lambda,\dot{\lambda},\theta) = -V_0\lambda^2 h_D(R_0;\lambda,\dot{\lambda},\theta), \tag{2.24}$$

where

$$\mathbf{T}_D(\mathcal{B}_0;\mathbf{F},\theta,\mathbf{L}) = t_D(R_0;\lambda,\dot{\lambda},\theta)\mathbf{1}, \quad \mathbf{L} = (\dot{\lambda}/\lambda)\mathbf{1},$$
$$t_D(R_0;\lambda,\dot{\lambda},\theta) = t(R_0;\lambda,\theta) + h_D(R_0;\lambda,\dot{\lambda},\theta), \tag{2.25}$$

is the generalized Cauchy stress tensor, and

$$\forall\theta \in I, \qquad h_D(R_0;\lambda,0,\theta) = 0, \qquad h_D(R_0;\lambda,\dot{\lambda},\theta)\dot{\lambda} \geq 0. \tag{2.26}$$

It should be stressed that the description of a spherical size-effect body introduced in this section is not a particular case of the model introduced in [3]. It is because we consider here a different thermodynamic system: this one for which the only admissible thermodynamic configurations are these corresponding to homothetic deformations, while in [3] the admissible thermodynamic configurations correspond to general homogeneous deformations. Nevertheless, the notions and the approach presented in [3] are applicable to this simpler case.

3. Liquid-like response of a spherical size-effect solid body

The definition of liquid-like response introduced in [3], Sec. 4 (Eqs. (4.3) and (4.4)) takes, in the case of a spherical size-effect body $\mathcal{B}_0$ of the radius R_0

considered in Sec. 2, the following form:

$$\Psi(R_0;\lambda,\theta)=\Phi_\theta(R_0\lambda),\qquad \lambda>0,\qquad \theta\in I \tag{3.1}$$

where

$$\begin{aligned}\Phi_\theta(R) &= a(\theta)V(R)+b(\theta)F(R)+c(\theta)M(R)+d(\theta),\\ V(R) &= (4/3)\pi R^3,\qquad F(R)=4\pi R^2,\quad M(R)=4\pi R.\end{aligned} \tag{3.2}$$

The generalized Cauchy stress function $t(R_0;\lambda,\theta)$ of Eq. (2.2) takes then the form:

$$t(R_0;\lambda,\theta)=T_\theta(R_0\lambda), \tag{3.3}$$

where

$$T_\theta(R)=3\left[a(\theta)+2b(\theta)R^{-1}+c(\theta)R^{-2}\right]. \tag{3.4}$$

The isothermal compressibility $K_\theta(R_0;\lambda)$ defined by Eq. (2.8) can be written, according to Eqs. (2.9), (3.3), and (3.4), in the form:

$$K_\theta(R_0;\lambda)=K_\theta(R_0\lambda), \tag{3.5}$$

where

$$K_\theta(R)=\frac{R}{3}\frac{dT_\theta(R)}{dR}=-2\left[b(\theta)R^{-1}+c(\theta)R^{-2}\right]. \tag{3.6}$$

The heat capacity $K_\lambda(R_0;\theta)$ (Eq. (2.14)) takes the form:

$$\begin{aligned}K_\lambda(R_0;\theta) &= -\theta\frac{d^2}{d\theta^2}C_{R_0\lambda}(\theta),\\ C_R(\theta) &= \Phi_\theta(R).\end{aligned} \tag{3.7}$$

It follows from Eqs. (2.3), (3.3), and (3.4) that the radius $R_0(\theta)$ of a natural spatial configuration $\mathcal{B}_0(\theta)$ of the spherical size-effect body is defined by the following equation:

$$a(\theta)R^2+2b(\theta)R+c(\theta)=0,\quad R>0 \tag{3.8}$$

that has a solution $R=R_0(\theta)$ iff

$$\forall\theta\in I,\qquad B(\theta)=b(\theta)^2-a(\theta)c(\theta)\geq 0. \tag{3.9}$$

If the condition (3.9) is fulfilled, then the generalized Cauchy stress function $t_\theta(\lambda)$ of Eq. (2.4) exists and, according to Eqs. (3.3) and (3.4), takes the form:

$$t_\theta(\lambda)=T(R_0(\theta)\lambda)=3\left[a(\theta)+2b(\theta)h_0(\theta)\lambda^{-1}+c(\theta)k_0(\theta)\lambda^{-2}\right] \tag{3.10}$$

where $h_0(\theta)$ and $k_0(\theta)$ denote the mean and Gaussian curvatures of the boundary surface $\partial\mathcal{B}_0(\theta)$ of the natural spatial configuration $\mathcal{B}_0(\theta)$:

$$h_0(\theta) = R_0(\theta)^{-1}, \quad k_0(\theta) = R_0(\theta)^{-2}. \tag{3.11}$$

The postulate of compressibility (2.5), applied to the generalized Cauchy stress function $t_\theta(\lambda)$ defined by Eqs. (3.9) – (3.11), leads to the following condition (cf. [3], Eq. (4.29)):

$$\forall\theta \in I, \qquad a(\theta) \geq 0, \qquad c(\theta) \leq 0. \tag{3.12}$$

Consequently, the radius $R_0(\theta)$ is uniquely defined at each temperature $\theta \in I$ and given by

$$\begin{aligned} R_0(\theta) &= \frac{1}{a(\theta)}\left[-b(\theta) + B(\theta)^{1/2}\right] \quad \text{if} \quad a(\theta) > 0,\ b(\theta) \leq 0, \\ &\qquad\qquad\qquad\qquad\qquad\qquad\qquad\qquad\qquad\qquad c(\theta) < 0, \\ R_0(\theta) &= -\frac{2b(\theta)}{a(\theta)} \quad \text{if} \quad a(\theta) > 0,\ b(\theta) < 0,\ c(\theta) = 0, \end{aligned} \tag{3.13}$$

or

$$\begin{aligned} R_0(\theta) &= \frac{1}{a(\theta)}\left[-b(\theta) + B(\theta)^{1/2}\right] \quad \text{if} \quad a(\theta) > 0,\ b(\theta) > 0, \\ &\qquad\qquad\qquad\qquad\qquad\qquad\qquad\qquad\qquad\qquad c(\theta) < 0, \\ R_0(\theta) &= -\frac{c(\theta)}{2b(\theta)} \quad \text{if} \quad a(\theta) = 0,\ b(\theta) > 0,\ c(\theta) < 0. \end{aligned} \tag{3.14}$$

It follows from Eqs. (2.16), (2.17), (3.5), (3.6) and (3.12) – (3.14) that the spherical size-effect solid body is, at each temperature $\theta \in I$ and for each reference configuration $\mathcal{B}_0$ of the radius R_0, *mechanically stable* iff

$$\forall\theta \in I, \quad a(\theta) > 0, \quad b(\theta) \leq 0, \quad b(\theta)^2 + c(\theta)^2 \neq 0 \tag{3.15}$$

or *mechanically stable of lower order* iff

$$\forall\theta \in I, \quad a(\theta) \geq 0, \quad b(\theta) > 0, \quad c(\theta) < 0. \tag{3.16}$$

The radius $R(\theta)$ of the mechanically stable of lower order spatial configuration $\mathcal{B}_{\mathrm{cr}}(\theta)$ is given by:

$$R(\theta) = -\frac{c(\theta)}{b(\theta)}, \quad \theta \in I. \tag{3.17}$$

It follows from Eqs. (3.4), (3.6) and (3.14) that, for the *critical spatial configuration* $\mathcal{B}_{\rm cr}(\theta)$ of the radius $R(\theta)$, the condition (2.19) of existence of a critical point of a phase transition, is not fulfilled within the range I of temperature. Since the unstressed natural spatial configurations $\mathcal{B}_0(\theta)$, $\theta \in I$, are preferred reference configurations of the spherical size-effect solid body, the *critical deformations* $\lambda_{\rm cr}(\theta)$ of Eq. (2.17) will be referred to these reference configurations:

$$\lambda_{\rm cr}(\theta) = \frac{R(\theta)}{R_0(\theta)} = \frac{e(\theta)}{[1+e(\theta)]^{1/2}-1} > 1 \quad \text{if} \quad a(\theta) > 0,$$

(3.18)

$$e(\theta) = -\frac{a(\theta)b(\theta)}{c(\theta)} > 0,$$

or

$$\lambda_{\rm cr}(\theta) = \frac{R(\theta)}{R_0(\theta)} = 2 \quad \text{if} \quad a(\theta) = 0. \tag{3.19}$$

The corresponding *critical generalized Cauchy stress* $t_{\rm cr}(\theta)$ is independent of the choice of a reference configuration and given by (see Eqs. (3.4), (3.10), and (3.17)):

$$t_{\rm cr}(\theta) = T_\theta(R(\theta)) = -\frac{B(\theta)}{c(\theta)} > 0, \tag{3.20}$$

where the conditions (3.9) and (3.16) were taken into account. It follows from Eq. (3.20) that $t_{\rm cr}(\theta)$ is the absolute maximum of the generalized stress function $T_\theta(R)$ defined by Eqs. (3.4) and (3.16). Thus, $t_{\rm cr}(\theta)$ defines a finite *upper elastic limit* of the mechanically stable of lower order elastic spherical size-effect solid body with the liquid-like response. The isothermal bulk modulus $K(\theta)$ of this size-effect body (Eq. (2.13)) has, according to Eqs. (3.5), (3.6) and (3.11), the following representation:

$$K(\theta) = K_\theta(R_0(\theta)) = -2\left[b(\theta)h_0(\theta) + c(\theta)k_0(\theta)\right] > 0, \tag{3.21}$$

where $R_0(\theta)$ of Eq. (3.11) is given by Eq. (3.14). Note that if the considered spherical size-effect body is mechanically stable, then the isothermal bulk modulus is given also by Eq. (3.21) but with the radius of $R_0(\theta)$ Eq. (3.11) defined by Eq. (3.13).

It follows from Eqs. (3.2), (3.4), and (3.6) that the influence of the body boundary surface causes the dependence on the body size of the isothermal generalized Cauchy stress $T_\theta(R)$ as well as the isothermal compressibility $K_\theta(R)$. Thereby, it is a phenomenological model of the influence of surface atoms on thermomechanical properties of spherical nanomaterial clusters (see [3], Secs. 1 and 4). If the elastic spherical size-effect solid body is mechanically stable, then

its asymptotic uniform expansion defines the finite isothermal generalized Cauchy stress $t(\theta)$:

$$t(\theta) = \lim_{R\to\infty} T_\theta(R) = 3a(\theta) > 0 \tag{3.22}$$

being a finite *asymptotic upper elastic limit* of this size-effect body (cf. [3], Eqs. (4.28) and (4.29)). Denoting by $p_\theta(R) = -T_\theta(R)$ the uniform pressure compensating the generalized Cauchy stress $T_\theta(R)$, we obtain the following properties of the asymptotic uniform compression:

$$\lim_{R\to 0} p_\theta(R) = \infty, \qquad \lim_{R\to 0} K_\theta(R) = \infty. \tag{3.23}$$

It means that, within the range I of temperature, the elastic spherical size-efect solid body of the very small size can carry a very high uniform pressure (compression). It agrees with the observation that macroscopically small nanocrystaline clusters can carry very high compressions ([3], Sec. 1). Moreover, it folbws from Eqs. (3.20), (3.22), and (3.23) that the considered size-effect solid body has unsymmetrical elastic properties under the conditions of uniform tension and compression. It agrees with elastic properties of crystalline materials.

4. Mechanically stable mesoscale clusters

Let us consider the mechanically stable, isotropic and elastic spherical size-effect solid body with the liquid-like response under the conditions of uniform pressure. It follows from Eqs. (2.4), (2.9), (2.16), (3.10) and (3.15) that the isothermal generalized stress function t_θ monotonically increases and has, according to Eqs. (3.22) and (3.23), the following asymptotic properties:

$$\begin{gathered} \lim_{\lambda\to 0} t_\theta(\lambda) = -\infty, \qquad t_\theta(1) = 0, \\ t(\theta) = \lim_{\lambda\to\infty} t_\theta(\lambda) = 3a(\theta) > 0. \end{gathered} \tag{4.1}$$

Moreover, we can identify the constant $a(\theta) > 0$ of the formula (3.2) with the free energy density $\varepsilon(\theta)$ needed to change the volume unit and conditioned by bulk interatomic interactions. Thus, taking into account the identification of constants $b(\theta)$ and $c(\theta)$ ([3], Sec. 4, remarks following Eqs. (4.10) and (4.11)), we obtain for the considered mechanically stable size-effect solid body the conditions see Eq. (3.15)):

$$a(\theta) = \varepsilon(\theta) > 0, \quad b(\theta) = -\gamma(\theta) < 0, \quad c(\theta) = -\omega(\theta) \leq 0, \tag{4.2}$$

where $\gamma(\theta)$ and $\omega(\theta)/2\pi$ are the free energy densities necessary to change the boundary surface field unit and to change the diameter $M(\mathcal{B})/2\pi = 2R$ unit of

the spherical body, respectively. The isothermal generalized stress function t_θ of Eq. (3.10) can be written then in the following form:

$$t_\theta(\lambda) = T_\theta(R_0(\theta)\lambda), \tag{4.3}$$

where

$$\begin{aligned} T_\theta(R) &= t(\theta) - 3\left[2\gamma(\theta)R^{-1} + \omega(\theta R^{-2}\right], \\ t(\theta) &= 3\varepsilon(\theta) > 0, \end{aligned} \tag{4.4}$$

and the isothermal bulk modulus $K(\theta)$ of Eq. (3.21) takes the form:

$$K(\theta) = 2\left[\gamma(\theta)h_0(\theta) + \omega(\theta)k_0(\theta)\right] > 0, \tag{4.5}$$

where $h_0(\theta)$ and $k_0(\theta)$ denote the mean and Gaussian curvatures (given by Eq. (3.11)) of the boundary surface of the natural spatial configuration $\mathcal{B}_0(\theta)$ of radius $R_0(\theta)$. Thus, in accordance with the observed properties of nanocrystaline macroscopically small clusters ([3], Sec. 1), the bulk modulus increases if the body $\mathcal{B}_0(\theta)$ size decreases. Note that, according to Eqs. (3.13) and (4.1), the radius $R_0(\theta)$ decreases if the upper elastic limit t_θ increases.

Let us observe that the term $\omega(\theta)R^{-2}$ appearing in Eq. (4.4) can be interpreted as the one corresponding to the long-range interactions between the surface atoms and bulk atoms located in a boundary layer (see [3], remarks following Eq. (4.11)). Thereby, in the case

$$\varepsilon(\theta) > 0, \qquad \gamma(\theta) > 0, \qquad \omega(\theta) = 0 \tag{4.6}$$

these interactions are neglected. Since in this case Eq. (4.4) takes the form

$$T_\theta(R) = 3\left[\varepsilon(\theta) - 2\gamma(\theta)R^{-1}\right], \tag{4.7}$$

the isothermal generalized Cauchy stress depends on interatomic bulk interactions ($\varepsilon(\theta) > 0$) as well as on interactions of the surface atoms located on the body boundary ($\gamma(\theta) > 0$). These interatomic interactions influence the radius $R_0(\theta)$ of a natural spatial configuration in the following manner (cf. Eqs. (3.13) and (4.7)):

$$R_0(\theta) = \frac{2\gamma(\theta)}{\varepsilon(\theta)}. \tag{4.8}$$

Consequently, according to Eqs. (4.5), (4.6), and (4.8), the isothermal bulk modulus reduces to:

$$K(\theta) = 2\gamma(\theta)R_0(\theta)^{-1} = \varepsilon(\theta), \tag{4.9}$$

and it follows from Eqs. (4.3), (4.7), and (4.9) that the isothermal generalized Cauchy stress $t_\theta(\lambda)$ (Eq. (3.10)), referred to the natural configuration of the radius $R_0(\theta)$ of Eq. (4.8), can be written in the form:

$$t_\theta(\lambda) = t(\theta)(1 - \lambda^{-1}), \qquad \lambda > 0, \tag{4.10}$$

where the asymptotic upper elastic limit $t(\theta)$ is related to the bulk modulus $K(\theta)$ according to the following formula:

$$t(\theta) = 3K(\theta). \tag{4.11}$$

The graph of this function t_θ is an equilateral hyperbola. Note that Eq. (4.9) means that the isothermal bulk modulus depends on interatomic bulk interactions only. It is a point of similarity between this bulk modulus and the macroscopic bulk modulus (see Sec. 1). On the other hand, the bulk modulus $K(\theta)$ of Eq. (4.9) is referred, contrary to the macroscopic bulk modulus, to the preferred spatial configuration of the body that is conditioned by the influence of surface atoms (Eq. (4.8)). It suggests that the spherical size-effect solid body defined by the conditions (4.2) and (4.6) can be considered as the one whose size lies in the upper range of the mesoscale observation levels (see [3], Sec. 1).

If

$$\omega(\theta) > 0 \tag{4.12}$$

then the radius $R_0(\theta)$, $\theta \in I$, of a natural spatial configuration (Eqs. (3.13) and (4.2)) becomes greater than that of the case (4.6) (Eq. (4.8)). The isothermal bulk modulus $K(\theta)$ reveals explicitly the size effect in a manner observed for macroscopically small nanomaterial clusters (see remarks following Eq. (4.5)) and the dependence of this modulus on interatomic bulk interactions is still preserved. Thus, the size of such natural configuration should lie also in the upper range of the mesoscale observation levels.

5. Fullerene-like response

Let us consider the mechanically stable of lower order, isotropic and elastic spherical size-effect solid body with the liquid-like response defined by Eqs. (3.1), (3.2) and by the conditions (3.16) written in the form (see [3], Eqs. (4.11), (4.9)):

$$a(\theta) = \varepsilon(\theta) \geq o, \quad b(\theta) = \gamma(\theta) > 0, \quad c(\theta) = -\omega(\theta) < 0. \tag{5.1}$$

The radius $R_0(\theta)$ of a natural configuration is defined by Eq. (3.14), the radius $R(\theta)$ of a critical spatial configuration can be written in the form (see Eq. (3.7)):

$$R(\theta) = \frac{\omega(\theta)}{\gamma(\theta)}, \tag{5.2}$$

and the isothermal generalized Cauchy stress $T_\theta(R)$ of Eq. (3.4) can be rewritten as:

$$
\begin{aligned}
T_\theta(R) &= t(\theta) + 3[2\gamma(\theta)R^{-1} - \omega(\theta)R^{-2}], \\
t(\theta) &= 3\varepsilon(\theta) \geq 0.
\end{aligned}
\tag{5.3}
$$

The isothermal compressibility of Eq. (3.6) takes then the form:

$$
\begin{aligned}
K_\theta(R) &= 2[-\gamma(\theta)R^{-1} + \omega(\theta)R^{-2}], \\
K_\theta(R(\theta)) &= 0.
\end{aligned}
\tag{5.4}
$$

If $\lambda_{\mathrm{cr}}(\theta)$ is the critical deformation of the spatial natural configuration $\mathcal{B}_0(\theta)$ defined by Eqs. (3.18) and (3.19), and $\delta_{\mathrm{cr}}(\theta)$ denotes the critical relative variation of the radius $R_0(\theta)$ of this configuration

$$
\delta_{\mathrm{cr}}(\theta) = \frac{R(\theta) - R_0(\theta)}{R_0(\theta)} = \lambda_{\mathrm{cr}}(\theta) - 1 > 0,
\tag{5.5}
$$

then the isothermal bulk modulus is given by:

$$
K(\theta) = K_\theta(R_0(\theta)) = 2\lambda_{\mathrm{cr}}(\theta)\delta_{\mathrm{cr}}(\theta)\frac{\gamma(\theta)}{R(\theta)} > 0.
\tag{5.6}
$$

The isothermal generalized Cauchy stress function t_θ, describing the elastic response of the spherical size-effect solid body with respect to its natural configuration and defined by Eqs. (3.10), and (5.1) – (5.3), takes the form:

$$
\begin{aligned}
t_\theta(\lambda) &= T_\theta(R_0(\theta)\lambda) = t(\theta) + s_\theta(\mu)_{|\mu=\lambda/\lambda_{\mathrm{cr}}(\theta)}, \\
s(\mu) &= s_{\mathrm{cr}}(\theta)(2\mu^{-1} - \mu^{-2}),
\end{aligned}
\tag{5.7}
$$

where it was denoted:

$$
s_{\mathrm{cr}}(\theta) = \frac{3\gamma(\theta)}{R(\theta)} = \frac{3\gamma(\theta)^2}{\omega(\theta)},
\tag{5.8}
$$

and takes its maximum value $t_{\mathrm{cr}}(\theta)$ for $\lambda = \lambda_{\mathrm{cr}}(\theta)$, that is in the critical spatial configuration $\mathcal{B}_{\mathrm{cr}}(\theta)$ of the radius $R(\theta)$:

$$
t_{\mathrm{cr}}(\theta) = T_\theta(R(\theta)) = t(\theta) + s_{\mathrm{cr}}(\theta).
\tag{5.9}
$$

It follows from Eqs. (5.1) – (5.9) that the case $\varepsilon(\theta) > 0$ means the existence of interatomic bulk interactions that influence the critical point $(\lambda_{\mathrm{cr}}(\theta), t_{\mathrm{cr}}(\theta))$.

However, the occurrence of size effect (Eqs. (5.6) and (5.8)) is independent of the existence of these interactions. This is why we restrict ourselves to the case

$$\varepsilon(\theta) = 0, \tag{5.10}$$

at which

$$\begin{aligned} &\lambda_{\mathrm{cr}}(\theta) = 2, \quad \text{i.e.} \quad \delta_{\mathrm{cr}}(\theta) = 1, \quad R(\theta) = 2R_0(\theta), \\ &t(\theta) = 0, \quad \text{i.e.} \quad t_{\mathrm{cr}}(\theta) = s_{\mathrm{cr}}(\theta). \end{aligned} \tag{5.11}$$

The isothermal bulk modulus $K(\theta)$ and the isothermal critical generalized Cauchy stress $t_{\mathrm{cr}}(\theta)$ reveal then the size effect of the form:

$$K(\theta)R_0(\theta) = 2\gamma(\theta), \tag{5.12}$$

and

$$t_{\mathrm{cr}}(\theta)R(\theta) = 3\gamma(\theta). \tag{5.13}$$

Note that the relation (5.12) is equivalent to the following representation of the bulk modulus:

$$K(\theta) = \frac{4\gamma(\theta)^2}{\omega(\theta)}, \tag{5.14}$$

and, according to Eqs. (5.11) and (5.13), we obtain:

$$t_{\mathrm{cr}}(\theta) = \frac{3}{4}K(\theta). \tag{5.15}$$

It follows from Eqs. (5.14) and (5.15) that the size effect appearing in Eqs. (5.12) and (5.13) depends only on interactions between surface atoms ($\gamma(\theta) > 0$) and on their long-range interactions with bulk atoms located in a boundary layer ($\omega(\theta) > 0$) (see [3], Sec. 4). Thereby, this size effect has a physical meaning that corresponds to the properties of the very nanostructures (see [3], Sec. 1). Consequently, we can expect that the case (5.1), (5.10) concerns nanomaterial spherical clusters smaller than mesoscale clusters discussed in Sec. 4.

The isothermal generalized stress function t_θ (Eq. (5.7)) takes in the case (5.10) the following form:

$$t_\theta(\lambda) = 4t_{\mathrm{cr}}(\theta)(\lambda^{-1} - \lambda^{-2}), \quad \lambda > 0. \tag{5.16}$$

The function t_θ of Eq. (5.16) monotonically increases (taking positive as well as negative values) in the interval $0 < \lambda < 2$ and for $\lambda = \lambda_{\mathrm{cr}}(\theta) = 2$ (being a critical deformation for which the isothermal compressibility vanishes) reaches the upper elastic limit $t_{\mathrm{cr}}(\theta)$ (see Sec. 3). For $\lambda > 2$ the stress function is positive

and decreases to zero if the uniform extension λ tends to infinity. It means that the elastic resistance to uniform tension decreases for $\lambda > \lambda_{\mathrm{cr}}$ (and vanishes at infinity). We will call this process the (nonlinear) *elastic flow effect*. Note that the similar relation between a uniform pressure (compression or tension) and the deformation of Eq. (1.1) was found for usual crystals by means of numerical computations based on the analysis of bound energy changes in cubic crystal lattices (direct, body-centered, and face-centered) [9]. In these computations the central binary interactions with Morse-type potential (or with an arbitrary type potential but for the case of nearest neighbour interactions only) and the natural reference configuration temperature 0 K, were assumed. Particularly, the elastic flow effect has been computed. This effect is, in the framework of the considered liquid-like response of the spherical elastic size-effect solid body, a consequence of the mechanical stability of lower order.

The liquid-like response manifests itself in the dependence of the total free energy as well as the generalized Cauchy stress on the actual spatial configurations only (Eqs. (3.2) and (5.9)). Therefore, the considered size-effect solid body reacts in a manner similar to a fluid body regarded as a material body having no preferred configuration (see [3], Secs. 2 and 4). On the other hand, the condition (5.1), defining the mechanical stability of lower order, means the existence of preferred configurations (the natural spatial configurations) and the existence of critical spatial configurations (being configurations of the mechanical stability of lower order). Since the critical spatial configurations are not associated with the existence of a critical point of a phase transition (see remarks following Eq. (3.17)) and reveal the elastic flow effect, they can be considered to exhibit the existence of solid state with the liquid-like elastic behaviour within a finite range of temperature. It can be interpreted as an elastical analogue of properties of small spherical fullerene C_{60} clusters that exhibit a coexistence of solid and liquid states within a finite range of temperature and for some particular sizes of these clusters only (see [3], Sec. 1). If so, the uniquely defined diameter $2R(\theta)$ of a critical spatial configuration (Eq. (5.2)) can be considered as a counterpart, at the temperature $\theta \in I$, of the particular size of a small fullerene C_{60} cluster. The mechanically stable of lower order, isotropic and elastic spherical size-effect solid body with the liquid-like response will be called, coming into line with the above analogy, a spherical size-effect body with the *fullerene-like response*.

Note that if the fullerene-like response is interpreted as an elastical analogue of the coexistence of solid and liquid states within a finite range of temperature, then it seems reasonable to admit that a *viscosity effect* (cf. Eqs. (2.24) – (2.26)) occurs in the critical spatial configurations. Unfortunately, viscosity properties of small nanomaterial clusters are not satisfactorily recognized.

6. Conclusions and remarks

The analysis of a homogeneous isotropic and elastic spherical size-effect solid body (Sec. 2) with the liquid-like response (Secs. 3-5) subjected, within a certain range of temperature, to a uniform pressure, shows that if the body is mechanically stable, then it can be considered to be a model of nanocrystalline (e.g. metallic) clusters with a size which lies in the upper range of the mesoscale observation levels. It has been shown that a part of the total surface energy, representing the long-range interactions between the surface atoms and bulk atoms located in a boundary layer, is then responsible for the explicit occurrence of the size effect (Sec. 4). If the body is mechanically stable of lower order, then it reveals the fullerene-like response that can be interpreted as an elastic analogue of the properties of small C_{60} clusters of a size corresponding to the very nanometer observation level scale (Sec. 5). In both cases a finite upper elastic limit appears. If the spherical size-effect body is mechanically stable, then the upper elastic limit is an asymptotic elastic property. If the spherical size-effect body is mechanically stable of lower order, then the upper elastic limit corresponds to a critical spatial configuration of the body and reveals a size effect (Eq. (5.13)). Moreover, in both cases, the body can carry a high pressure (compression) with very small elastic deformations (Sec. 3). This asymmetry of elastic properties under a uniform tension and compression is a characteristic feature of crystalline solid clusters, of usual as well as nanostructured materials. In fact, the domain of physically admissible elastic homogeneous deformations of a nanomaterial cluster is bounded by a hypersurface defined by the elastic limit. The hypersurface is dependent on the body uniform temperature (cf. [10] and [11]) and can depend on the body itself (cf. Eqs. (2.17) and (2.18)).

The isothermal bulk modulus $K(\theta)$ of the spherical size-effect solid body with the liquid-like response increases if the radius $R_0(\theta)$ of its unstressed spatial configuration $\mathcal{B}_0(\theta)$ decreases (Eq. (3.21)). For the body being mechanically stable of lower order, the bulk modulus has the representation given by Eq. (5.6) from which it follows that if the critical deformation $\lambda_{\mathrm{cr}}(\theta)$ of $\mathcal{B}_0(\theta)$ (Eqs. (3.18) and (3.19)) is constant, then this bulk modulus is inversely proportional to the radius $R(\theta)$ of the critical spatial configuration $\mathcal{B}_{\mathrm{cr}}(\theta)$. Particularly, if the bulk interatomic interactions can be neglected (cf. [3], Secs. 1 and 4), then $\lambda_{\mathrm{cr}}(\theta) = 2$ for each $\theta \in I$ and this size effect reduces to (Sec. 5):

$$K(\theta)R_0(\theta) = 2\gamma(\theta) \tag{6.1}$$

where

$$R(\theta) = 2R_0(\theta) = \omega(\theta)/\gamma(\theta). \tag{6.2}$$

It follows from Eqs. (6.1) and (6.2) that the isothermal bulk modulus depends only on the interactions of the boundary surface atoms ($\gamma(\theta) > 0$) and on the

long-range interactions between these atoms and the bulk atoms located in a boundary layer ($\omega(\theta) > 0$ (Sec. 5). Note that if the body is mechanically stable and the long-range interactions between the surface atoms and bulk atoms of a boundary layer are neglected ($\omega(\theta) = 0$), then the formula (6.1) is also valid but in this case the radius $R_0(\theta)$ is given by

$$R_0(\theta) = 2\gamma(\theta)/\varepsilon(\theta), \tag{6.3}$$

where $\varepsilon(\theta) > 0$ is the volumetric free energy density conditioned by the interatomic bulk interactions (Sec. 4). Let us denote by $\alpha(\theta)$ the coefficient of linear thermal expansion of an unstressed configuration $\mathcal{B}_0(\theta)$ of the spherical size-effect solid body, and by $\beta(\theta)$ – the temperature bulk compressibility coefficient of this configuration:

$$\begin{aligned} \alpha(\theta) &= \frac{1}{R_0(\theta)}\frac{dR_0(\theta)}{d\theta} = \frac{1}{3V_0(\theta)}\frac{dV_0(\theta)}{d\theta}, \\ \beta(\theta) &= \frac{1}{K(\theta)}\frac{dK(\theta)}{d\theta}, \quad V_0(\theta) = (4/3)\pi R_0(\theta)^3. \end{aligned} \tag{6.4}$$

Differentiating the relation (6.1) with respect to the parameter θ, and taking into account that if the temperature increases from 0 K to $\theta \in I$, then the surface tension $\gamma(\theta)$ monotonically decreases [1] and $\alpha(\theta) > 0$ because almost all material bodies expand under heating, we obtain that the following conditions would be fulfilled:

$$\begin{aligned} &\alpha(\theta) > 0, \quad d\gamma(\theta)/d\theta < 0, \quad \beta(\theta) < 0, \\ &|\beta(\theta)| > \alpha(\theta), \quad \theta \in I, \end{aligned} \tag{6.5}$$

and

$$\begin{aligned} d\varepsilon(\theta)/d\theta < 0 \quad &\text{if} \quad \omega(\theta) = 0, \\ d\omega(\theta)/d\theta < 0 \quad &\text{if} \quad \varepsilon(\theta) = 0. \end{aligned} \tag{6.6}$$

It is known that the macroscopic bulk moduli of usual crystals decrease if the temperature increases [1]. We see that the mesoscale as well as the nanoscale bulk modulus has the same property. It agrees with the observation that the elevated temperatures have the effect of degrading the mechanical properties of nanomaterials [11]. The case of bulk modulus suggests that the phenomena of thermal expansion and decreasing of free energy densities (superficial as well as volumetric) have a contribution to this effect.

Note that the problem when a cluster can be treated as the macroscopic one, has as yet no accurate general solution. For example, a cluster of an inert gas can be considered as a macroscopic particle if it consists of more than 10^4 atoms under the condition that the cluster temperature is not too low [12]. This example, the properties of small fullerene clusters ([3], Sec. 1), and the effect of degrading mechanical properties of nanomaterials at elevated temperatures, lead to a conclusion that the size effect in macroscopically small nanomaterial clusters should be related to thermomechanical properties of these clusters rather than to their purely mechanical properties only.

The classical thermodynamic is applied in this paper to macroscopically small systems that can contain even less than 200 atoms [13]. Consequently, such systems may not be satisfactorily described, in a manner consistent with the classical thermodynamics, by means of the classical statistical physics. However, for example, a finite system of mutually interacting identical particles, the dynamical behaviour of which is random, can admit the thermodynamical interpretation of the Markovian-type evolution of the system [14]. Namely, the existence of thermodynamically permitted Markov processes can be shown that are consistent with the assumption of thermal character of the interaction of the system with the environment, with the first and second laws of thermodynamics, with the postulate of existence of the equilibrium state, and with the relaxation postulate (stating that the process relax, independently of the choice of the initial condition, towards the state of thermodynamical equilibrium). Moreover, if the environment of the system is a thermostat, then we can generalize, replacing the uniform temperature of the system with the (uniform) temperature of the thermostat, the equilibrium definition of the free energy to the nonequilibrium situation [14]. This example shows that the classical thermodynamics can be also consistent with the randomness of microstate dynamics of macroscopically small systems containing a small number of atoms.

References

1. A. COTTREL, *The mechanical properties of matter*, John Willey & Sons, New York 1964.
2. N. W. ASHEROFT and N. D. MERMIN, *Solid state physics* [Polish edition], PWN, Warsaw 1986.
3. A. TRZĘSOWSKI, *Nanomaterial clusters as macroscopically small size-effect bodies.* I, Arch. Mech., this issue.
4. A. TRZĘSOWSKI, *On the compressibility of a spherical solid body*, Arch. Mech., **33**, 11–20, 1981.
5. C. TRUESDELL, *A first course in rational continuum mechanics*, John Hopkins University Press, Baltimore 1972.
6. A. S. KOMPANIEV, *Course of theoretical physics*, Part II [in Russian], Prosveščenie, Moscow 1975.

7. P. GLANDSDORF and I. PRIGOGINE, *Thermodynamical theory of structure, stability and fluctuations*, Willey-Interscience, London 1973.

8. B. MRYGOŃ, *Fluctuational model of a system in the phase transition domain* [in Polish], IP-PAS Reports 77, Ossolineum, Wrocław 1978.

9. F. M. MILSTEIN and R. HILL, *Theoretical properties of cubic crystals at arbitrary pressure. I*, Mech. Phys. Solids, **25**, 457, 1977.

10. A. TRZĘSOWSKI, *The size effect*, Bull. Acad. Polon. Sci., Serie Sci. Techn., **XXVII**, 255–267, 1979.

11. V. PROVENZANO, N. P. LOAT, M. A. IMAM and K. SANDANANDO, *Ultrafine superstrength materials*, Nanostruct. Mat., **1**, 89–94, 1992.

12. B. M. SMIRNOV, *Transition cluster-macroscopic system* [in Russian], J. Exp. Theor. Phys., **108**, 1810–1820, 1995.

13. J. M. MONTEJANO-CARRIZALIVES and J. L. MORÁN-LOPEZ, *Geometrical characteristics of compact nanoclusters*, Nanostruct. Mat., **1**, 397–409, 1992.

14. A. TRZĘSOWSKI and S. PIEKARSKI, *Markovian description of irreversible processes and the time randomization*, Il Nuovo Cimento, **D14**, 767–787, 1992.

Received June 18, 1999; revised version November 19, 1999.

INSTITUTE OF FUNDAMENTAL TECHNOLOGICAL RESEARCH
is publishing the following periodicals:

ARCHIVES OF MECHANICS – bimontly (in English)
ARCHIVES OF ACOUSTICS – quarterly (in English)
ARCHIVES OF CIVIL ENGINEERING – quarterly (in English)
ENGINEERING TRANSACTIONS – quarterly (in English)
COMPUTER ASSISTED MECHANICS AND ENGINEERING SCIENCES – quarterly (in English)
JOURNAL OF TECHNICAL PHYSICS – quarterly (in English)

Subscription orders for the journals edit by IFTR may be sent directly to the
Editorial Office
Institute of Fundamental Technological Research,
Świętokrzyska 21, p. 508,
00-049 WARSZAWA, Poland.

DIRECTIONS FOR THE AUTHORS

The journal *ARCHIVES OF MECHANICS (ARCHIWUM MECHANIKI STOSOWANEJ)* deals with the printing of original papers which should not appear in other periodicals.

As a rule, the volume of a paper should not exceed 40 000 typographic signs, that is about 20 type-written pages, format: 210×297 mm, leaded. The papers should be submitted in two copies. They must be set in accordance with the norms established by the Editorial Office. Special importance is attached to the following directions:

1. The title of the paper should be as short as possible.

2. The text should be preceded by a brief introduction; it is also desirable that a list of notations used in the paper should be given.

3. The formula number consists of two figures: the first represents the section number and the other the formula number in that section. Thus the division into subsections does not influence the numbering of formulae. Only such formulae should be numbered to which the author refers throughout the paper, and also the resulting formulae. The formula number should be written on the left-hand side of the formula; round brackets are necessary to avoid any misunderstanding. For instance, if the author refers to the third formula of the set (2.1), a subscript should be added to denote the formula, viz. $(2.1)_3$.

4. All the notations should be written very distinctly. Special care must be taken to write small and capital letters as precisely as possible. Semi-bold type should be underlined in black pencil. Explanations should be given on the margin of the manuscript in case of special type face.

5. It has been established to denote vectors by semi-bold type. Trigonometric functions are denoted by sin, cos, tg and ctg, inverse functions – by arc sin, arc cos, arc tg and arc ctg; hyperbolic functions are denoted by sh, ch, th and cth, inverse functions – by Arsh, Arch, Arth and Arcth.

6. Figures in square brackets denote reference titles. Items appearing in the reference list should include the initials of the first name of the author and his surname, also the full title of the paper (in the language of the original paper); moreover;

a) In the case of books, the publisher's name, the place and year of publication should be given, e.g.,

5. S. Ziemba, *Vibration analysis*, PWN, Warszawa 1970;

b) In the case of a periodical, the full title of the periodical, consecutive volume number, current issue number, pp. from ... to ..., year of publication should be mentioned; the annual volume number must be marked in black pencil so as to distinguish it from the current issue number, e.g.,

6. M. Sokołowski, *A thermoelastic problem for a strip with discontinuous boundary conditions*, Arch. Mech., **13**, 3, 337–354, 1961.

7. The authors should enclose a summary of the paper. The volume of the summary is to be about 100 words.

8. The authors are kindly requested to enclose the figures prepared on diskettes (format PCX, BitMap or PostScript).

Upon receipt of the paper, the Editorial Office forwards it to the reviewer. His opinion is the basis for the Editorial Committee to determine whether the paper can be accepted for publication or not.

The printing of the paper completed, the author receives 25 copies of reprints free of charge. The authors wishing to get more copies should advise the Editorial Office accordingly, not later than the date of obtaining the galley proofs.

The papers submitted for publication in the journal should be written in English. No royalty is paid to the authors.

Please send us, in addition to the typescript, the same text prepared on a diskette (flopy disk) 3 1/2″ as an ASCII file, preferably in the TEX or LATEX format in Dos or Unix format.

EDITORIAL COMMITTEE
ARCHIVES OF MECHANICS
(ARCHIWUM MECHANIKI STOSOWANEJ)

Archives of Mechanics

Contents of issue 1 vol. 52

Arch. Mech., **52**, nr 1, str. 1–200, Warszawa 2000